UNIVERSITAT DE BARCELONA

The role of cyclin-dependent kinase 5 (Cdk5) in colorectal cancer

Sara Kjaergaard Bystrup

UNIVERSITAT DE BARCELONA

FACUTAT DE MEDICINA

PROGRAMA DE DOCTORAT EN BIOMEDICINA

THE ROLE OF CYCLIN-DEPENDENT KINASE 5 (CDK5) IN CORLORECTAL CANCER PROGRESSION

SARA KJAERGAARD BYSTRUP

Resistance, chemotherapy and biomarkers group
Germans Trias i Pujol Research institut

May 2021

Memòria de tesi doctoral presentada per Sara Kjaergaard Bystrup per optar al grau de doctora per la Universitat de Barcelona

Dra. Eva Martinez Balibrea
Director

Dr. Victor Moreno
Tutor

Sara Kjaergaard Bystrup
Author

PMPPC Program for Predictive and Personalized Medicine of Cancer | IGTP Germans Trias i Pujol Research Institute | Program Against Cancer Therapeutic Resistance ProCURE | ICO Institut Català d'Oncolog

Eva Martinez Balibrea, leader of the “Resistance, chemotherapy and biomarkers group” at the Germans Trias i Pujol Research institut (IGTP) and **Victor Moreno Aguado**, leader of the “Colorectal Cancer Research Group” at The Bellvitge Institute for Biomedical Research (IDIBELL) give the approval of the presentation of the PhD thesis written by Sara Kjaergaard Bystrup with the title:

The role of cyclin-dependent kinase 5 (Cdk5) in colorectal cancer

MARTINEZ BALIBREA EVA - 38139505P
Valid signature
Firmado digitalmente por MARTINEZ BREA EVA - 38139505P
Fecha: 2021.05.31 09:24:44 +02'00'

Eva Martinez Balibrea
Director

BYSTRUP --- SARA KJAERGAARD - X5883126W
Digitally signed by BYSTRUP --- SARA KJAERGAARD - X5883126W
Date: 2021.05.31 10:09:28 +02'00'

Sara Kjaergaard Bystrup
Author

Digitally signed by MORENO AGUADO VICTOR RAUL - 35046710T
Date: 2021.05.29 12:43:32 +02'00'

Victor Moreno Aguado
Tutor

Barcelona May 2021

Table of contents

List of figures

List of tables

List of abbreviations

5-FU: Fluorouracil
ABC: ATP-binding cassette
AKT: Protein kinase B
APC: Adenomatous polyposis coli
APCs: Antigen presenting cells
AR: Androgen receptor
ATM: Ataxia-telangiectasia mutated
BRAF: v-Raf murine sarcoma viral homolog B
CAPOX: Capecitabine plus oxaliplatin
CD: Cluster of differentiation
Cdk5: Cyclind ependent kinase 5
Cdks: Cyclin dependent kinases
cDNA: Coding DNA
CIMP: CpG island methylator phenotype
CIN: Chromosomal instability
CMS: Consensus molecular subtype
CNV: Copy number variation
COAD: Colon adenocarcinoma
CRC: Colorectal cancer
ctDNA: Circulating tumor DNA
CTLA-4: cytotoxic T-lymphocyte-associated protein 4
DACH: Diaminocyclohexane
DDR: DNA damage repair
DE: Differentially expressed
DFS: Disease free survival
dMMR: deficient mismatch repair
EGFR: Epithelial growth factor receptor
EMT: Epithelial mesenchymal transition
Erk1/2: Mitogen-activated protein kinase 3/1
EZH2: Enhancer of zeste homolog 2
FACS: Fluorescence-activated cell sorting
FAK: Focal adhesion kinase
FAP: Familial adenomatous polyposis
FDR: False discovery rate
FOBT: Fecal occult blood testing
FOLFIRI: Leucovorin/5-fluorouracil/irinotecan
FOLFOX: Leucovorin/5-fluorouracil/oxaliplatin
GO: Gene ontology
gRNA: guide RNA
HER2: human epidermal growth factor receptor 2
IP: Immunoprecipitation
IRF2: Interferon regulatory factor 2
IRF2BP: Interferon regulatory factor 2 binding protein
KD: Knockdown
KRAS: Kirsten rat sarcoma virus
LS: Lynch syndrome
MAPK: Mitogen-activated protein kinase
mCRC: Metastatic colorectal cancer
MDOTS: Murine derived organotypic spheroids
MEK: Mitogen-activated protein kinase kinase
MHC: Major histocompatibility complex

MLH1: mutL homology 1
MMR: Mismatch repair
MSH2: MutS homolog 2
MSH6: MutS homolog 6
MSI-H: High microsatellite instability
MSI: Microsatellite instability
NER: Nucleotide excision repair
NRAS: Neuroblastoma RAS viral oncogene homolog
NSCLC: Non small cell lung cancer
OS: Overall curvival
p35/p39: Cyclin-dependent kinase 5 activator 1/2
PAK1: P21 activated kinase-1
PCR: Polymerase chain reaction
PD-1: Programmed cell death protein 1
PD-L1: Programmed death-ligand 1
PFS: Progression free survival
PI3K: Phosphoinositide 3-kinase
PI3KCA: Phosphatidylinositol 3-kinase
PMS2: Post-Meitotic Segregation Increased 2
PPAR: peroxisome proliferator-activated receptors
qPCR: Quantitative polymerase chain reaction
Rb: Retinoblastoma
SD: Standard deviation
SEM: Standard error of the mean
siRNA: Small interfering RNA
SMAD4: Mothers against decapentaplegic homolog 4
STAT3: Signal transducer and activator of transcription 3
TCGA: The cancer genome atlas
TGF: Transcription growth factor
TMA: Tissue microarray
TNBC: Triple negative breast cancer
TP53: Tumor protein P53
TTP: Time to progression
VEGF: Vascular epithelial growth factor
WT: Wildtype

Tesi en format clàssic amb 1 article annexat.

Vicenç Ruiz de Porras†, **Sara Bystrup†**, Sara Cabrero-de Las Heras, Eva Musulén, Luis Palomero, Maria Henar Alonso, Rocio Nieto, Diego Arango, Víctor Moreno, Cristina Queralt, José Luis Manzano, Laura Layos , Cristina Bugés , Eva Martinez-Balibrea.
Tumor Expression of Cyclin-Dependent Kinase 5 (Cdk5) Is a Prognostic Biomarker and Predicts Outcome of Oxaliplatin-Treated Metastatic Colorectal Cancer Patients.
Cancers 2019, 11, 1540.
† Vicenç Ruiz de Porras and Sara Bystrup contributed equally.

Cancers (ISSN 2072-6694)
Journal Citation Report – Quartil 1 (*Oncology*)
Impact Factor: 6.126 (2019)

Summary

Colorectal cancer (CRC) is the third most common cancer in men and the second in women worldwide. Although 5-year survival rates in early stages are above 90% the situation dramatically changes in the metastatic setting. Only few advances have been made in the treatment of CRC in the last decades, as it still consists of different regimes of chemotherapy, possibly combined with one of the few effective targeted therapies. Hence, there is a need for finding new targets, along with prognostic and predictive biomarkers to optimize the efficiency of current and upcoming treatments.

Cyclin dependent kinase 5 (Cdk5) is best known for its functions in the nervous system, however in the last decade it has been demonstrated that it is also involved in many of the hallmarks of cancer. In this study, we investigated the expression pattern of Cdk5 in CRC cell lines and in a large number of tumor samples in order to evaluate its relevance in this pathogenesis. We found that Cdk5 is highly expressed and activated in CRC cell lines and while it does not affect proliferation, its silencing decreases cell invasion and migration, particularly in cell lines with activating mutations downstream of the epithelial growth factor receptor. Functional enrichment analyses and transcriptional effects seen upon its knockdown also confirmed the involvement of Cdk5 in cancer motility. In tumor tissues, *CDK5* is overexpressed compared to normal tissues due to a copy number gain. In patients with localized disease, we found that high Cdk5 levels correlate with poor prognosis, particularly in patients harboring *KRAS* mutations. In the metastatic setting, Cdk5 is only predictive for patients receiving an oxaliplatin-based treatment, which was corroborated by in vitro studies of oxaliplatin and irinotecan resistant cell lines. When exploring the Cdk5 levels in the consensus molecular subtypes, we found the lowest levels in subtype 1, where high Cdk5 again was associated with a poorer prognosis, however *in vitro*, *in vivo* and *ex vivo* studies do not indicate a role for Cdk5 in immune infiltration or response to immune checkpoint blockage in CRC.

Overall the results of this PhD thesis confirm the relevance of Cdk5 in CRC, and even though further studies are needed, we suggest that Cdk5 could be used either as a biomarker for adjuvant therapy in early stage CRC or for prediction of response to chemotherapies. Alternatively, Cdk5 inhibition could be used in an adjuvant setting to prevent disease relapse or in a metastatic setting in combination with oxaliplatin.

Resum

El càncer colorectal (CCR) és el tercer càncer més freqüent en homes i el segon en dones a nivell mundial. Tot i que les taxes de supervivència a 5 anys en els primers estadis superen el 90%, la situació canvia dràsticament en pacients metastàtics. S'han vist pocs avenços en el tractament del CCR en les darreres dècades, el qual encara consisteix en diferents règims de quimioteràpia, amb la possibilitat de ser combinats amb una de les poques teràpies dirigides que són efectives. Per tant, es necessita trobar noves dianes terapèutiques, juntament amb biomarcadors pronòstics i predictius per optimitzar l'eficiència dels tractaments actuals i futurs.

La cinasa dependent de la ciclina 5 (Cdk5) és més coneguda per les seves funcions en el sistema nerviós, però en l'última dècada s'ha demostrat que també està involucrada en molts processos propis del càncer. En aquest estudi, hem investigat l'expressió de Cdk5 en línies cel·lulars de CCR i en un gran nombre de mostres tumorals per tal d'avaluar la seva rellevància en aquesta patogènesi. Vam trobar que Cdk5 s'expressa i està molt activa en les línies cel·lulars de CCR i tot i que no afecta la proliferació, el seu silenciament gènic disminueix la invasió i la migració cel·lular, particularment en les línies cel·lulars amb mutacions activadores per sota del receptor del factor de creixement epitelial. Els anàlisis d'enriquiment funcional i els efectes transcripcionals com a conseqüència de l'eliminació del gen *CDK5*, també van confirmar la participació d'aquesta proteïna en la motilitat del càncer. En els teixits tumorals, Cdk5 es troba sobre-expressada en comparació amb els teixits normals a causa d'un guany en el nombre de còpies. En pacients amb malaltia localitzada, vam trobar que els nivells alts de Cdk5 es correlacionen amb un pitjor pronòstic, especialment en pacients que tenen mutacions en *KRAS*. En el context metastàtic, Cdk5 prediu la resposta en pacients tractats amb oxaliplatí, essent aquest fet corroborat per estudis in vitro amb línies cel·lulars resistents a l'oxaliplatí i no donant-se en el cas de l'irinotecan. En explorar els nivells de Cdk5 en els subtipus moleculars consensuats, vam trobar els nivells més baixos en el subtipus 1, on uns nivells elevats de Cdk5 es va tornar a associar amb un pitjor pronòstic, tot i que els estudis *in vitro*, *in vivo* i *ex vivo* no indiquen un paper per a la Cdk5 en infiltració immunitària o resposta al bloqueig del punt de control immunitari en CCR.

Els resultats d'aquesta tesi doctoral confirmen la rellevància de Cdk5 en CCR, i tot i que es necessiten estudis addicionals, suggerim que la Cdk5 es podria utilitzar com a biomarcador per a la teràpia adjuvant en CCR en estadis inicials o per predir la resposta a quimioteràpies. Alternativament, la inhibició de la Cdk5 es podria utilitzar en la

adjuvancia per evitar la recaiguda de la malaltia o en un entorn metastàtic en combinació amb oxaliplatí.

1 Introduction

1.1 Colorectal cancer

1.1.1 Epidemiology

Colorectal cancer (CRC) represents gastrointestinal malignancies from the colon to the rectum. They can be defined as colon or rectal cancers, depending on their location, however they are usually considered together as they have many biological and clinical common features. Globally, CRC is the third most diagnosed cancer, behind lung and breast, with more than 1.8 million new cases and 861,000 deaths in 2018, according to the data from the World Health Organization GLOBOCAN. The disease represents approximately 1.4% of all-cause and 8.9% of cancer-related deaths. An increase of 30% CRC deaths has been observed during the past 15 years and a further 25% growth is expected by the year 2030. The incidence rates vary greatly worldwide, with Australia, Europe and North America having the highest (1). In some of these countries a slight reduction has been observed both in incidence rates and death rates, thanks to great effort with screening and early detection along with improved treatment options. The reason why a global growth in the incidence rates is still expected is due to the rapid increase seen mainly in Asiatic and Arabic countries (2).

The risk of CRC increases with the age. It is more common in people above 50, with a median age at diagnosis of 72 in women and 68 in men, respectively. Noteworthy, in some eastern and Arabic countries the average age at diagnosis is considerably lower (2). The incidence rate is 31% higher in men than in women, with the largest differences found in rectal tumors. However, the accumulative lifetime risk for developing the disease is similar in the two sexes, 4,4% for men and 4,1% for women, because women have a longer life expectancy (3).

1.1.2 Risk factors

A risk factor is anything that increases a person's chance of developing a specific disease. They do not directly cause cancer; however, they can jointly increase the probability. Generally, 95% of cancers develop sporadically, while only 5% are considered as familial, with genetic changes or mutations passing on through generations. When looking globally at the CRC risk factors, inherited susceptibility causes the most striking increase in the risk of developing CRC, and it is currently the only reason for recommendation of more frequent screening. Other leading risk factors include inflammatory

bowel syndromes, tall stature, physical inactivity, overweight, large intake of alcoholic beverages, high consumption of red or processed meat, as well as modest intake of dairy products and foods containing wholegrains or dietary fiber. Many indications suggest that there are a number of ways to lower the risk of developing CRC as well, besides of course maintaining a healthy body weight and being physical active, high consumptions of calcium, dairy aliments, vegetables and fruit as well multivitamins and vitamin D are recommendable (1).

Among the hereditary CRC syndromes, the most common one is the Lynch syndrome (LS), which is caused by germline mutations in one of the mismatch repair (MMR) genes: *mutL homology 1* (*MLH1*)*, MutS homolog 2* (*MSH2*)*, MutS homolog 6* (*MSH6*)*, Post-Meitotic Segregation Increased 2* (*PMS2*) or *epithelial cell adhesion molecule (EPCAM).* Impaired MMR during replication leads to accumulation of mutations in the DNA, particularly in the microsatellite fragments with repetitive nucleotide sequences. Over time, the accumulation of such mutations in microsatellites and elsewhere in the genome can drive tumorigenesis. A number of other cancers are also associated with the Lynch syndrome, including endometrial, ovary, stomach and urothelial tract (4). Familial adenomatous polyposis (FAP) is the second most common hereditary CRC syndrome. This syndrome is caused by mutations in the *adenomatous polyposis coli* (*APC)* gene, which is a key tumor suppressor gene that is involved in the β-Catenin/Wnt signaling pathway. Most patients with familial adenomatous polyposis develop a large number of colorectal adenomas leading to early development of CRC. Other hereditary CRC syndromes are also polyposis associated including Peutz Jeghers syndrome, serrated polyposis and juvenile polyposis coli. Common for these syndromes is that the polyps end up undergoing carcinogenesis, however the exact route differ from condition to condition (4).

1.1.3 Screening and detection

CRC is among the cancer types more suitable for broad population screening. Firstly, CRC has a long preclinical stage, secondly, the incidence of the disease is high and outcome for a significant proportion of affected patients is poor and thirdly, because adenomas and early cancers are easy detectable and treatable. Most programs are based on a primary screen, with fecal occult blood tests. Both early and advanced premalignant lesions can bleed and shed cells into the bowel lumen, which can be detected. In those that test positive a colonoscopy is indicated.

Other tests take advantage of DNA shed by epithelial cells, which can also be isolated from stool samples. Mutations of Kirsten rat sarcoma virus (*KRAS)* and *APC* or other

typical CRC mutations can be detected, however the accuracy of these tests still needs to be improved. Other potential useful diagnostic markers under investigation include circulating tumor mRNA, microRNA and circulating Cytokeratin (4).

Typical symptoms for CRC include blood in stools, change in bowel habits and abdominal pain. This is often accompanied with fatigue, anemia-related symptoms, shortness of breath and weight loss. When a person presents with a combination of these symptoms a colonoscopy is the physicians' preferred method for investigation. During the colonoscopy the gastroenterologists will take biopsies of any suspicious polyps. Additionally, modern imaging techniques improve detection and clinical staging. The depth of local tumor invasion and the presence of regional and distant metastases are assessed by computed tomography scan (CT) and magnetic resonance imaging (MRI).

1.2 CRC pathogenesis

1.2.1 From adenoma to carcinoma

In order to understand the development of a CRC it is important to understand the setting in which it arises. The wall of the colon consists of an epithelial crypt layer followed by layers of connective tissue, a thin muscle layer, submucosa, a thick muscle layer and at last the serosa (figure 1). The epithelial layer has two principal functions: absorbing useful substances from digested food and at the same time restricting the entry of any harmful substances.

CRC development is initiated with transformations in the normal epithelium mucosa leading to a hyper-proliferative epithelium that can form adenomas. However, adenomas in the epithelial cell layer are not considered malignant adenocarcinomas until they have invaded through to the submucosa layer. This process is referred to as the "adenoma-carcinoma sequence". It is a slow process estimated to take up to between 7-10 years (5). During this period the epithelial cells accumulate genomic instability and activating mutations in oncogenes accompanied by inactivation of tumor suppressor genes. Another important feature of this development is attaining the ability to escape immune surveillance.

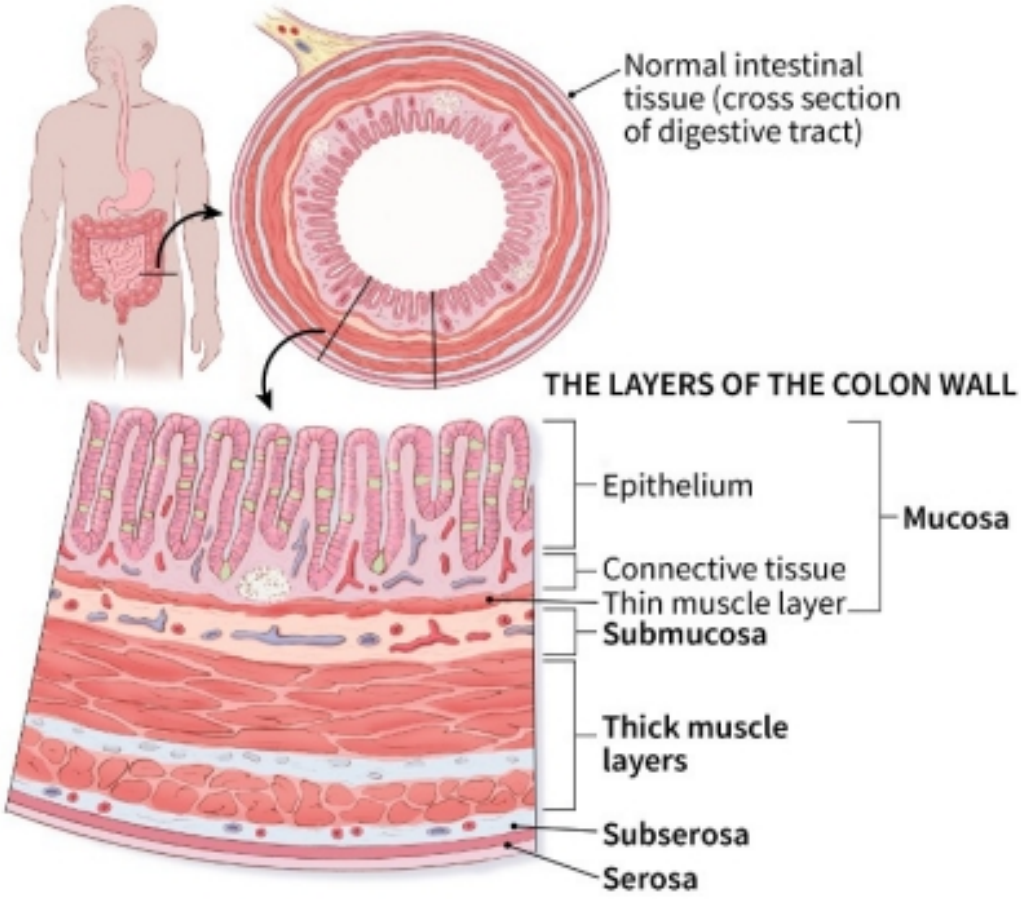

***Figure 1**. Layers of the epithelial wall. From www.cancer.com (6)*

CRC is a very heterogeneous disease with distinctive backgrounds. Understanding the complexity of each tumor is crucial in order to determine the best choice of treatment. In general CRC results from the progressive accumulation of numerous genetic and epigenetic aberrations within cells. This development from adenoma to carcinoma is considered to be caused by one or a combination of three major molecular pathways: Microsatellite instability (MSI), chromosomal instability (CIN) and CpG island methylator phenotype (CIMP) (figure 2). These 3 pathways are not mutually exclusive and some tumors exhibit features of multiple pathways. The molecular aspects of these pathways are used clinically in the diagnosis and in the management of patients with CRC.

1.2.2 MSI

Tumors with deficient MMR (dMMR) have high rates of mutations that particularly accumulate in the microsatellites, resulting in genomic instability. Microsatellites are small (1-6 base pairs) repeating stretches of DNA found throughout the entire genome. They account for around 3 % of the human genome. Due to their repeated structure, mi-

crosatellites are prone to have high mutation rate. Approximately 15% of CRC are dMMR, which in the tumor results in a hypermutable phenotype MSI. Three percent of these are associated with Lynch syndrome, with germline mutation in a MMR gene (*MLH1, MSH2, MSH6, PMS2*), while the remaining 12% are primarily caused by sporadic epigenetic inactivation of the *MLH1* MMR gene. As a result of the dMMR these tumors also accumulate different driver mutations, with *v-Raf murine sarcoma viral homolog B* (*BRAF) and Transforming growth factor, beta receptor II (TGFBR2)* being the most common ones (7). Colorectal tumors with MSI have distinctive features, including a tendency to arise in the proximal colon, lymphocytic infiltrate, and a poorly differentiated, mucinous or signet ring appearance. When diagnosed at an early stage they have a better prognosis than colorectal tumors without MSI and display different response to chemotherapeutics. These tumors are more frequently diagnosed in stage II and relatively uncommon among metastatic tumors (8).

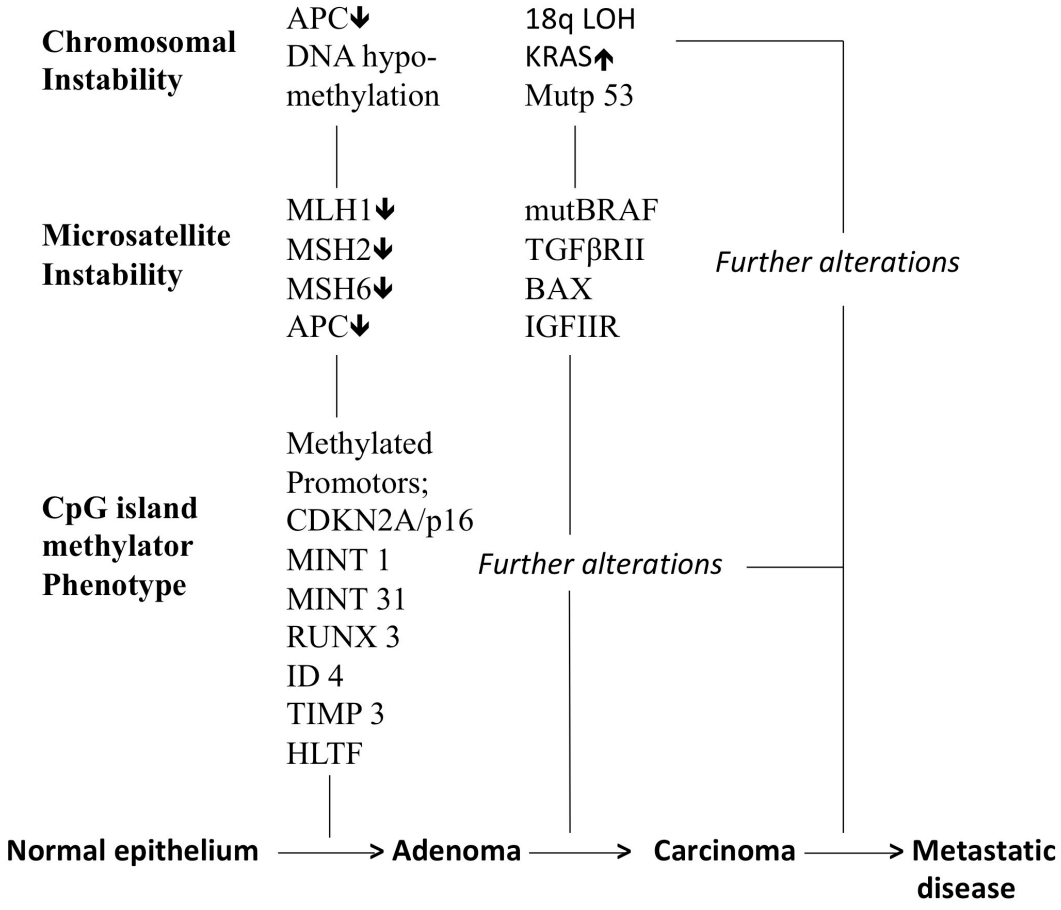

***Figure 2**: Important molecular, genetic and epigenetic changes with respect to CRC disease progression. Based on Tariq et al Cancer biology and medicine 2016 (9)*

1.2.3 CIN

With approximately 85% of colorectal tumors, chromosomal instability represents the most common form. These tumors are characterized by chromosomal rearrangements with gains, losses or rearrangement of large segments of chromosomes mainly caused by defects in mitotic checkpoints. Along with these karyotype abnormalities CIN tumors show a characteristic set of mutations in tumor suppressor genes (e.g. *APC, Mothers against decapentaplegic homolog 4 (SMAD4)* and Tumor protein P53 (*TP53*)) and oncogenes (e.g. *KRAS)* and Phosphatidylinositol 3-kinase (*PI3KCA*)), which leads to the activation of pathways that are critical for the initiation and progression of CRC (10). The CIN colorectal carcinogenesis model proposed by Fearon and Vogelstein in 1990 is still widely accepted for tumor progression(11). Inactivation of the *APC* gene resulting in hyper activation of the Wnt signaling pathway is considered a key-initiating event. Alternatively, epigenetic changes in β-catenin equally result in such activation. Both events lead to dysregulation of cell proliferation and differentiation and consequently the progression to adenomas. This is followed by oncogenic *KRAS* mutations and *TP53* loss or mutations ultimately leading to carcinoma development.

1.2.4 CIMP

The third pathway described for CRC development is the CpG island methylator phenotype. This is an epigenetic phenotype where tumor suppressor gene transcription is silenced by hypermethylation of CpG islands found in the promotor region of the gene. These tumors have distinct clinical, pathological and molecular features. Hence, they show high rates of *KRAS* or *BRAF* mutations, low frequency of TP53 mutations, proximal colon location, poor differentiation and a higher occurrence in females and older patients (12), (13). It is estimated that 20-30% of CRC tumors harbors the CIMP phenotype, however due to discrepancies between the cut-off values and markers included in different technique this number varies greatly (14). At present several panels exist to define the CIMP phenotype, these verify the transcriptional inactivation of different genes involved in carcinogenic development (15, 16).

1.2.5 Relevant mutations

It is worth highlighting some of the major oncogenes in CRC as they become more and more important, mainly as predictive markers but also for future non-invasive monitorization through liquid biopsies. In CRC mutations in *KRAS* are present in 42% of pa-

tients. Mutations in *BRAF*, the direct downstream target of Kras, are less frequent and found in 10% (7). The Kras protein is located on the inner surface of the membrane and it transmits signals upon epithelial growth factor receptor (EGFR) transmembrane receptor activation to the effectors in the mitogen-activated protein kinase (MAPK)- and Phosphoinositide 3-kinase (PI3K) / Protein kinase B (AKT)-signaling pathways in the cytoplasm, ultimately leading to cell survival and proliferation. Certain mutations in either of the *RAS/RAF* genes result in constitutive signaling through these pathways. Almost all *RAS* activating mutations occur in codons 12, 13 and 61, with G12D, G12V, G13D being the most frequent (17). The main activating mutation in *BRAF* is V600E substitution, a central amino acid in the kinase domain. V600 is required to maintain RAF in its inactive conformation without stimulation. Such receptor-independent pathway activation makes cancerous cells unresponsive to anti-EGFR therapies (18).
In contrast to the *KRAS/BRAF* mutations, mutations in tumor suppressor genes disrupts the normal function of the gene. Around 54% of CRC patients have dysfunctioning p53 (7). p53 plays a crucial role in cancer progression as it is an important regulator of cellular processes such as apoptosis, DNA damage, response to stress and aberrant proliferative signals. Basically, p53 is responsible for stopping the cell cycle in damaged cells during reparation, otherwise apoptosis is initiated. Mutations in the *TP53 gene do* not only abrogate the tumor suppressor function, but it also gains novel oncogenic function, which promotes a more aggressive, metastatic cancer phenotype (19).
Another important tumor suppressor is the APC protein. As many as 75% of sporadic CRC patients show mutations in this gene (7), and as mentioned it is also related with the FAP syndrome. Disruption of the *APC* gene is an early event in CRC development. APC interacts with and counteracts β-catenin, why loss of APC leads to constitutive activation of the canonical Wnt signaling and thus deregulation of cell proliferation, survival/apoptosis and differentiation (20).

1.2.6 From local to advanced disease

About 20% of the patients with CRC present with metastases at the time of diagnosis. Furthermore, 35–45% of the patients with localized disease have distant recurrence within 5 years of surgery. In CRC the most common sites for metastasis are the liver and lungs and these metastases are by far the most frequent cause of CRC-related death (21). To be able to metastasize a cancer cell needs to require the ability to invade the surrounding tissues, survive in circulation (bloodstream or the lymphatic system), colonize a foreign organ and eventually resume growth (figure 3) (22, 23). This complex process remains one of the least understood in cancer biology, however in the

last decade noticeable progress has been made, elucidating many aspects of metastasis formation.

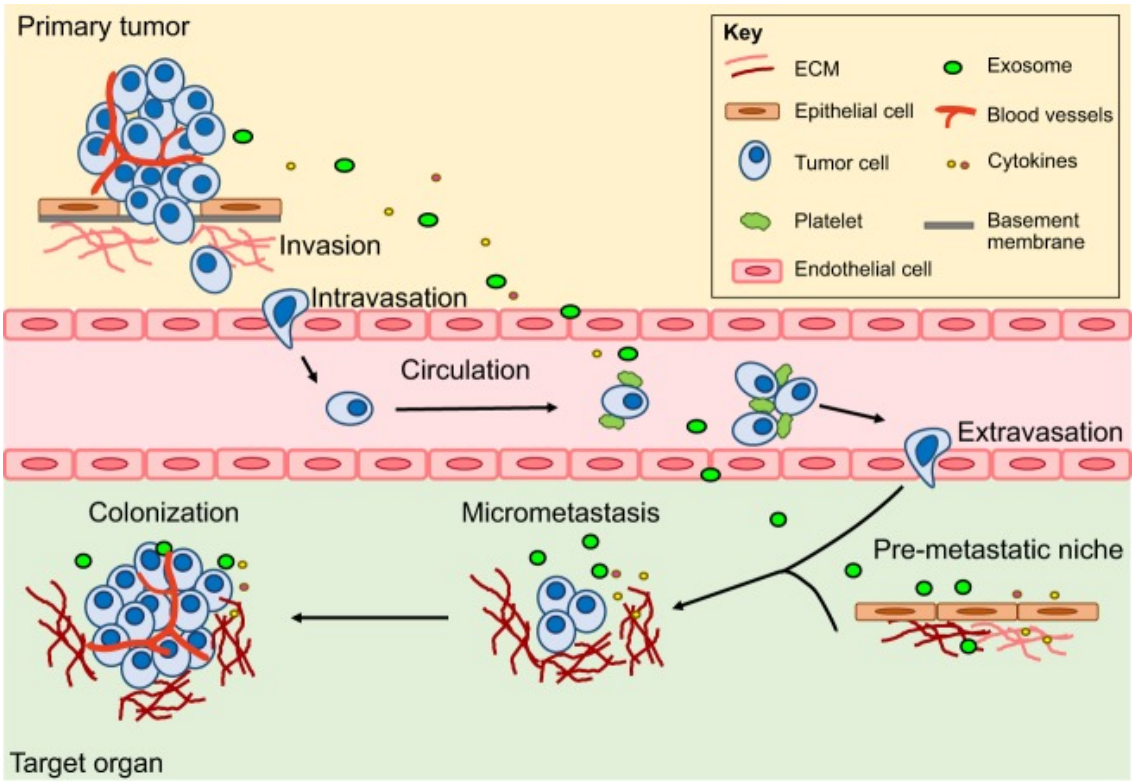

Figure 3: *Metastatic cascade. Gomez-Cuadrado et al. Diesease models and Mechanisms 2017 (24)*

An important initial step of tumor dissemination is widely agreed upon to be though epithelial to mesenchymal transition (EMT) (25). In this process epithelial cells increase their motility, invasiveness and ability to degrade components of the extracellular matrix. The program is orchestrated by a series of transcription factors, such as Snail, Slug, Twist and Zeb1 (23, 26). Additionally, several types of cancers, among them CRC, have been shown to acquire tumor-initiating capacity following EMT induction, an important trait for cancer stem cells (27). The subsequent intravasation and dissemination through either the bloodstream or lymphatic system can occur as single cells or tumor cell clusters. For collective migrating clusters of cells with mesenchymal traits can be observed at the invasive fronts of the primary tumor (28). Whether single cells or cell clusters are the main cause of metastasis still remains to be demonstrated, however recent evidence show that when clusters are introduced experimentally into venous circulation in mice they are far more efficient compared to single carcinoma cells in seeding metastatic colonies (29). Circulating cells (single or clusters) persist in circulation until getting physically trapped in micro vessels of distant tissues. The bloodstream represents a hostile environment for circulating tumor cells, as they are

exposed to for example natural killer cells or fragmentation due to physical stress. Platelet coating and neutrophil binding are some of the mechanisms that serve as protection (30, 31). Extravasation requires the carcinoma cells to traverse the endothelial wall. A number of different proteins, among them Vascular epithelial growth factor (VEGF), Matrix metalloproteinases (MMPs) and Disintegrin and metalloproteinase domain-containing protein 12 (ADAM12) have been reported to be secreted by the tumor cells to increase permeability of the vasculature. Some of these have been reported to be important both for intravasation and extravasation (32). Once in the new distant location the tumor cells need to adapt to a new microenvironment. Several dormancy programs and niches have been described allowing the newly metastasized cells to persist in a dormant state until having adapted to these new surroundings. Next it is believed that it is only cancer cells with stem cell traits are capable of being the founders of new metastatic colonies. E.g. in lung cancer it has been shown that this ability is dependent on a maintenance of a stem cell population though enhanced Wnt signaling (33). Thus, it seems that the metastatic potential of a carcinoma is closely linked to the ability of dispatching populations of circulating stem cells (CSC) that can re-initiate tumor growth following arrival at distant sites (34).

The whole process of metastasizing luckily has a very low efficiency, evidence indicate that as low as 0,01% of injected tumor cells are indeed able to carry out all steps needed to form an actual metastasis (35). Hence the high frequency of liver metastasis in CRC might simply be the result of the sheer number of CTCs filtering strait into the liver through the portal vein that drains the gut (36). Whether this dissemination is an early or late event in the CRC disease still remains unclear. The lack of larger hypothesis generating studies comparing paired primary and metastasis tumors is the main limiting factor. A recent study of 12 paired tumors with comprehensive whole genome sequencing found the mutational landscape to be very similar in the majority of the cases, which supports a late dissemination theory (37). Surely this is an aspect of CRC disease progression that with the modern techniques now available should soon be further clarified.

1.3 Diagnosis and staging

1.3.1 Histopathology

The pathologists play a very important role in CRC diagnosis. Apart from the molecular testing of MSI, *BRAF* and *KRAS* mutations among others, the histopathological information still remains the basis for tumor characterization, pathological staging and

search for prognostic and predictive parameters. The vast majority of colorectal cancers are adenocarcinomas and develop from cells of the epithelial mucosa layer. And as mentioned earlier the defining malignant feature is the invasion into the submucosa (13). Typical adenocarcinomas (>90%) of the colon are composed of columnar epithelial cells arranged in gland-like structures that mimic colon crypts. At diagnosis tumors are graded depending on the extent of these gland-like structures. Tumors with more than 50% gland formation are graded as low grade (well and moderate differentiation) while tumors with less than 50% gland formation are graded as high (poorly and undifferentiated) (38). The high grade/ poorly differentiated tumors are associated with poor survival (39) .

The World Health Organization (WHO) has apart from the most frequent adenocarcinoma classified a number of histological variants of colorectal carcinomas, such as mucinous, signet ring cell, medullary, micropapillary, serrated cribriform comedo-type, adenosquamous, spindle cell and undifferentiated. Recent effort has aimed at correlating such features with genomic alterations in these tumors, which could have clinical implications (40)

Pathologists are also starting to report findings of tumor budding. Tumor budding is defined as single or small clusters of tumor cells, which have detached from the main tumor (41). This is a marker of tumor dissemination and an indicator of an aggressive tumor (42). Evidence has correlated tumor budding with epithelial mesenchymal changes in the tumor microenvironment often found in then Consensus molecular subtype 4 (CMS4) subtype (described below) (43).

1.3.2 Tumor staging

At the time of diagnosis, CRC is divided into a number of clinical stages. This facilitates the clinical management and provides a prognostic accuracy. The current staging system is developed by the American Joint committee on Cancer and it is based on depth of Tumor invasion (T), presence of nodal metastasis (N) and distant metastasis (M), also known as the TNM classification (described in table 1)(44). The TNM system has now completely replaced the Dukes classification, which was the first effort to stage CRC. A definitive staging can first be done after surgery and a histopathological study. Based on the spreading of the tumor (and a number of other factors) the oncologist will choose what the appropriate treatment is. Tumors with no distant metastases are in general first resected, and adjuvant therapy is subsequently offered to a part of the patients. In the case of distant metastasis chemotherapy is often administered prior to possible a surgery (see section 1.5.4).

AJCC stage	TNM stage	TNM stage criteria for colorectal cancer
Stage 0	Tis N0 M0	Tis: Tumor confined to mucosa; cancer-in-situ
Stage I	T1 N0 M0	T1: Tumor invades submucosa
Stage I	T2 N0 M0	T2: Tumor invades muscularis propria
Stage II-A	T3 N0 M0	T3: Tumor invades subserosa or beyond (without other organs involved)
Stage II-B	T4 N0 M0	T4: Tumor invades adjacent organs or perforates the visceral peritoneum
Stage III-A	T1-2 N1 M0	N1: Metastasis to 1 to 3 regional lymph nodes. T1 or T2.
Stage III-B	T3-4 N1 M0	N1: Metastasis to 1 to 3 regional lymph nodes. T3 or T4.
Stage III-C	any T, N2 M0	N2: Metastasis to 4 or more regional lymph nodes. Any T.
Stage IV	any T, any N, M1	M1: Distant metastases present. Any T, any N.

Table 1. *American Joint Commitee on Cancer (AJCC) staging for CRC. Tumor (T), Nodes (N), Metastasis (M).*

1.4 Classification approaches

The aim of the molecular classifications is to provide an insight toward the etiology and characteristics of the tumor, which, eventually should lead to better clinical stratification and targeted personalized interventions. The first attempt for such classification was from the group of Sjoblom in 2006 (45) with the Candidate cancer gene (CAN) concept. Since then numerous classifications have been published, however they show great differences between them, for example varying in the number of subtypes identified. The differences can partly be attributed to methodological differences and statistical and algorithm bias (46). Worth highlighting is The Cancer Genome Atlas (TCGA) project which was based on genomic and transcriptomic characterization. This approach identified 2 major groups: hypermutated cancer with MSI (16%) and non-hypermutated cancers with MSS and a high number of somatic DNA copy number alterations and mutations in *APC, TP53, KRAS, SMAD4,* and *PIK3CA* (84%) (7). In order to unify all the data available on subtypes the international CRC Subtyping Consortium was created in 2014. Based on this comprehensive multi-omic characterization, finally 4 Consensus Molecular Subtypes (CMS) were proposed in 2015, see figure 4 (47). This clarified previous confusions and importantly unified the taxonomies.

The CMS1 is the so-called immune subtype (14% of early-stage tumors) and it comprises most of the MSI tumors. It is characterized by hypermutation, hypermethylation, *BRAF* mutations and infiltration of immune cells. The remaining MSS tumors are divided into 3 subtypes. CMS2 is the canonical subtype (37% of early-stage tumors), characterized by epithelial features, CIN and activated WNT and MYC signaling pathways. The CMS3 is the metabolic subtype (13% of early-stage tumors), in which deregulation of metabolic pathways can be observed. *KRAS* mutations are frequent and they furthermore show low levels of CIN and CIMP. The CMS4 is the mesenchymal subtype (23% of early-stage tumors), which is characterized by upregulation of EMT, transcription growth factor (TGF)-beta activation, angiogenesis and stromal infiltration. Nevertheless, still 13% of tumors remained unassigned due to mixed phenotypes of several CMS or intra-tumoral heterogeneity (47). As can be appreciated in figure 4, the four subtypes have different relapse-free and overall survival, with the best prognosis found in the CMS1 and the worst in CMS4.

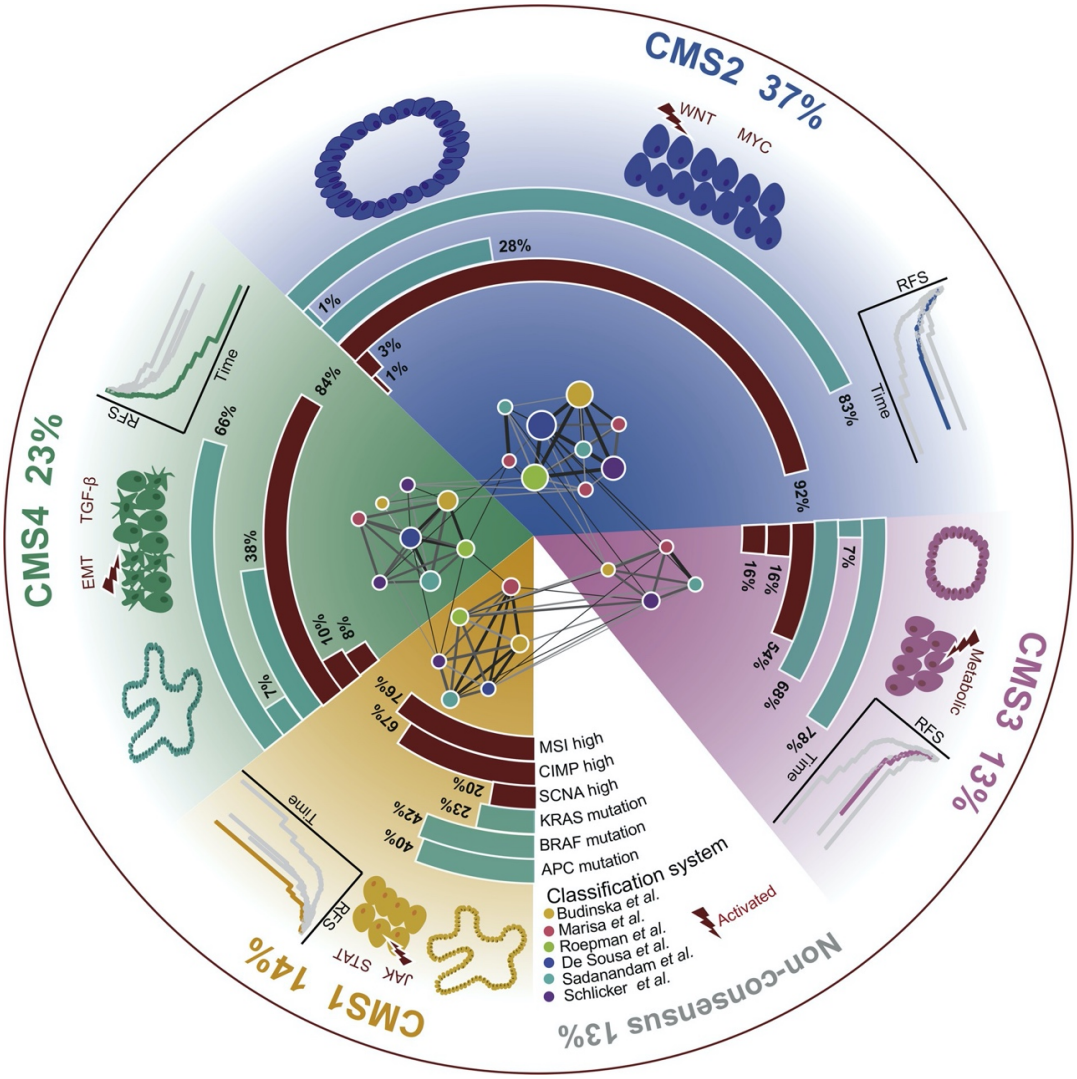

***Figure 4**: The CRC consensus molecular subtyping (CMS) system. Wang et al. Seminar Cancer Biology 2018 (46)*

The CMS has since 2015 been considered the most robust classification system and it is currently widely used both for clinical stratification but also in research purposes. Hence, a recent publication classified preclinical models into the CMS, thereby facilitating the translation from these models, especially in regards to specific drug sensitivity studies (48). The identification of molecularly distinct subtypes should provide subsets of patients on which to test new treatments as well as clues for specific biological pathways to target for these subgroups. It also opens up for a possible need to reevaluate possible treatments as they might have been discarded due to overall low response rates, thus hiding possible beneficial effects in a single subtype (49)

1.5 Colorectal cancer treatment

Overall survival rates of CRC patients have been improving over the last decades. This is thanks to major advances in the diagnostic process and better understanding of molecular mechanisms in CRC pathogenesis having led to new treatment options. Ensuring a successful management of CRC requires accurate staging and a multidisciplinary treatment plan. Currently the treatment is tailored to the burden of the disease, the patient's performance status, goals of care, and expected survival.

1.5.1 Surgery

The main curative treatment for non-metastatic cancer is surgery aiming at removing the tumor along with the nearby draining lymph nodes, ensuring clean surgical margins. More and more surgeries are now done laparoscopically making them less invasive. Patients with tumors in the sigmoid colon or rectum might require postoperative placement of a colostomy.

For stage IV metastatic CRC whether the primary tumor initially is removed depends on the symptoms that it causes. Perforated tumors, tumors causing complete bowel obstruction or tumors with severe bleeding warrant resection. In the case of asymptomatic primary tumors, the removal depends primarily on whether the metastatic disease is resectable or not. If this is the case, which is more likely for liver metastasis, the resection can either be in stages or simultaneous. Studies have shown similar overall survival (OS) for both approaches (50, 51). In the case of synchronous unresectable metastatic disease, several meta-analysis showed improved OS in patients who underwent resection of the primary tumor, however selection bias appears to affect most studies as patients with better performance status and lower disease burden where more likely to be chosen for surgical resection (52). It has indeed been a highly debated issue in

the last decade. Very recent findings from a randomized trial, assigning patients to either chemotherapy treatment or primary tumor resection followed by chemotherapy, provide strong evidence that the resection of asymptomatic primary tumors does not improve the overall survival. As a matter of fact the phase III trial was stopped due to surgery-related complications and higher morbidity in the postoperative period (53). Additional studies are needed to better identify patients who could benefit from either curative or palliative resection.

At the time of diagnosis of CRC with liver metastases only 10-20% of patients are candidates for metastasis resection. In some cases a good response to systemic chemotherapy will allow for subsequent resection. The criteria for potentially curative resection includes; no tumor present at margins, at least 20-40% (depending on injury) liver remnant left and functional vascular inflow and vascular/biliary outflow. The technical strategy for resection is determined by metastatic volume and location. Metastasis to the lung are rarely the only site of disease spreading, thus the consideration of pulmonary metastectomy usually depends on outcomes of therapy for other sites (54). The most common procedure is a “wedge resection with parenchymal sparing. Patients with peritoneal metastases usually have the worst prognosis (55), however cytoreductive surgery removing all visible tumor along with hyperthermic intra-peritoneal chemotherapy has become standard care in peritoneal surface malignancies (56).

1.5.2 Radiation therapy

Radiation therapy is not commonly used for colon cancers as the bowel is too sensitive. However, in combination with chemotherapy, it is recommended in neoadjuvant treatment of intermediate - and advanced stage rectal cancer. Some patients achieve complete clinical responses, and surgery can be postponed (57).

1.5.3 Systemic treatment for primary disease

For stage II CRC the rate of patients cured by surgery is high. However, guidelines recommend adjuvant treatment in high-risk cases such as poorly differentiated tumors, in tumors with vascular, lymphatic or peritoneal invasion, and in cases which obstructive and perforated tumors and pT4 (58). The aim of such treatment is to eradicate any possible micrometastasis already present at the time of surgery. Few prospective studies exist, however a small but statistically significant benefit of adjuvant chemotherapy, has been reported in patients with low likelihood of recurrence (59). However, in multiple post hoc analyses of patients with stage II CRC, the use of adjuvant chemotherapy

in the stage II setting has been questioned (60). Surely better patient stratification will help select the patients where assuming the secondary effects of adjuvant therapy is compensated by the decrease in reoccurrence risk.
In stage III tumors, 6 months of adjuvant therapy is the standard treatment. The protocols for adjuvant therapy with FOLFOX (leucovorin/5-fluorouracil/oxaliplatin) or CAPOX (capecitabine plus oxaliplatin) are the current standard of care (61). With these regimens the 5-year disease free survival (DFS) is around 70% (62). Recent studies have shown that the 6 months of adjuvant therapy could be cut down to 3 months without affecting the DFS, especially in low risk patients. Importantly, this shortening of treatment significantly reduced adverse effects of the treatment (63).

1.5.4 Systemic treatment for metastatic disease

The survival of patients with metastatic disease has substantially improved over the past three decades, with median overall survival now exceeding 30 months. This can be attributed to chemotherapeutics, such as oxaliplatin and irinotecan, targeted therapies along with improved surgical resection of mainly liver metastases. The backbones for first line treatment are the FOLFOX or FOLFIRI (leucovorin/5-fluorouracil plus oxaliplatin or irinotecan, respectively) regimens, which contain two cytotoxic agents. The addition of monoclonal antibodies such as bevacizumab (anti-VEGF) and cetuximab/panitumumab (anti-EGFR) to the first line chemotherapy backbones has been shown to improve the clinical outcome. Upon failure of the first line treatment a second line is usually offered switching the backbone and possibly changing the targeted therapy. If progression is found on the second line of treatment a third line can be applied seeking new combinations of treatment, always taking performance status and overall quality of life in to consideration (see figure 5) (64). Interestingly, the concept of rechallenging a tumor with for examples anti-EGFR treatment after withdrawal from the treatment has recently showed promising results. The idea is that a clonal expansion of *KRAS*-wild type (WT) cells during the withdrawal can be targeted again (65).

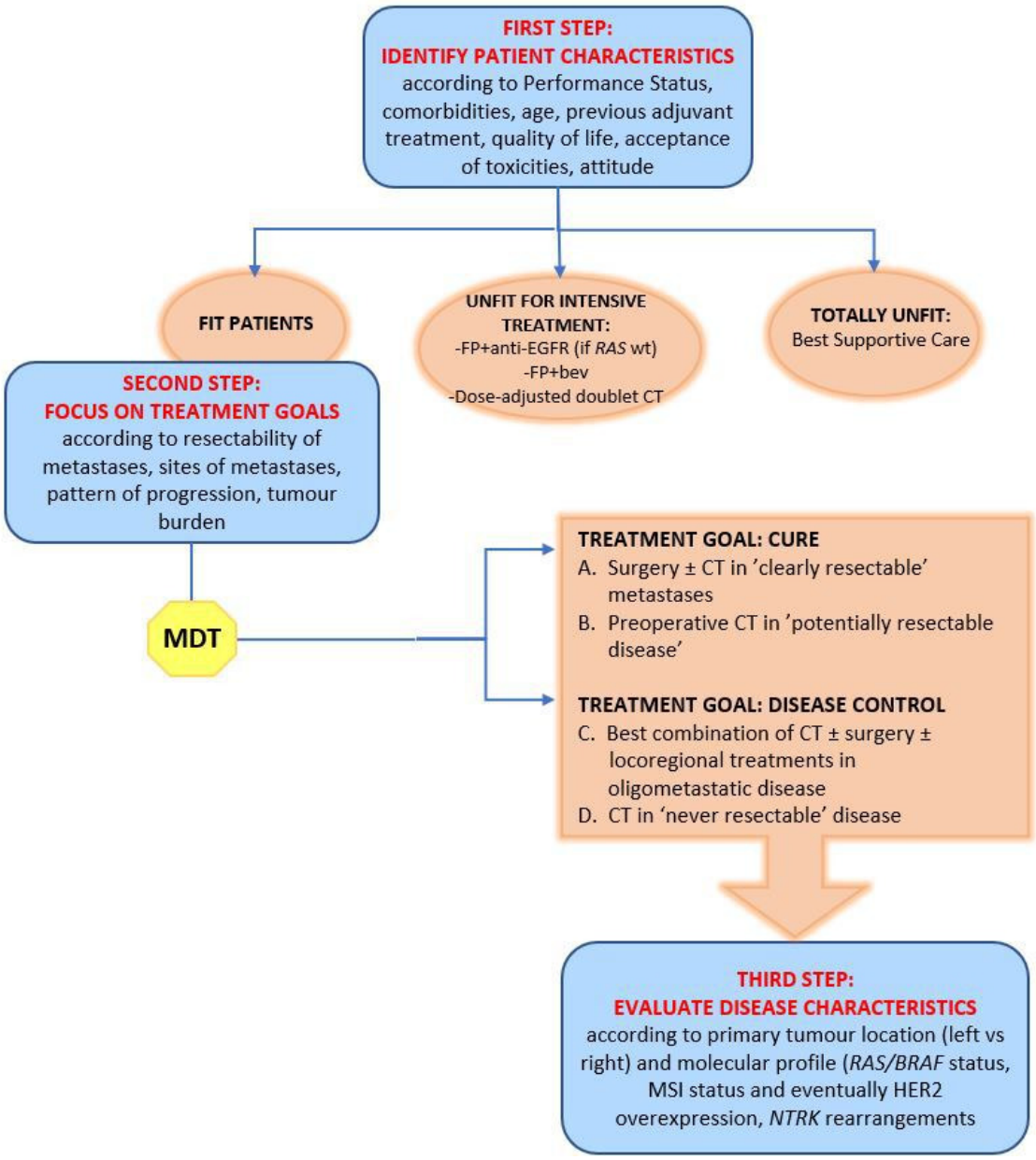

Figure 5: *Algorithm for treatment of metastatic colorectal cancer. Bevacizumab (bev), fluoropyrimidine (FP), multidisciplinary team (MDT), neurotrophic tyrosine receptor kinase (NTRK). De Falco et al. ESMO open 2020. (66)*

1.5.5 Chemotherapies

Chemotherapy is a systemic treatment with the goal of damaging and stressing the cancer cells for them to initiate cell death pathways. The effects are however not specific, and other rapidly dividing normal cells are also damaged resulting in many side effects, such as immunosuppression, gastrointestinal distress, nausea and neuropathy to mention just a few. In metastatic CRC (mRCR) treatment the three main chemotherapeutic agents are fluorouracil, irinotecan and oxaliplatin.

1.5.6 Fluoropyrimidines

Fluorouracil (5-FU) has since the late 1950s been the base for both adjuvant - and metastatic chemotherapy treatment of CRC. 5-FU is a thymidylate synthase inhibitor. This enzyme methylates deoxyuridine monophosphate to form thymidine monophosphate. Inhibition of this process leads to a shortage of the nucleotide pyrimidine thymidylate necessary for RNA and DNA synthesis, ultimately leading to apoptosis in rapidly dividing cancer cells (67). Usually Leucovorin folinic acid is administered with 5-FU in CRC to enhance the effects. Capecitabine is a pro-drug developed to mimic the continuous infusion of 5-FU. Instead of intravenous administration it is given as pills and once absorbed it is converted into enzymatically active 5-FU. The two drugs have shown equal results when combined with other cytotoxic agents (68).

1.5.7 Irinotecan

Irinotecan was approved for CRC treatment in the late 1990s followed by oxaliplatin in the early 2000s after they both had shown to improve the outcome for CRC patients treated with 5-Fu/leucovorin (69, 70)). This lead to the implementation of the regimens FOLFOX and FOLFIRI, which are still the standard of care today. Irinotecan is a semisynthetic analog of camptothecin originally extracted from a Chinese ornamental tree. Irinotecan is hydrolyzed mainly in the liver into its active metabolite SN38, which is a Topoisomerase I inhibitor. Topoisomerases are enzymes that participate in the over - and underwinding of the DNA strand ahead of the replication fork during replication and transcription. SN38 stacks against the base pairs just next to a topoisomerase cleavage site, rendering the enzyme inactive causing irreversible inhibition of DNA synthesis with double-strand DNA breaks and ultimately cell death (71).

1.5.8 Oxaliplatin

Oxaliplatin is a platinum based antineoplastic drug, containing a square planar platinum in the center, a bidentate oxalate group and a diaminocyclohexane (DACH) ring. The presence of the DACH ring makes it larger than the other widely used platinum drugs Cisplatin and Carboplatin, explaining the different spectrums of activity. Upon intravenous administration, oxaliplatin is rapidly biotransformed into its active derivate losing the oxalate group and incorporating chlorine molecules. oxaliplatin forms crosslinks in DNA through a multi-step process involving cellular uptake and hydratization, monofunctional adduct formation between adjacent guanines or guanine and adenine resi-

dues and closure to bifunctional adducts. These adducts prevent replication and transcription. Unless nucleotide excision repair (NER), which is the main repair mechanism activated by oxaliplatin, resolves these crosslinks they ultimately end up causing cell death (72, 73).

1.5.9 Biological targeted agents

Biologic agents targeting specific oncogenic pathways have improved survival in mCRC patients. They include the humanized monoclonal antibodies against EGFR (cetuximab and panitumumab) and VEGF (bevacizumab) (see figure 6). More biological agents exist targeting these pathways, however cetuximab, panitumumab and bevacizumab to date remain the only ones approved for first line mCRC treatment.

VEGF-A binds to tyrosine receptors VEGFRs on the cell surface causing dimerization and activation through transphosphorylation. Such binding stimulates signaling cascades promoting endothelial cell proliferation, vascular permeability and angiogenesis. The necessity of a vascular network in growing tumors has for long been well established, as tumors generally have high metabolic rates and thus high need for nutrients and oxygen (74). Bevacizumab binds to circulating VEGF thus inhibiting the binding and activation of the VEGFRs. This inhibition reduces the microvascular growth and thereby limits the blood supply to tumor tissues. Clinical trials have demonstrated that adding the bevacizumab to both FOLFIRI and FOLFOX regimens improves Progression Free Survival (PFS) (75, 76).

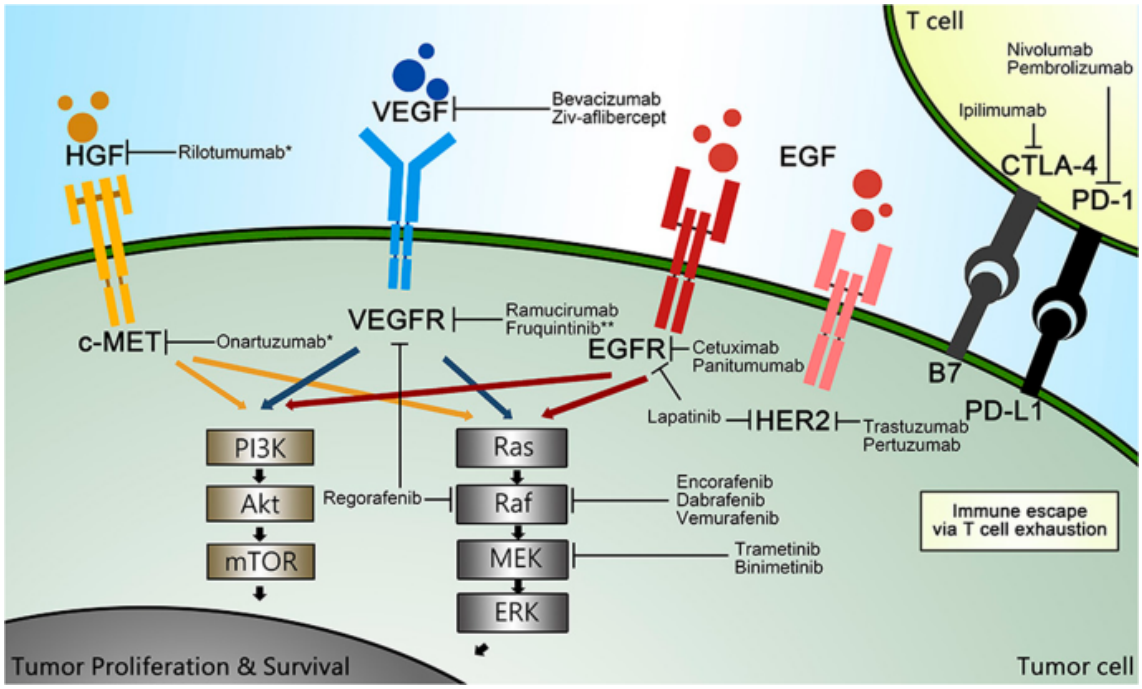

***Figure 6**: Overview of recommended targeted agents in CRC. Xie et al Signal Trasnduct Target Ther. 2020 [73].*

EGFR receptor is expressed in normal epithelial tissues and in several types of human cancers. Upon binding by EGF to its receptor multiple intracellular downstream signaling pathways are activated, including the RAS/RAF/MAPK/PI3K/AKT/mTOR pathways, ultimately promoting cell proliferation (77). Anti-EGFR monoclonal antibodies cetuximab and panitumumab bind to the extracellular domains of the receptors blocking any possible growth stimuli. In mCRC these two antibodies are approved for the use in *KRAS* WT tumors. *KRAS* mutations in codon 12 and 13 render the GTPase constitutively active, thus bypassing the anti-EGFR effect. The National comprehensive cancer network now recommends genotyping not only for *KRAS* but also neuroblastoma RAS viral oncogene homolog (*NRAS)* and *BRAF* before administering cetuximab or panitumumab.

Molecular profiling and understanding of mutations and their possible implications for treatments is increasing. Such detailed knowledge of each tumor opens up for new treatment possibilities, currently especially in third line treatments and beyond. Indeed, several new promising targets of interest have been described, among them human epidermal growth factor receptor 2 (*HER2)* amplifications, non-V600E *BRAF* mutations and dMMR/MSI status. HER2-directed therapy with either trastuzumab or pertuzumab have shown promising results in a small group of patients with HER2 amplifications (78). New evidence has shown that a triple regimen of Braf, mitogen-activated protein kinase kinase (MEK) and EGFR inhibitor (encorafenib, binimetinib, and cetuximab) in *BRAF* mutated patients offered significantly better survival benefit (79). Other targeted therapies like regorafenib (a multitargeted kinase-inhibitor) and ramucirumab (angiogenesis inhibitor) have also shown good results in chemorefractory mCRC (80-82).

With an expanding number of targeted drugs available, knowing the molecular profile of the tumor cells after several lines of treatment becomes more and more important. Treatment pressure obviously favors clonal selection, why both primary tumors and metastases might show different mutational landscape compared to initial biopsies. Detection of oncogenic mutations in circulating tumor DNA (ctDNA) shows great promises, allowing for continuous non-invasive monitorization. This could help guide the choice of sequence therapy in order to get maximal exploration of these new targeted therapies.

1.5.10 Immune checkpoint blockage

In addition to agents directly blocking pathways involved in tumor growth and spreading, accumulating evidence show that targeting pathways involved immunorecognition is also effective. While results similar to what have been seen in melanoma and lung

cancer is not expected for CRC, as it is known to be a notorious cold cancer, a subgroup of patients do indeed respond very well to such therapies (83).

Under normal conditions malignant cells harboring genetic alterations will present abnormal antigens on the surface through the major histocompatibility complex (MHC)-I leading to recognition and obliviating by the immune system. Cancer cells adapt a number of processes to avoid detection: secretion of immunosuppressive factors, downregulation of MHC-I and recruitment of immunosuppressive cells. Importantly they also express programmed death-ligands 1 (PD-L1) and 2 (PD-L2) on the cell surface, which are ligands of T-cell immune checkpoint receptors programmed cell death protein 1 (PD-1) and cluster of differentiation (CD279). Such binding results in inactivation and exhaustion of T-cells. Yet another central checkpoint exists between antigen presenting cells (APCs) and T-cells, namely cytotoxic T-lymphocyte-associated protein 4 (CTLA-4) and CD80/CD86. Immune checkpoint targeted therapy aims at blocking the tumors attempt to escape from T cell detection, and thus stimulate immune surveillance and clearance (84, 85). As mentioned, only a subgroup of mCRC patients responds to ICB therapy, the ones with a high mutational burden (dMMR) and high levels of microsatellite instability (MSI-H). It is believed to be due to higher levels of neoantigens derived from mutations, which attract attention from immune cells and thus increase T-cell infiltration (86). The PD-1 blocker Pembrolizumab has indeed shown great results as monotherapy in this subgroup with progression free survival (PFS) of 16.5 months compared to the 8.2 months for the chemotherapy group. Noticeably the duration of the response at 24 months was 83% compared to 35% for the control group (87). Equally encouraging results has been observed with another PD-1 inhibitor Nivolumab and the CTLA-4 inhibitor Ipilimumab (88).

1.5.11 Treatment resistance

Even though the medical treatment of CRC has made advances in the later decades with strategies including chemotherapy and the targeted therapies as described above, the 5-year overall survival for mCRC is still only around 12 percent (89). This is mainly due to treatment resistance. The first hurdle for the systemic treatment is to successfully reach the tumor cells. This is affected by factors such as absorption, distribution, metabolism and excretion (90). Once in the tumor, cells can be intrinsically resistant or acquire resistance during a treatment. The most commonly described mechanisms include altered transport of the drug across the plasma membrane, genetic responses, enhanced DNA repair, alteration in target molecules, metabolic effects and growth factors.

One of the most universal forms of resistance against antineoplastic agents is by the action of a group of membrane transporters, the ATP-binding cassette (ABC) proteins. By extruding cytotoxic molecules, the ABC-transporters keep the intracellular drug concentration below cell-killing threshold. This is one of the possible mechanisms leading to multidrug resistance, due to broad drug specificity (91). Defects in the apoptotic pathway represent another common mode of therapy resistance. The p53 protein is an important regulator of the cell cycle as a sensor of genotoxic stress, inducing G1 arrest and/or apoptosis preventing replication of defective cells. Drugs, which increase DNA damage, therefore cause p53-mediated cell death. Loss of p53 function, which is common in CRC, allow cells with damaged DNA to replicate, thus leading to resistance to DNA damaging drugs (92). Resistance is of course also related with the specific mechanism of action of the drug. Example of such specific mechanisms is gene amplification in thymidylate synthase in 5-FU treated patients (93) and upregulation of genes involved in NER repairs, eg the excision repair cross-complementing group 1 (ERCC1) in oxaliplatin treated patients (94).

Resistance to treatment is unfortunately just as common for targeted therapies. A mechanism of resistance to anti-EGFR therapy in *RAS* and *BRAF*-WT tumors is the emergence of *RAS* and *BRAF* mutations during cetuximab or panitumumab therapy. Indeed, it has been demonstrated that a majority of patients with WT tumors test positive for one or more MAPK pathways mutations in their coding DNA (cDNA) or on repeat tumor biopsy at the time of anti-EGFR resistance (95). Another resistance mechanism is the upregulation of alternative signaling pathways. In this context, recent preclinical studies have demonstrated the reversal of acquired anti-EGFR resistance when MEK inhibitors are added to the anti-EGFR treatment (96).

Further improvement in outcomes for mCRC highly depends on identifying and targeting mechanisms of drug resistance. Importantly this can also help improve initial patient selection and thus possibly avoid treatment with non-effective toxic drugs. Identification of biomarkers of resistance should indeed receive greater attention in order to better guide oncologists in their decision-making.

1.6 Prognostic and predictive biomarkers

A lot of advances have been made in the molecular and biological characterization of CRC. The genetic profile is indeed becoming more and more important in CRC disease management. To make the most of this knowledge it is crucial to have sensitive and specific biomarkers. They play key roles both in prevention and early diagnosis and also later in the choice of targeted therapies and in the prediction of drug response.

There are 4 main types of biomarkers: diagnostic markers, prognostic markers, predictive markers and surveillance markers. Diagnostic markers are used for disease detection and risk assessment, while prognostic markers indicate the likelihood of disease progression. Predictive markers are used to predict the patient's response to a given therapy, and lastly, surveillance markers are used to monitor possible disease recurrences.

The diagnostic biomarkers used in the clinic today are mainly found in stools. The fecal occult blood testing (FOBT) and Fecal immunochemical test (FIT) are commonly used, and part of many screening programs as mentioned earlier, however they show high false positivity rates (97). DNA-based methods represent another strategy for CRC detection, as they show diagnostic advantage over FOBT, however these systems are not suitable for screening programs due to their high expense. Blood-based tests are ideal for screening purposes, indeed several biomarkers, including Carcinoembriogenic antigen (CEA) and Carbohydrate antigen (CA) 19-9 are well established in clinical practice. Unfortunately they both show low specificity and sensitivity (98). An alternative strategy is multivariate classification models, which based on measurements of numerous biomarkers calculate probability of having the disease. A panel of 15 biomarkers did indeed discriminate better between healthy subjects and CRC patients compared to single markers (99).

As previously mentioned, surgical removal of the tumor is the treatment of choice for early-stage cancers (I-III). In stage II it is currently clinicopathological features, and not biomarkers that decides whether adjuvant therapy is given. Adjuvant chemotherapy is given to all stage III patients while stage IV patients receive a multimodality treatment, including surgery and systemic treatments with chemotherapy and biologicals. The prognostic/predictive tissue biomarkers currently used in CRC management are MSI high, *KRAS/NRAS* and *BRAF* mutations.

Stage II MSI patients have better prognosis and do not require chemotherapy, hence no benefit has been observed from 5-FU based chemotherapy treatment in this subgroup (100),(101). In stage III tumors the MSI/MSS status is currently not useful as no differences in risk have been observed (102). Interestingly, trials are testing MSI-high as a predictive marker for immunotherapy in stage III. This has already been implemented for stage IV CRC, where Pembrolizumab is approved for first line treatment and Nivolumumab and Ipilimumab for refractory disease (103). In these patients there is a high demand for more predictive biomarkers, as PD-L1 has not shown to predict better survival outcomes in patients treated with immunotherapy (104).

In non-metastatic CRC *KRAS* mutations (codon 12 and 13) is a marker of poor prognosis. Patients with *KRAS* mutated tumors have a 1.5 higher risk of relapse and death

compared to *KRAS*-WT (105). This was believed to be the case also for metastatic patients, however a meta-analysis has showed that in the metastatic setting it is mainly the *KRAS* G12C and G13D variants that associate with poor OS rather than the G12V and G12D ones (106). As for the predictive value of KRAS mutations it has for long been known that only *KRAS* WT patients benefit from addition of an anti-EGFR to a chemotherapy regimen (107).

Like *KRAS* mutations, *BRAF* mutations, typically V600E, is also a marker for poor prognosis in stage III and IV CRC. Until recently testing *BRAF* mutational status has purely been a prognostic marker, however the recent BEACON study showed that *BRAF* mutated mCRC patients could benefit from a doublet or triplet with Braf, EGFR and MEK inhibitors (79). Data concerning the possible benefit of treating BRAF mutated patients with anti-EGFR treatment remains conflicting, as meta-analyses exist concluding both lack of response (108) and equal response (109).

Numerous additional biomarkers show promising result, and hopefully in the coming years they can become translated into the clinical setting. It has been well demonstrated that ctDNA from liquid biopsies can help assess surgical tumor clearance, choice appropriate targeted treatment and monitor treatment response (110). Now the main challenge remaining for ctDNA is standardization of methods and technologies before it can widely become implemented in the clinic. A rather new concept in mCRC is the sidedness of the tumor. Several studies show that right-sided colon cancers show worse prognosis than the left-sided ones do (111), why more intensive chemotherapy triplets could be used for this group. Additionally, current guidelines recommend limiting anti-EGFR to left sided *KRAS* WT tumors, as right-sided *KRAS* WT tumors did not benefit from the treatment (112). Another upcoming predictive marker is HER2. Recent studies showed clinical benefit from dual HER2 blockage in patients with HER2 amplification. Studies have also shown that HER2 amplifications negatively predict efficiency of anti-EGFR therapies and furthermore is associated with development of resistance to them (113).

Even though there are great advance in the discovery of biomarkers for CRC, more prospective studies are needed to validate novel candidates in large cohorts. In particularly in regards to immunotherapy, biomarkers predicting possible efficacy is needed. Another area with high need of biomarkers is early-stage CRC, in order to avoid overtreating patients who will not benefit from adjuvant therapy. Hopefully a combination of new biomarkers and advances in the technology of liquid biopsies will allow to personalized treatment in the near future.

1.7 Cdk5

Cyclin dependent kinases (Cdks) are serine/threonine kinases that are activated upon binding and complex formation with cyclins. Once activated Cdks can phosphorylate target proteins at serine and threonine residues directly next to a proline. These kinases are well known to regulate the progression through the cell cycle in all eukaryotic cells (114). Cdk5 is an atypical Cdk, as its enzymatic activity does not depend on cyclins, rather it binds with either cyclin-dependent kinase 5 activator p35 or p39 (*CDKR1* and *CDKR2*). Also, Cdk5 has not been shown to play any role in cell cycle regulation. Instead, most Cdk5 substrates are part of the cytoskeleton or neuronal signaling molecules (115, 116).

Cdk5 is ubiquitously expressed in all tissues, however the highest expression is found in the nervous system and the brain. It is also in this context that Cdk5 is best characterized. During embryogenesis, Cdk5 is indispensable for proper brain development. In the adult brain, Cdk5 is essential for numerous neuronal processes, including cognitive functions such as learning and memory formation, neuronal outgrowth and migration (117). Its activity is known to be deregulated in several neurological disorders, such as Alzheimer's disease, Parkinson's disease and Huntington's disease, leading to neurotoxicity (116). As for non-neuronal functions it has been shown to be involved in vastly different process as for example regulation of monocyte differentiation (118), development and regeneration of muscle cells by Nestin phosphorylating (119), and promotion of angiogenesis (120). Moreover, during the last decade, it has been described to promote progression in numerous solid tumors.

1.7.1 Cdk5 activity

It was indeed in the nervous system where Cdk5’s binding partners, p35 and p39 were first identified. Even though these activators share little sequence similarity to cyclins, computer modelling has shown that p35 actually adopts cyclin-like tertiary structure (121). Crystallization of the complex shows that p35/p39 bind to the T-loop of Cdk5. The number of hydrogen bonds is reduced between p39 and Cdk5 compared to p35, explaining why this complex is more labile and dissociates easier (122). As illustrated in Figure 7 unbound Cdk5 is found mainly in the cytosol, while both p35 and p39 contain a myristolation signal directing them for the cell membrane. Upon activation Cdk5 is also found in the cell periphery (123). The p35 protein levels tightly regulate the activity of the Cdk5-p35 complex, as its half-life is of only 20-30 min. It has been demonstrated that Cdk5 phosphorylates p35 targeting it for ubiquitin-dependent proteasomal

degradation. In this way an autoregulatory negative feedback loop exists for the Cdk5 kinase activity (124).

Interestingly, calpain-cleaved forms of both p35 and p39 exist, p25 and p29 respectively, which lack the myristolation modification, making them more soluble and allowing them to locate elsewhere within the cell (figure 7) (126). Translocation of the complex to the nucleus has been widely demonstrated in neurons upon different kinds of stress (127, 128). Furthermore, the Cdk5-p25 complex has been shown to have prolonged activation (5-10 times longer), as p25 loses the signal for ubiquitination. The Cdk5-p25 complex is suggested to play an important role in neurodegenerative diseases (129). In contrast to other Cdks, Cdk5 does not need phosphorylation for its activity, as the complex Cdk5-p35/p39 is constitutively active. However, Tyrosine 15 phosphorylation, by Cables or c-Abl, has been shown to increase the activity of the complex (130).

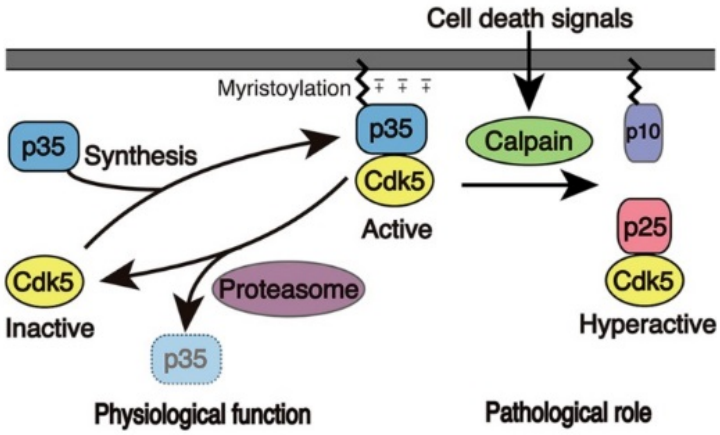

Figure 7. *Activation mechanism of Cdk5. Kimura et al. Front Mol Neurosci 2014 (125)*

Most of what is known about the transcriptional regulation of both *CDK5* and *CDKR1* is from the brain, where their transcription is partly regulated through the Mitogen-activated protein kinase 3/1 (ERK1/2) signaling. For *CDK5* this is mediated by transcription factors Fos and CREB (116). Transcriptional *CDK5* regulation outside of the nervous system still needs further clarification.

1.7.2 Cdk5 targets

Along with the characterization of Cdk5 function in more and more cell types and tissues, the list of direct or indirect targets is also growing. Indeed, the functions seem to differ depending on the setting. Figure 8 illustrates just a few. For example, in pancreatic beta-cells it has been shown that Cdk5 reduces insulin secretion in response to glucose abundance through phosphorylation of Ca2+ channels (131). In lymphatic vessels Cdk5 was shown to phosphorylate Foxc2, which in turn regulates the expression of *connexin 37*, a protein involved in GAP junctions between cells which is crucial for lymphatic valve formation (132). Within the immune system Dorand et al demonstrated that in medulloblastoma Cdk5 disruption resulted in decrease PD-L1 expression

through up-regulation of transcriptional repressors Interferon regulatory factor 2 (IRF2) and Interferon regulatory factor 2 binding protein (IRF2BP) (133). As previously mentioned Cdk5 is implicated in neuronal migration, where for example Caldesmon is one of the direct targets. It has been shown that Cdk5 indeed also plays an important role in cancer cell migration and cytoskeletal organization and thus metastasis formation. These last two aspects will be discussed in further detail below.

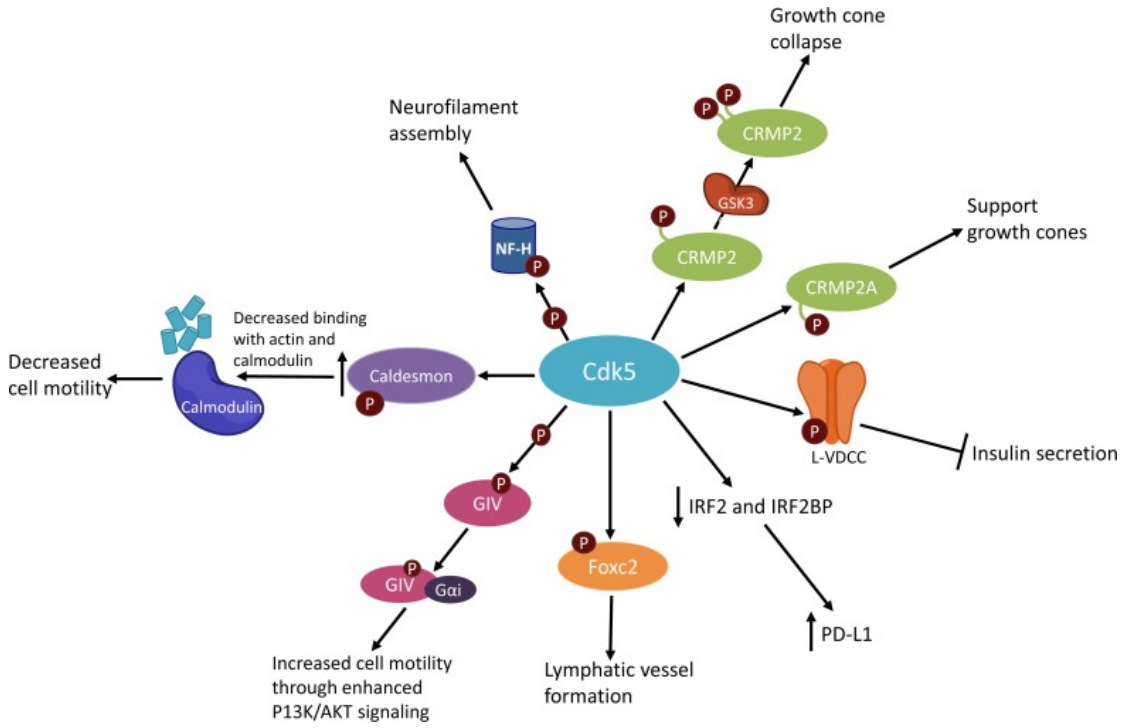

***Figure 8**. Simplified schematic representation of Cdk5 activities. Shupp et al. Oncotarget 2017 (134)*

1.7.3 Cdk5 inhibition

There is increasing evidence that the inhibition of Cdk5 could be an attractive therapeutic target in pathologies such as neurodegenerative diseases (135), diabetes (136) and many types of solid tumors. Unfortunately, no specific Cdk5 inhibitors are currently available. Therefore, most of the *in vivo* studies carried out to date use pan-Cdk inhibitors targeting the ATP binding site of the Cdks, which even though often described as specific, they actually inhibit several other kinases. Among the most studied inhibitors are Roscovitine and Dinaciclib, both included in on-going clinical trials for numerous pathologies (137). Both have shown promising results in preliminary *in vitro* studies both as monotherapy or combined with current treatments. Many different small molecule inhibitors have also been developed, like AT7519 and 20-223 (138, 139), however

as Cdk5 shares many structural similarities with other Cdks and particularly with Cdk2, designing mono-specific inhibitor is indeed proving to be a very challenging task (140). When developing an inhibitor, one also need to keep in mind that Cdk5 has some crucial functions in the nervous system, but neurological side effects can possibly be minimized taking advantage of the blood brain barrier.

It is worth mentioning that alternative strategies have been considered to interfere with Cdk5 activity, particularly in diabetes. A small peptide containing 125 amino acid residues of p35, called Cdk5 inhibitory peptide (CIP), specifically inhibits the hyper-activation of Cdk5 by p25, while having no effect on physiological activation of CDK5 by p35/p39 (141). An even smaller 24 amino acid derivative of p25 was found to display a greater inhibitory potential than CIP in neurons (142). These peptides could also be a valid strategy for Cdk5 inhibition however, it is only the hyper-activated Cdk5-p25 complex that is inhibited which limits the applicability.

1.8 Cdk5 in Oncology

In the last decade accumulating evidence supports the role of Cdk5 in mechanisms driving tumor formation and progression, and the kinase has indeed become an attractive target for developments of new cancer therapies. Both the expression and activity of Cdk5 has been shown to be upregulated in most cancers. Partly due to gene amplifications, which can be observed in as many as 20% of breast and prostate cancer patients (140). High Cdk5 levels overall confers poor prognosis in osteosarcoma (143), breast (144), lung (145), colorectal (146), liver (147) and skin cancer (148), to mention just a few. The only publication pointing to the contrary is in gastric cancer where Cdk5 was decreased compared to normal tissue and overexpression of Cdk5 inhibits gastric tumorigenesis (149).

At the mechanistic level, Cdk5 has been shown to be involved in processes as diverse as proliferation, migration, invasion, anchorage-independent growth, angiogenesis and immune escape, which will be described in more detail below. Table 2 summarizes the most important publications concerning Cdk5 in cancer including the proposed molecular mechanisms. The most common study design is inhibition of Cdk5, pharmacologic or genetic, followed by *in vitro* and *in vivo* studies to determine the consequences. Some publications reveal the Cdk5 phosphorylation targets and affected pathways. Taken together, high levels of Cdk5 leads to a similar more progressive phenotype in all the mentioned cancer models, however the underlying mechanisms seem to be very context-dependent.

Cancers	Study design	Effects of Cdk5 inhibition or loss	Molecular mechanism	Ref.
Breast cancer	Cdk5 gene knockdown *in vitro* Roscovitine-based inhibition *in vitro* and *in vivo* Cdk5 shRNA in mice model CRISPR/Cas9 *in vivo* knockdown	Inhibition of proliferation and growth Induction of apoptosis Blockage of metastasis Increased sensitivity to irradiation Increased sensitivity to etoposide and hydroxyurea Increased sensitivity to PARP inhibitors T-cell mediated immune response Decreased cellular invasion	Increased p21Cip1 degradation Impaired tumor establishment in vivo Impairing DNA damage repair Blockage of TGF - mediated EMT activation Reduced FAK phosphorylation Upregulated Foxo1-Bim pathway Downregulation of PD-L1 expression Decreased ADD1 phosphorylation PIPKγ90 phosphorylation and enhanced Fibronectin secretion	(144, 150-156)
Pancreatic cancer	Expression of the dominant-negative Cdk5 allele siRNA-mediated Cdk5 knockdown and inhibition by Roscovitine Xenograft mouse models	Inhibition of tumor formation, invasion, migration and growth Induction of synergistic effect when combined with inhibitors of MEK and PI3K	Suppression of RAS–Ral signaling pathway	(157, 158)
Medullary thyroid carcinoma	Introduction Cdk5-dead cell lines Cdk5 knockdown *in vitro* and in animal models	Cell cycle arrest and inhibition of cell proliferation Retardation of tumor formation in vivo	Downregulation of Rb protein Downregulation of cell cycle CDKs Reduction of phospho-STAT3	(159-161)
Hepatocellular carcinoma	Cdk5 knockdown and pharmacologic inhibition with Roscovitine in cell-based assays and xenograft mouse models	Reduced cell proliferation and induction of apoptosis Synergistic with doxorubicin and etoposide in vitro and in vivo Induction of antiangiogenic effects	Reduced phosphorylation of ATM Abolition of STAT3-mediated phosphorylation of an endonuclease Eme1 Downregulation of VEGFA Reduced TPX2 phosphorylation	(161-164)
Melanoma (cutaneous)	Cdk5 knockout mouse models Various endothelial and tumor cell-based assays Tumor xenograft models CRISPR/Cas9 *in vivo* knockdown	Excessive but malfunctioned vessel formation Marked inhibition of invasion, migration, and growth of tumor cells Blockage of metastasis to liver and lung T-cell mediated immune response	Decreased Dll4-induced NICD Dephosphorylation of Caldesmon to halt metastasis Decreased Vimentin phosphorylation Downregulation of PD-L1 expression Downregulation of p-CREB	(120, 148, 165-169)
Lung cancer	Functional inhibition using Roscovitine and siRNA *in vitro* and *in vivo* Endothelial-specific Cdk5 KO mice	Suppression in proliferation, motility and invasiveness of cancer cells Sensitization of tumor cells to anti-VEGF treatment Decreased vasculogenic mimicry formation	Impaired tumor cell cytoskeleton remodeling and microfilament formation Downregulated notch pathway-dependent endothelial functions Decreased FAK/AKT signaling	(170, 171)
Ovarian cancer	Multiple ovarian cancer cell lines and xenografts treated with Cdk5 siRNA	G1 cell cycle arrest and inhibition of proliferation Apoptosis induction and metastasis blockage Enhanced paclitaxel sensitivity	Attenuation of Akt activation of p53 and p27 and induction of p21 Blockage of Caldesmon-mediated invadopodia formation Increased intratumoral retention of drugs	(172, 173)
Leukemia	*In vitro* Cdk5 knockdown study	Increased apoptotic cancer cell death Diminished tumor growth	Increased nuclear pool of Noxa via impaired phosphorylation, and enhanced suppression of miR-23(a) activity Impaired glucose utilization	(174)
Colorectal cancer	*In vitro* pharmacologic and siRNA inhibition In vivo Cdk5 knockdown Xenograft mouse models	Decreased cancer cells proliferation, growth, survival, migration and metastasis Reduced tumor growth	Inhibition of PPAR- phosphorylation Abrogation of ERK5-AP-1 oncogenic axis	(139, 146, 175, 176)
Medulloblastoma	shRNA/CRISPR/Cas9 KD *in vitro* and *in vivo*	Reduced PD-L1 expression and CD4+ T-cell mediated tumor rejection	Persistent expression of IRF2 and IRF2BP2	(133)
Prostate cancer	Cdk5 *in vitro* knockdown or inhibition Mouse xenografts	Decreased proliferation Decreased AR activation Decreased cell mobility and loss of polarity Decreased metastasis formation	AR phosphorylation and AKT activation Reduced STAT3 phosphorylation	(177) (178)

***Table 2**. Preclinical studies on Cdk5 in cancer. Adapted and updated from Lenjisa et al. Future Med. Chem. 2017 (140)*

1.8.1 Cdk5 and proliferation

Sustaining proliferative signaling is an important part of cancer development and progression. Even though Cdk5, in contrast to other Cdks, has not historically been considered as a regulator of cell cycle and cell proliferation, some studies suggest its involvement in pathways affecting these (figure 9A). In neuroendocrine thyroid cancer Cdk5 has been shown to phosphorylate retinoblastoma (Rb) protein, which controls the transition from the G0/G1 to S-phase through E2F transcription factor release leading to transcription of genes required for cell cycle progression (179). Another important activator of cell cycle progression is signal transducer and activator of transcription 3 (STAT3). This well-known transcription factor is activated upon stimulation of various pathways and controls cell cycle genes. In medullary thyroid cancer, Cdk5 has been shown to phosphorylate Signal transducer and activator of transcription 3 (STAT3) at Ser727, which in turn up-regulates STAT3 target genes, such as c-*Fos* and *JunB*, and ultimately leads to cell cycle progression (160). In prostate cancer Cdk5 has been found to phosphorylate androgen receptor (AR) at Ser-308 and Ser-81 enabling the transcription of AR induced genes and hence also promoting cell proliferation (177, 178). A more direct participation of Cdk5 in cell cycle control has also been suggested recently, as Cyclin I-like (CCNI2), a homolog of Cyclin I, was shown to bind and activate Cdk5 affecting cell cycle progression (180).

Interestingly in neurons Cdk5 has been proposed to suppress cell cycle (181), in contrast to the above-mentioned correlations with Rb, STAT3 and AR. Similar findings have been reported in gastric cancer, where nuclear accumulation of Cdk5 actually inhibits cell proliferation. Thus, the involvement of Cdk5 in cell cycle control and proliferation still remains controversial, and as Pozo et al. has suggested, dysregulated Cdk5 might promote tumorigenesis in some malignancies while exerting the opposite effects in others (182).

1.8.2 DNA damaging and repair

At the molecular level Cdk5 has been linked to the initiation of DNA damage response (DDR) and DNA repair, as illustrated in figure 9B. Both mechanisms are initiated upon exposure to classical chemotherapy and radiotherapy. Cdk5 is activated in cells or tissues exposed to DNA-damaging therapies or genotoxic agents (150, 183) possibly due to up regulation of p35 via the Early growth response protein 1 (Egr1) promoter as is the case in neurons (184). Cdk5 has been shown to phosphorylate Ataxia-telangiectasia mutated (ATM), a crucial regulator of DNA damage repair, at Ser-794

switching on its kinase activity in several types of cancers (162, 185). Such phosphorylation causes activation of tumor suppressor genes, as p53, allowing the cells to complete repair before entering the next cell cycle. In line with these findings the blockage of Cdk5 prevents the ATM phosphorylation and subsequently the initiation of the DDR signaling cascade to repair the double strand breaks caused by irinotecan in hepatic cancer cell lines (162). Cdk5 can also transduce signals necessary for the expression of DNA-repair molecules, such as the DNA repair endonuclease Eme1. Cdk5 phosphorylates STAT3 on Ser-727, which in turn interacts with the promoter of the Eme1 gene in CRC cell lines (163).

Indeed, our group started studying Cdk5 because we observed that Cdk5 was upregulated in 4 cell lines that had been made resistant to oxaliplatin (186). Due to its function in DDR and DNA repair, other groups have also linked Cdk5 to resistance to several DNA damaging therapies. Treatment with Roscovitine both in non-small cell lung cancer (NSCLC) cell lines and hepatocellular carcinoma (HCC) xenograft mouse models increase sensitivity to radiotherapy and chemotherapy respectively (162, 187). Such results indicate that a combination of a DNA-damaging drug and Cdk5 inhibition could be a possible future treatment strategy.

1.8.3 Dissemination

In order to successfully metastasize, cancer cells need to undergo a series of steps, such as invasion, intravasation, migration and extravasation as previously explained. Cdk5 has been described to be involved in all of these processes. This is not surprising as some of them are very similar to the known roles described for Cdk5 in the nervous system, where it is involved in neuronal migration, cytoskeleton remodeling and axonal guidance to mention just a few (188). Numerous *in vivo* studies in mice have shown that inhibition or knockdown of Cdk5 drastically decreases metastasis formation in solid tumors such as prostate (189), pancreas (190), melanoma (166), lung (191), pituitary (192) and CRC (146).

Some of the proposed Cdk5 downstream modulators of cell motility are more specifically part of the actin and microtubule cytoskeleton and focal adhesion, both important components of invadopodia formation (see figure 9C). Cdk5 phosphorylates and activates Focal adhesion kinase (FAK) which is an important step for the initiation of cell migration (144, 171). Additionally, the actin regulatory protein Caldesmon (166), cytoskeletal protein Talin (193) and intermediate filament protein Vimentin (148) can all be directly phosphorylated in cancer cells by Cdk5.

In pancreatic cancer Cdk5 has also been found to phosphorylate FAK as well as p21-activated kinase-1 (PAK1), another important regulator of cytoskeletal remodeling (194), as part of cell morphology alterations in migrating cells. Interestingly the authors demonstrated that Cdk5 was hyperactivated downstream of mutant KRAS signaling, as they observed an increased *CDKR1* expression, p35 to p25 cleavage and phosphorylation of Cdk5 substrates FAK and PAK1. The effect of Cdk5 inhibition on migration and invasion were only found in the *KRAS* mutant setting (158). The importance of Cdk5 activity in signaling downstream of Kras in pancreatic cancer was reinforced by another paper, as Feldmann et al. showed that Cdk5 was essential for RAS signaling through the critical effectors RalA and RalB (157). Pancreatic cancer is the cancer with the highest frequency of *KRAS* mutations (>90%). Other solid cancers with high rates of *KRAS* mutation include lung and CRC. Studies with Dinaciclib (CDK1/2/5/9 inhibitor) in NSCLC show that acquisition of *KRAS* mutations enhances sensitivity towards the treatment (195). However, further studies are needed in order to clarify whether a similar relationship between Cdk5 and KRAS signaling exists in other kinds of tumors. Although not considering the mutational of *KRAS*, another publication places Cdk5 down-

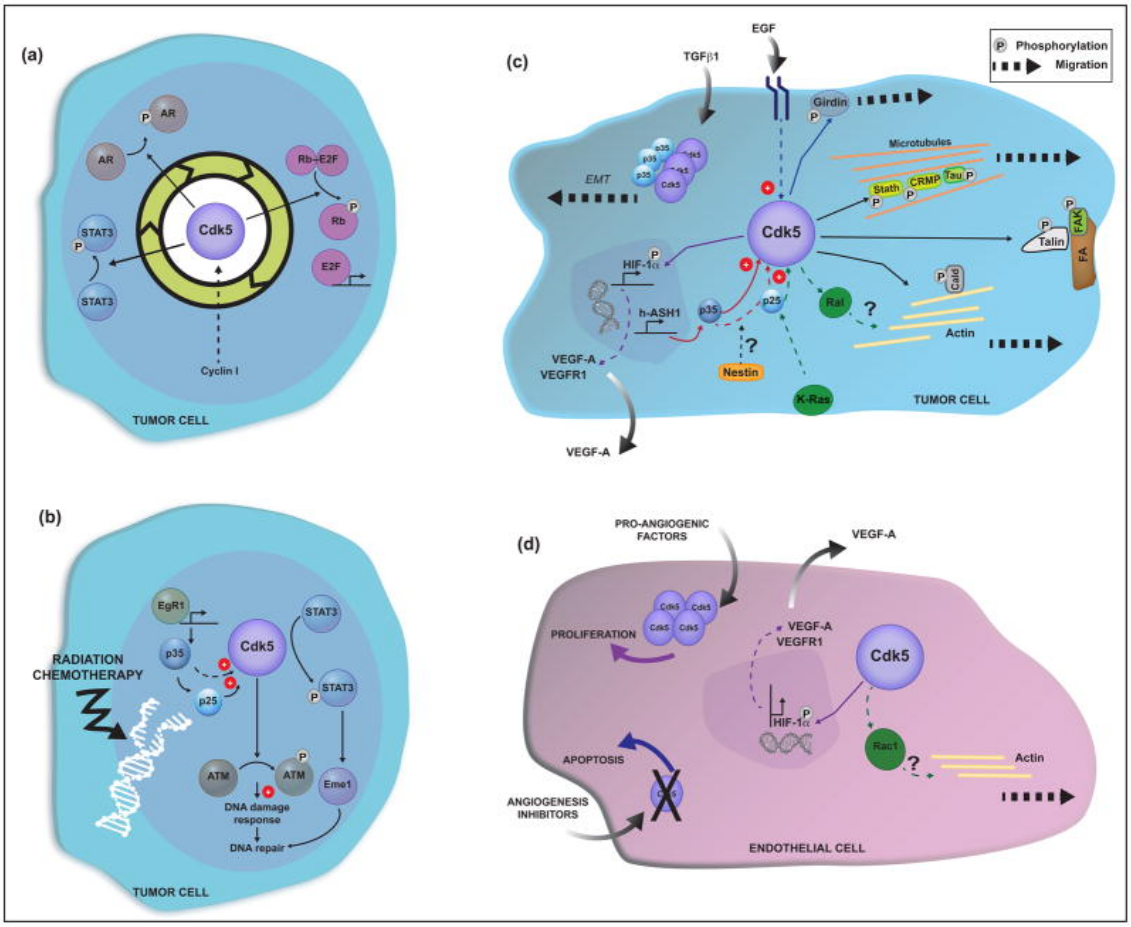

Figure 9. *Involvement of Cdk5 in cancer related processes. a) Cdk5 contribution to cell cycle and proliferation. b) Cdk5 in the DNA-damage response and DNA-repair. c) Cdk5 in cell motility. d) Cdk5 in epithelial cell proliferation and migration. Pozo et al. Trends in cancer 2016 (182)*

stream of EGF signaling, as Bhandari et al. showed that Cdk5 phosphorylates guanine exchange factor GIV(Girdin), which is important in the migration–proliferation dichotomy. Phosphorylated GIV enhances pro-migratory AKT signals, while mitogenic MAPK signaling is limited, hence triggering cell migration (196).

1.8.4 Cdk5 and Angiogenesis

In order for tumors to grow beyond a certain size they need dedicated blood supply to provide oxygen and other nutrients. By secreting growth factors, e.g. VEGF, tumor cells stimulate capillary growth within the tumor. This pro cess is referred to as tumor angiogenesis. Importantly lymphatic and blood vessels also allows for removal of metabolic waste from the tumor. At the same time, they also represent the main escape route for migrating cancer cells. This process therefore represents an interesting target in cancer treatment and antiangiogenic drugs have indeed shown good clinical results in the treatment of various cancers (197).

Cdk5 has been shown to be expressed in the endothelial cells lining the blood vessels (198) and quite a few studies have shown implications for Cdk5 in the angiogenic process (Figure 9D). Different roles have been proposed. For example, that Cdk5 promotes endothelial migration and angiogenesis by remodeling of the cytoskeleton. More specifically by controlling the localization of the GTPase Rac1 to the leading edge of migrating cells (120). In highly vascularized cancers, such as hepatocellular carcinoma and gliomas, genetic knockdown and pharmacological inhibition of Cdk5 impairs angiogenesis and subsequently also tumor growth (162, 165). At the molecular level Cdk5 stimulates Notch-driven angiogenesis, which along with hypoxia inducible factor1-α (HIF-1α) leads to the activation of both VEGF-A and VEGF receptor 1. Both are essential for the formation of blood vessels growing tumors. Taken together these studies suggest that Cdk5 could be a target for anti-angiogenic treatments for cancer therapy.

1.8.5 Immune infiltration and Cdk5

Immunotherapy has gotten a lot of attention in the last decade. Such treatments target immune checkpoint interactions, between mainly PD-1 and its ligand PD-L1 along with CTLA-4 and its ligand B7. The PD-L1 - PD-1 binding is between tumor cells and T-cell respectively and it prevents the T-cell from killing the tumor cell. CTLA-4 is found on the surface of inactive T-cells and the B7 receptor on antigen presenting cells, and the binding prevents the T-cell activation. Cancer cell PD-L1 upregulation hence allows the cell to escape immune detection (199).

In the recent years a connection between Cdk5 and tumor immune cell infiltration and subsequently response to immune checkpoint blockage has been demonstrated. Dorand et al. discovered how Cdk5 allows tumor cells to evade immune-surveillance by transcriptional activation of *PD-L1* in Medulloblastoma. Cdk5 disruption induced expression of PD-L1 transcriptional repressors *IRF2* and *IRF2BP2*, which resulted in CD4+ T-cell mediated tumor rejection as a consequence of PD-L1 down-regulation (133). This is supported by another group who demonstrated that the combination of anti-PD-1 and Dinaciclib, a Cdk inhibitor with highest affinity for Cdk2 and Cdk5, increased the T-cell infiltration in bladder and colorectal murine tumor models (200). Furthermore a study in melanoma and breast cancer showed that CRISPR/Cas9 mediated KO of Cdk5 elicited strong T-cell mediated immune response in the tumor microenvironment (154). In triple negative breast cancer (TNBC), the most aggressive subtype, it has recently been shown that Cdk5 increases the stemness of TNBC cells, which is closely related with metastatic progression. Strikingly, Cdk5 blockage diminishes stemness transformation, which reverses an immunosuppressive microenvironment enhancing anti-PD-1 therapeutic efficacy (201). Collectively, these results indicate that at least in some tumors the co-inhibition of Cdk5 and PD-1/PD-L1 binding could enhance the efficacy of the immunotherapy.

1.8.6 Cdk5 in CRC

As reviewed above, in an extensive number of solid tumors Cdk5 has been related to many hallmarks of cancer, such as proliferation, angiogenesis, DNA damage repair, immune evasion and dissemination. Quite different mechanisms and pathways have been suggested, seemingly varying greatly dependent on the cancer type. However, it is clear that high levels are generally associates with poor prognosis.

As for CRC the first publication concerning Cdk5 is from 2006, where Kim et al. reported that Cdk5 was elevated in the CRC cell line HT29 and that treatment with a peroxisome proliferator-activated receptors (PPAR)gamma ligand decreased Cdk5 activity and cell proliferation(175). Next, in 2009 our group showed that Cdk5 was significantly upregulated in a panel of CRC cell lines made resistant to oxaliplatin (186). Shortly after Courapied et al. showed that upon SN38 treatment (the active metabolite of irinotecan) Cdk5 was up-regulated and found to co-immunoprecipitate (IP) with STAT3. The STAT3-Cdk5 pathway reduced DNA damage through up-regulation of Eme1, an endonuclease involved in DNA repair (163).

In 2016 Zhuang et al. showed increased Cdk5 expression in CRC tissues compared to normal tissues and in a mixed cohort of CRC patients they found high Cdk5 levels to

correlate with tumor aggressiveness and poor overall survival. In *in vitro* studies they showed that abrogation of Cdk5 activity, either by shRNA or Roscovitine treatment, decreased proliferation and colony formation in CRC cell lines. They observed the contrary when overexpressing Cdk5. When studying the migratory and invasive capacity in vitro and in vivo they also found it to be affected by Cdk5. For example, the number of metastatic lesions in mouse models were drastically decreased upon Cdk5 inhibition, while the opposite effect was observed when Cdk5 was overexpressed. They further revealed a mechanistic link between Cdk5 and the oncogenic ERK5-AP-1 signaling pathway in the pathogenesis of CRC (146). In another recent publication, a Cdk2 and Cdk5 inhibitor showed inhibition of migration and proliferation in CRC cell lines and tumor growth inhibition in xenograft models (139).

Many aspects remain to be studied regarding the importance of Cdk5 in CRC development and progression. Therefore, with the work presented in this thesis we wanted to do a thorough evaluation of its expressional pattern and role in key processes such as proliferation, cancer dissemination and immune infiltration. Ultimately, determining which clinical relevance there could be in studying Cdk5 levels in CRC tumors or which advantages there could be in inhibiting this kinase.

Hypothesis

While treatment options rapidly increase for other types of cancer, only few advances have been made in the treatment of CRC in the last decades. The treatment still consists of different regimes of chemotherapy possibly combined with a targeted therapy of choice. Unfortunately, the list to choose from is very short. Hence, there is an unmet need for new druggable targets, along with prognostic and predictive biomarkers to optimize the efficiency of current and upcoming treatments.

Research in different types of cancer shows that Cdk5 is associated with a more aggressive phenotype and that high levels of this kinase mark poor prognosis. Mechanistically, Cdk5 has been linked to many of the cancer hallmarks such as proliferation, cancer dissemination, immune infiltration and DNA damage response. When it comes to CRC only few publications exist investigating the role of Cdk5, but a possible involvement in proliferation and migration is indicated (146). Our group has previously found Cdk5 to be upregulated in oxaliplatin resistant CRC cell lines and others found Cdk5 to be involved in DNA damage repair upon irinotecan treatment (163).

Based on this preexisting knowledge about Cdk5 from CRC and other solid tumors, we hypothesize that Cdk5 plays an important role in CRC progression and that tumors with high levels of Cdk5 are more aggressive and prone to disseminate to distant organs. Furthermore, we hypothesize that tumor Cdk5 levels could serve as a prognostic and/or predictive biomarker for CRC patients' outcome. If our hypothesis is confirmed the studies of Cdk5 in CRC could broaden and optimize the current treatment of CRC. In order to test our hypotheses and establish whether further investigation into specific inhibition of Cdk5 in CRC is warranted we proposed the objectives specified below.

Objectives

The general objective is to expand the knowledge about Cdk5 in CRC and determine the applicability of Cdk5 as a prognostic and/or predictive marker.

In order to achieve this, we propose four specific objectives:

1. **To describe the expressional patterns and activity of Cdk5 in patient's samples and in *in vitro* models.**

2. **To study the involvement of Cdk5 in key aspects of cancer progression such as proliferation, dissemination and clonogenic capacity in *in vitro* models.**

3. **To identify transcriptional effects of *CDK5* knock down on individual genes and pathways in a panel of CRC cell lines.**

4. **To determine the usability of Cdk5 is a prognostic or predictive marker in CRC.**
   a) Investigating whether Cdk5 levels are associated with disease- and/or overall survival of untreated stage II-III CRC patients.
   b) Studying whether the presence of Cdk5 affects the response to DNA damaging agents commonly used in the treatment of stage IV CRC.
   c) Studying whether Cdk5 could serve as a biomarker for alternative drugs.
   d) Determining if Cdk5 affects the immune infiltration and response to immune checkpoint blockage in CRC tumors.

2 Materials and methods

2.1 Cell culture

The CRC cell lines used in the studies are listed below along with important molecular characteristics (Table 3). All cell lines were passed on from other research groups, apart from the LoVo cell line which was purchased from the American Type Culture Collection (ATCC) and the SW48 cell line, with or without a *KRAS* mutation (G12D) introduced, which was bought at Horizon Discovery Ltd. In non-purchased cell lines we performed an authentication analysis by short tandem repeat (STR) profile characterization (Thermo Fisher). All of them were shown to be the expected cell lines.

Cell lines:

Human	**Origen**	**Medium**	**CMS**	**Microsatellite**	***KRAS* status**	***BRAF* status**	**Tp53**
HT29	Colon	DMEM	3	MSS	WT	Mut V600E	Mut
LoVo	Colon	F-12	1	MSI	Mut G13D	WT	WT
HCT116	Colon	RPMI	4	MSI	Mut G13D	WT	WT
Difi	Rectum	DMEM/F-12	2	MSS	WT	WT	Mut
SW48	Colon	RPMI	1	MSI	WT	WT	WT
DLD1	Colon	RPMI	No label	MSI	Mut G13D	WT	Mut
A293T	Embryonic kidney	DMEM	-	-	-	-	-
Murine							
MC38	Colon	RPMI	-	MMR deficient	WT	W487C	Mut
CT26	Colon	RPMI	-	MMR proficient	Mut G12D	WT	WT

Table 3. *Human and murine colorectal cancer cell lines. Mutational and microsatellite statis from Sveen et al. Clin. Cancer Res. 2018 (48)*

Cell lines were grown as monolayer in the medium indicated in table 3. All cell lines were cultured at 37°C in a humidified atmosphere of 5% CO2. Cells were passaged weekly using Trypsin-EDTA (Thermo Fisher) at 3X and the number of passages were limited to 10. All cell lines were routinely checked for contamination of mycoplasma with a polymerase chain reaction (PCR)-based assay (Stratagene).

For the generation of the oxaliplatin-resistant cell lines HTOXAR3 and LoVOXAR3, HT29 and LoVo cell lines were used as the parental cells. These sublines were developed as a result of continuous exposure to increasing doses of oxaliplatin as described

previously (186). The DLDIRI and LoVIRI cell lines were achieved by following the same principle exposing the DLD1 and LoVo cells, respectively, to increasing concentrations of irinotecan.

DMEM: Dulbecco's Modified Eagle medium, 10% FBS (Reactiva), 1% Penicillin/Streptomycin 10.000 I.U/mL (Life technologies), 2,05mM L-Glutamine (AppliChem), 2,60mM HEPES (AppliChem).
RPMI: RPMI medium 1640, 10% FBS, 1% Penicillin/Streptomycin 10.000 I.U/mL, 2,05mM L-Glutamine, 2,60mM HEPES.
F-12: Ham's F12 Nutrient Mixture, 20% FBS, 1% Penicillin/Streptomycin 10.000 I.U/mL

2.1.1 Cryopreservation

Approximately 10^6 cells were resuspended in FBS (Reactiva) and DMSO at 9:1 in cryogenic tubes and placed in a Mr. Frosty Freezing container (Thermo Fisher) and placed at -80°C. For long/time storage the cells were moved to liquid nitrogen. For the defrosting of cell lines, the cell containing solution was quickly defrosted in the appropriate warm medium, cells were pelleted and seeded in cell culture flasks.

2.2 *CDK5* gene manipulation techniques

2.2.1 Gene silencing by siRNA

A pool of 3 Silencer Select validated siRNAs against *CDK5* at 5nM (s2826, s2825 and s2827, Ambion) or 3nM non-targeting control (siNTC) (Dharmacon) along with lipofectamine RNAimax (Invitrogen) were diluted in Optimem medium (Gibco). In all experiments we included a non-transfected negative control (Mock) to evaluate the toxicity of the siRNA. $2.5x10^5$ cells were seeded per well in 6-well plates (2 wells per condition) and treated with the mixture of oligonucleotides, lipofectamine and Optimem. After 24h the transfection medium was replaced by fresh medium and after yet another 24h the cells were counted and used for subsequent studies. The inhibition was evaluated by WB and experiments with target downregulation above 75% were included.

2.2.2 Gene knockdown (KD) by CRISPR/Cas9

Gene knockdown was carried out with the CRISPR/Cas9 technique in the human HT29, HTOXA, LoVo, LoVOXA, and SW48 cell lines and in the murine cell lines CT26 and MC38. The pLentiCRISPR v2 plasmids were purchased at Genscript. The Long Terminal Repeat (LTR) sequences facilitate the integration into the host genome, and whatever is found between the two is integrated. This includes a U6 promotor in front of the gRNA and gRNA scaffold sequences, followed by an EFS promotor and the Cas9 sequence, and at last a Puromycin resistance gene (Figure 10). 20-nucleotide long gRNA were chosen to target early exons in the *CDK5* gene (see Table 4). Low specificity for other genes was checked as well. A plasmid containing a gRNA with no human or murine target was also purchased to serve as a negative control (crNTC) in the experiments with the knockdown cell lines.

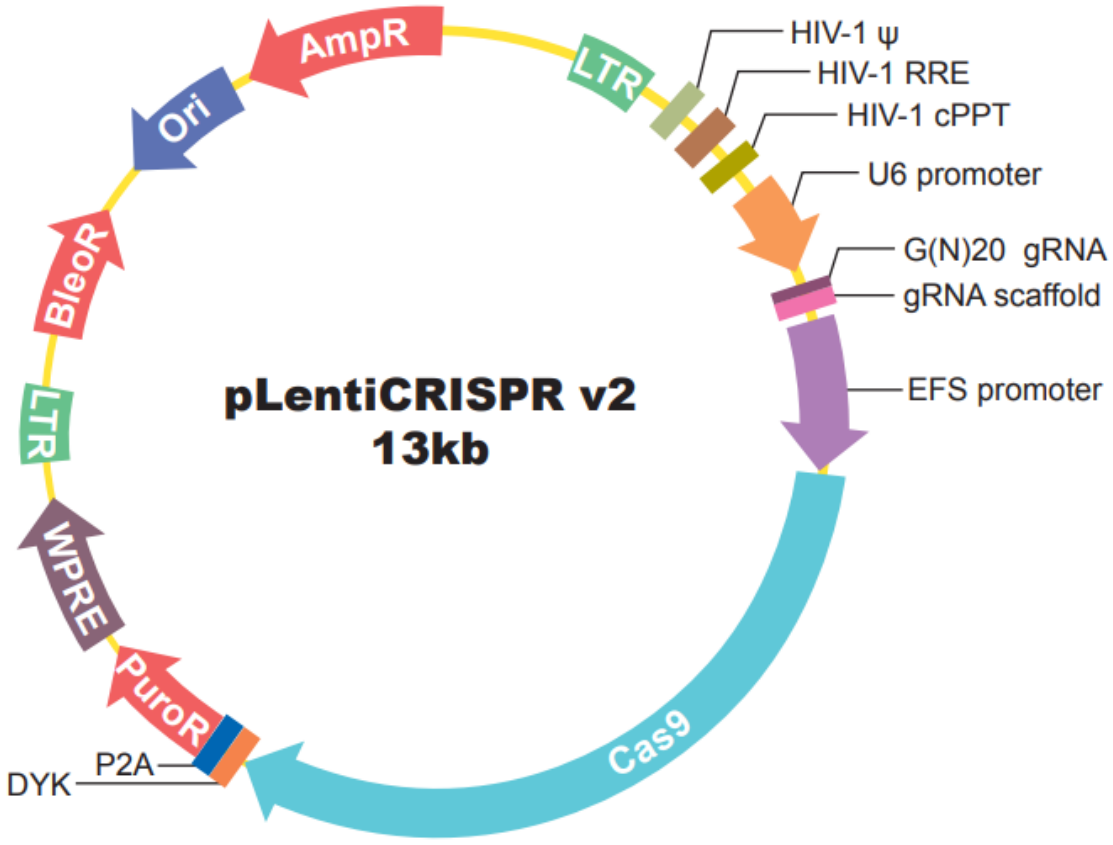

***Figure 10**. Simplyfied pLentiCRISPR/Cas9 plasmid map. www.genscript.com*

Target	gRNA sequence
Human *CDK5* gRNA1	GGCCTTGAACACAGTTCCGT
Human *CDK5* gRNA2	GTGTGCCGAGTTCCGCCCTC
Human *CDK5* gRNA3	ATCTCCCGGAGGGCGGAACT
Murine *CDK5* gRNA1	CAGGCTGGATGATGACGATG
Murine *CDK5* gRNA3	TCAGCTTCTTGTCACTATGC
Non-target	ACGGAGGCTAAGCGTCGCAA

Table 4. *gRNA used for CRSPR/Cas9 CDK5 KD. www.genscript.com*

Small amounts of the plasmids are provided and therefore an initial amplification step was performed. 100µL competent *E.coli* Stbl3 bacteria were incubated with 200ng plasmid for 30 minutes on ice. A thermic shock was given for the plasmid to enter the bacteria and next 300µL SOC was added and the mix was incubated for 50 minutes at 37ºC in the shaker. The bacteria were streaked on 100µg/mL ampicillin containing agar plates and left to grow overnight at 37ºC. Bacteria colonies were picked for each plasmid and inoculated in 5mL LB medium with Ampicillin overnight. Next 1mL of this LB medium was again left overnight in 150mL LB medium with Ampicillin. The plasmids were extracted from the bacteria with the Extract Me Plasmid Maxi Endotoxin-Free kit (DNA Gdansk) following the instructions. The plasmids were quantified on the nanodrop and a digestion was performed to confirm the plasmid integrity. The EcoRI and BamHI restriction enzymes were used for the digestion. Both linearizations with a single enzyme and double cut with both enzymes were carried out. The digested fragments were loaded on 0,5% agarose gels. The identity was confirmed by analyzing the bands observed.

For the lentivirus production we used two additional plasmids psPAX2 and pVSVg. psPAX2 (Addgene # 12260) is a second-generation lentiviral packaging plasmid. It encodes for the Gag, Pro and Pol genes derived from HIV. The promoter is the chicken β actin promoter and the polyadenylation signal is the rabbit β globin poly A. It also contains an ampicillin resistance cassette. pVSVg (AddGene #8454) is an envelope plasmid used for lentiviral production. It expresses the 6 glycoproteins of VSV virus (Vesicular Stromatitis Virus) under control of CMV immediate-early promoter. It mediates viral entry by interacting with phospholipid components of the target cell membrane and fosters the fusion of viral and cellular membranes. It also includes IVS, a synthetic intron known to enhance the stability of mRNA, the ColE1 origin of replication and an ampicillin resistance cassette for propagation and antibiotic selection in bacteria.

For the lentivirus production A293T cells were seeded 24h prior to use in order to have approximately 60% confluence at the time of transfection. The virus producing cells

were transfected with lipofectamine 2000 (Thermo Fisher) to introduce p-lentiCRISPR plasmids with gRNAs for *CDK5* or a sequence with no target (Genscript), along with the transfer plasmid Pax2 and the envelope plasmid VSV-G and left 48h to produce lentivirus. The total amount of plasmid used was 3.2µg at a ratio of 1:1:1. After the 48h the virus-containing medium was collected and filtered through 45-micron filters and the virus from the two/three different gRNA plasmids against *CDK5* was joined. The virus-containing medium was mixed 1:1 with fresh medium, and this medium was added to the cells to infect along with Polybrene at 8µg/mL. This medium was changed after 4h incubation and the cells were left 48h before Puromycin selection was started. The optimal concentration of Puromycin had previously been determined for each cell line by titration. *CDK5* KD was confirmed by Western blot and q-PCR.

2.3 Functional assays

2.3.1 Proliferation assay

Cdk5 was silenced using siRNA (as described in 2.2.1). $5x10^4$ cells were seeded in a 24 well plate. Cell proliferation of mock, siNTC and siCdk5 cells was evaluated after 24, 48, 72 and 96 hours by disrupting the cells with 1.7% triton x100 and next staining them with Propidium iodide at 30µM (Sigma Aldrich). After 10 minutes the red fluorescence was measured on a microplate reader (Varioscan, Thermo Scientific), at excitation wavelength of 470nm and emission wavelength of 620nm. Cell number was assessed by quantifying the fluorescent signal and subtracting the signal form a blank. Values are presented as means ± SD of at least three independent experiments. Statistical differences were assessed by the students t-test.

2.3.2 Migration and invasion assays

The role of Cdk5 on the migration/invasion potential was investigated *in vitro* using a Boyden chamber. A total of 10^5 or 10^4 cells was seeded to test migration and invasion respectively onto the 8µm pore membrane (HTS Transwell® polyester membrane tissue culture treated; Corning, NY, USA). The upper and lower chambers were filled with medium containing 2% and 10% FBS respectively, thereby stimulating the cells to invade and migrate. For the invasion assay the upper chambers were coated with 21µl of Geltrex™ (Thermofisher®). After 48 or 72 hours of incubation at 37 °C, cells above the membrane were removed, the membrane washed with PBS and fixed with 4% paraformaldehyde (Sigma-Aldrich) and stained with 0.5% crystal violet (MERCK). To re-

move remaining cells that did not migrate through the membrane, the surface of the membrane within the well was gently scrubbed with a sterile cotton bud. Pictures were taken with a microscope (x4 magnification, NIS-Element) and migrated cells quantified by Image J (five random fields per membrane). At least three independent experiments were performed, and the data are presented as mean±S.D. Statistical differences were calculated by the students t-test.

2.4 Co-immunoprecipitation

Cells were washed with PBS and incubated with 200µl lysis buffer (50mM Tris pH7.4, Triton X, 1mM EDTA, 135mM NaCl, protease inhibitor and H2O) for 5 minutes on ice. Next, they were scraped off the petri dish and mechanically disrupted with a tissue grinding pestle. After centrifugation (12000rpm) for 20 minutes at 4°C, the supernatant from the cell lysate was collected and incubated with either 30µl α-Cdk5 (Santa Cruz) or 30µl α-p35 (Santa Cruz) overnight at 4°C on a rotator. For each condition, 50µl of bead suspension (PureProteomeTM Protein G Magnetic Beads, Millipore) were washed with PBS-T (0.1%) and incubated for 2 hours with the cell lysates, containing the antibody. After incubation the beads were washed 3 times with the lysis buffer containing triton-X (with concentrations increasing up to 1%). Beads were then resuspended in 2x loading buffer, boiled for 5 minutes at 95°C and after removing the beads samples were stored at -20°C until western blotting. For the western blot 50µl of the eluted proteins were loaded onto 10% SDS-PAGE gels.

2.5 Protein extraction

2.5.1 Cell lines

Cells were washed with PBS and a RIPA plus buffer (PBS; NP-40 1%; Na deoxycholate 0.5%; SDS 0.1%; EDTA 1mM; NaF 50mM; NaVO3 5mM) containing a mixture of EDTA-free protease inhibitors (Roche) was added to the cell pellet or cell culture dish. After homogenization the mixture was incubated for 20 minutes at 4°C on a shaker. Afterwards, cell lysates were centrifuged for 20 minutes at 4°C at 12000rpm and the protein containing supernatant was collected and frozen down. The protein concentration was measured through the Bradford method, using the DCTM Protein Assay (Bio-Rad) according to the manuals instructions and bovine serum albumin diluted in RIPA buffer as a standard. Reagent A was mixed 50 to 1 with reagent A'. 5µl protein sample were pipetted in duplicates onto a 96-well plate and 25µl of the reagent A/A' mixture was added to each sample. Lastly 200µl reagent B was added to each sample and the

plate was covered with aluminum foil, placed on a shaker for a moment to mix the solutions and then incubated for 15 minutes. Plates were then measured with a microplate reader (Varioscan, ThermoScientific) at 562nm and protein concentrations were calculated.

2.5.2 Tumor tissue

Frozen tissue samples (Cohort A, table 8) were disintegrated and homogenized manually with the gentleMACS Dissociator system (Milteny Biotech, Bergisch Gladbach, Germany). The RIPA plus buffer was used for the subsequent protein extraction as described above for the cultured cells.

2.6 Western Blotting

For the western blot 50µg of protein were loaded in a 10% SDS-PAGE gels (Invitrogen, Life Technologies) and subjected to electrophoresis in a MOPS buffer (50nM MOPS, 50nM Tris, 0.1% SDS, 1mM EDTA at ph 7.7). Novex™ Sharp Pre-stained Protein Standard (Thermo Fisher) was loaded for subsequent molecular weight estimationn. Afterwards, proteins were transferred onto a polyvinylidene difluoride (PVDF) membrane (BioRad) by wet transfer in Transfer buffer (27nM Tris, 197nM Glycine and 20% Methanol). The membranes were blocked for 2h with Odyssey blocking buffer (LICOR Biosciences) and then incubated overnight at 4 °C with specific primary antibodies at the indicated dilution (Table 5). ß-Actin or α-Tubulin was used as reference proteins. Membranes were incubated with IRDye rabbit and/or mouse secondary antibodies (1:10000) (LI-COR Biosciences) for 50 minutes protected from the light. Membranes were scanned with an Odyssey Imaging System, and band signal was quantified with the build-in software. Each band was referenced to either α -Tubulin or ß-Actin bands from the same sample.

Primary Antibodies	**Source**	**Dilution**
Cdk5 (#2506 Cell Signaling)	Rabbit	WB 1:1.000, IHC 1:200
Cdk5 (#sc-6247 Santa Cruz)	Mouse	IP 30 µl
Cdk5 (#ab40773 Abcam)	Rabbit	IHC 1:200
p35 (#2680S Cell Signaling)	Rabbit	WB 1:1.000 / 1:300
P35 (#sc-820 Santa Cruz)	Rabbit	IP 30 µl
IgG (#sc-69786 Santa Cruz)	Rabbit	IP 30 µl
Caldesmon (#12503 Cell signaling)	Rabbit	WB 1:500 / 1:1000

METLL7A (#MA5-27225 Thermo Fisher)	Mouse	WB: 1000
METTL7A (#PA596971 Thermo Fisher)	Rabbit	WB: 1000
α-Tubulin (#T6074 Sigma-Aldrich)	Mouse	WB 1:20.000
ß-Actin (#A2066 Sigma-Aldrich)	Rabbit	WB 1:20.000
Secondary antibodies		
IRDye 680 anti-rabbit	Rabbit	WB 1:10.000
IRDye 800 anti-rabbit	Rabbit	WB 1:10.000
IRDye 800 anti-mouse	Mouse	WB 1:15.000

Table 5. *List of primary and secundary antibodies.*

2.7 Drug responses

2.7.1 MTT assay

Human CRC cells were seeded in a 96-well microtiter plates and allowed to attach for 24h. The number of cells depended on the cell line and the duration of the experiment. Prior to the experiments the optimal cell number for each experiment was determined by titration to obtain an OD between 1.5 and 2 in the untreated wells after addition of the MTT. We have previously found that the OD saturates above 2. Medium containing the drug to be tested was added after 24h. Dose ranges depended on the drug tested, however for all experiments it was the aim to achieve viabilities between 10 and 90%. After the treatment period fresh medium was added to each well and the cells were allowed to grow for 72h. For treatments with Taxanes the MTT solution was added immediately after the treatment. A mixture of non-complemented RPMI medium, 10% MTT and 10% FBS was prepared and added for 4h. The MTT salts aggregates were dissolved with 20% SDS and 0,02M HCL and the absorbance was read at 590nm the following day on a microplate reader (Varioscan, Thermo Scientific, or Luminometer, Berthold technologies). Survival for each treatment dosage was determined for each experiment using the median effect line method. This method consists of a graphical representation of $\log_{10}((1/fn)-1)$, where fn is different fractions of the viability obtained for $\log_{10}$ of the drug dose. The GraphPad Prism software was used to create the dose response curves and calculate EC50 values. Data represent the mean ± S.D. of three independent experiments. Statistical differences were determined by paired t-test.

2.7.2 Colony assay

A serial dilution of the cells was made in order to seed only approximately 200cells/well in a 6-well plate, and the cells were left 24h to adhere. In Colony assays with drug treatments, cells were treated for 24h at their respective EC50 values starting 24h after seeding. Cells were left a total of 12 days in culture for colonies to form performing regular medium changes. Cells were subsequently washed, fixed with a methanol/acetic acid (3:1) solution for 10 min and stained with a solution of 0.5% crystal violet (MERCK) for 10 min. After the staining, cells were washed with PBS and colonies were counted manually. Data represent the mean ± S.D. of three independent experiments and student's t-test was used to determine statistical differences.

2.8 DNA extraction

DNA extraction was performed with the E.Z.N.A. Tissue DNA Kit (Omega Bio-tek) following the manufacturer's instructions. Briefly, the cell suspension was treated with OB Protease Solution and cells were lysed with BL Buffer. 100% ethanol is added to the centrifuged cell solution and the whole sample is transferred to a HiBind DNA mini-column. The sample is centrifuged, and filtrate is discarded. HBC buffer is diluted with 100% isopropanol, added to the column and again the sample is centrifuged. The filtrate is discarded, and the column is then washed twice with DNA Wash Buffer. One last time, the filtrate is discarded, and the empty column is centrifuged to dry. To elute the DNA from the column, pre heated Elution buffer is added to the column, incubated for 2 minutes and centrifuged one last time. The resulting DNA was quantified on the Nanodrop spectrophotometer (Nucliber).

2.9 RNA extraction and quantitative PCR

Total RNA was extracted from cell pellets using a commercial kit (RNA mini kit, Qiagen) following the manufacturer's instructions. TRK lysis buffer was added to cell pellets, and the cells were homogenized with a homogenizer. 70% Ethanol is added and the solution was transferred to Hibind RNA column and centrifuged. The column was washed twice with wash buffers I and II. The RNA was eluted with nuclease free water and stored at -80°C. The RNA was quantified using the Nanodrop spectrophotometer (Nucliber). Before the retrotranscription the RNA was treated with DNAse (Invitrogen). DNase buffer and DNase were added to the RNA sample and incubated at 37°C for 30

minutes. The DNase inactivation reagent was added to the sample before centrifuging. The supernatant contains the purified RNA sample.

For the retro-transcription (RT) from RNA to cDNA we used the M-MLV reverse transcriptase (Thermo Fisher). Depending on the RNA concentration of each sample an initial volume of RNA was taken (final concentration of ended RT of 200 – 300ng/μl) and brought up to 10μl. 1μl of 10mM dNTPs (Ecogen) and 1μl 250ng/mL Random Hexamer Primers (Thermo Fisher) was added and incubated at 65°C for 5 minutes. Next 2μl of 0,1M dithiotreitol (DTT) (Thermo Fisher) 4μl of reaction buffer 5X (Thermo Fisher), 1μl RNAse OUT (Thermo Fisher) and 1μl M-MLV reverse transcriptase (Thermo Fisher) was added. The following program was used for the RT reaction: Annealing: 10 min. at 25°C, Extension: 45 min. at 37°C, Inactivation: 10 min. at 70°C. The resulting cDNA samples were stored at -20°C.

For the quantitative (q)-PCR analysis of *CDK5* we used the commercially available TaqMan Gene Expression Assay (Hs00358991_g1). Diluted template cDNA from the RT reaction (37,5ng/rxn) was mixed with TaqMan Universal Master Mix (6,25μl/rxn) (Applied Biosystems), Taqman® primers and probes (15μM stock) (0,08μl/rxn) (Thermo Fisher) and PCR grade H2O (to final volume of 10μl). β-actin (IDT DNA) was included as endogenic control gene. The qPCR analysis was run on the AbiPrism 7900 equipment

For the qPCR analysis of *PD-L1*, *METTL7A* and *CALD1* expression the Roche Lightcycler 480 II was used. Template cDNA (100ng/rxn) was mixed with SYBRgreen master mix (5μl/rxn) (Thermo Fisher) and specific primers (5μM stock) (1μl/rxn) and PCR grade H2O (to final volume of 10μl). Again, *β-ACTIN* was included as endogenous control gene.

	Forward primer (5´-3´)	Reverse primer (3´-5´)
PD-L1	TCCATCCTGTTGTTCCTCATTG	ACGATCTACCACTCTTTACACC
METTL7A	TTCCAAGTCGAACACTCAGC	AAGAACCAGGAGCGGATTC
CALD1	GCAGAAGCAGGAGGAAGAATC	GTTCTGTTGGTGGTGTTTGTG
β-ACTIN	TGAGCGCGGCTACGCTT	TCCTTAATGTCACGCACGATTT

Table 6. *IDT DNA primers used in the study.*

The q-PCR was carried out in 354 well plates. For each sample 3 *β-ACTIN* replicates and 3 replicates of the studied genes were carried out. To control the presence of genomic DNA contamination an RT-minus (from RNA prior to the RT reaction) sample was included for *β-ACTIN* expression. Each primer mix was also run to check for signal. Furthermore, a human RNA reference (Stratagene) was included in each run al-

lowing to compare results from difference experiments. The thermal cycling can be seen in table 7.

	Taqman AbiPrism 7900 equipment			**Sybrgreen Roche Lightcycler 480 II**		
	Cycles	Temperature	Time	Cycles	Temperature	Time
Pre-incubation	1	95°C	10 min	1	95°C	5 min
Amplification	40	95°C	15 sec	40	95°C	10 sec
		60°C	1 min		60°C	20 sec
					72°C	10 sec
Cooling	1	4 °C	∞		4 °C	∞

Table 7. *Thermal cycles for qPCR experiments*

The quantification of gene expression was calculated by the $2^{-\Delta\Delta Ct}$ method. This method is the standard way to calculate relative gene expression levels between different samples, directly using the cycle threshold (Cts) generated by the qPCR system (202). The Ct of a reaction is defined as the cycle number when the fluorescence of a PCR product can be detected above the background signal. First the ΔCt is calculated, which is the difference between the studied gene (gene X) and the endogenous control gene:

$$\Delta Ct = Ct_{\text{gene X}} - Ct_{\text{Control gene}}$$

To be able to compare results from different experiments the expression was normalized to the human RNA reference sample:

$$\Delta\Delta Ct = \Delta Ct_{\text{sample}} - \Delta Ct_{\text{RNA ref}}$$

Finally, the $2^{-\Delta\Delta Ct}$ was calculated, which shows how the gene studied is expressed in any sample compared to the reference RNA sample.

In order to ensure very low contamination from genomic DNA the percentage of signal in any sample coming from genomic DNA was calculated. The amount of signal coming from genomic DNA should be below 5 %. The following formula was used:

$$2^{-\Delta\Delta Ct}_{\text{RT-minus}} = 2^{\text{Ct RT-minus control gene} - \text{Ct control gene}}$$

$$\% \text{ genomic DNA} = 100 / 2^{-\Delta\Delta Ct}_{\text{RT-minus}}$$

For each experiment 3 replicates were carried out with RNA coming from 3 independent experiments. Results with standard deviations between the 3 replicates below 0,25

where accepted. Student's t-test was used to determine statistical differences between conditions.

2.10 RNAseq

For the RNAseq experiments, RNA was extracted as previously mentioned from the HT29, LoVo and SW48 crNTC and *CDK5* KD cell lines in triplicates. It was quantified on the Nanodrop spectrophotometer (Nucliber) and the integrity of the RNA was confirmed on a 1% agarose gel. The reverse transcription and the actual RNAseq were carried out by Centre Nacional d'Anàlisi Genòmica (CNAG-CRG, Barcelona).
RNA-seq reads were mapped against human reference genome (GRCh38) using STAR software version 2.5.3a (203) with ENCODE parameters. Genes were quantified using RSEM version 1.3.0 (204) with default parameters and annotation file from GENCODE version 33. Differential expression analysis was performed with DESeq2 v1.18. R package (205) using the Wald test to compare the experimental conditions. We considered differentially expressed (DE) genes those with FDR < 0.05 and absolute fold-change |FC|> 1.5. PCA plots and heatmaps were generated using the DESeq2 rlog transformed counts with the 'ggplot2' and the 'pheatmap' R packages. A Functional gene Ontology (GO) enrichment analysis of the differentially expressed genes was performed with the g:Profiler v0.7.0 (206) R package. Gene expression correlations were computed with the 'Hmisc::rcorr' function and boxplots were performed with the 'ggboxplot' function of ggplot2. Venn diagram was performed with the R package 'VennDiagram'. For the survival analyses (*METTL7A* and *CALD1*), we used the COAD TCGA PanCancer expression and clinical data from the cbioportal (version 2018). The Kaplan-Meier curves were performed with the functions 'surv_cutpoint'(minprop=0.2), 'surv_categorize', 'survfit' and 'ggsurvplot' from the R packages 'survival' and 'survminer'.

2.11 Achilles study

We used the Achilles database from the Cancer Dependency Map (Broad Institute/Dana Farber Cancer Institute). Achilles gives a value of a gene dependency for each gene in each cell line included in the Achilles study (genome-wide RNAi and CRISPR loss-of-function screens). This gene dependency was correlated with the *CDK5* expression levels in CRC cell lines, looking at all cell lines (24), *KRAS* mutated (13) and *KRAS* WT (11) separately. The mutational and expressional data for the cell lines were extracted from the cbioportal (https://www.cbioportal.org/ study?id=cellline

_ccle_broad). See table 8 for the cell lines included and their *KRAS* mutational status. This results in a list of genes, which are crucial for cell survival in cells with high expression of *CDK5*. A list of possible drugs targeting these protein dependencies was also made. MTT assays were carried out (as described in section 2.7.1) with drug inhibitors specific for four of these proteins in the crNTC and *CDK5* KD HT29 and LoVo cell lines

***KRAS* WT cell lines**	***KRAS* mutated cell lines**
HT29	LOVO
CCK81	SW1463
SW48	CL40
RKO	LS180
OUMS23	SW837
SNU503	HCC56
HT55	NCIH747
MDST8	LS513
KM12	SW620
HT115	LS1034
C2BBE1	NCIH716
	SW403
	T84

***Table 8**. List of cell lines included in the Achilles study.*

2.12 Tissue microarrays

Tissue microarrays (TMA) had previously been built (207); hematoxylin-eosin-stained slides of all primary tumors were reviewed to identify the most well-preserved areas. Tissues corresponding to these areas were randomly sampled from paraffin blocks, with no special preference for the different parts of the tumor (*e.g.*, superficial zone *vs*. infiltrating border). Three cylindrical cores, each measuring 0.6 mm in diameter, were obtained from every donor block using a TMA workstation MTA-1 (Beecher Instruments). Subsequently immunohistochemistry procedures were applied. Specific Cdk5 antibodies were used (Abcam ab40773 1:200 and Cell Signaling 2506 1:200 for validation). Cell lines in which Cdk5 expression had been silenced by siRNA techniques were used as negative controls. Sections were scored as negative or positive.

2.13 Immunohistochemistry

Five micrometer thick sections were deparaffinized, hydrated, immersed in buffered citrate pH 6 and autoclaved. Afterward, sections were incubated for 30 min in rabbit serum. Incubations with a 1:200 dilution of anti-Cdk5 antibody (Abcam) were carried out for 22h at room temperature. Slides were washed and incubated with biotinylated rabbit anti-mouse Ig antibodies at a 1:700 dilution and then incubated in PBS/6% hydrogen peroxide for 15 min at room temperature before addition of avidin-biotin peroxidase complex (Dakopatts). The chromogen 3,3′-diaminobenzidine tetrachloride (Serva) was applied, and counterstaining was performed with Harris hematoxylin. A non-immnune mouse serum and a human hepatocellular carcinoma were used as negative and positive controls, respectively. Quantification of the results was adapted to the staining expression of Cdk5 antibody, and thus, it was evaluated as negative, low and strong positive.

2.14 Subcutaneous tumor growth in mice and Murine organotypic tumor spheroids (MDOTS) generation

Murine cell lines MC38 and CT26 were cultured in complete RPMI medium under the same conditions as described for the human cell lines. In preparation for cell inoculation cells were trypsinized and counted. For each injection 100ul was prepared consisting of 50ul culture medium with 10^6 cells and 50ul of matrigel (Corning). The cell solutions were prepared individually for each animal and kept on ice until injection. Balb/C and C57BL6 (females between 8-10 weeks at the time of injection) mice were anesthetized with inhalation of 4% isoflurane and 100% Oxygen, during the maintenance period of the anesthesia the isoflurane was lowered to 2%. The flanks of the mice were shaved and disinfected and the subcutaneous injection was carried out by pinching the skin with two fingers and inserting the needle between them approximately 1 cm. The cell suspension was injected slowly. Cells were injected on both sides, non-target cells on the left and KD *CDK5* cells on the right. The tumor growth was monitored every 3 days and the tumors were excised when one of the tumors reached a diameter of approximately 1cm. The final tumor volume was calculated using the formula V = (L x W x W)/2. The mice were euthanized by cervical dislocation and the tumors were removed with scalpels. Tumor samples were kept in RPMI medium and on ice until the start of the tissue digestion. For the MDOTS generation we followed the protocol described by Jenkins et al. in Cancer Discovery in 2018 with minor modifications (208). The piece of tumor is placed on a Petri dish and the medium is removed and replaced by 1mL of

medium containing 100 U/mL of collagenase IV (Thermo Fisher). Using scalpels, the tumor was cut until the pieces are below 1mm and the medium has become cloudy. Any blood cloths were removed. The presence of spheroids in the dish was confirmed under the microscope. The media and tumor pieces were filtered through a 100µm filter into 50mL conical tube. The bottom of the petri dish was washed fresh media and this was also filtered through same filter. The 100µm filter was inverted over a 6-well dish, and 5mL media was filtered through backwards. The uncut tumor fragments were saved and ice and later frozen down. The Solution that has passed through the 100µm filter was next filtered through a 40µm filter. The solution that has passed though was kept on ice for subsequent Fluorescence-activated cell sorting (FACS) analysis. The 40µm filter was also inverted over another well in the 6-well dish and again 5mL medium was run through backwards to elute the spheroids found on top of the filter with sizes between 40 and 100µm. The spheroid solutions were span down at 300rcf for 4 minutes. The medium was removed and the pellets containing the spheroids were resuspended in 1:4 medium with 50% FBS and Vitrogel (Tebu) (diluted 1:1 in PBS). For the culture of the spheroids we used the microfluidic chambers from Aim Biotech (see figure 11). 10ul of the spheroid solution was injected into the middle gel inlet. The chambers were placed in the designated holders with humidity chambers and left 40 min for the gel to solidify. Subsequently media with or without treatments was added to the media channels. Treatments applied were IgG isotype control (#16-4321-81), α-PD-1 (#16-9982-81) and α-CTLA-4 (#16-1521-81) at 10µg/mL (Life Technologies). The chambers were placed in the incubator for 6 days, with one medium change at day 3. The growth of the spheroids was monitored every 2 days.

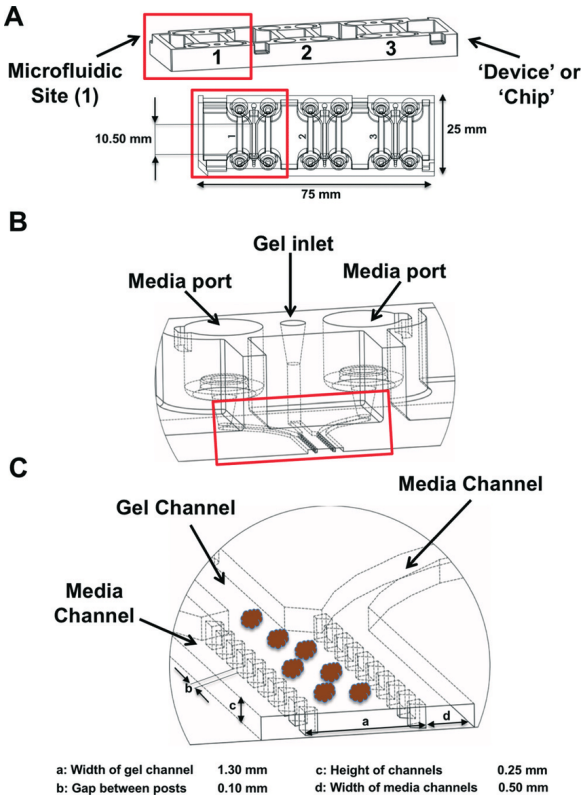

Figure 11. *Graphical illustration of microfluidic chamber (Aim Biotech).*

After the 6 days incubation the medium was removed and PBS was gently washed though the medium channels twice. Next PBS containing Propidium iodide (2,5µg/mL, Sigma) and Acridine orange (5µg/mL, Invitrogen) was added for an incubation of 5

minutes in the dark followed by another wash with PBS. Images of cell viability were captured on the Zeiss microscope with the red and green filter and 20X objective. The same Fluorescent threshold settings were used for all the images within an experiment. The quantification of the cell viability was carried out with the ImageJ software as follows. The green/red images were converted to black and white and the threshold was adjusted and the signal from each dye was quantified. The total signal was calculated by adding the red and green signal from this the percentages of death and live cells were calculated. Student's t-test was used to evaluate differences between conditions. The protocol can be seen in the following link https://youtu.be/p4KF7w7fO7Q.

2.15 Tumor immune infiltration

The infiltration of immune cells into the tumor tissue was evaluated by FACS. The cell suspension filtered through the 2 filters during the MDOTS generation was pelleted and washed once with 1x PBS + 1% FBS. Approximately 10^6 cells were suspended in 1mL and incubated with x 1,25μl of the viability dye. Next another wash was carried out with PBS+FBS. The cell pellet was resuspended in 100μl PBS and incubated with antibodies against CD3 (2μl) (#553062), CD4 (5μl) (#562891), CD8 (2,5μl) (#553035) and CD45 (2,5μl) (#557235) (Becton Dickinson) for 15 min. After another wash the solution was suspended in 200ul of PBS+FBS and cells were acquired on the FACS Canto II cytometer and analyzed with the FlowJo software. Student's t-test was used to determine statistical differences between conditions.

2.16 Patient's samples

Six different cohorts (named A to F), with a total of 811 samples from different patients, were used in this study. Table 9 shows the characteristics of each cohort. Samples from cohort C are all from stage III CRC patients and were collected at the Duran and Reynals Hospital. The qPCR was carried out in our laboratory. Samples from cohorts D and E belong to a private collection previously collected by our group (ISCIII registered number C.0001505). These consist of stage IV patients treated with either oxaliplatin or irinotecan based chemotherapy. All the samples were collected according to standard local protocols and after obtaining informed consent.

Cohort	Type of samples	Cdk5 measured by	N	Sex	Age	Metastasis	Stage	Treatment	Origin of samples	Available at	Molecular data available	Clinical data available
A	Frozen tissue Tumor/ adjacent	WB	12	Male 7 (78%) Female 2 (22%)	72	Liver 8 (89%) Lung 1 (11%)	IV	N/A	Tumor Biobank	N/A	-	-
B	In silico data	Micro array	98	Male 72 (57%) Female 28 (43%)	72 (43-87)	-	II, MSS	Radical surgery 96 (98%)	Colonomics project	Colonomics .org	RAS, CMS, etc	DFS, OS
C	Frozen tissue	qPCR	37	Male 21 (57%) Female 16 (43%)	78 (37-91)	-	III	Radical surgery 36 (97%)	Duran y Reynals Hospital	N/A	-	DFS (mean 36.3 months) OS (mean 42 months)
D	FFPE – TMA	IHC	52	Male 29 (56%) Female 23 (44%)	62 (37-76)	Liver 37 (71%) Lung 5 (10%) Others 10 (19%)	IV	5-FU/OXA (77%) CAPE/OXA (23%)	Private collection	ISCIII	-	DFS (mean 9.6 months)
E	FFPE – TMA	IHC	139	Male 78 (69%) Female 35 (31%)	62 (29-75)	Liver 97 (70%) Lung 46 (33%) Others 20 (14%)	IV	5-FU/LV/IRI (47%) 5-FU/IRI (53%)	Private collection	ISCIII	-	DFS (mean 9.4 months) OS (mean 20.3 months)
F	In silico data	RNA seq	473	Male 259 (54%) Female 225 (46%)	66 (31-90)	-	I-IV	Various	TCGA project	https://cancergenome.nih.gov	CNV, RAS, CMS, etc	PFI, OS

***Table 9**. CRC cohorts used in the study.*

2.17 In silico data

Two publicly available cohorts were used: Colonomics (NCBI BioProject PRJNA188510) and TCGA. The Colonomics cohort (cohort B) consisted of 98 paired adjacent-normal and tumor tissues from stage II microsatellite stable patients and 50 colon mucosae samples from healthy donors (246 samples in total). Gene expression data, assessed by Affymetrix Human Genome U219 expression array, had previously been analyzed [29]. For studies using the TCGA cohort (cohort F), we included all samples annotated as TCGA-colon adenocarcinoma (COAD) (n = 448) and 25 samples annotated as stage IV TCGA-rectum adenocarcinoma (READ), 473 samples in total. The classification of TCGA samples into four CMS was in agreement with Guinney et al. (209). Different survival event data were retrieved according to Liu et al. (210)

2.18 Statistics

Data coming from *in vitro* experiments are presented as mean ± S.D. of at least three independent experiments and statistical analysis was performed with Graphpad Prism V.4 software (San Diego, CA, USA). Comparisons among different experimental conditions were carried out through the student's t-test. Values of $p \leq 0.05$ were considered significant. The Graphpad Prism software was also used to calculate EC50 values for the MTT analysis (detailed in section 2.7.1).

For cohort survival analysis the survminer R packages were used. Kaplan–Meier curves depicting disease-free survival (DFS), time to progression (TTP), progression-free interval (PFI), and overall survival (OS) were accompanied with the log-rank test to verify significance in survival curve differences. The Cox regression hazards models were performed to quantify the effect of gene expression and survival (adjusted for age and stage). Differences in response to treatment were evaluated in cohorts D and E by contingency tables and chi-square or Fisher's exact tests as appropriate.

Regarding TCGA data, comparison between primary and normal tumor samples (gene expression and copy number alteration segment mean) were performed using paired samples t-tests. Both variables were compared using the Pearson correlation test. *CDK5* gene expression comparison between different CMS subtypes was performed using one-way ANOVA.

3 Results

3.1 Objective 1

3.1.1 Characterization of *CDK5* expression in human CRC

We studied the Cdk5 levels in 6 CRC patient cohorts available, as explained in the materials and methods section. We observed significant higher *CDK5* mRNA levels in tumor versus normal adjacent colon samples in two different data sets (Colonomics, cohort B, Figure 12A and TCGA, cohort F, Figure 12B). The Colonomics cohort consists of 98 stage II MSS CRC patients and from the TCGA we had paired expression data from 38 stage I-IV patients.

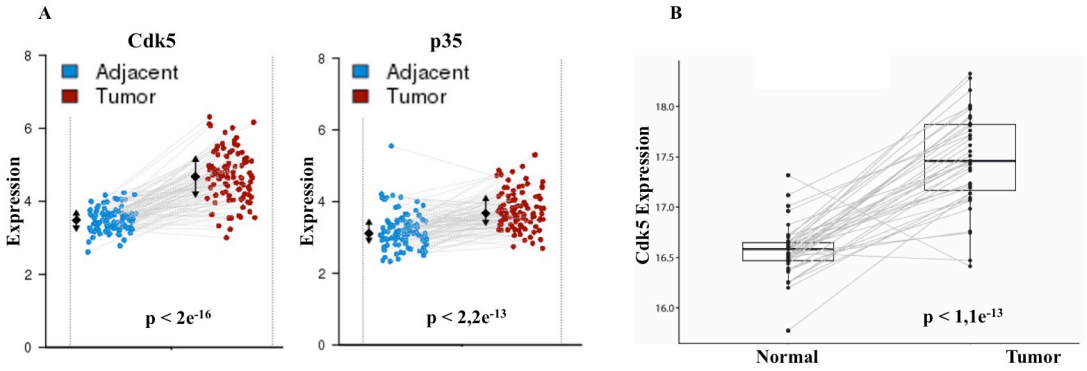

***Figure 12**. CDK5 expression in normal and tumoral tissues. (A) Graphic representation of CDK5 and p35 mRNA expression in 98-paired adjacent normal and tumor tissues from stage II microsatellite stable (MSS) CRC patients (cohort B). (B) Graphic representation of CDK5 mRNA expression in normal and tumor tissues of 38 I-IV CRC patients. Data were obtained from The Cancer Genome Atlas (TCGA) database (cohort F).*

In a cohort with 12 paired normal and tumour samples from stage IV CRC patients (cohort A) we found protein levels of Cdk5 and p35 to be increased in the malignant tissue as compared to the adjacent tissue (figure 13A-C). We could also detect Cdk5 protein by immunohistochemistry (IHC) in primary colorectal tumors from cohort D, consisting of 52 stage IV patients. In collaboration with pathologists the staining was scored as either negative or positive (weak and strong staining) (Figure 13D). A total of 75% of the tumors were positive for Cdk5 staining.

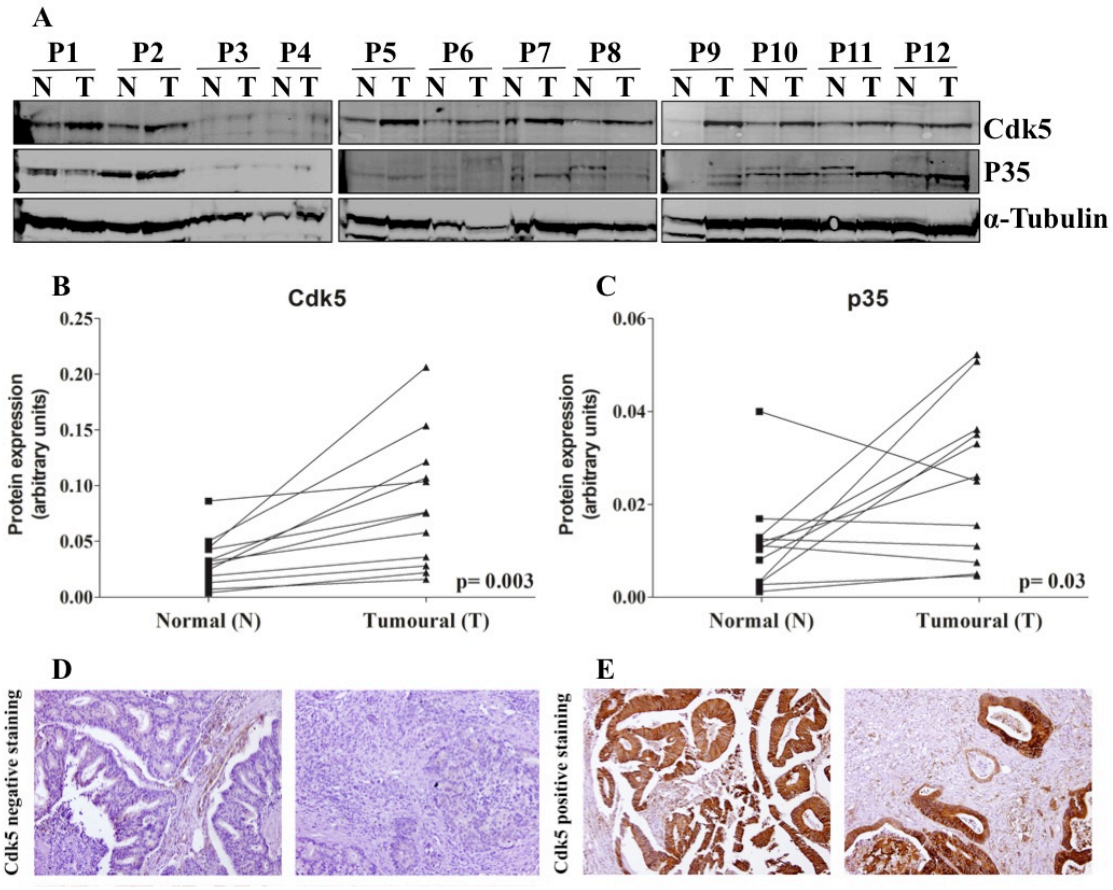

Figure 13. *Cdk5 protein levels in normal and tumoral tissues. Western blot (A) and graphic representation (B,C) of Cdk5 and p35 protein expression, respectively, in tumoral (T) and normal adjacent (N) tissues of 12 stage IV CRC patients (cohort A). Alpha-tubulin was used as endogenous control. The p-value was calculated by paired t-test. (D, E) Representative immunohistochemistry images of Cdk5 staining in CRC tumor tissues. Left negative staining (D) and right positive staining (E).*

We wanted to study further what was behind the increase in Cdk5 expression. Genomic rearrangements, such as copy number changes due to deletions or amplifications, are common in cancer and can drive its development through several mechanisms. Again, using TCGA data (cohort F), we analysed the *CDK5* gene CNV at region chr7:151054008–151057848. We observed a statistically significant increase ($p=7.59\times10-7$) in the *CDK5* copy number in primary tumors as compared to the corresponding adjacent normal colon tissues (Figure 14A). We found that the CNV of the *CDK5* gene was strongly correlated ($r=0.55$, $p=7.16\times10^{-7}$) to *CDK5* expression levels in tumor tissue (Figure 14B). Taking advantage of the Cancer Cell Line Encyclopedia database (Broad Institute), which among other information, contains cell line gene expression and copy number information, we studied a panel of 63 CRC cell lines. As expected, we found that there was a clear correlation between *CDK5* expression and

CNV also in cell lines (r=0.54, p=4.6x10^{-6}) (Figure 14C). Hence, the higher expression of *CDK5* in CRC is mainly due to a gain in copy number of the gene.

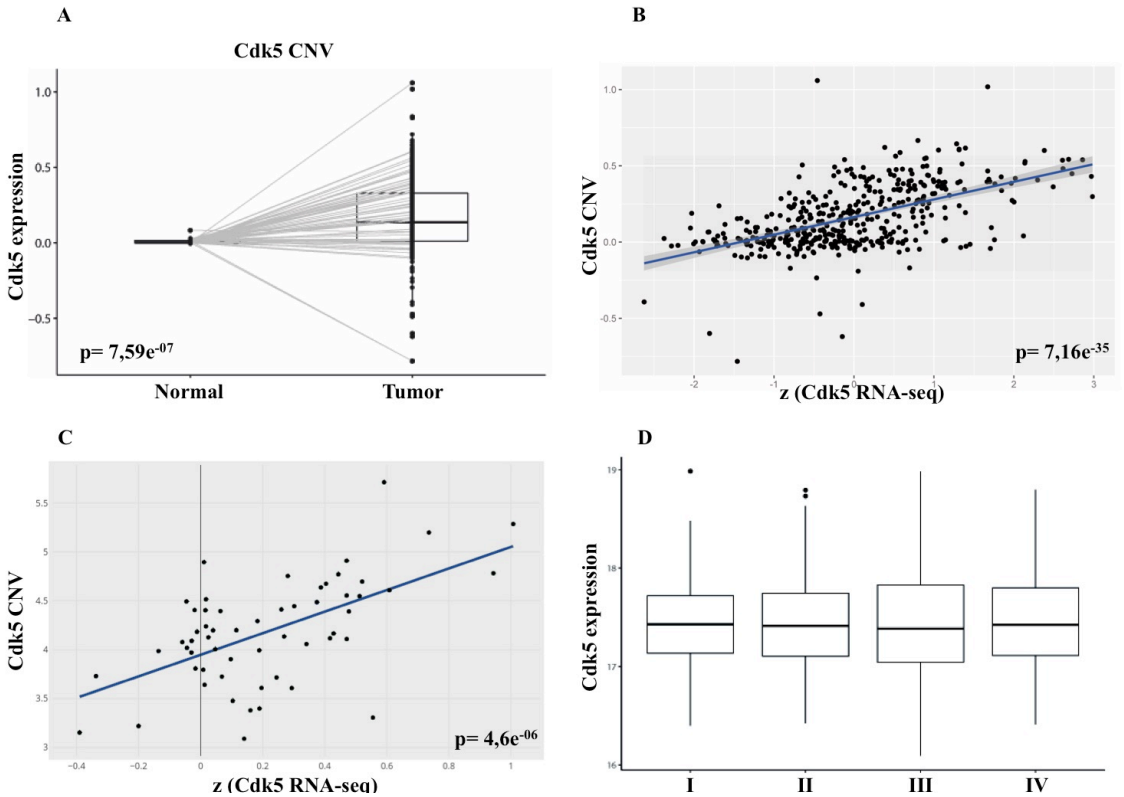

***Figure 14**. CDK5 copy number gain. (A) Graph representing the CDK5 copy number (CNV) change between normal and tumoral tissues in 67 stage I–IV CRC patients (cohort F). (B) Correlation between CDK5 CNV and CDK5 gene expression in 473 stage I–IV CRC patients. p-value according to Pearson correlation test (cohort F). (C) Correlation between CDK5 CNV and Cdk5 gene expression in 63 CRC cell lines. The p-value was according to Pearson correlation test. Data from the Broad Institute Cancer Cell Line Encyclopedia. (D) CDK5 expression in 473 stage I–IV CRC patients (cohort F).*

Having seen that the Cdk5 mRNA and protein levels are generally higher in tumor tissue compared to normal tissue, we studied whether it increases gradually with disease progression. For this we used the TCGA cohort (Cohort F), which consists of local and advanced disease patients. As can be seen in figure 14D *CDK5* mRNA levels do not differ depending on disease stage, suggesting that the *CDK5* copy number gain probably is an early event in CRC development and apparently, it is not selected along the progression process.

We also wanted to study whether Cdk5 levels differed between primary and metastatic lesions. Unfortunately, due to the lack of paired biospecimens very few larger cohorts exist. According to the Human Cancer Metastasis Database (http://hcmdb.i-sanger.com/index), which collects microRNA and RNA sequencing data from Gene Expression Omnibus (GEO) at the National Center for Biotechnology Information

(NCBI), the biggest cohort with matched samples consist of 18 patients analysed by cDNA microarray (211). When we compared the levels of Cdk5 between primary tumors and metastasis we did not find any differences (P=0,941).

In the process of characterizing Cdk5 in CRC we also took advantage of the CRC TCGA dataset (cohort F) to perform a gene set enrichment analysis (GSEA). This is a computational method that determines if there is a correlation between pre-defined sets of genes and expression of a specific gene or phenotype. This represents a very common and useful method to gain insights into which biological process and pathways a given gene is related to. We found 14 gene sets to be positively correlated with *CDK5* expression with FDR q-values below 0,05 (figure 15). The analysis of the leading edge shows that for the Anastassiou cancer mesenchymal transition signature (GSEA M2572), which contain known EMT genes such as Snail, Slug and Fibronectin, as many as 83% of the genes are positively correlated with *CDK5* and contribute to the enrichment score, as can be appreciated in figure 15.

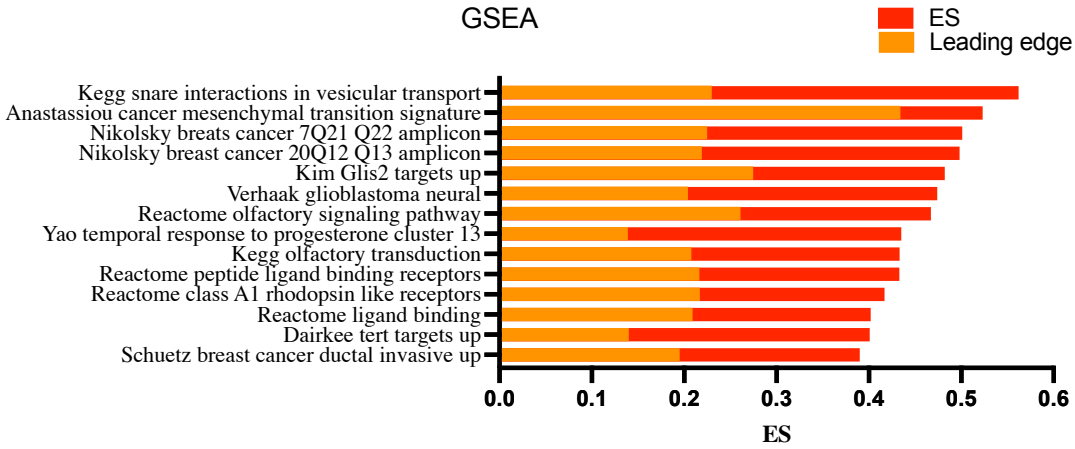

Figure 15. *Gene set enrichment analysis (GSEA) of correlations with Cdk5 in the TCGA cohort (Cohort F). Displayed are gene sets with FDR q-values above 0,05. (ES) Enrichment score.*

In summary, we have here shown a clear increase of *CDK5* mRNA and protein levels malignant tissue compared to normal adjacent. We believe this is an early event in the CRC progression as we observed no differences in the Cdk5 levels when comparing different disease stages and primary and metastatic lesions. This increase is most likely due to a *CDK5* copy number gain.

3.2 Objective 2

3.2.1 *In vitro* characterization of Cdk5 in key aspects of cancer progression

Now we wanted to confirm that Cdk5 was also present in our CRC cell lines. We studied a panel of 10 cell lines where it was observed that both Cdk5 and its activator p35 were present at high levels in all cell lines (Figure 16).

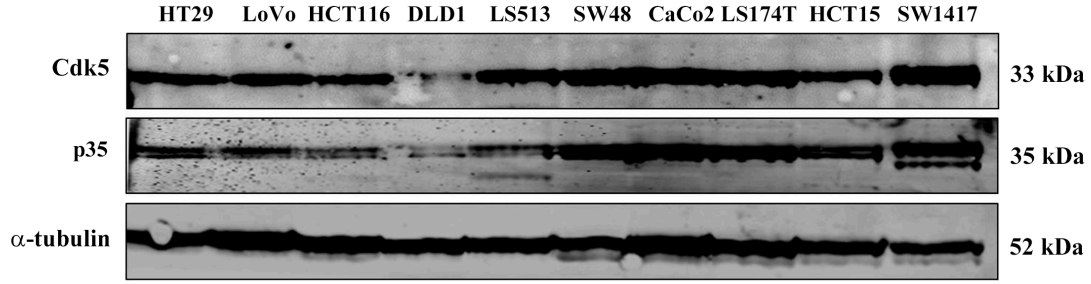

Figure 16. *Cdk5 and p35 in CRC cell lines. Western blot analysis of Cdk5 and p35 basal protein levels in a panel of 10 CRC cell lines. Alpha-tubulin was used as endogenous control.*

Then, we wanted to determine whether it was indeed also active in these cells. It was intended to determine the degree of Cdk5 Tyr15 phosphorylation, which is a marker for kinase activation (212). However the epitopes against which these antibodies are raised, are highly homologous between Cdk1, Cdk2 and Cdk5 making the detection of solely Cdk5 Tyr15 phosphorylation extremely difficult and confusing. We decided to use an alternative strategy aimed at detecting the binding of Cdk5 to its main activator p35, or its cleaved form p25, by co-IP with protein G coupled magnetic beads. This technique allows isolating Cdk5 along with any protein bound to it. We found that Cdk5 in HT29, LoVo, HCT116 and DiFi cell lines is primarily bound to p25, as p35 cannot be detected (see figure 17). As mentioned in the introduction, different to p35 the truncated p25 is not bound to the membrane and the p25-Cdk5 complex has a longer activation period. This indicates that the complex is highly active and could move freely within the cell to phosphorylate its substrates.

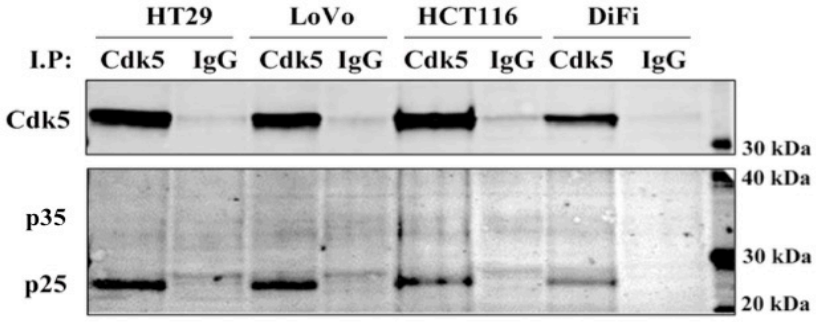

Figure 17. *Representative WB images showing the co-immunoprecipitation (IP) of Cdk5 and p35/p25 in the indicated cell lines. Co-IP with an immunoglobin G (IgG) antibody was used as a negative control. The results were obtained from at least three independent experiments*

When performing our in vitro studies we observed that the protein levels varied greatly depending on the time of cell collection, so we decided to study this further. As can be seen in figure 18A-D protein levels of Cdk5 and p35 increased greatly with time after cell seeding in HT29, LoVo and HCT116 cell lines. Protein levels are ultimately a result of transcription, translation and turnover, all processes that are tightly regulated. We therefore examined the gene expression levels of Cdk5, which were also increasing (figure 18E-G) during the 4-day cell culture, however not too the same degree as the protein levels. Thus, it is most likely a result of both increased transcription and a decrease in protein turnover. In order to understand why we were observing this we tested whether it depended on cell confluence, factors accumulating in the media or lack of nutrients. Nevertheless, the same pattern could be observed at the different time points independent of cell number, daily medium changes and medium addition (data not shown).

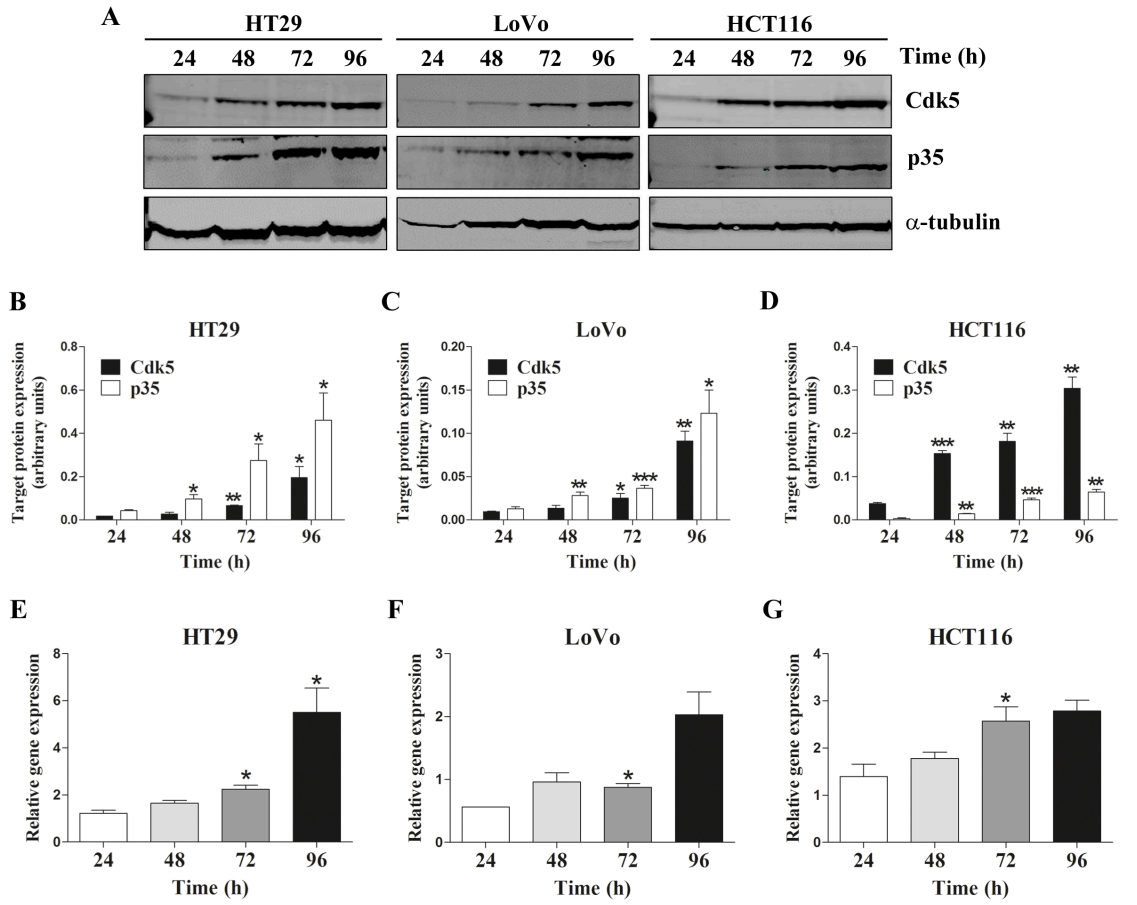

***Figure 18**. Cdk5 expression at different time points after cell seeding. (A) Representative Western blot images of Cdk5, p35 and endogenous control α-tubulin at 24, 48, 72 and 96 hours after cell seeding of the indicated cell lines. (B-D) Graphics showing the protein quantification of three independent experiments. (E-G) Graphics showing the Cdk5 gene expression at 24, 48, 72 and 96 hours after cell seeding of the indicated cell lines. Student's t-test was used to evaluate differences between time points. *p-value<0,05, **p-value<0,01, ***p-value<0,001.*

Three important characteristics of cancer progression are proliferation, migration and invasion. In other solid tumors Cdk5 has been linked to all three processes. To study the importance of Cdk5 in relation to cell proliferation we transiently silenced the gene by siRNA. Cells with gene inhibition (between 70-90%), a negative control of the transfection (siNTC) along with the Mock (DNA free transfection) were seeded and left to proliferate for up to 96H. At different time points cells were permeabilized with Triton X-100 and stained with Propidium iodide, which is a fluorescent agent binding to DNA. Hence, the fluorescent signal is proportional to the number of cells. We saw that for the HT29, LoVo, HCT116 and DiFi cell lines the presence of Cdk5 did not affect the cell proliferation significantly (Figure 19).

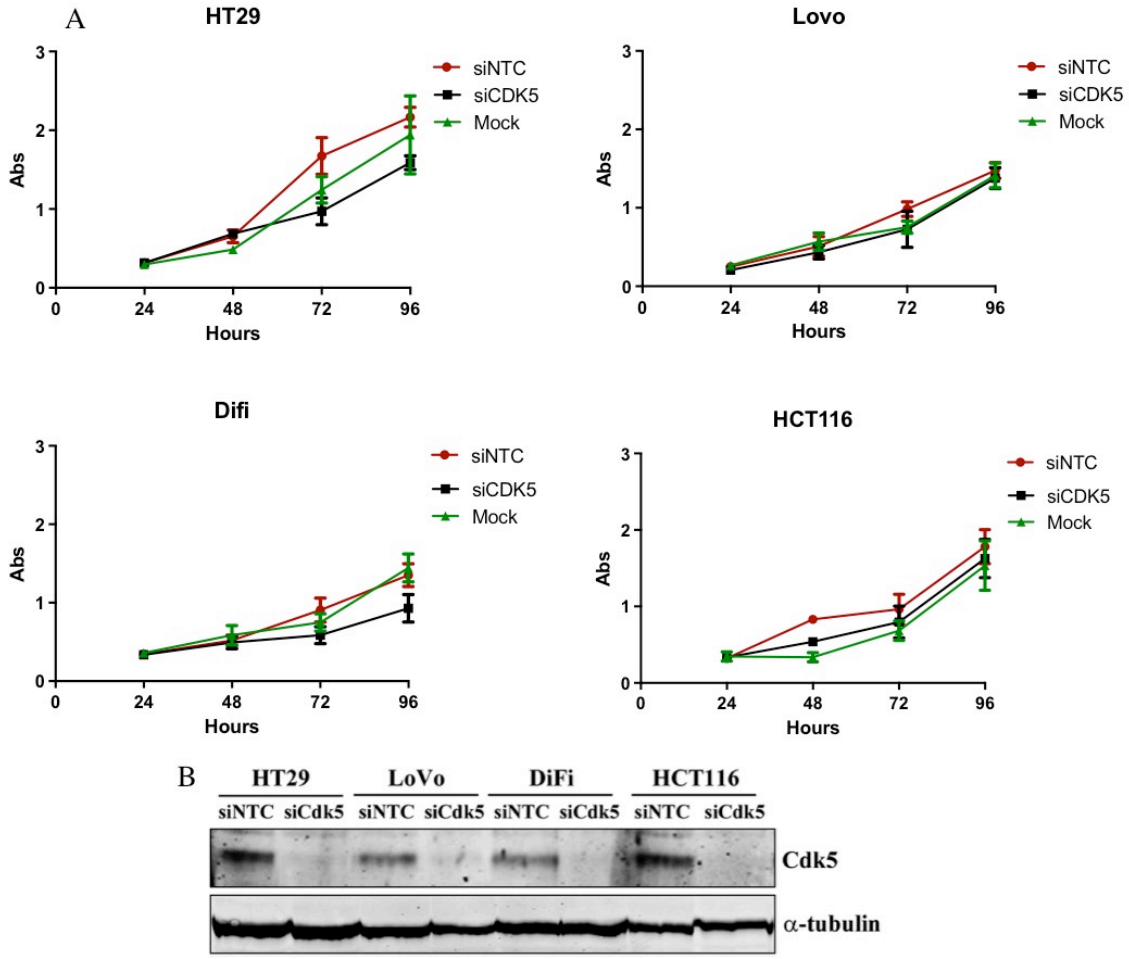

Figure 19. *Cdk5 and cell proliferation. (A) Graphic representation of HT29, LoVo, DiFi, and HCT116 time-dependent cell proliferation after Cdk5 gene silencing measured by propidium iodide (PI). Student's t-test was used to evaluate differences between conditions. (B) Western blot showing the degree of siRNA Cdk5 silencing. Experiments with silencing above 70% were included. α-Tubulin was included as endogenous control. Degree of silencing was calculated by referencing to the siNTC Cdk5 band after normalizing to the endogenous control.*

Again using the cells with siRNA Cdk5 silencing we studied whether the presence of Cdk5 affected the migration and invasion. This was done using Transwell assays where cells are seeded above a porous membrane, and stimulated to migrate by higher FBS concentrations in the bottom chamber. To create an invasion assay the pores in the membrane are covered with a gel composed of extracellular matrix proteins meant to simulate the typical matrices that tumour cells encounter during the invasion process. We found significantly reduced migration and invasion in HT29 and LoVo siCdk5-transfected cell lines as compared to siNTC cells. In contrast, silencing of Cdk5 did not decrease the migration and invasion ability of DiFi cells (Figure 20). As HT29 and LoVo cell lines harbour mutations in genes (*BRAF* and *KRAS*, respectively), downstream of the EGFR, constitutively activating the mitogen activated protein kinase (MAPK) signalling pathway, and the DiFi cell line is considered to be wild type, we wondered whether this fact could be behind the observed differences. We took advantage of another *KRAS* WT cell line SW48 that was engineered to express a mutant form of *KRAS* (G12D). Cdk5 silencing caused a modest but statistically significant decrease in migration only in the SW48 *KRAS* G12D cell line and not in the *KRAS* WT. No differences in invasion ability after Cdk5 silencing were observed in either SW48 cell line.

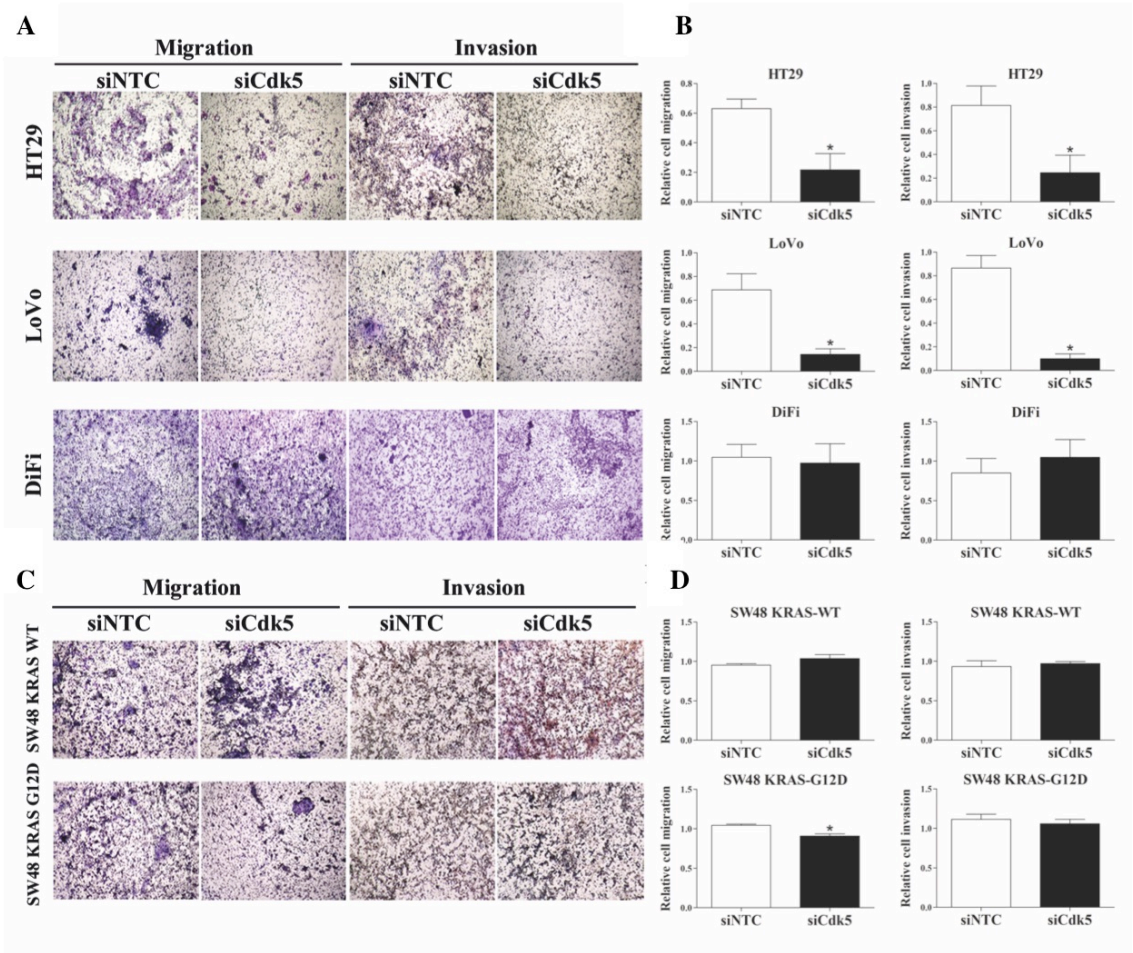

Figure 20. *Cdk5 in cellular migration and invasion. (A,C) Representative Boyden chamber migration and invasion assays images (4× magnification) and (B,D) bar graphs showing (mean ± S.D.) relative cell migration and invasion after Cdk5 silencing in the indicated cell lines. * p-value < 0.05 relative to control cells siRNA non-target control (siNTC) tested by Students t-test. The results were obtained from at least three independent experiments.*

Another important characteristic of cancer cells is their ability to undergo an unlimited number of divisions. To study the implications of Cdk5 in the long-term clonogenic capability of CRC cells, we performed colony formation assays in the HT29 and LoVo cell lines with the siRNA silenced cells. Even though the silencing with this technique is transient, we controlled that the inhibition of Cdk5 was maintained. As can be visualized in figure 21A, even with the lowest siRNA concentration (5nM), the Cdk5 silencing resulted in above 70% inhibition for at least 96h. It is indeed in this period that the clonogenicity is pivotal. We observed a decrease in the number of colonies for siCdk5-transfected cells compared to siNTC cells in both lines, however, these were only sta-

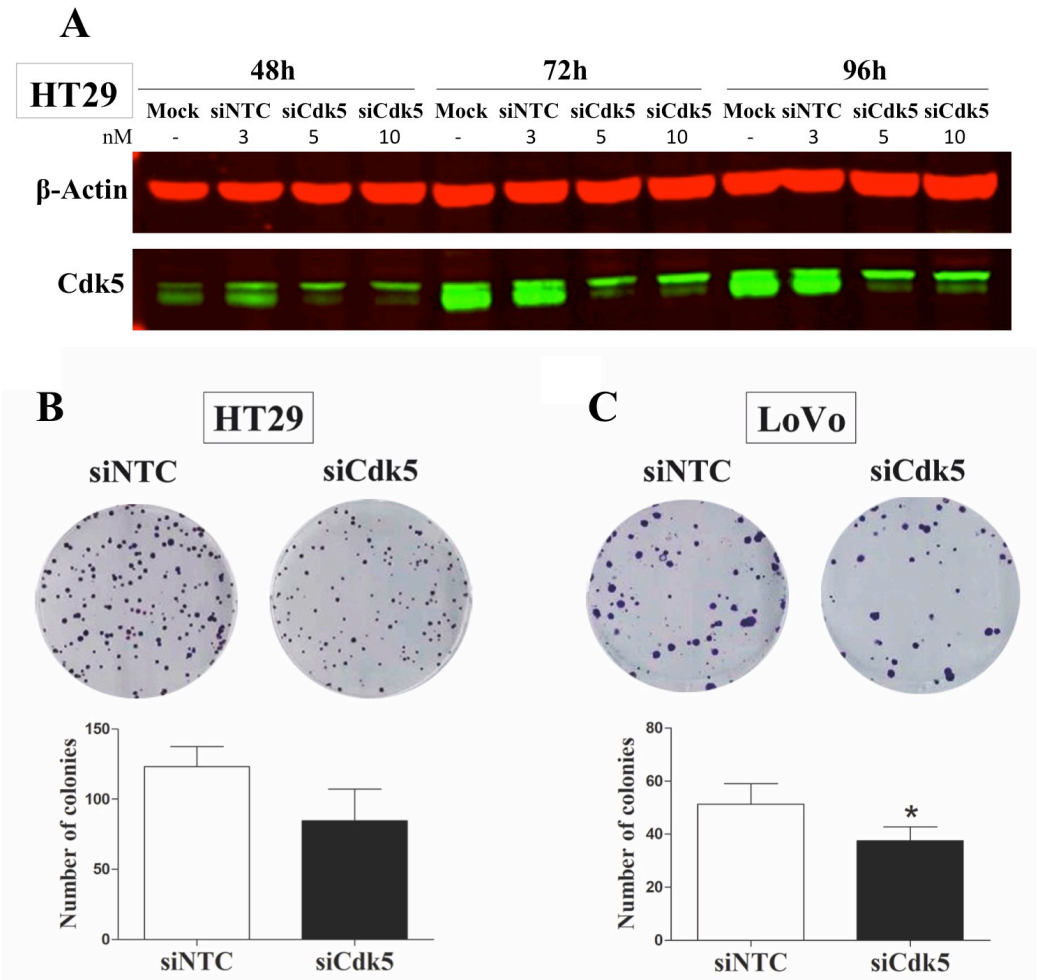

Figure 21. *Cdk5 in colony formation. (A) Western blot image showing the siRNA silencing efficiency of Cdk5 at 48, 72 and 96h in HT29 cells with the indicated concentration of siRNAs. . Degree of silencing was calculated by referencing to the siNTC Cdk5 band after normalizing to the endogenous control (B) Representative images of colony formation in HT29 and LoVo cells after siRNA silencing. Results were obtained from at least three independent experiments. Statistical differences were determined by students t-test. *p-value < 0.05.*

tistically significant for the LoVo cells (p-values 0.198 and 0.046, respectively), as can be seen in Figure 21B.

Studying Cdk5 in our CRC cell lines, we have confirmed the presence of this kinase and its activator p35. Interestingly when precipitating this complex we found that Cdk5 was mainly bound to p25, indicating a hyperactivation. When studying the importance of Cdk5 in different pocesses of cancer progression, we found that the proliferation is not affected, while migration, invasion and colony formation is decreased in the HT29 and LoVo cells upon *CDK5* silencing. This is however not the case for the *KRAS/BRAF* WT cell lines Difi and SW48, where migration and invasion is not affected, suggesting that Cdk5 plays an important role in particular when this pathway is continuously active.

3.3 Objective 3

3.3.1 Transcriptional effects of *CDK5* knock down

To continue our *in vitro* studies we decided to develop a cellular model with a permanent inhibition or down regulation of Cdk5. At this time the CRISPR/Cas9 technique was becoming more widely accessible, and we decided on this strategy. As can be visualize in figure 22 we achieved a high degree of knock down (KD), which was maintained during passaging of the cells. Having a stable KD of *CDK5* did not affect the proliferation of any of the silenced cell lines, as the doubling times remained unaffected, confirming the previous proliferation studies carried out with the siRNA approach.

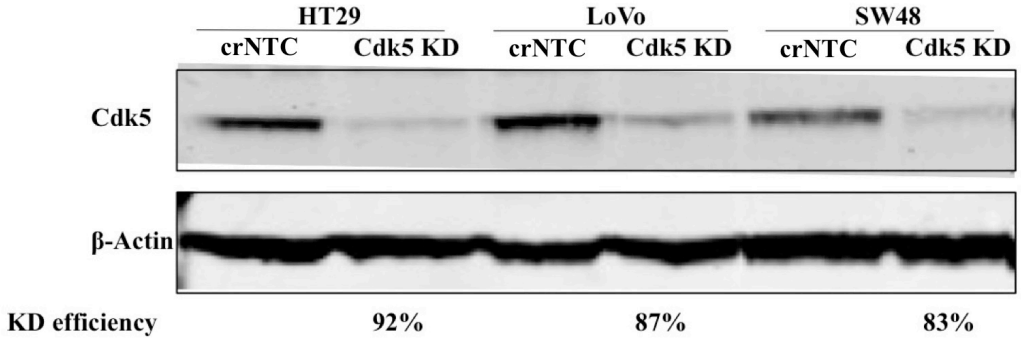

***Figure 22**. CRISPR/Cas9 KD of Cdk5. Representative Western blot images showing the Cdk5 protein levels. β-actin was used as endogenous control. Degree of KD was calculated by referencing to the crNTC Cdk5 band after normalizing to the endogenous control.*

An important part of our characterization was to gain information about the cellular signaling effects of *CDK5* KD along with its direct and indirect interactions. We also wanted to study whether this differed between cell lines with different characteristics, such as CMS and EGFR-pathway mutational status. For this study we used 3 of the Cdk5

KD cell line pairs generated with the CRISPR/Cas9 technique, HT29, LoVo (in which the Cdk5 silencing led to a decreased invasion and migration) and SW48 (in which the Cdk5 silencing did not reduce invasion and migration).

The RNAseq was carried out at the CNAG and the data passed their quality control pipeline, was mapped and quantified. A differential expression analysis (DE) was carried out, comparing each CRISPR/Cas9 non-target control (crNTC) cell lines with the *CDK5* KD cell line. The first thing we did was to confirm the transcriptional KD of *CDK5* in our 3 cell lines, which was 62% in the case of SW48, 68% in HT29 and 71% in LoVo cells. Of note, by western blot we had observed higher levels of KD. It is possible that reads mapped to the 3' end of the gene prior to the site complementary to the first CRIPSR gRNA increase the total gene count.

In order to understand the biological processes related to Cdk5 we carried out a gene enrichment analysis. Genes have been grouped together in gene sets (KEGG, Gene ontology, Reactome etc.) based on their involvement in the same biological pathway facilitating the biological translation of large identification. With this analysis we can get an overview of pathways, which are up or down regulated in the *CDK5* KD cells compared to the control. When we looked for enriched datasets among the up- or down-regulated genes we found no overlap between the 3 cell lines. Looking at the gene sets in the down regulated genes we found 5 that were both significant in LoVo and SW48 cells, namely Cellular response to chemical stimulus, Biological adhesion, cell adhesion, Extracellular region and Rheumatoid arthritis. Noteworthy, Biological adhesion and Cell adhesion also came up as significant in the up regulated genes in the LoVo cell line. These are large dataset with more than thousand genes, why it is possible that a number of these genes are up regulated and others down regulated when Cdk5 is removed. Hence, it cannot be concluded whether cell adhesion is up or down regulated, however genes from these gene sets are clearly affected by the *CDK5* KD.

Then we turned our attention to single gene changes. The Venn diagram shows the genes with a Fold change (FC) gene expression of 1,5 or above upon *CDK5* KD (Figure 23). The biggest impact of *CDK5* KD could be seen in the LoVo cell line, where 1004 and 459 genes where up-regulated or down-regulated, respectively. In the diagram it can also be appreciated that the LoVo cell line shows similarities to both HT29 and SW48 while few changed genes are common between HT29 and SW48. This could be related to the fact that both LoVo and SW48 are MSI and that LoVo and HT29 are *KRAS* and *BRAF* mutated, respectively, placing the LoVo cell lines somewhat in between the other two cell lines.

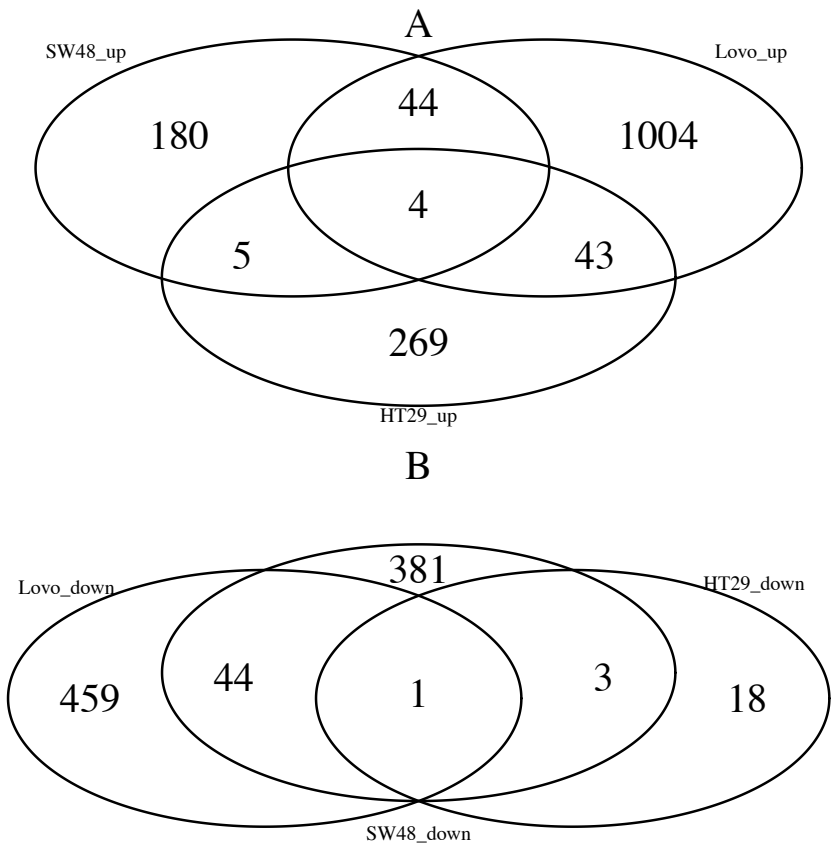

Figure 23. *Venn diagram of differentially expressed (DE) genes after Cdk5 KD. (A) Upregulated genes with Fold change (FC) above 1,5. (B) Downregulated genes with FC below -1,5.*

Using a criterion of a minimum of 1,5 gene FC upon *CDK5* KD we found 4 genes to be upregulated, *VSNL1, NCMAP, PLEKHA4* and *ATP8B3* in all 3 cell lines and none to be downregulated (besides Cdk5 itself) (Table 10). Apart from *VSNL1*, a neuronal calcium sensor protein, none of the genes have been related to cancer. VSNL1 has been shown to inhibit EMT and migration in squamous carcinoma (213, 214), while in CRC it has been linked with high rate of lymph node metastasis and poor prognosis (215). Grouping only 2 cell lines we logically found a lot more genes to have FC above 1,5, specifically 104 upregulated and 50 downregulated. We then applied a second arbitrary filter of a FC above 2 in both cell lines to find the genes with the highest changes in expression (up or down) in the cell lines upon *CDK5* KD (Table 10).

RNAseq	HT29		LoVo		SW48	
	FC	P adj.	FC	P adj.	FC	P adj.
HT29, LoVo and SW48 (FC>1,5)						
VSNL1	8,68	2,7E-07	1,66	7,3E-50	1,83	3,3E-111
NCMAP	1,93	1,8E-02	2,22	6,9E-04	2,00	3,0E-02
ATP8B3	1,65	2,8E-02	1,81	6,7E-06	2,44	4,9E-09
PLEKHA4	1,52	6,0E-03	4,37	3,9E-45	2,38	2,4E-04
CDK5	-3,13	1,46E-52	-3,55	1,60E-60	-2,67	7,67E-43

HT29 and LoVo (FC>2)						
ADGRV1	18,13	2,8E-02	3,41	3,8E-06		
SMIM31	10,90	3,6E-02	5,13	2,7E-02		
ABCB1	8,51	1,8E-05	3,28	1,6E-134		
CALD1	6,73	4,0E-03	2,53	7,9E-120		
CDK14	4,47	2,4E-02	2,70	2,0E-31		
DNAJC12	3,22	9,0E-03	4,64	8,5E-04		
TTLL7	2,86	8,8E-08	3,08	1,4E-30		
ISG20	2,85	5,5E-05	2,11	1,7E-03		
RNASE4	2,80	3,3E-02	2,43	3,9E-02		
TMEM140	2,68	5,0E-03	3,82	5,7E-12		
SLC16A4	2,58	2,9E-02	9,78	3,9E-10		
TPPP3	2,29	1,1E-02	8,00	3,9E-07		
TENM3	2,09	3,5E-02	2,19	5,0E-42		
INSC	2,08	8,0E-03	5,34	3,0E-03		
TUBA1A	2,04	1,2E-04	3,88	6,0E-29		
HT29 and SW48 (FC>2)						
LoVo and SW48 (FC>2)						
DLC1			8,14	2,6E-06	2,83	4,9E-02
RAMP1			6,53	6,9E-07	4,79	6,9E-05
DHRS2			5,51	2,9E-248	4,54	8,7E-254
MSR1			4,38	2,9E-05	15,18	1,9E-02
PLEKHA4			4,37	3,9E-45	2,38	2,4E-04
METTL7A			4,33	1,7E-10	6,42	5,2E-03
CA12			2,89	1,2E-72	4,11	4,5E-11
ESAM			2,71	1,2E-73	2,01	6,3E-16
SP5			2,68	1,0E-05	4,86	3,5E-57
CGNL1			2,51	1,7E-06	2,35	1,1E-03
APBA2			2,48	3,0E-02	2,21	4,0E-03
VIL1			2,32	3,5E-11	2,25	8,0E-03
GOLT1A			2,22	2,1E-02	2,42	8,1E-03
CALB2			2,04	1,7E-06	2,13	2,3E-02
ASB4			2,03	1,4E-21	5,35	0,0E+00
PCDH7			-7,60	2,3E-13	-2,12	5,0E-03
HLA-DPA1			-7,26	0,0E+00	-15,88	3,8E-17
FBN2			-5,92	8,1E-53	-2,25	1,8E-02
CD74			-4,65	0,0E+00	-9,14	4,8E-02
WDR72			-4,27	3,5E-22	-2,14	4,2E-03
ANO1			-3,77	2,9E-22	-4,00	5,3E-10
NTRK2			-3,34	3,5E-170	-2,08	3,0E-02
VWA2			-3,05	5,0E-58	-2,54	1,1E-03
SYT1			-2,88	1,5E-59	-2,19	9,1E-03
MME			-2,18	1,2E-06	-2,18	2,3E-38

Table 10. *RNAseq results of CDK5 KD cell lines. Genes with FC>(-) 1,5 (3 cell lines) or FC> (-) 2 (2 cell lines) included.*

We used the Cancertool website to study the correlations between the selected genes with FC above 1,5 in three cell lines or FC above 2 in two cell lines (Table 10) and CDK5 in CRC tumors (http://genomics.cicbiogune.es/CANCERTOOL/). This website gathers information from 7 publicly available CRC datasets with mRNA data. We looked for genes that were upregulated in the KD cell lines that had a negative correlation with Cdk5 in tumor tissues, while for genes downregulated in the KD cell lines we looked for a positive correlation. *CALD1* and *METLL7A* were upregulated with a FC above 2 in two cell lines, and also inversely correlated with Cdk5 in all datasets (except *CALD1* that was non-significantly positively correlated in the Colonomics dataset) (Figure 24A). We furthermore checked whether any of these genes had prognostic value in the CRC TCGA cohort in a similar direction as *CDK5 (Figure 24B-C)*. High *CALD1* had poorer OS (p=0,013), just like *CDK5* (according to the literature (146) and our results (see below), which contradicts the inverse relation. Patients with low *METTL7A* expression had poorer OS (p=0,035), in concordance with the fact that patients with high *CDK5* have poorer OS.

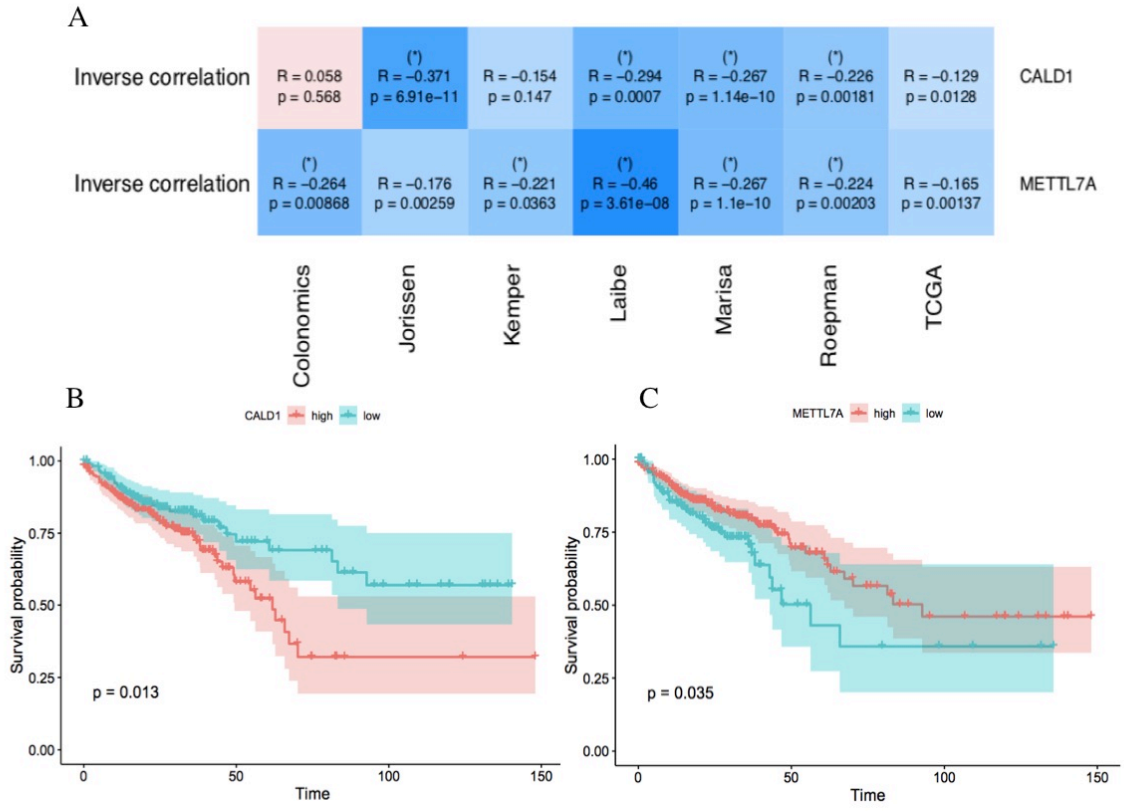

Figure 24*. Caldesmon and METTL7A correlations with CDK5 and prognostic values. (A) Inverse correlations between CDK5 and METLL7A/CALD1 in 7 different publically available CRC datasets. *R>0.2. (B,C) Kaplan Meier and log-rank test analysis of survival probability in the TCGA COAD of patients with high and low CALD1 and METTL7A expression.*

METTL7A is an integral membrane protein anchored into the endoplasmic reticulum membrane where it recruits cellular proteins for lipid droplet formation (216). METTL7A is downregulated in all stages of colorectal cancer (Colonomics.org, CanSarBlack icr.ac.uk). Scarce information exists about the involvement of METLL7A in cancer, however one study in thyroid cancer describes how METTL7A transcription is repressed through gene body methylation by Enhancer of zeste homolog 2 (EZH2), a subunit of polycomb repressor complex 2 (217). According to Cancertool a very positive correlation exists between *CDK5* and *EZH2* in CRC. Interestingly, EZH2 has been shown to be phosphorylated by Cdk5, which leads to its degradation (218). On this basis we wished to study further the relation between Cdk5 and METTL7A, possibly though EZH2. We started out validating *METTL7A* by qPCR, and confirmed upregulation in the LoVo (3,6 fold) and SW48 (2,8 fold) cell lines upon *CDK5* KD (figure 25). We furthermore checked *EZH2* transcription, however, just like in the RNAseq results no difference could be observe between the control and KD cell lines (data not shown). We continued on to study METT7LA by western blot however in spite of trying several antibodies we were unable to detect the protein due to very low specificity.

The *CALD1* gene encodes for Caldesmon, a Calmodulin binding protein, which plays an essential role in the regulation of smooth muscle and non-muscle contractions, where it stabilizes actin filaments (219). Just like *METTL7A, CALD1* is also transcribed at lower levels in all stage of CRC cancer compared to normal tissue (Colonomics.org, CanSarBlack icr.ac.uk), which is in concordance with the inverse relation with *CDK5*. In cancer Caldesmon has been related to EMT in several studies (166, 220). Interestingly, Cdk5 has been shown to regulate cell motility in melanoma partly through Caldesmon. In melanoma cells *CDK5* KD was accompanied by dephosphorylation and overexpression of *CALD1* inhibiting invasion/migration, colony formation, and anchorage-independent growth (166). We observe the same characteristics in our *KRAS/BRAF* mutated cell lines, regarding cell motility and *CALD1* overexpression upon *CDK5* KD. Hence, we wanted to study the relation between Cdk5 and Caldesmon further. We started out confirming our RNAseq results by qPCR, as *CALD1* was upregulation in HT29 (3,7 fold) and LoVo (4 fold) (Figure 25). Despite trying several antibodies for Caldesmon, we only got very weak bands, making it very difficult to evaluate whether the upregulation we observe at transcriptional level is indeed also translated into higher protein levels.

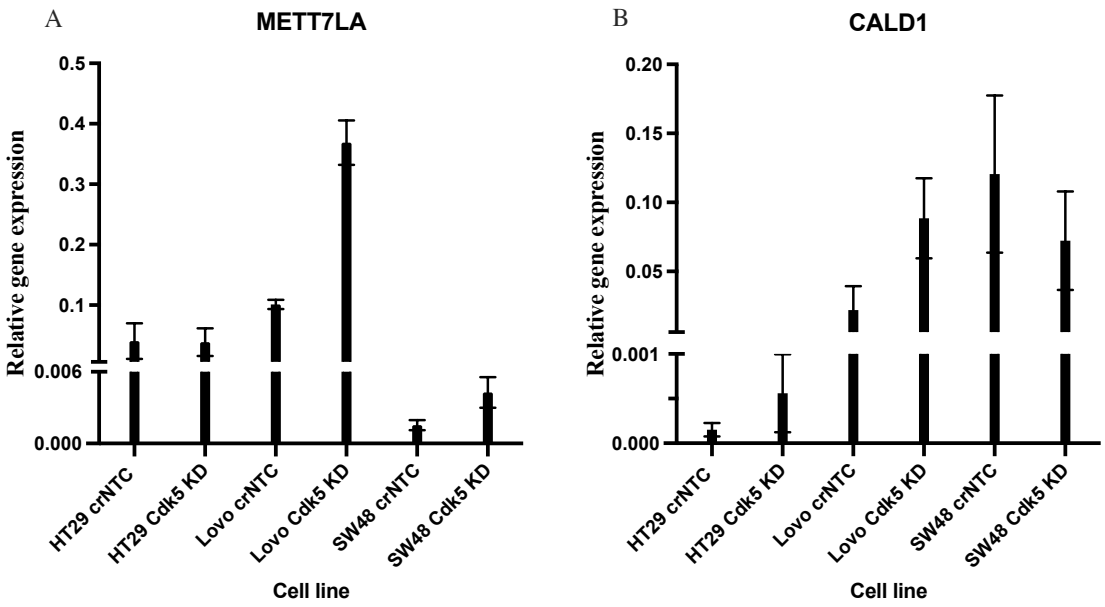

***Figure 25**. METTL7A and CALD1 gene expression in crNTC and CDK5 KD cell lines. (A,B) Validation of METTL7A and CALD1 uprgeulation upon CDK5 KD by qPCR. 3 independent experiments were carried out and the FCs were calculated based on average gene expression.*

With our RNAseq study we have shown high transcriptional effects of the *CDK5* KD in 3 very different and representative CRC cell lines. In the gene enrichment analysis, we found cell adhesion gene sets to be affected by the *CDK5* KD. When studying individual DE genes, we chose the ones affected in two or three of the cell lines, in order to assure broad relevance of the findings, ruling out effects limited to one cell line. When looking at the individual DE genes we focused on the ones with appropriate correlations (respective the RNAseq result) in at least 4 out of 7 CRC datasets, namely *METLL7A* and *CALD1.* Both represent interesting connections with Cdk5 and ongoing experiments are aiming at describing these further.

3.4 Objective 4

Objective 4a

3.4.1 Prognostic value of Cdk5

An important part of translational cancer research is to evaluate whether *in vitro* findings indeed have applicability in the clinical practice. We wondered whether Cdk5 expression could be a good prognostic and/or predictive biomarker in CRC patients. To study this possibility, we used several of our 6 cohorts with clinical patient history in which the expression of Cdk5 was determined depending on pre-existing data or type of available material (TMA, RNA): IHC (in TMAs), microarray (in the case of data coming from the Colonomics database), qPCR (RNA from tissue) or RNAseq (in the case

of data coming from the TCGA) (Table 9). Data was categorized into high and low Cdk5 expression groups as follows: In cohorts using continuous data (cohorts B, C and F), patients were assigned to low or high groups according to Cdk5 values below or above the median, respectively; in those using categorical data (cohorts D and E), patients were grouped as low when IHC staining was negative or weak and as high when it was strong (Figure 13D-E).

The prognostic value of *CDK5* expression was studied in two highly homogenous cohorts of localized microsatellite stable (MSS) CRC cancer patients (cohorts B and C, Table 9). Patients from cohorts B and C were diagnosed with stage II or stage III cancer, respectively, underwent surgery and did not receive any adjuvant treatment. In both the cohorts, high *CDK5* levels were associated with shorter disease-free survival (DFS) (p=0.049, 95% confidence interval (CI) 0.98–5.88 for cohort B and p=0.048, 95%

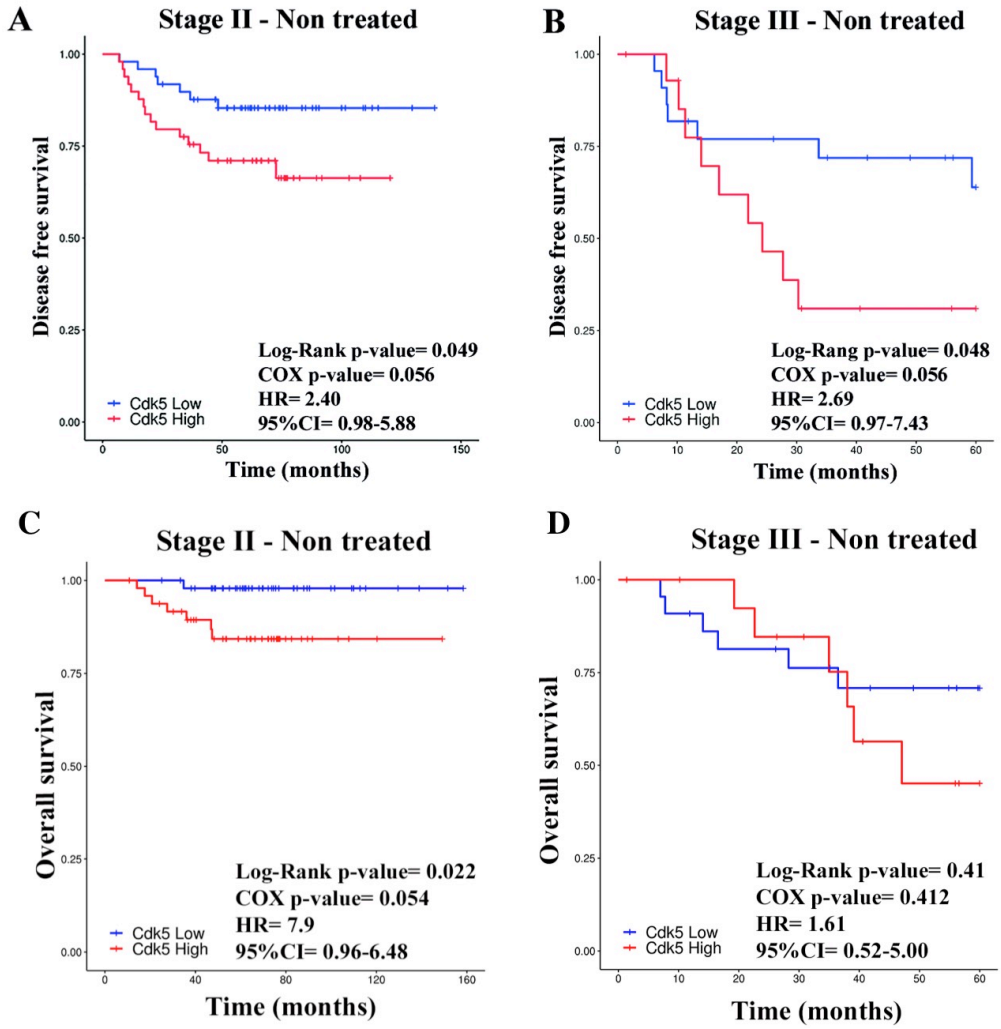

Figure 26. *Kaplan–Meier analysis of disease free survival (DFS) and overall survival (OS) depending on CDK5 levels. (A) DFS in 98 stage II CRC patients split by the median of CDK5 expression (cohort B). (C) DFS in 37 non-treated stage III CRC patients split by the median of CDK5 expression (cohort C). OS in 98 stage II CRC patients split by the median of CDK5 expression (cohort B). (D) OS in 37 non-treated stage III CRC patients split by the median of CDK5 expression (cohort C).*

CI 0.97–7.43 for cohort C) (Figure 26A-B), and also with overall survival (OS) in cohort B (p=0.022, 95% CI 0.96–6.48), while no differences could be observed in OS in cohort C (Figure 26C-D).

We had previously observed a difference in the effect of Cdk5 silencing in cell lines depending on their *KRAS* mutational status when studying the migration and invasion of the cells. Furthermore, it has been reported that Cdk5 is involved in the signaling cascade downstream of the EGFR receptor [7]. Thus, we wanted to know whether there was a difference in the prognostic value of Cdk5 according to *KRAS* mutations. Patients from cohort B, containing stage II patients, were split according to *KRAS* mutational status (WT or mutated) and *CDK5* expression was again categorized as high or low. In the *KRAS* WT group, patients with high or low *CDK5* levels had similar DFS; however, in the group with *KRAS* mutated, high Cdk5 levels predicted a statistically

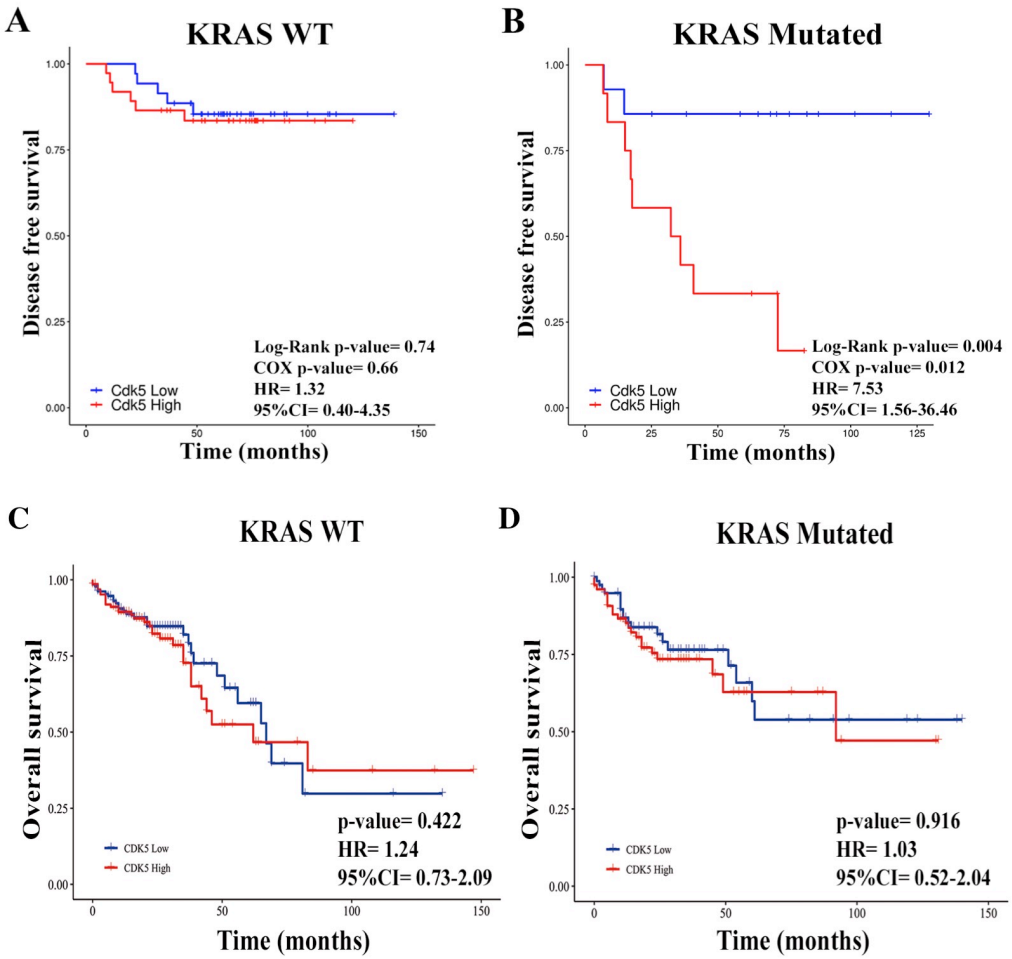

***Figure 27**. Kaplan–Meier analysis of disease free survival (DFS) and Overall survival (OS) depending on Cdk5 expression and Kirsten rat sarcoma oncogene (KRAS) mutational status. (A) DFS for 72 stage II CRC patients with wildtype (WT) KRAS and split by the median of Cdk5 expression. (B) DFS for 26 stage II CRC patients with mutated KRAS and split by the median of Cdk5 expression (cohort B). (C) OS for 72 stage II CRC patients with WT KRAS and split by the median of Cdk5 expression. (D) OS for 26 stage II CRC patients with mutated KRAS and split by the median of Cdk5 expression (cohort B).*

very significant poorer DFS compared to the *CDK5* low group (p=0.004, 95% CI 1.56–36.46) (Figure 27A-B). We did not observe any differences in OS in this cohort when grouping according to the *KRAS* mutational status (Figure 27C-D).

When analyzing the entire TCGA cohort (n=473, stages I to IV, treated and non-treated), no differences could be observed in PFI and OS. However, we took advantage of having CMS subtype information in this cohort. We then studied whether *CDK5* had prognostic value when grouping patients according to CMS. When we analyzed the PFI, we found that high *CDK5* in the CMS1 correlated with poorer outcomes (*p*=0.036, 95% CI 1.07–8.10) (Figure 28C), while no differences were found in the three remaining molecular subtypes. We then compared the OS between patients with high or low *CDK5* levels in the TCGA cohort and did not observe any differences in any of the CMS. When studying the Cdk5 expression in the four CMS, we found that the CMS1 displayed the lowest levels of *CDK5* (Figure 28A-B), both in the stage II Colonomics cohort and in the mixed TCGA cohort

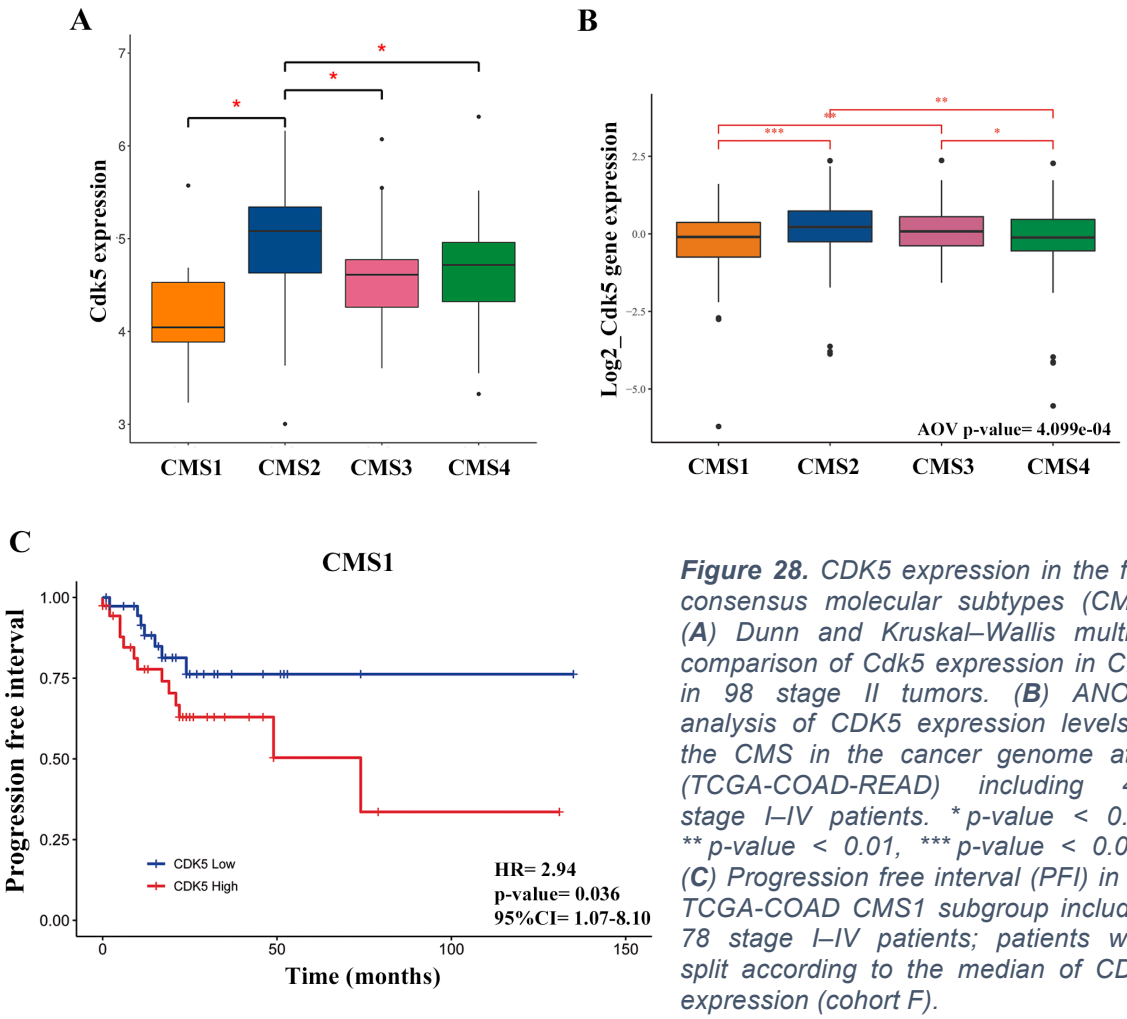

Figure 28. *CDK5 expression in the four consensus molecular subtypes (CMS). (**A**) Dunn and Kruskal–Wallis multiple comparison of Cdk5 expression in CMS in 98 stage II tumors. (**B**) ANOVA analysis of CDK5 expression levels in the CMS in the cancer genome atlas (TCGA-COAD-READ) including 410 stage I–IV patients. * p-value < 0.05, ** p-value < 0.01, *** p-value < 0.001. (**C**) Progression free interval (PFI) in the TCGA-COAD CMS1 subgroup including 78 stage I–IV patients; patients were split according to the median of CDK5 expression (cohort F).*

Objective 4b

3.4.2 Predictive value of Cdk5

To study the predictive value of Cdk5 expression in the metastatic setting, we used two different, but again, quite homogenous cohorts of patients. Cohort D consisted of stage IV CRC patients treated with oxaliplatin and 5-fluorouracil as the first-line treatment, while patients from cohort E were treated with different schedules combining irinotecan and 5-fluorouracil (Table 9). As shown in Figure 29 high Cdk5 levels were associated with shorter TTP only in the patients that received an oxaliplatin-based treatment (median 8.095 vs. 18.23 months, p=0.043, 95% CI 1.01–4.71) (cohort D, Figure 29), as no differences could be observed in the patients treated with irinotecan (median 8.95 vs. 8.42 months, p=0.45, 95% CI 0.59–1.27) (cohort E, Figure 29). Similarly, when analyzing the response rates (Chi-square), we only found differences according to Cdk5 levels in the oxaliplatin-treated patients (cohort D) as 87% (13 out of 15 patients) of the low Cdk5 group had complete or partial response, while only 53% (18 out of 34) of the high Cdk5 group responded (p=0.029).

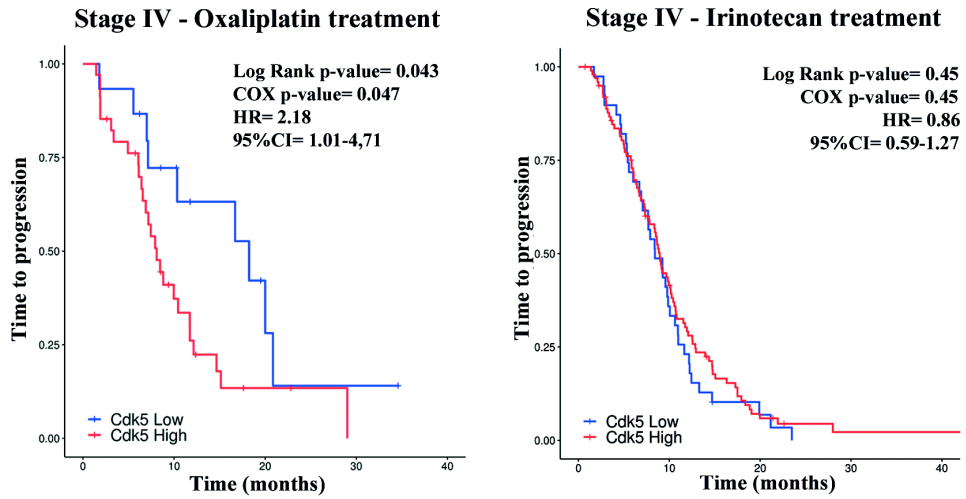

Figure 29. *Kaplan–Meier analysis of time to progression (TTP) depending Cdk5 levels in advanced CRC (A) TTP in 52 stage IV oxaliplatin-treated patients, grouped depending on negative (n = 18) or positive Cdk5 (n = 34) immunohistochemistry (IHC) staining (cohort D). (**B**) TTP in 139 stage IV irinotecan-treated patients grouped depending on negative (n = 73) and positive (n = 66) Cdk5 IHC staining (cohort E).*

Our results indicate that high *CDK5* mRNA levels is associated with poor prognosis in early-stage CRC patients who have not received any treatment, particularly in those harbouring activating *KRAS* mutations. In cohorts with mixed CRC stages this is only the case for the CMS1 subtype. We also found that Cdk5 predicts poor response to oxaliplatin- but not to irinotecan-based treatment in metastatic patients. Based on these results, data from the literature and results from our *in vitro* studies, we saw three pos-

sible translational applications for Cdk5 that we have evaluated further: i) Cdk5 could be used as predictive biomarker of response to oxaliplatin-based chemotherapy; ii) Cdk5 could serve as a biomarker for other already approved drugs and iii) Cdk5 could be related to tumor immune infiltration and response to immune checkpoint blockage (ICB).

3.4.3 Cdk5 association with chemotherapy response *in vitro*

There is quite a lot of evidence that Cdk5 contributes to the initiation of the DNA damage response (DDR) and DNA repair, which are associated with tumorigenesis and resistance to conventional DNA-damaging agents-based cancer treatments. Taking this into account, our findings here showing the predictive value of Cdk5 and previous results by our group reporting an upregulation of this kinase in cell lines with acquired resistance to oxaliplatin (186), we wanted to study this further *in vitro*. We thus hypothesized that Cdk5 inhibition may be a valid strategy to overcome chemotherapy resistance, primarily to oxaliplatin.

To evaluate the cytotoxic effect of Oxaliplatin, and whether this was affected by the removal of Cdk5 we used MTT assays. The assay was carried out in two pairs of parental and oxaliplatin resistant cell lines, HT29/HTOXA and LoVo/LoVOXA with CRISPR/Cas9 *CDK5* KD (Figure 30). The oxaliplatin resistant cell lines have previously been generated in the laboratory by gradually exposing the cells to increasing doses of the drug, until reaching at least 3 times increase in the EC50 values (concentration of a drug needed to achieve 50% of the maximum response). After transcriptomic profiling and real time qPCR validation we found that HTOXA and LOVOXA cells doubled the expression of *CDK5* as compared to the parental cells (186).

KD of *CDK5* in HTOXA and LoVOXA cells resulted in a EC50 decrease of 30% and 22%, respectively, as compared to the control non-target cells. No differences could be observed when studying the parental HT29 and LoVo cells.

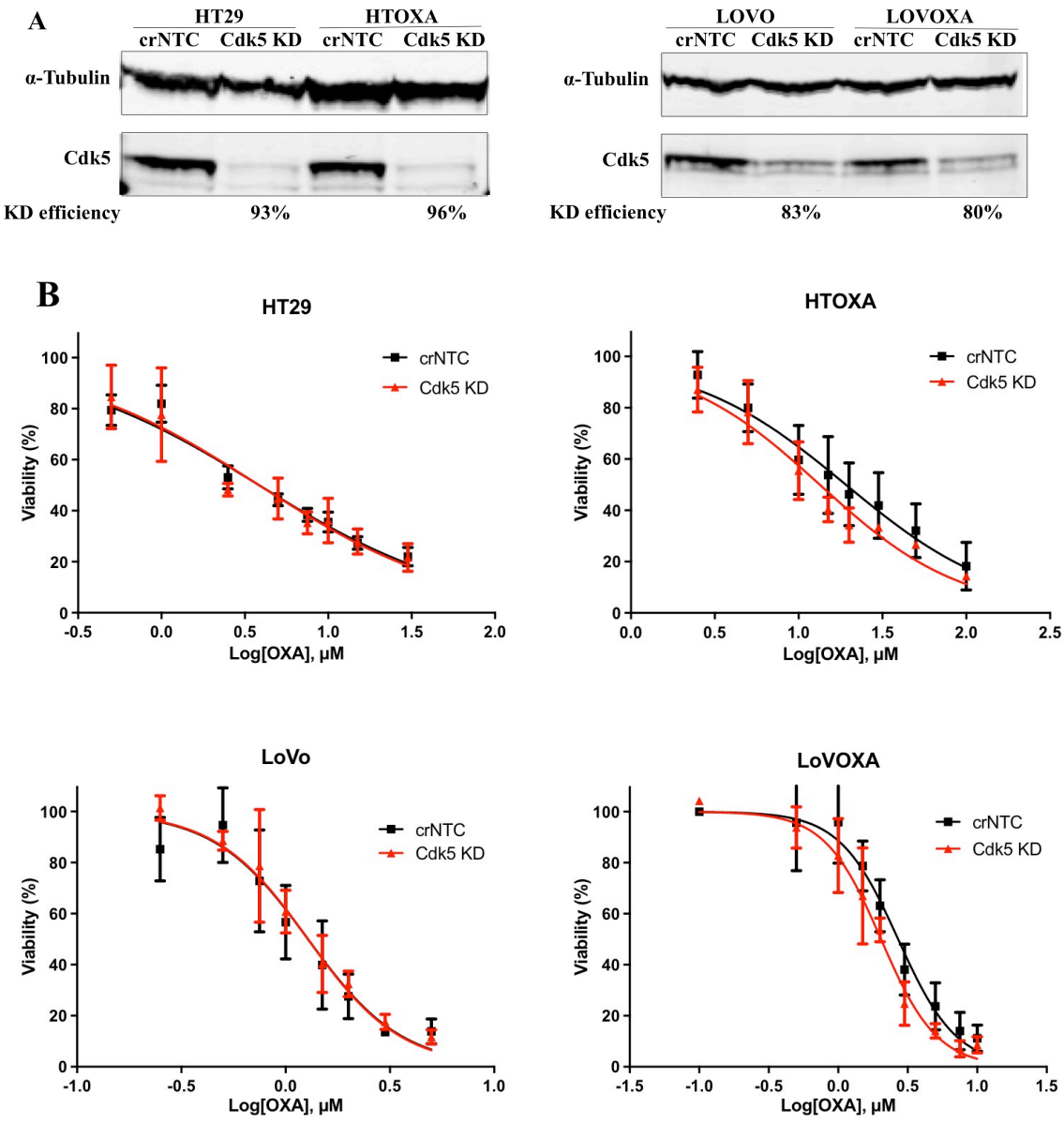

HT29	crNTC	*CDK5* KD	LoVo	crNTC	*CDK5* KD
EC50 (µM)	3,93	3,78		1,24	1,32
95% CI	3,36 - 4,58	2,91 - 4,93		1,04 - 1,48	1,18 - 1,47
R^2	0,94	0,85		0,86	0,94
EC50 reduction		**3,8%**			**0%**
p-value		0,81			0,52
HTOXA	crNTC	*CDK5* KD	**LoVOXA**	crNTC	*CDK5* KD
EC50 (µM)	19,14	13,38		2,70	2,03
95% CI	15,57 - 23,52	11,37 - 15,74		2,34 - 3,12	1,81 - 2,29
R^2	0,82	0,90		0,92	0,94
EC50 reduction		**30,1%**			**24,8%**
p-value		0,008			0,003

Figure 30. Effect of Cdk5 knockdown (KD) on the toxicity of oxaliplatin. (A) Western blot showing the Cdk5 KD efficiency of the CRISPR/Cas9 editing. α-Tubulin was used as endogenous control. Degree of KD was calculated by referencing to the crNTC Cdk5 band after normalizing to the endogenous control. (B) Dose response curves of MTT viability assay in the HT29/HTOXA and LoVo/LoVOXA cell lines with and without CDK5 KD. Vertical bars correspond to ± standard deviation (SD) of at least 3 independent experiments. In the table below the EC50 values of oxaliplatin can be found for each cell line and condition. Correlation coefficient (R^2).

As reported in section 3.2.1 the silencing of Cdk5 affected the colony formation capacity in HT29 and LoVo cell lines (only statistically significant for the LoVo cells). We performed a similar study including the resistant cell lines with *CDK5* KD by Crispr/Cas9. Here we found that the clonogenic capacity was lowered in the KD cell lines, however only statistically significant in the LoVOXA cells (p=0,003). In the context of oxaliplatin response, we studied the colony formation capacity in the *CDK5* KD pairs HT29/HTOXA and LoVo/LoVOXA after a 24H oxaliplatin treatment. Only small decreases in colony numbers could be observed after treating the cells at their respective EC50 oxaliplatin doses. A decrease that was not affected by Cdk5. Taken together the number colonies formed are decreased when Cdk5 is removed, however the clonogenic capacity after exposure to oxaliplatin is not affected by the presence of Cdk5 (Figure 31).

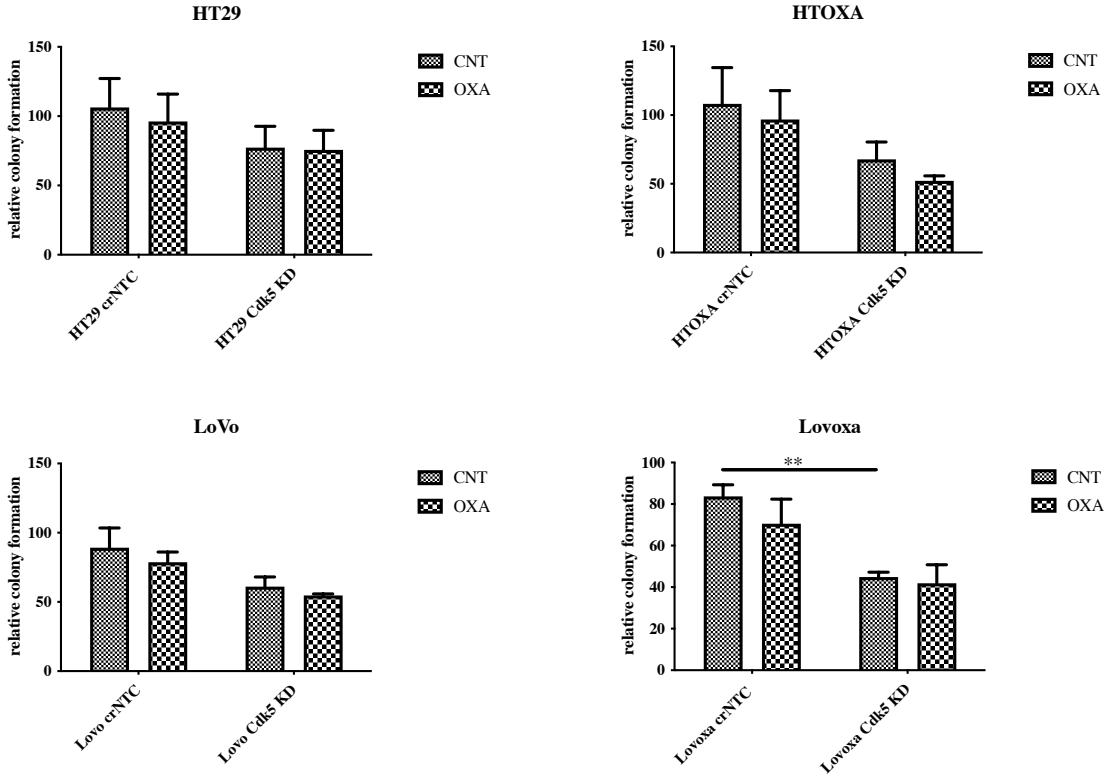

***Figure 31**. Effect of CDK5 KD and oxaliplatin treatment on colony formation. Cell lines were treated with their respective approx. EC50 oxaliplatin values (HT29 4μM, HTOXA 20μM, LoVo 1μM and LoVOXA 2,5μM) for 24H 24H after being seeded. Results were obtained from at least three independent experiments. Statistical differences were evaluated by students t-test. **p-value < 0.01.*

During the elaboration of this thesis, we were able to successfully develop two pairs of parental/resistant cell lines to irinotecan/SN38 in a similar manner to the oxaliplatin resistant cell lines. Unfortunately, we were unable to reach a stable resistant phenotype in the HT29 cells, why we could only study the LoVo/LoVIRI and DLD1/DLDIRI pairs. We first checked the mRNA levels in these cell pairs by qPCR and indeed we could observe a slight non-significant decrease in the Cdk5 expression in the irinotecan resistant cell lines (Figure 32). Hence the upregulation of *CDK5* seems to be specific to the acquisition of oxaliplatin resistance. We furthermore tested whether the sensitivity to irinotecan was affected by the knock down of *CDK5* in the Ht29 and the LoVo cell, however this was not the case for either (Figure 33).

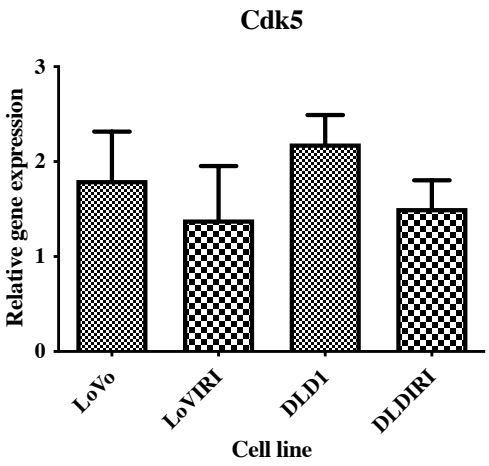

***Figure 32**. Cdk5 expression in irinotecan resistant cell lines. Cdk5 mRNA levels were assessed by qPCR. Statistical differences of at least three independent experiments were analysed by students t-test.*

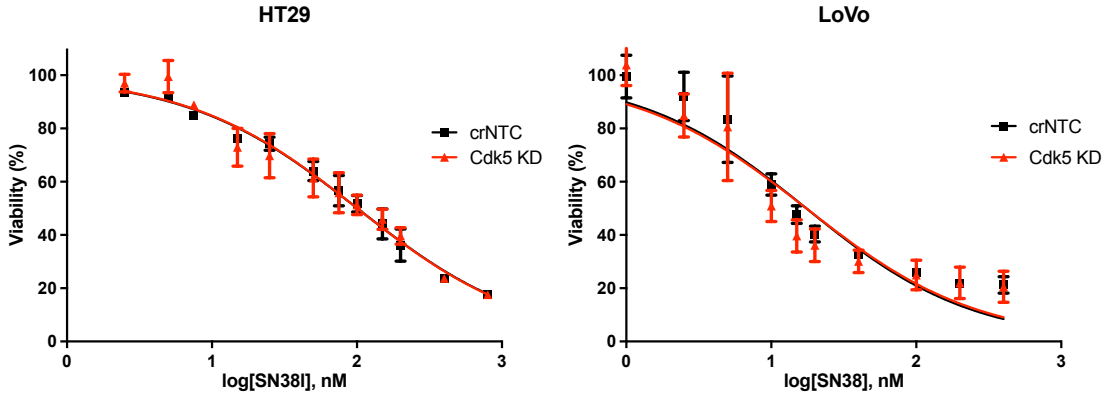

HT29	crNTC	*CDK5* KD	**LoVo**	crNTC	*CDK5* KD
EC50 (nM)	100,4	100,9		19,66	15,40
95% CI	92,1 - 109,6	87,3 - 116,5		15,03 - 25,71	11,01 - 24,54
R^2	0,98	0,95		0,89	0,85
EC50 reduction		**0%**			**21,7%**
p-value		0,959			0,252

***Figure 33.** Effect of Cdk5 knockdown (KD) on the toxicity of irinotecan. Dose response curves of MTT viability assay in the HT29 and LoVo cell lines with and without Cdk5 KD. Vertical bars correspond to ± standard deviation (SD) of at least 3 independent experiments. In the table below the EC50 values of irinitecan can be found for each cell line and condition. Correlation coefficient (R^2).*

Our *in vitro* studies support our findings in patient cohorts, showing that high *CDK5* mRNA levels are predictive of a poor response to oxaliplatin-based treatments. Cdk5 levels are increased upon resistance development and these oxaliplatin resistant cell

lines are more sensitive to oxaliplatin upon *CDK5* KD. While further studies are needed, our results indicate that metastatic CRC patients with high Cdk5 levels could possibly benefit from concomitant treatment with oxaliplatin and a putative Cdk5 inhibitor.

Objective 4c

3.4.4 Cdk5 as a biomarker for alternative drugs

So far, our results are indicative of a relevance of Cdk5 in the treatment of CRC; however and as commented before, current Cdk5 inhibitors are highly unspecific. We therefore wanted to explore whether it could serve as a predictive biomarker for other drugs already approved or that are in later stages of clinical investigation. For this we used the “Achilles project”, which is a collaboration between the Broad Institute and the Dana-Farber cancer Institute (Massachusetts, USA) and it is part of the bigger project "Cancer Dependency Map". With the "Cancer Dependency Map" they wish to systematically identify genetic and pharmacologic dependencies and the biomarkers that could possibly predict them. Within this effort, the Achilles project provides the foundation with a genome-wide-Loss of Function (LOF) screen using both lentiviral-based pooled RNAi and CRISPR-Cas9 libraries to silence or knockout individual genes. This allows for the stable suppression of each gene individually in a subset of cells within a pooled format allowing for genome scale identification of those genes that then become crucial for cell survival.

We crossed the data for gene dependencies with the expression of *CDK5* in the panel of 24 CRC cell lines. Taking into account our results, we additionally split the cell lines according to *KRAS* mutational status in to two subgroups in order to identify dependencies specific to subsets of cell lines. A negative correlation indicates that a certain gene is important for cell survival when the *CDK5* levels are high. Figure 34 shows volcano plots for all, *KRAS* WT and *KRAS* mutated cell lines with the left sides of the plots showing the genes with the lowest and more significant Achilles score. These are the genes that show the highest genetic vulnerability in cell lines with high *CDK5* expression. Part of the data accumulated in the Achilles project is also information about drugs, approved or in late-phase trials.

First, we observed that *KRAS* mutations indeed affect the gene dependencies in cell lines with high *CDK5* levels. Apart from the Xanthine Dehydrogenase, which show high dependency in all cell lines and both subgroups, the rest of the genes only come up in all cell lines and in either of the two subgroups. This supports the fact that *KRAS* mutations are so-called driver mutation affecting the entire transcriptional network of the cell

lines, and hence also the genes on which the cell lines depend for survival and proliferation.

Interestingly, METTL7A is among the genes with the lowest gene dependency score taking into consideration the effect of *CDK5* when looking at all cell lines. We have reported this gene to be upregulated in all three cell lines upon *CDK5* KD (see section 3.3.1). However, as no drug inhibiting METT7A exists this gene is not included in our subsequent study. Worth mentioning, *CDK5* also shows high genetic vulnerability when looking at all cell lines, which supports our hypothesis about the relevance of this protein in CRC.

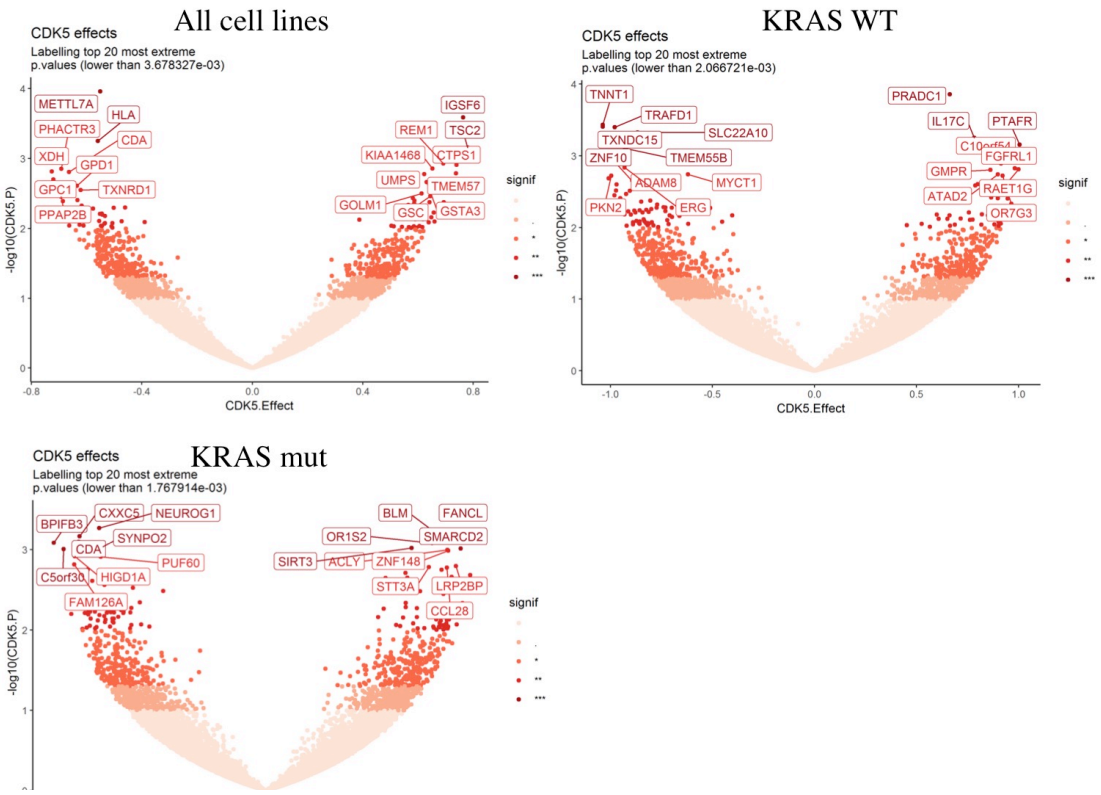

Figure 34. *Effect of CDK5 levels on gene dependencies. Volcano plots showing Achilles dependency scores correlated with CDK5 expression in all (54), KRAS WT (29) and KRAS mutated (24) CRC cell lines. The darker the red color the more significant the correlation. *p-value < 0.05, **p-value < 0.01, ***p-value < 0.001.*

Among the top genes with inhibitors that have been clinically approved or are in late phase clinical trials are: Cytidine Deaminase (CDA) (inhibited by Tetrahydrouridine) significant in all and *KRAS* mutated cell lines, Xanthine Dehydrogenase (XDH) (inhibited by Febuxostat) significant across the three groups of cell lines, Tubulin (inhibited by Taxanes) significant in all and *KRAS* mutated cell lines and lastly Phosphatidylinositol-4,5-Bisphosphate 3-Kinase Catalytic Subunit Beta (PIK3CB) (inhibited by AZD6482) significant in WT cell lines. We decided to study whether the effect of inhibiting these

proteins differed in the cell lines depending on whether Cdk5 was present (HT29 and LoVo crNTC cells) or not (*CDK5* KD cells). We hypothesize that, in the parental crNTC cell lines where Cdk5 is high, the inhibition of these proteins could affect the cell proliferation and viability to a higher degree than in the cell lines without Cdk5. Hence, an indication for a such treatment in CRC patients could be the high tumor levels of Cdk5.

Figure 35 shows the MTT results from treatments with Tetrahydrouridine, Febuxostat, AZD6482 and 3 different Taxane chemotherapies (Docetaxel, Cabazitaxel and Paclitaxel). Tetrahydrouridine, inhibiting CDA, did not affect the cell proliferation of either HT29 or LoVo. The crNTC HT29 cell line is more sensitive to AZD6482 (PIK3CB) and Docetaxel (Tubulin), 39% and 32% respectively. No differences could be observed with the other treatments. The crNTC LoVo cells were more sensitive to all 3 taxanes as compared to the *CDK5* KD, however only statistically significant results were found in the case of Cabazitaxel (48%). As for the rest of the treatments, whether Cdk5 was present or not did not affect the cellular response.

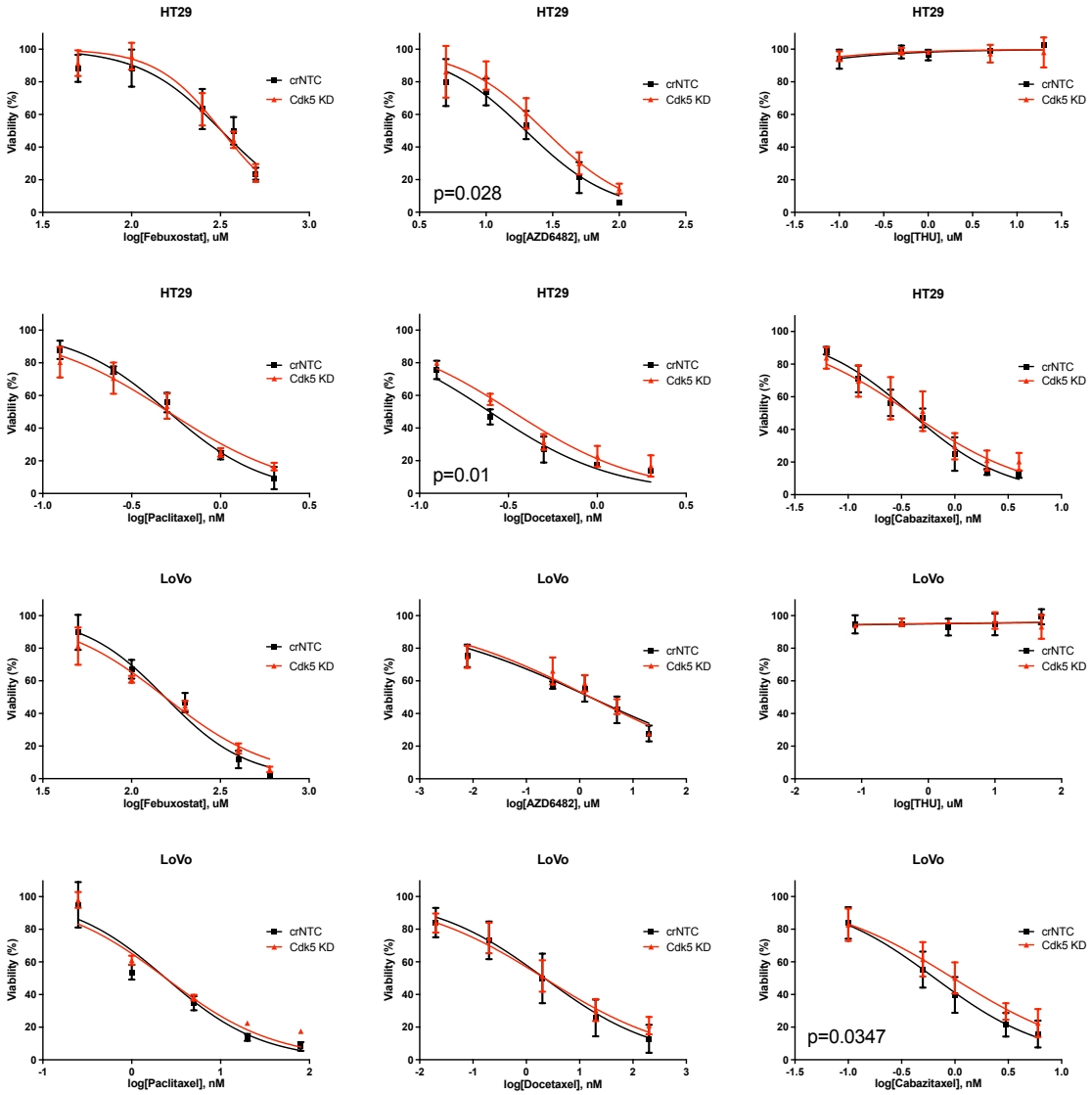

		HT29	crNTC	*CDK5* KD	LoVo	crNTC	*CDK5* KD
Febuxostat	**EC50 (μM)**		320,2	321,0		160,7	146,3
	95% CI		268,6-381,8	286,5-359,7		142,6-181,0	130-164,6
	R^2		0,87	0,94		0,95	0,95
	EC50 change			**0,3%**			**9,0%**
	p-value			0,98			0,26
		HT29	crNTC	*CDK5* KD	**LoVo**	crNTC	*CDK5* KD
AZD6482	**EC50 (μM)**		19,83	27,57		1,21	1,96
	95% CI		15,92-24,71	22,27-34,14		0,66-2,24	1,12-3,43
	R^2		0,91	0,92		0,83	0,83
	EC50 change			**28,1%**			**38,3%**
	p-value			0,028			0,23
		HT29	crNTC	*CDK5* KD	**LoVo**	crNTC	C*DK5* KD
Paclitaxel	**EC50 (nM)**		0,52	0,49		1,69	3,08
	95% CI		0,47-0,58	0,41-0,58		1,17-3,28	1,81-5,22
	R^2		0,97	0,93		0,93	0,93
	EC50 change			**5,8%**			**45,1%**
	p-value			0,50			0,18
		HT29	crNTC	*CDK5* KD	**LoVo**	crNTC	*CDK5* KD
Docetaxel	**EC50 (nM)**		0,25	0,33		1,82	2,70
	95% CI		0,21-0,30	0,29-0,39		0,87-3,83	1,52-4,81
	R^2		0,92	0,95		0,89	0,93
	EC50 change			**24,2%**			**32,6%**
	p-value			0,01			0,38
		HT29	crNTC	*CDK5* KD	**LoVo**	crNTC	*CDK5* KD
Cabazitaxel	**EC50 (nM)**		0,36	0,42		0,65	0,96
	95% CI		0,31-0,42	0,33-0,53		0,50-0,85	0,74-1,26
	R^2		0,94	0,87		0,90	0,89
	EC50 change			**14,3%**			**32,3%**
	p-value			0,25			0,034

***Figure 35**. Effect of Cdk5 on the cellular sensitivity to Achilles inhibitors. Dose response curves of MTT viability assay in the HT29 and LoVo cell lines with and without CDK5 KD. Vertical bars correspond to ± standard deviation (SD) of at least 3 independent experiments. In the table below the EC50 values of each drug can be found for each cell line and condition. Correlation coefficient (R^2). Worth noting, the statistics for the treatments with Tetrahydrouridine are not included in the table as EC50 values could not be calculated.*

With these results we show that the effect of targeting proteins, which have shown correlation between their dependency and Cdk5 levels, is for some indeed affected by whether Cdk5 is present or not. And while further studies are needed in a higher number of cell lines to confirm the results from the taxanes and the PIK3CB inhibitor, this suggest an applicability of Cdk5 levels as predictive of response to other drugs.

Objective 4d

3.3.5 Cdk5 and immune aspects

Unfortunately, almost all CRC patients are intrinsically resistant to treatments with immune checkpoint blockers. Only about 5% of the metastatic patients whose tumors harbor a great amount of mutations (MSI tumors, hypermutated) have been shown to benefit from these therapies. Therefore, it is important to study ways to promote immune cell infiltration in cold CRC tumors, for them to become sensitive to immunotherapies. As described in the introduction, recent studies in medulloblastoma, colorectal, bladder and melanoma have described a connection between high Cdk5 and low immune infiltration in the tumor microenvironment and subsequently lack of response to immune checkpoint inhibitors (133, 154, 200). These discoveries combined with our finding of prognostic value in the CMS1 immune subtype encouraged us to study this further.

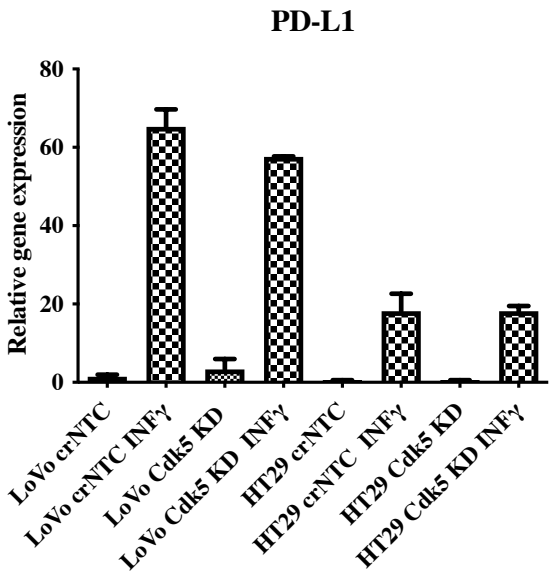

***Figure 36**. PD-L1 expression in crNTC and Cdk5 KD cell lines. PD-L1 mRNA levels were assessed by qPCR. Statistical differences of at least three independent experiments were analysed by students t-test.*

Dorand et al. reported that disruption of *CDK5* expression in meduloblastoma cell lines suppressed PD-L1 expression both with and without interferon(IFN)-γ stimulation. We studied the PD-L1 expression in the *CDK5* KD HT29 and LoVo cell lines, at basal levels and with 100ng/mL IFN-γ stimulation. The PD-L1 expression levels were very low without stimulation in both cell lines, but increased clearly upon IFN-γ addition. The levels of PD-L1 are clearly higher in the LoVo cell line, both at basal levels and after IFN-γ stimulation, in accordance with it being CMS1. It was clear that in these two cell lines the PD-L1 expression was not affected by whether Cdk5 was present or not, as no differences could be detected between the crNTC and *CDK5* KD cells (figure 36).

Even though this first results did not show any direct link between Cdk5 and PD-L1, there are many more aspects related to a possible response to ICB. In order to study this properly we need to have models with fully functioning innate and adaptive immune systems. In CRC there are two main syngeneic mouse models: C57BL/6/MC38

and the Balb/c/CT26. Both MC38 and CT26 cell lines are derived from mouse colon adenocarcinomas induced by continuous exposure to carcinogenic compounds. Both the C57BL/6 and the Balb/c mice have normal immune systems making them particularly relevant for studies of immunotherapy. We therefore knocked down *CDK5* in these two cell lines by CRISPR/CAS9. A complete loss of the Cdk5 protein could be observed by western blot (Figure 37A). Next we studied the subcutaneous tumor growth of CT26 and MC38 in Balb/C and C57BL6 mice, respectively. One million of crNTC and *CDK5* KD cells were injected subcutaneously in the left and right flank of the mouse, respectively. In the Balb/c mice injected with the syngeneic cell line CT26 we saw bilateral tumor growth with the tumor reaching maximal size approximately one month after injection. No differences could be observed in the tumor growth rate or final size between the CT26 crNTC and *CDK5* KD, which is in agreement with our previous observations in human CRC cells where we did not find any effects of *CDK5* KD on cellular proliferation. Western Blot analysis showed that the KD of *CDK5* was 68% in the subcutaneous CT26/C57BL6 tumors (figure 37B-C). This increase of Cdk5 after subcutaneous growth could be ascribed to non-tumor cells found within the tumor. In the case of the C57BL6 mice injected with the MC38 cell line initial tumor growth was observed followed by a striking reduction in tumor size. Three weeks after injection no tumor could be seen, indicating that the mice were able to reject both the crNTC and *CDK5* KD tumor cells (Figure 37D). Unfortunately, we were unable to get

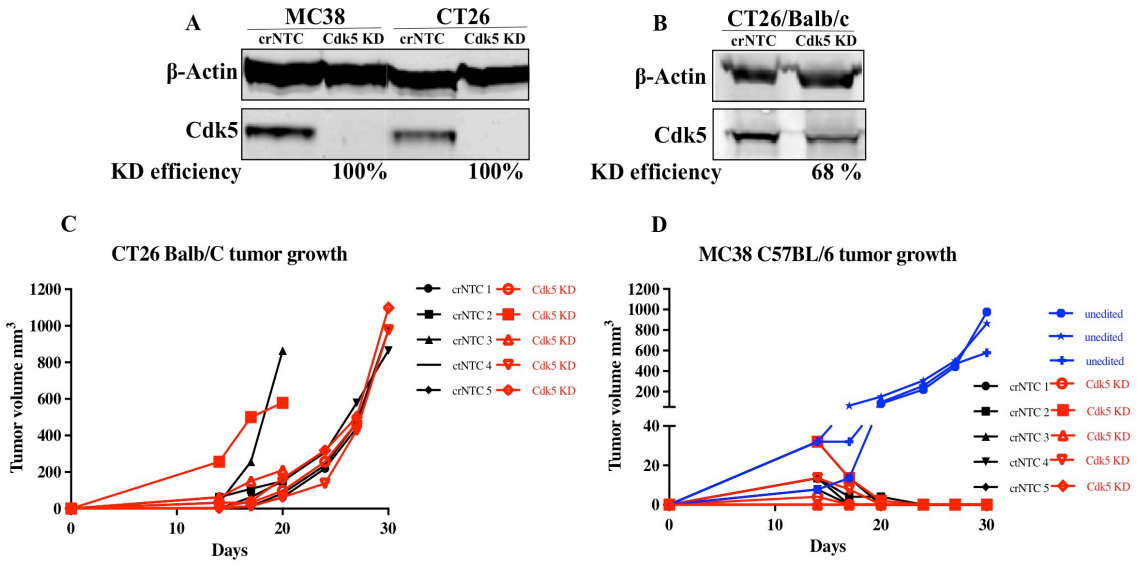

***Figure 37**. Subcutaneous tumor growth of MC38 and CT26 cell lines. (A) Western Blot (WB) of CRISPR/Cas9 KD of CDK5 in MC38 and CT26 murine cell lines. β-Actin was used as endogenous control. (B) Representative WB image of Cdk5 levels in CT26/B57BL/6 subcutaneous tumors. α-Tubulin was used as endogenous control. (C-D) Growth curves for CT26/B57BL/6 and MC38/Balb/c crNTC and CDK5 KD subcutaneous tumors (n=5). Unedited MC38 cells were also injected to check the tumor growth capacity (n=3).*

crNTC or *CDK5* KD tumors from the C57bl/6/MC38 model, which is known to be the more immunogenic of the two (221). In attempts to explain the tumor rejection we found that Cas9 from Streptococcus Pyogenes from the CRISPR modification has been shown to cause immune-mediated responses (222). To test this we tried to grow subcutaneous tumors with MC38 cell without the CRISPR/CAS9 modifications and observed tumor growth in all 3 animals (Figure 37D).

We studied the lymphoid infiltration in the Balb/c/CT26 tumors by flow cytometry, comparing single cells from the crNTC tumors with the *CDK5* KD. We used a simple panel identifying mainly helper and cytotoxic T cells, which together with natural killer cells, are the main players in the elimination of cancer cells. An example of the applied gating can be visualized in figure 38. As can be seen in figure 38 the number CD45+ lymphocytes was slightly lower in the *CDK5* KD tumors. However, a slightly higher percentage

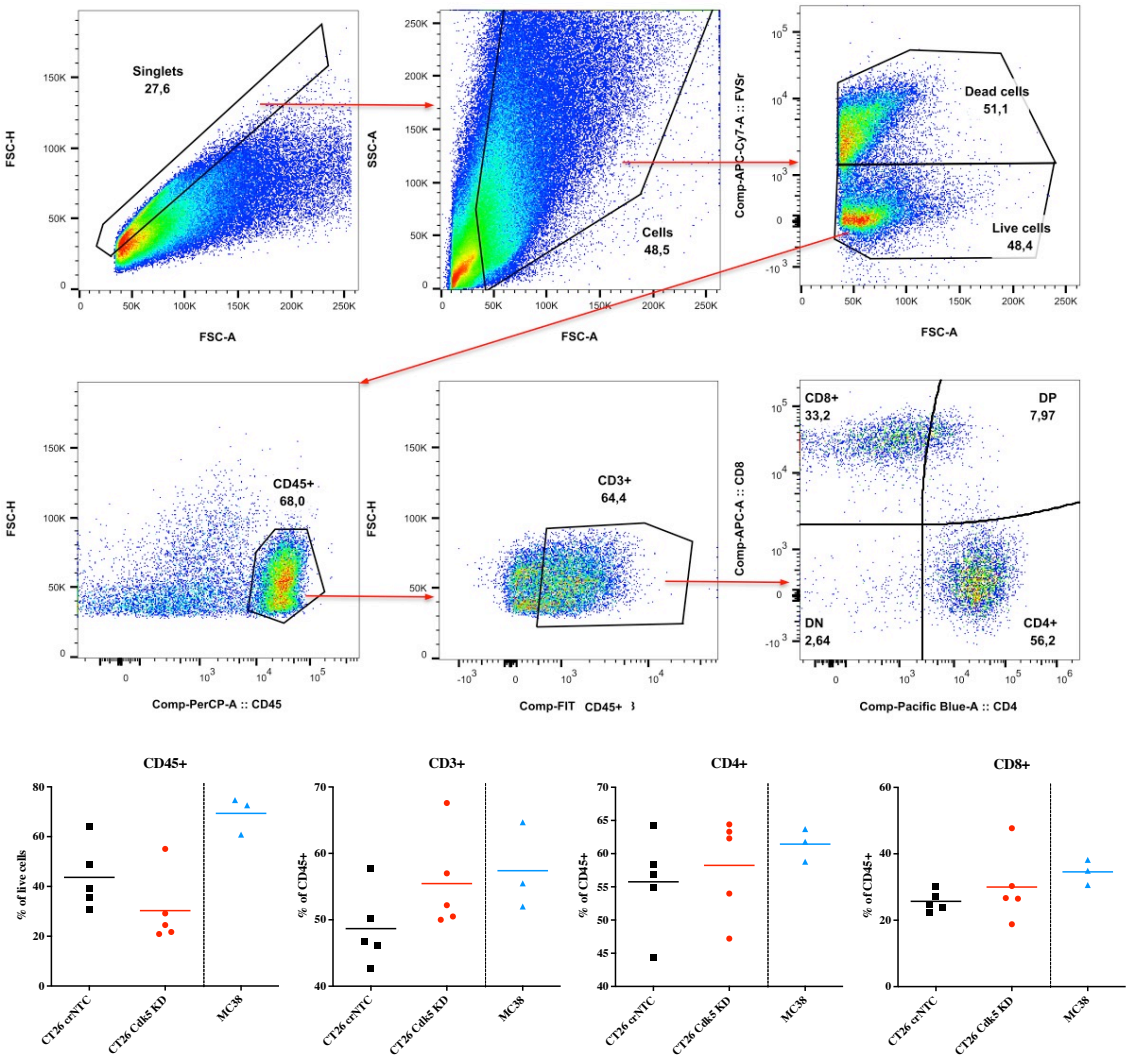

Figure 38. *Immune infiltration in CT26/B57BL/6 tumors. Top, flow cytometric gating strategy for detection of T cells. Bottom, CD45+ cells in the CT26 crNTC (black)./CDK5 KD (red) and unedited MC38 (blue) tumors. CD3+, CD4+ and CD8+ cells as percentage of CD45+ cells in the CT26 crNTC/CDK5 KD and unedited MC38 tumors. Student's t-test was used to evaluate differences between CT26 crNTC and CT26 Cdk5 KD tumors.*

of the lymphocytes were CD3+, CD4+ and CD8+ in the *CDK5* KD cells, leading us to estimate that the actual numbers of cytotoxic and regulatory T cells present in the tumors are actually quite similar. Unfortunately, we were not able to do the same comparison between crNTC and *CDK5* KD cells in the C57BL/6/MC38 model. However, in the tumors without any editing we found a higher lymphoid infiltration compared to the Balb/c/CT26 tumors, confirming an immune rich microenvironment as expected.

With the aim of studying the implications of Cdk5 in response to immune checkpoint blockage we chose to use tumor spheroids – MDOTS. This is an ex-vivo technique that from one tumor allows testing many different drug combinations, significantly minimizing the number of animals needed. The technique is very useful in studies of ICB, as the spheroids maintain the tumor microenvironment, including possible infiltrating immune cells, during the 6 days incubation time (223). The Balb/c/CT26 tumors were degraded and subjected to a number of filtration steps, allowing to us to isolate spheroids between 40 and 100microns. These spheroids were resuspended in a collagen solution and injected into microfluidic chambers, as shown in Figure 39. For each tumor four chambers with spheroids were generated and treated with an IgG isotype control, α-PD-1, α-CTLA4 or both for 6 days.

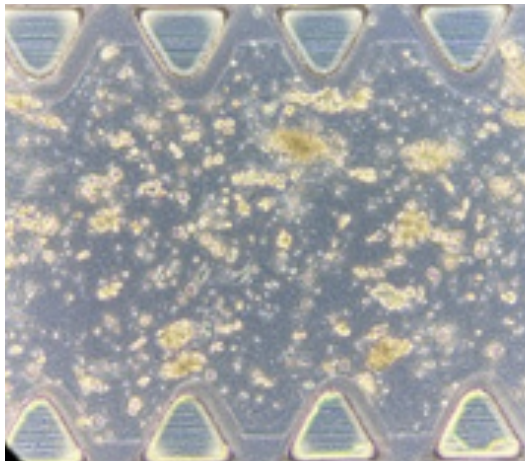

***Figure 39**. Murine derived organotypic tumor spheroids (MDOTS) in microfluidic chambers. Representative imatge of MDOTS from CT26/Balb/c tumors in the microfluidic chamber.*

The viability of the spheroids was evaluated by Acridine orange (green/alive) and Propidium iodide (red/dead) staining visualized by fluorescent microscopy as previously described (208). Figure 40 shows an example of how the live cells within the spheroids are stained green and the dead cells are stained red. The green and red staining was quantified for at least 15 spheroids per condition in ImageJ. As can be seen in figure 41 the treatments with immune checkpoint inhibitors did not affect cell viability in MDOTS from the Balb/c/CT26 model, as the viability remains high in all condition. Hence, the removal of Cdk5 did not result in an increase in the response to ICB either.

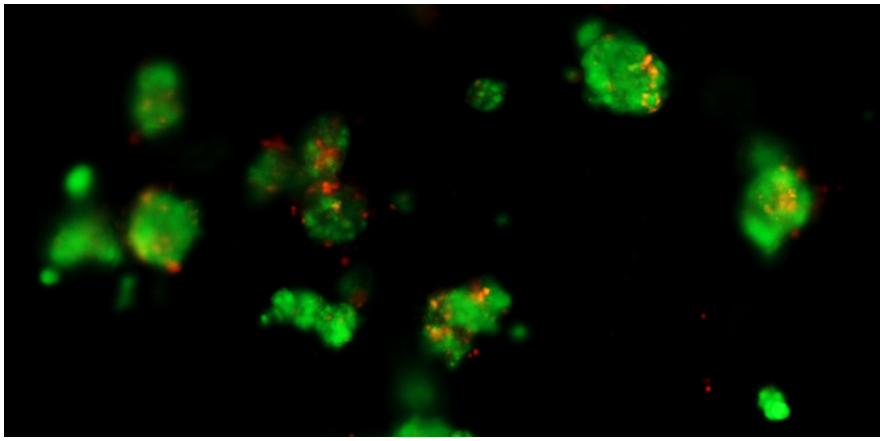

Figure 40. *Example of viability staining of Murine derived organotypic tumor spheroids (MDOTS). Representative immunofluorescence image of CT26/Balb/c spheroids, green (Acridine Orange) mark live cells and red (Propidium iodide) mark dead cells.*

As we could not generate MDOTS from the C57bl/6/MC38 model transduced with CRISPR/Cas9 plasmids, we decided to generate them from the subcutaneous tumors grown without genetic modifications and as an approximation of *CDK5* KD we used Roscovitine treatment, which is a pan-Cdk inhibitor with lowest IC_{50} value for Cdk5. As can be seen is figure 41A α-PD-1 alone affected the viability of the MDOTS significantly, while no effect could be observed with individual α-CTLA4 or Roscovitine treatment. Concomitant treatment with Roscovitine increases the responses to α-CTLA4 and combined CTLA4 plus α-PD-1 treatment. To our surprise, we observed higher viability in spheroids treated with CTLA4 and α-PD-1 as compared to those treated with α-PD-1 alone (Figure 41A)

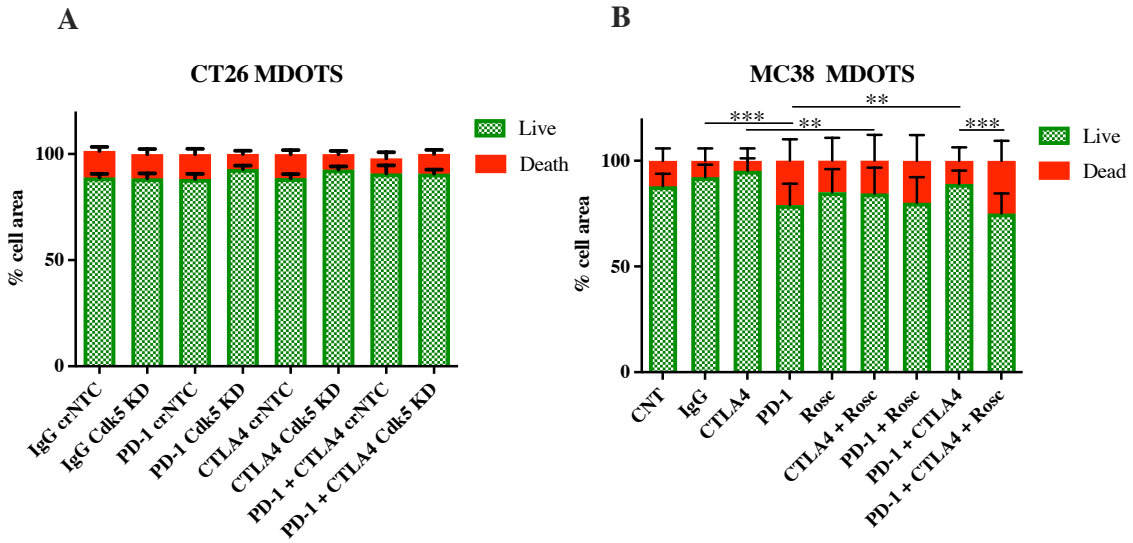

Figure 41. *Quantification of viability staining of Murine derived Organotypic tumor spheroids (MDOTS). Viability was assessed by Acridine Orange (AO) and Propidium Iodide (PI) immunofluorescence staining of live MDOTS. (A) CT26/Balb/c spheroids from crNTC and CDK5 KD tumors treated with an IgG control, α-PD-1 or α-CTLA4 antibodies. (B) Spheroids from MC38/C57BL/6 tumors without CRISPR/Cas9 editing treated with an IgG control, α-PD-1 or α-CTLA4 antibodies combined with Roscovitine for Cdk5 inhibition. Statistical differences between*

*treatment conditions were determined by students t-test. *p-value < 0.05, **p-value < 0.01, ***p-value < 0.001.*

Based on the results presented here, it is unlikely that Cdk5 plays a major role in the tumor immune cell infiltration or in response to ICB in CRC. The lymphoid infiltration does not differ between crNTC and *CDK5* KD Balb/c/CT26 tumors. It should be kept in mind that these are results form only one model, as we were not able to analyze this in the C57bl/6/MC38 model. Experiments are currently on going to study this (discussed below). Regarding ICB response, *CDK5* KD does not affect the tumor cell PD-L1 expression or ICB response in the Balb/c/CT26 spheroids. Roscovitine does slightly increase the response to α-CTLA4 and α-CTLA4/ α-PD-1 in the more immune C57bl/6/MC38 spheroids, however further studies are needed with a specific inhibition to confirm this.

4 Discussion

Only few drugs have been added to the armamentarium of CRC treatment in the last decades and chemotherapy still remains to be the therapy backbone. There is an unmet need for new treatment options and biomarkers for current and upcoming therapies. With this PhD thesis we aimed at expanding the knowledge about Cdk5 in CRC and determine the applicability of this kinase as a prognostic and/or predictive marker and as a candidate drug target. In order to achieve this, we have studied the expression and activity of Cdk5 in CRC along with its relevance in different aspects of cancer progression, such as proliferation, cell motility and immune response, and evaluated its prognostic and predictive value. In the following sections, I will try to discuss all these findings.

4.1 Cdk5 is overexpresses and highly active in CRC

We started out by showing that both Cdk5 and p35 were found at higher levels in colorectal cancer tumors as compared to normal adjacent colon tissues. This is both the case for mRNA and protein, and with the use of different techniques making our results more robust. These results are in agreement with those reported by Zhuang et al. (146), which is what we consider the reference work in CRC, and confirm previous data obtained in other types of cancer (144, 158, 164). We furthermore describe that this increase is likely due to a copy number gain, which has also been reported by Robb et al. (139). As a matter of fact, this is probably due to whole chromosome aneuploidies commonly affecting chromosomes 7, 13 and 20, that occur prior to the transition from adenoma to adenocarcinoma (224). Trisomy of chromosome 7, where *CDK5* is located, has been reported in as many as 74% of CRC tumors (225). Our findings support the fact that *CDK5* copy number gain is an early event in CRC development, as we observe no differences in the Cdk5 levels among disease stages or paired primary and metastasis lesions.

As mentioned in the introduction, the majority of the research concerning Cdk5 is from the nervous system and in relation to different neurological disorders where it has been shown that both inactivation and hyperactivation of Cdk5 is toxic. Loss of Cdk5 function has been related to epilepsy, mental retardation and schizophrenia while hyperactivation occurs in many neurodegenerative diseases, as summarized by Shah et al. (116). Binding of Cdk5 to p25, resulting in such a hyperactive complex, has been described for example in pancreatic cancer (158), where they showed a correlation between mu-

tated *KRAS* and increased p35 cleavage; however, the mechanism behind the p35 cleavage in cancer remains unclear. In neurons it is mainly due to the protease activity of calpain, which is controlled by calcium concentrations (226), while for myoblasts the turnover is related to nestin (227). To our surprise, we observed that Cdk5 is primarily bound to p25 in our CRC cell lines, as we could not detect any p35 band on the WB of the IP eluate. Noteworthy, when we do a regular WB of the same four cell lines, we only detect the p35 band, and no band for p25. When performing the cell lysis prior to IP among other agents we did not include SDS for denaturation, as it can interfere with and compromise antibody binding and protein interactions. The gentler IP lysis might mean that some of the Cdk5-p35 bound to the membrane is not liberated, while the Cdk5-p25 complex is soluble and easily extracted, possibly affecting the amounts of p25/35 detected. It could also be a reflection of the fact that the binding between Cdk5 and p25 is more stable, and therefore to a higher degree visualized by the IP. Most likely Cdk5 is found both in complex with p25 and p35 in CRC cell line. To our knowledge this is the first description of the presence of the Cdk5-p25 complex in CRC cancer. Combining the fact that Cdk5 is expressed at higher levels in malignant tissue, and what is known from the nervous system about this hyperactive form, our hypothesis is that Cdk5 indeed is highly active and possibly relevant in CRC progression is reinforced. This evidence could have therapeutic repercussions as one possibility could be to design an inhibitor that specifically disrupts the binding between Cdk5-p25, which would be more tumor-specific and probably would have less side effects.

4.2 Cdk5 is not involved in cellular proliferation

Some authors reported a role of Cdk5 in promoting cell proliferation in different types of cancer, such as medullary thyroid carcinoma, non-small cell lung cancer and also CRC (145, 146, 179), while others have reported that it indeed has no effect on proliferation in melanoma and pancreatic cancer (157, 166). When we KD *CDK5* in a panel of 4 CRC cell lines we did not observe any significant effect on cell proliferation. Noteworthy, Zhuang et al. reported that in HCT116, Cdk5 removal almost stops proliferation for 5 days, while we did not observe any effect in this cell line. Such big differences in the results can unlikely be ascribed to differences between methodology or medium compositions, leaving only the cell line itself as a possible explanation. The failure to reproduce research has been an issue for long, and in a recent multi-omics study of HeLa cell lines collected from laboratories all over the world Liu et al. showed great heterogeneity (228). This is in line with what was reported by Ben-David et al. (229) when they tested 321 anti-cancer compounds in 27 MCF7 strains. Seventy-five percent of

compounds that strongly inhibited some strains were completely inactive in others. We therefore speculate that clonal selection of the HCT116 cell line could explain the different results reported. Both mentioned papers advocate for cell line authentication beyond STR profile, suggesting documenting the precise molecular makeup of the cells, for example by transcript or proteome profiling. Unfortunately, this will most likely take years to be widely implemented due to the current elevated cost. Such inter-laboratory differences furthermore underscore the need to carry out *in vitro* studies in panels of cell lines in order to reach reliable conclusions. Based on our studies in four cell lines, we can conclude with a high degree of certainty that Cdk5 does not affect the proliferative capacity in CRC *in vitro*.

Moreover, we evaluated the proliferation of the murine CRC CT26 cell line grown subcutaneously in Balb/c mice and found no differences in the growth rate or final tumor size between the crNTC and *CDK5* KD cells. This is in concordance with the fact that we do not see any differences in vitro proliferation in the human cell lines. Zhuang et al. have previously reported that genetic KD and overexpression of Cdk5 causes reduction and promotion, respectively, of subcutaneous tumor growth in nude mice (139, 146). A 46% inhibition of subcutaneous tumor growth has been reported for the CT26 cell line upon treatment with Dinaciclib (200). Yet another study using xenografts originating from the GEO cell line, also report growth reduction when treating with 20-223, a small molecule inhibitor of Cdk5 (139). However, neither of the two inhibitors is specific against Cdk5, making it hard to compare directly, and it is very possible that the inhibitory effect can be attributed to the inhibition of Cdk2, which is known to be an important regulator of cell cycle progression (230). Our results, which are the first from genetic KD of *CDK5* carried out in immunocompetent mice, contradicts what has previously been reported. Hence, further studies with genetic silencing or specific inhibitors are needed to conclude which effects Cdk5 has on tumor growth *in vivo.*

4.3 Cdk5 affects cell motility in CRC

Several studies in CRC, melanoma and pancreatic cancer among others, have shown the involvement of Cdk5 in promoting metastasis formation *in vitro* and *in vivo* (146, 148, 157). To form a metastasis, tumor cells need to invade surrounding tissue, extravasate, survive in non-attachment conditions and proliferate in new distant organs. *In vitro*, we can evaluate some of these features by studying the invasive, migrative and colony formation capacities of tumor cell lines. We observed a decrease in both migration and invasion capacity of HT29 and Lovo cells when Cdk5 was silenced, which was also the case for the HCT116 and SW480 cell lines, as reported by Zhuang et al (146).

However, we showed that this was not the case for *KRAS/BRAF* wild type cells, DiFi and SW48. Upon introduction of the most common *KRAS* mutation in the SW48 cell line, a subtle but significant effect of Cdk5 silencing could be observed in the migratory capacity. Indeed, signaling through the MAPKs is one of the main deregulated pathways in CRC and other authors have reported an interaction between Cdk5 and different effectors of this pathway. For example, in pancreatic cancer Eggers et al. and Feldman et al. found that Cdk5 acts in concert with mutated *KRAS*, possibly through effectors RalA and RalB, suggesting a dependency on the constitutive activation of this oncogenic pathway (157, 158). Indeed when we split the Colonomics cohort with stage II patients according to the mutational status of *KRAS*, we found that only in patients harboring *KRAS* mutations did high Cdk5 correlate with shorter DFS. This supports our in vitro results about Cdk5 being particularly important in combination with activating mutations in this pathway.

In the *KRAS* mutant HCT116 cell line, it has previously been shown that Cdk5 can phosphorylate ERK5 and that the effects of abrogation of *CDK5* expression on proliferation and cellular movement were due to the inhibition of ERK5-AP-1 signaling (146). However, we think that this is unlikely as CRC cell lines with *KRAS* or *BRAF* mutations seem to preferentially activate ERK1/2 and when treated with ERK5 inhibitors, cell proliferation is unaffected (231, 232). When we checked the cluster of genes that the authors reported to be affected downstream of ERK5 in our RNAseq data we did not observe the same pattern of changes upon *CDK5* KD. Only in the LoVo cell line, which harbors the exact same mutation (G13D), we found two out of the nine genes to be upregulated in a similar manner. Hence, the signaling through the ERK5-AP- axis might be somehow context-dependent, underlining the importance of doing *in vitro* studies in panels of cell lines to increase the chance of translation into the clinic.

Once a tumor cell reaches a distant organ another important trait of cancer cells with tumor initiating capabilities is the ability to start a colony and next undergo unlimited division. This is commonly tested by colony assay. When we studied the consequences of Cdk5 silencing we saw a decrease in the capacity of forming new colonies, which is in concordance with what was reported by Zhuang et al. in CRC (146) and also for numerous other solid tumors (164, 166). In breast cancer Cdk5 has indeed been linked to tumor initiating cells and stem cell properties, either through the anti-apoptotic FOXO1-Bim pathway (153) or by enhancing CD44 alternative splicing from CD44s to the CD44v isoform promoting self-renewal (201). This represents an interesting area for further research, as tumor-initiating cells are the main cause of tumor recurrence, establishment of metastasis and resistance towards cancer therapies.

We also studied the effects of *CDK5* KD on cell transcriptional patterns in HT29, LoVo and SW48 cells which, as commented, represent different mutational status for typical CRC cancer mutation (*BRAF, KRAS* and WT, respectively) along with different molecular subtypes (CMS3, CMS1, CMS1). Regardless of these genetic profiles, among the gene sets that come up in the DE genes is “Cell adhesion”. Among the upregulated individual genes upon *CDK5* KD in HT29 and LoVo is *CALD1*, which also shows a very negative correlation with Cdk5 in tumors tissues. These results together with those from the GSEA analysis of the TCGA dataset indicate a clear positive association between *CDK5* expression and genes from the EMT signature, supporting the idea of Cdk5 having a role in CRC progression.

Interestingly one study exists showing a connection between Cdk5 and Caldesmon in cancer. In Melanoma, *CDK5* KD caused dephosphorylation (Tyr27) and overexpression of Caldesmon resulting in a marked inhibition of cell motility. Concomitant *CALD1* KD rescued cell motility and invasive phenotype (166). Such tyrosine phosphorylation of Caldesmon has been found to cause its dissociation from actin, thereby contributing to actin microfilament disassembly (219). Without examining the phosphorylation status, another study demonstrated that elevated Caldesmon levels reduced the number of podosomes/invadopodia and therefore represses cancer cell invasion (233). As Cdk5 is a Ser/Thr kinase it cannot directly phosphorylate Tyr27, however numerous Caldesmon Ser/Thr phosphorylation sites have been described for similar kinases such as Pak2 (234), Cdk2 (235) and Erk1/2 (236).

We speculated that in CRC cells with *KRAS/BRAF* mutations (HT29 and LoVo), which is also where we see a clear decrease in migration and invasion, CDK5 KD causes increased Caldesmon expression, decreased Caldesmon phosphorylation levels and ultimately affecting cell adhesion and actin remodeling during cell movement. In this context it is worth mentioning that Cdk5 has also been shown to regulate actin dynamics through interactions with other important actin regulatory proteins, such as PAK-1 and p27 (237, 238). We were very eager to study this possible connection between Cdk5 and Caldesmon further and clarify its implication for cell motility in CRC. Unfortunately, we have not been able to detect the Caldesmon protein by Western blot in our CRC cell lines and there are no longer any phosphor-Tyr27 Caldesmon antibodies on the market.

Obviously, the dynamics of cell matrix adhesions are very complex, involving creation of adhesion points, maturation and lastly the resolution. All processes are highly controlled, partly by posttranslational modifications. Possibly, it is the phosphorylation of key amino acids that are relevant for migration and cancer spreading, which is in line with other studies (239, 240). Hence, in order to study the Cdk5-Caldesmon connection

further and possibly identify new CRC Cdk5 phophorylation targets, a phosphoproteome profiling study could be a possibility.

Although not studied deeply, we find it interesting to comment on METTL7A, which like Caldesmon was upregulated upon *CDK5* KD in our RNAseq study. This methyltransferase is an integral membrane protein, anchored into the endoplasmic reticulum (ER) membrane recruiting cellular proteins for lipid droplet formation (241). METLL7A was upregulated in the LoVo and SW48 cell lines upon *CDK5* KD, both defined as MSI, CMS1. We observed a strong inverse correlation with Cdk5 in tumor tissues and low *METTL7A* expression was correlated with poor prognosis. No previous connection has been reported between Cdk5 and METTL7A, and they seem to have very distinct cellular location and functions, however with so many indicators of a connection we studied this further. A direct connection is unlikely, as no possible Cdk5 phosphorylation sites exist in the *METTL7A* amino acid sequence. Three proteins have been reported to regulate *METTL7A* expression, however none of these, ADAR1/2 (242), EZH2 (217) or RhoBTB2 (243), are affected by the *CDK5* KD. Hence, if there is a connection in CRC it is most likely through other undescribed interactions. Unfortunately, our wish to study this further was hindered by the lack of specific antibodies, why we have not been able to determine whether the transcriptional upregulation is reflected at protein levels as well.

4.5 Cdk5 has prognostic value in CRC

An important part of our research as a translation laboratory is to study the clinical relevance of our pre-clinical findings. For this we took advantage of private and publicly available cohorts, where Cdk5 has been determined by different methods. According to our results, we expected that high Cdk5 tumor levels would be associated with worse DFS. This was indeed demonstrated in a cohort of stage II and in another one of stage III CRC patients that importantly, had not received any treatment after primary tumor resection. As discussed above, this was particularly true in patients with *KRAS*-mutant tumors, at least in stage II patients. These results point to the prognostic value of Cdk5, which seems to be related with a more aggressive phenotype as we demonstrated in our in vitro experiments and are in line with results from other groups (139, 146). It should be kept in mind that the significance of Cdk5 as a prognostic biomarker seems to be highest when looking at the DFS, as for the stage III non-treated cohort the OS did not differ between the low and high Cdk5 groups. The DFS refers to the period before recurrence, hence indicating that tumors expressing high levels of Cdk5 could

have an enhanced capacity to invade and migrate from primary sites to metastatic sites and also to initiate growth at new sites.

We also observed the same trend in the CMS1 subtype when studying the TCGA cohort. We believe that this has to do with the CMS1 being the most uniform of the 4 subtypes. The CMS1 is known to have good prognosis and the relapse rate is very low, why fewer of the patients in the CMS1 group would have received treatments and most of them had indeed early stage tumors. Furthermore, the CMS1 is known to have the highest prevalence of *BRAF* mutations at 42%, which along with the 23% of *KRAS* mutations adds up to approximately two thirds of the CMS1 having this pathway affected.

Despite the relatively small size of our cohorts, they are quite homogeneous, making the possibility of additional factors being involved unlikely. Moreover, our results confirm those from other authors pointing out a role of *KRAS/BRAF* activating mutations. As mentioned in the introduction it is important to have good prognostic biomarkers to support the pathological features in identifying on one hand the CRC patients that can benefit from adjuvant therapy or on the other hand, those in which we should avoid overtreatments. This is particularly important in stage II patients where a benefit of adjuvant treatment has not been demonstrated. Our results identify a specific group of patients with *KRAS* mutations and high levels of Cdk5 that have a really bad prognostic. Further studies are warranted to elucidate if Cdk5 could be a candidate to consider for inclusion in future standardized prognostic panels for early stage CRC tumors.

4.5 Cdk5 predicts response to oxaliplatin

Several studies have shown that Cdk5 plays a role in DNA damage repair and resistance, including the ones induced by oxaliplatin and irinotecan (186, 244). Therefore we investigated the predictive value of Cdk5 through analysis of the association between tumor protein expression and the outcomes of metastatic CRC patients receiving two standard CRC chemotherapy regimens: oxaliplatin plus 5-fluorouracil and irinotecan plus 5-fluorouracil. We observed a clear association between high Cdk5 protein levels and a lower response rate and worse TTP in patients treated with the oxaliplatin based treatment. Again, the homogeneity of our patients' cohorts is an added value of our results. Moreover, they were also supported by *in vitro* studies of Cdk5 in the context of chemotherapy treatment also pointing at a role particularly in relation to oxaliplatin response and resistance. Our group has previously reported that Cdk5 overexpression was associated with oxaliplatin resistance acquisition in four cell line models (186), and here we show that this is not the case for irinotecan resistant cell lines. Rather we observed a slight decrease in the expression. Cdk5 silencing in our cell lines

followed by treatment with either irinotecan or oxaliplatin does not affect the cell viability. Interestingly, when we silenced Cdk5 in the oxaliplatin resistant cell lines we observed a clear sensitization to the drug. Unfortunately, due to the timing of the irinotecan resistant cell lines establishment, we have not yet studied the effect of Cdk5 silencing in these cells. Hence, based on the Cdk5 expression, cell viability studies and our data from the cohorts, we believe that Cdk5 contributes mainly to oxaliplatin resistance. While Cdk5 in hepatocellular carcinoma had been linked to ATM phosphorylation in the response to irinotecan treatment (162) no study exists regarding the role of Cdk5 in oxaliplatin treatment. The acquisition of oxaliplatin resistance involves numerous molecular pathways, as reviewed by our group (245). Based on our results we cannot pinpoint any pathway, however we can probably exclude the more common ones that would also affect irinotecan sensitivity, such as for example the ABC family of drug efflux transporters. Putting all this together, we can summarize our findings in figure 42. Cdk5 levels rise upon the acquisition of oxaliplatin resistance. Inhibition of Cdk5 could possibly revert this resistance. Including a Cdk5 inhibitor when administering an oxaliplatin-based regimen could possibly avoid the effects of Cdk5 upregulation on drug sensitivity. While further studies are needed, another possibility is that high Cdk5 tumor levels could serve as a biomarker for avoiding treatment with oxaliplatin and instead, treat these patients with irinotecan, as Cdk5 does not seem to affect responses to this drug.

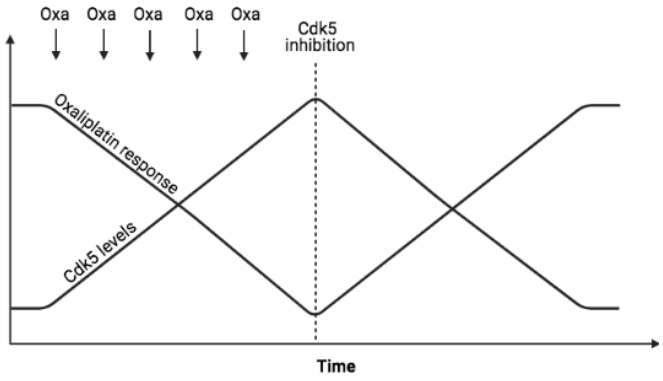

***Figure 42**. Proposed relation between Cdk5 levels and response to oxaliplatin (Oxa).*

Taken together, our results suggest that Cdk5 could be a good target to develop drugs against. Such drugs could both be used in an adjuvant setting to prevent disease relapse and in a metastatic setting in combination with oxaliplatin. Unfortunately, although huge efforts have been made, as deliberated in the introduction, the development of specific inhibitors is still an outstanding issue. Apart from the nervous system, Cdk5 is primarily expressed in malignant tissue, which could possibly limit side effects. In the drug design one could possibly take advantage of the blood brain barrier to avoid unwanted neurological side effects. In this sense, I would like to stress that we have indeed been granted by the Spanish association against cancer (AECC) to carry out proof of concept studies of the use of Proteolysis-targeting chimeric molecules

(PROTACs) for Cdk5 degradation. PROTACs® work by hijacking the intracellular ubiquitin proteasome system in cells to degrade the target, and have shown great potential in targeting otherwise “undruggable” proteins. Clinical trials are ongoing evaluating the efficacy of PROTACS® against both androgen and estrogen receptors in prostate and breast cancer, respectively. As designing specific PROTAC® is expensive and time-consuming, we are going to use the dTAG system instead (246). The dTAG system allows us to carry out a proof-of-concept study confirming the applicability of the technique before endeavoring an actual PROTAC® project.

4.6 Cdk5 as a biomarker for the use of alternative drugs

Drug repurposing has gained popularity as a strategy to accelerate the approval of new drugs’ indications by regulatory agencies. This is because approved drugs have been already assessed for safety, speeding up the time and lowering the cost from bench to bedside compared to new untested drugs. Examples of repositioning of drugs that have been approved for cancer treatments include rapamycin, chloroquine, metformin and thalidomide (247). In the recent years, advances in genomic and high-throughput technologies alongside with computational modeling have speeded up the discovery of new applications for drugs. An important side of the drug repurposing is the discovery of associated biomarkers.

We took advantage of the Achilles study to ascertain whether high Cdk5 expression could serve as a biomarker for possible dependency of other genes. This was done considering all the cell lines or subsets according to the *KRAS* mutational status. We found out that the HT29 cells expressing Cdk5 were more sensitive to docetaxel and a PIK3CB inhibitor, while in the case of LoVo, the presence of Cdk5 was associated with higher sensitive to cabazitaxel. This indicates that the vulnerability to these drugs is somehow affected by the presence of Cdk5 in our cell lines. The differences are not big, however significant.

Docetaxel and cabacitaxel are a class of drugs called taxanes that block tumor cells’ division by disrupting microtubules function through the stabilization of the GDP bound Tubulin. While they are widely used for the treatment of prostate, ovarian, NSCLC and breast cancer, they have been shown to be inefficacious in CRC (248). One could speculate that if patients in these clinical trials had been stratified according to Cdk5 expression, a possible effect in those patients with high Cdk5 levels could have been observed. Thus, further investigation is needed to understand the implication of these results and whether Cdk5 could be used as a biomarker of response to these kinds of drugs.

High dependency of *PIK3CB* was found in *KRAS* WT cells expressing high levels of *CDK5*. This gene encodes an isoform of the catalytic subunit of PI3K. The PI3K/AKT/mTOR pathway is frequently deregulated in CRC and many other types of cancer and associated with tumorigenesis, proliferation, apoptosis, EMT and drug resistance to mention a few aspects. Our results demonstrated that the effect of AZD6482 is indeed higher when *CDK5* expression is maintained in the HT29 (*KRAS* WT), suggesting that the signaling level through this key pathway is higher in these cells. Indeed, studies in ovarian and prostate cancer have shown that the phosphorylation of AKT at Ser473 is decreased upon Cdk5 downregulation (172, 177). Based on our results regarding PIK3CB inhibition, only seen in one of the two cell lines, we could only speculate how Cdk5 potentiates such signaling. Nonetheless, such indications are very much in line with the goal of the Achilles project: to identify genetic vulnerabilities. It is possible that some *KRAS* WT cell lines with higher Cdk5 levels depend more on the PI3K/AKT/mTOR pathway for cell proliferation and survival, hence making them more susceptible to such inhibition.

4.7 Cdk5 and tumor immune aspects

As mentioned before, we found that when splitting the TCGA cohort according to CMS, high Cdk5 levels were predictive of a worse PFI only in the CMS1 subtype. CMS1 is the so-called immune subtype and it is enriched in microsatellite instable (MSI), hypermutated, and highly lymphocyte-infiltrated tumors, which usually are responsive to immune checkpoint blockers (ICB). The CMS1 subtype has better relapse-free survival but worse overall survival after relapse compared with the other subtypes.

We furthermore found that in the TCGA and Colonomics cohorts, CMS1 tumors had the lowest levels of Cdk5. The fact that *CDK5* expression is lowest in the CMS1 subtype is in line with what has been demonstrated by other groups, who have shown an inverse relation between Cdk5 levels and T-cell infiltration (154, 200). One of the studies carried out in CT26 and MC38 tumors showed that the Cdk2/5/9 inhibitor Dinaciclib elicited immunogenic cell death in the tumors, why the combination therapy with α-PD-1 was highly effective (200). Yet another group showed that Cdk5 promoted transcription of PD-L1 expression in medulloblastoma models (133). Therefore, we hypothesized that Cdk5 levels could also affect immune infiltration and PD-L1 levels in CRC. However, we did not find changes in the PD-L1 expression upon IFN-γ treatment according to Cdk5 presence or absence. Moreover, our experiments in syngeneic mouse models did not reveal a clear increase in lymphocyte infiltration in tumors without *CDK5* expression. Unfortunately, we were not able to study the MC38 model due to immune

rejection because of the CRISPR/Cas9 editing. We confirmed this hypothesis as native MC38 cells did indeed result in tumor formation and growth. The differences in tumor establishment between the two models could very well be due to the MC38 cell line itself being more immunogenic than the CT26, creating more T-cell inflamed tumor microenvironment (221). When comparing the lymphoid infiltration in the two models, the C57BL/6/MC38 tumors did indeed show approximately twice the levels of CD45+ cells. This is agreement with what has previously been described about the immunophenotypic characteristics and responsiveness to ICB for MC38 and CT26 lines. These models in fact, mirror what is observed in the clinic with MSS (CT26) and MSI (MC38) colorectal cancer patients (249).

As we could not study the genetic ablation of *CDK5* in the MC38 model, we treated MOCK MDOTS with Roscovitine for Cdk5 inhibition with inconclusive results. Trying to solve this, we have attempted a transient transfection of CRISPR/Cas9 plasmids, followed by antibiotic selection and clonal expansion. The idea is that the CRISPR/Cas9 complex is present in the cell long enough to induce DSB in the *CDK5* gene without being incorporated into the genome. We were only able to achieve an approximately 50% KD of *CDK5*, most likely a reflection of gene KD on only one allele. An experiment in the C57BL/6/MC38 model with the dTAG Cdk5 degradation is contemplated within the AECC study, and should allow us to study whether specifically inhibiting Cdk5 changes the tumor immune infiltration.

Nevertheless, we could not observe a clear effect of *CDK5* KD in the response to anti-PD1 or CTLA4 in MDOTS experiments. The total absence of CTLA4 response could indicate the low levels of antigen presenting cells (APC), such as macrophages, B-cells and dendritic cells, in the spheroids. As described in the introduction this treatment inhibits exactly the binding between APC cells and T-cells, stimulating the maturation of the latter. With the simple flow cytometry panel we have used, these populations cannot be detected.

When performing studies involving aspects of the immune system it is important to keep in mind that there are significant differences between the mice and human. As syngeneic mice models are fully immunocompetent they are particularly useful in the evaluation of immuno-oncology agents. It is however important to keep in mind that there are limitations in terms of translatability to human tumors. These tumors do not develop spontaneously and often grow very rapidly, why they often do not contain the microenvironment or heterogeneity of human tumors of equivalent origin. Newer models that are becoming more common are genetically engineered mouse models (GEMM) or patient-derived xenografts (PDX) mice with human immune reconstitution though hematopoietic engraftment (249). However, the timeframe and the complexity

of these models are far greater. For our *in-vivo* studies we chose the syngeneic models as the cell lines can be modified genetically, they have well characterized responses to ICB and the rapid tumor establishment.
Taking into account our results in CMS1 patients, to study the C57BL6/MC38 model was of particular interest. It will be interesting to see whether the immune cell populations within the tumor are affected in this more CMS1-like model upon targeted degradation Cdk5 with the dTAG. If a role of Cdk5 in predicting response to ICB is confirmed, levels of Cdk5 could be used as a biomarker of immunotherapy selection.

With results of this thesis we strengthen the evidence of a role for Cdk5 in the CRC pathogenesis. We found Cdk5 to be overexpressed and highly active in CRC tumors correlating with an aggressive phenotype. Clinical applications for Cdk5 could be either as a biomarker for adjuvant therapy in early-stage CRC or for prediction of response to chemotherapy regimens. Our results furthermore suggest that Cdk5 could be a good target to develop drugs against, either to be used in an adjuvant setting to prevent disease relapse or in a metastatic setting in combination with oxaliplatin. Unfortunately, although huge efforts have been made, the development of specific inhibitors is still an outstanding issue. We believe that PROTACs® could be a possibility for specific Cdk5 inhibition, which we aim at evaluating in a proof-of-concept study with the dTAG system.

Conclusions

1) *CDK5* is expressed at high levels in CRC, which is mostly due to a gain in the gene copy number arising early on in the CRC development. The fact that we found it bound to p25 is indicative of a high activity.

2) Cdk5 does not affect CRC cell proliferation in our human *in vitro* models or when grown as subcutaneous tumors in syngeneic mice models. However, Cdk5 silencing decreases colony formation capacity as well as migration and invasion in human CRC cell lines with a deregulated MAPK pathway.

3) *CDK5* KD has a clear effect on gene expression profiles of the cell lines studied. Association with Cell adhesion signatures and specific upregulated genes, such as *CALD1,* support a connection between Cdk5 and an invasive/migratory phenotype.

4) Cdk5 levels have a prognostic value in patients with MSS, early-stage non-treated CRC, particularly those harboring *KRAS* mutations. In these patients, presenting high levels of Cdk5 are associated with shorter PFI, which is indicative of a more aggressive subset of tumors.

5) High Cdk5 levels are predictive of a shorter TTP in patients treated with an oxaliplatin-based therapy but not in those treated with an irinotecan-based treatment. *In vitro*, *CDK5* KD increases sensitivity to oxaliplatin in cell lines presenting high levels of Cdk5 expression as a consequence of acquired resistance to this drug. Acquisition of resistance to irinotecan was not associated with an increase in Cdk5 levels in the same cell lines.

6) According to data from the Achilles study, *CDK5* expression is indicative of several gene-dependencies affecting CRC cells' survival. These gene dependencies vary according to *KRAS* mutations. Experimentally, we found that cells with high levels of Cdk5 show a dependency on TUBB expression, which makes them more sensitive to anti-microtubule drugs.

7) Among all four CMS, *CDK5* is expressed at the lowest levels in the CMS1 subtype; in this group of patients, high Cdk5 levels are associated with shorter PFI.

Experimentally, *CDK5* KD does not influence PD-L1 expression in CRC cell lines upon IFN-γ stimulation. In the CT26/Balb/c model neither tumor growth, immune infiltration or response to ICB are affected by the presence of Cdk5. In spheroids from MC38/C57BL6 tumors treatment with Roscovitine and ICB did not show synergism.

References

1. Mattiuzzi C, Sanchis-Gomar F, Lippi G. Concise update on colorectal cancer epidemiology. Ann Transl Med. 2019;7(21):609.
2. Marley AR, Nan H. Epidemiology of colorectal cancer. Int J Mol Epidemiol Genet. 2016;7(3):105-14.
3. Siegel RL, Miller KD, Goding Sauer A, Fedewa SA, Butterly LF, Anderson JC, et al. Colorectal cancer statistics, 2020. CA: A Cancer Journal for Clinicians.n/a(n/a).
4. Ma H, Brosens LAA, Offerhaus GJA, Giardiello FM, de Leng WWJ, Montgomery EA. Pathology and genetics of hereditary colorectal cancer. Pathology. 2018;50(1):49-59.
5. Kanwar SS, Nautiyal J, Majumdar AP. EGFR(S) inhibitors in the treatment of gastro-intestinal cancers: what's new? Curr Drug Targets. 2010;11(6):682-98.
6. http://www.cancer.com. Layers of the intestinal wall [Available from: https://www.cancer.org/cancer/small-intestine-cancer/detection-diagnosis-staging/staging.html.
7. Cancer Genome Atlas N. Comprehensive molecular characterization of human colon and rectal cancer. Nature. 2012;487(7407):330-7.
8. Jenkins MA, Hayashi S, O'Shea AM, Burgart LJ, Smyrk TC, Shimizu D, et al. Pathology features in Bethesda guidelines predict colorectal cancer microsatellite instability: a population-based study. Gastroenterology. 2007;133(1):48-56.
9. Tariq K, Ghias K. Colorectal cancer carcinogenesis: a review of mechanisms. Cancer Biol Med. 2016;13(1):120-35.
10. Pino MS, Chung DC. The chromosomal instability pathway in colon cancer. Gastroenterology. 2010;138(6):2059-72.
11. Fearon ER, Vogelstein B. A genetic model for colorectal tumorigenesis. Cell. 1990;61(5):759-67.
12. De Palma FDE, D'Argenio V, Pol J, Kroemer G, Maiuri MC, Salvatore F. The Molecular Hallmarks of the Serrated Pathway in Colorectal Cancer. Cancers (Basel). 2019;11(7).
13. Issa JP. CpG island methylator phenotype in cancer. Nat Rev Cancer. 2004;4(12):988-93.
14. Hughes LA, Khalid-de Bakker CA, Smits KM, van den Brandt PA, Jonkers D, Ahuja N, et al. The CpG island methylator phenotype in colorectal cancer: progress and problems. Biochim Biophys Acta. 2012;1825(1):77-85.
15. Toyota M, Ahuja N, Ohe-Toyota M, Herman JG, Baylin SB, Issa JP. CpG island methylator phenotype in colorectal cancer. Proc Natl Acad Sci U S A. 1999;96(15):8681-6.
16. Weisenberger DJ, Siegmund KD, Campan M, Young J, Long TI, Faasse MA, et al. CpG island methylator phenotype underlies sporadic microsatellite instability and is tightly associated with BRAF mutation in colorectal cancer. Nat Genet. 2006;38(7):787-93.
17. Scheffzek K, Ahmadian MR, Kabsch W, Wiesmuller L, Lautwein A, Schmitz F, et al. The Ras-RasGAP complex: structural basis for GTPase activation and its loss in oncogenic Ras mutants. Science (New York, NY). 1997;277(5324):333-8.

18. Bardelli A, Siena S. Molecular mechanisms of resistance to cetuximab and panitumumab in colorectal cancer. J Clin Oncol. 2010;28(7):1254-61.
19. Li H, Zhang J, Tong JHM, Chan AWH, Yu J, Kang W, et al. Targeting the Oncogenic p53 Mutants in Colorectal Cancer and Other Solid Tumors. Int J Mol Sci. 2019;20(23).
20. Fodde R. The APC gene in colorectal cancer. Eur J Cancer. 2002;38(7):867-71.
21. Torre LA, Bray F, Siegel RL, Ferlay J, Lortet-Tieulent J, Jemal A. Global cancer statistics, 2012. CA Cancer J Clin. 2015;65(2):87-108.
22. Akasaka T, Nakata A, Rudolf M, Wang WW, Yamada M, Suzuki M, et al. Synthesis and Photoinduced Electron-Transfer Reactions in a La2 @Ih -C80 - Phenoxazine Conjugate. Chempluschem. 2017;82(7):1067-72.
23. Massague J, Obenauf AC. Metastatic colonization by circulating tumour cells. Nature. 2016;529(7586):298-306.
24. Gomez-Cuadrado L, Tracey N, Ma R, Qian B, Brunton VG. Mouse models of metastasis: progress and prospects. Dis Model Mech. 2017;10(9):1061-74.
25. van Zijl F, Krupitza G, Mikulits W. Initial steps of metastasis: cell invasion and endothelial transmigration. Mutation research. 2011;728(1-2):23-34.
26. Lamouille S, Xu J, Derynck R. Molecular mechanisms of epithelial-mesenchymal transition. Nat Rev Mol Cell Biol. 2014;15(3):178-96.
27. Fan F, Samuel S, Evans KW, Lu J, Xia L, Zhou Y, et al. Overexpression of snail induces epithelial-mesenchymal transition and a cancer stem cell-like phenotype in human colorectal cancer cells. Cancer Med. 2012;1(1):5-16.
28. Revenu C, Gilmour D. EMT 2.0: shaping epithelia through collective migration. Curr Opin Genet Dev. 2009;19(4):338-42.
29. Aceto N, Bardia A, Miyamoto DT, Donaldson MC, Wittner BS, Spencer JA, et al. Circulating tumor cell clusters are oligoclonal precursors of breast cancer metastasis. Cell. 2014;158(5):1110-22.
30. Gay LJ, Felding-Habermann B. Contribution of platelets to tumour metastasis. Nat Rev Cancer. 2011;11(2):123-34.
31. Spiegel A, Brooks MW, Houshyar S, Reinhardt F, Ardolino M, Fessler E, et al. Neutrophils Suppress Intraluminal NK Cell-Mediated Tumor Cell Clearance and Enhance Extravasation of Disseminated Carcinoma Cells. Cancer discovery. 2016;6(6):630-49.
32. Reymond N, d'Agua BB, Ridley AJ. Crossing the endothelial barrier during metastasis. Nat Rev Cancer. 2013;13(12):858-70.
33. Malanchi I, Santamaria-Martinez A, Susanto E, Peng H, Lehr HA, Delaloye JF, et al. Interactions between cancer stem cells and their niche govern metastatic colonization. Nature. 2011;481(7379):85-9.
34. Oskarsson T, Batlle E, Massague J. Metastatic stem cells: sources, niches, and vital pathways. Cell Stem Cell. 2014;14(3):306-21.
35. Chambers AF, Groom AC, MacDonald IC. Dissemination and growth of cancer cells in metastatic sites. Nat Rev Cancer. 2002;2(8):563-72.
36. Gupta GP, Massague J. Cancer metastasis: building a framework. Cell. 2006;127(4):679-95.
37. Ishaque N, Abba ML, Hauser C, Patil N, Paramasivam N, Huebschmann D, et al. Whole genome sequencing puts forward hypotheses on metastasis evolution and therapy in colorectal cancer. Nature communications. 2018;9(1):4782.
38. Fleming M, Ravula S, Tatishchev SF, Wang HL. Colorectal carcinoma: Pathologic aspects. J Gastrointest Oncol. 2012;3(3):153-73.

39. Jass JR, Atkin WS, Cuzick J, Bussey HJ, Morson BC, Northover JM, et al. The grading of rectal cancer: historical perspectives and a multivariate analysis of 447 cases. Histopathology. 1986;10(5):437-59.
40. Shia J, Schultz N, Kuk D, Vakiani E, Middha S, Segal NH, et al. Morphological characterization of colorectal cancers in The Cancer Genome Atlas reveals distinct morphology-molecular associations: clinical and biological implications. Mod Pathol. 2017;30(4):599-609.
41. Lugli A, Kirsch R, Ajioka Y, Bosman F, Cathomas G, Dawson H, et al. Recommendations for reporting tumor budding in colorectal cancer based on the International Tumor Budding Consensus Conference (ITBCC) 2016. Mod Pathol. 2017;30(9):1299-311.
42. Zlobec I, Lugli A. Tumour budding in colorectal cancer: molecular rationale for clinical translation. Nat Rev Cancer. 2018;18(4):203-4.
43. Trinh A, Ladrach C, Dawson HE, Ten Hoorn S, Kuppen PJK, Reimers MS, et al. Tumour budding is associated with the mesenchymal colon cancer subtype and RAS/RAF mutations: a study of 1320 colorectal cancers with Consensus Molecular Subgroup (CMS) data. British journal of cancer. 2018;119(10):1244-51.
44. Edge SB, Compton CC. The American Joint Committee on Cancer: the 7th edition of the AJCC cancer staging manual and the future of TNM. Ann Surg Oncol. 2010;17(6):1471-4.
45. Sjoblom T, Jones S, Wood LD, Parsons DW, Lin J, Barber TD, et al. The consensus coding sequences of human breast and colorectal cancers. Science (New York, NY). 2006;314(5797):268-74.
46. Wang W, Kandimalla R, Huang H, Zhu L, Li Y, Gao F, et al. Molecular subtyping of colorectal cancer: Recent progress, new challenges and emerging opportunities. Semin Cancer Biol. 2019;55:37-52.
47. Guinney J, Dienstmann R, Wang X, de Reynies A, Schlicker A, Soneson C, et al. The consensus molecular subtypes of colorectal cancer. Nat Med. 2015;21(11):1350-6.
48. Sveen A, Bruun J, Eide PW, Eilertsen IA, Ramirez L, Murumagi A, et al. Colorectal Cancer Consensus Molecular Subtypes Translated to Preclinical Models Uncover Potentially Targetable Cancer Cell Dependencies. Clin Cancer Res. 2018;24(4):794-806.
49. Menter DG, Davis JS, Broom BM, Overman MJ, Morris J, Kopetz S. Back to the Colorectal Cancer Consensus Molecular Subtype Future. Curr Gastroenterol Rep. 2019;21(2):5.
50. Silberhumer GR, Paty PB, Denton B, Guillem J, Gonen M, Araujo RLC, et al. Long-term oncologic outcomes for simultaneous resection of synchronous metastatic liver and primary colorectal cancer. Surgery. 2016;160(1):67-73.
51. Mayo SC, Pulitano C, Marques H, Lamelas J, Wolfgang CL, de Saussure W, et al. Surgical management of patients with synchronous colorectal liver metastasis: a multicenter international analysis. J Am Coll Surg. 2013;216(4):707-16; discussion 16-8.
52. Feo L, Polcino M, Nash GM. Resection of the Primary Tumor in Stage IV Colorectal Cancer: When Is It Necessary? Surg Clin North Am. 2017;97(3):657-69.
53. Kanemitsu Y, Shitara K, Mizusawa J, Hamaguchi T, Shida D, Komori K, et al. Primary Tumor Resection Plus Chemotherapy Versus Chemotherapy Alone for Colorectal Cancer Patients With Asymptomatic, Synchronous Unresectable

Metastases (JCOG1007; iPACS): A Randomized Clinical Trial. J Clin Oncol. 2021:Jco2002447.
54. Tan KK, Lopes Gde L, Jr., Sim R. How uncommon are isolated lung metastases in colorectal cancer? A review from database of 754 patients over 4 years. J Gastrointest Surg. 2009;13(4):642-8.
55. Franko J, Shi Q, Meyers JP, Maughan TS, Adams RA, Seymour MT, et al. Prognosis of patients with peritoneal metastatic colorectal cancer given systemic therapy: an analysis of individual patient data from prospective randomised trials from the Analysis and Research in Cancers of the Digestive System (ARCAD) database. The Lancet Oncology. 2016;17(12):1709-19.
56. Sugarbaker PH. Peritonectomy procedures. Cancer Treat Res. 1996;82:235-53.
57. Habr-Gama A, Perez R, Proscurshim I, Gama-Rodrigues J. Complete clinical response after neoadjuvant chemoradiation for distal rectal cancer. Surg Oncol Clin N Am. 2010;19(4):829-45.
58. Labianca R, Nordlinger B, Beretta GD, Mosconi S, Mandala M, Cervantes A, et al. Early colon cancer: ESMO Clinical Practice Guidelines for diagnosis, treatment and follow-up. Ann Oncol. 2013;24 Suppl 6:vi64-72.
59. Quasar Collaborative G, Gray R, Barnwell J, McConkey C, Hills RK, Williams NS, et al. Adjuvant chemotherapy versus observation in patients with colorectal cancer: a randomised study. Lancet. 2007;370(9604):2020-9.
60. Varghese A. Chemotherapy for Stage II Colon Cancer. Clin Colon Rectal Surg. 2015;28(4):256-61.
61. Argiles G, Tabernero J, Labianca R, Hochhauser D, Salazar R, Iveson T, et al. Localised colon cancer: ESMO Clinical Practice Guidelines for diagnosis, treatment and follow-up. Ann Oncol. 2020;31(10):1291-305.
62. Andre T, Boni C, Navarro M, Tabernero J, Hickish T, Topham C, et al. Improved overall survival with oxaliplatin, fluorouracil, and leucovorin as adjuvant treatment in stage II or III colon cancer in the MOSAIC trial. J Clin Oncol. 2009;27(19):3109-16.
63. Iveson TJ, Kerr RS, Saunders MP, Cassidy J, Hollander NH, Tabernero J, et al. 3 versus 6 months of adjuvant oxaliplatin-fluoropyrimidine combination therapy for colorectal cancer (SCOT): an international, randomised, phase 3, non-inferiority trial. The Lancet Oncology. 2018;19(4):562-78.
64. Van Cutsem E, Cervantes A, Adam R, Sobrero A, Van Krieken JH, Aderka D, et al. ESMO consensus guidelines for the management of patients with metastatic colorectal cancer. Ann Oncol. 2016;27(8):1386-422.
65. Parseghian CM, Loree JM, Morris VK, Liu X, Clifton KK, Napolitano S, et al. Anti-EGFR-resistant clones decay exponentially after progression: implications for anti-EGFR re-challenge. Ann Oncol. 2019;30(2):243-9.
66. De Falco V, Napolitano S, Rosello S, Huerta M, Cervantes A, Ciardiello F, et al. How we treat metastatic colorectal cancer. ESMO Open. 2020;4(Suppl 2).
67. Longley DB, Harkin DP, Johnston PG. 5-fluorouracil: mechanisms of action and clinical strategies. Nat Rev Cancer. 2003;3(5):330-8.
68. Chintala L, Vaka S, Baranda J, Williamson SK. Capecitabine versus 5-fluorouracil in colorectal cancer: where are we now? Oncology Reviews. 2011;5(2):129-40.
69. Tournigand C, Andre T, Achille E, Lledo G, Flesh M, Mery-Mignard D, et al. FOLFIRI followed by FOLFOX6 or the reverse sequence in advanced colorectal cancer: a randomized GERCOR study. J Clin Oncol. 2004;22(2):229-37.

70. Colucci G, Gebbia V, Paoletti G, Giuliani F, Caruso M, Gebbia N, et al. Phase III randomized trial of FOLFIRI versus FOLFOX4 in the treatment of advanced colorectal cancer: a multicenter study of the Gruppo Oncologico Dell'Italia Meridionale. J Clin Oncol. 2005;23(22):4866-75.
71. Pommier Y. Drugging topoisomerases: lessons and challenges. ACS Chem Biol. 2013;8(1):82-95.
72. Ahmad S. Platinum-DNA interactions and subsequent cellular processes controlling sensitivity to anticancer platinum complexes. Chem Biodivers. 2010;7(3):543-66.
73. Di Francesco AM, Ruggiero A, Riccardi R. Cellular and molecular aspects of drugs of the future: oxaliplatin. Cell Mol Life Sci. 2002;59(11):1914-27.
74. Ferrara N, Hillan KJ, Gerber HP, Novotny W. Discovery and development of bevacizumab, an anti-VEGF antibody for treating cancer. Nature reviews Drug discovery. 2004;3(5):391-400.
75. Loupakis F, Cremolini C, Masi G, Lonardi S, Zagonel V, Salvatore L, et al. Initial therapy with FOLFOXIRI and bevacizumab for metastatic colorectal cancer. N Engl J Med. 2014;371(17):1609-18.
76. Saltz LB, Clarke S, Diaz-Rubio E, Scheithauer W, Figer A, Wong R, et al. Bevacizumab in combination with oxaliplatin-based chemotherapy as first-line therapy in metastatic colorectal cancer: a randomized phase III study. J Clin Oncol. 2008;26(12):2013-9.
77. Herbst RS. Review of epidermal growth factor receptor biology. Int J Radiat Oncol Biol Phys. 2004;59(2 Suppl):21-6.
78. Siena S, Sartore-Bianchi A, Trusolino L, Martino C, Bencardino K, Lonardi S, et al. Abstract CT005: Final results of the HERACLES trial in HER2-amplified colorectal cancer. Cancer Res. 2017;77(13 Supplement):CT005-CT.
79. Kopetz S, Grothey A, Yaeger R, Van Cutsem E, Desai J, Yoshino T, et al. Encorafenib, Binimetinib, and Cetuximab in BRAF V600E-Mutated Colorectal Cancer. N Engl J Med. 2019;381(17):1632-43.
80. Adenis A, de la Fouchardiere C, Paule B, Burtin P, Tougeron D, Wallet J, et al. Survival, safety, and prognostic factors for outcome with Regorafenib in patients with metastatic colorectal cancer refractory to standard therapies: results from a multicenter study (REBECCA) nested within a compassionate use program. BMC cancer. 2016;16:412.
81. Mayer RJ, Van Cutsem E, Falcone A, Yoshino T, Garcia-Carbonero R, Mizunuma N, et al. Randomized trial of TAS-102 for refractory metastatic colorectal cancer. N Engl J Med. 2015;372(20):1909-19.
82. Tabernero J, Yoshino T, Cohn AL, Obermannova R, Bodoky G, Garcia-Carbonero R, et al. Ramucirumab versus placebo in combination with second-line FOLFIRI in patients with metastatic colorectal carcinoma that progressed during or after first-line therapy with bevacizumab, oxaliplatin, and a fluoropyrimidine (RAISE): a randomised, double-blind, multicentre, phase 3 study. The Lancet Oncology. 2015;16(5):499-508.
83. Markman JL, Shiao SL. Impact of the immune system and immunotherapy in colorectal cancer. J Gastrointest Oncol. 2015;6(2):208-23.
84. Xie YH, Chen YX, Fang JY. Comprehensive review of targeted therapy for colorectal cancer. Signal transduction and targeted therapy. 2020;5(1):22.
85. Seidel JA, Otsuka A, Kabashima K. Anti-PD-1 and Anti-CTLA-4 Therapies in Cancer: Mechanisms of Action, Efficacy, and Limitations. Front Oncol. 2018;8:86.

86. McGranahan N, Furness AJ, Rosenthal R, Ramskov S, Lyngaa R, Saini SK, et al. Clonal neoantigens elicit T cell immunoreactivity and sensitivity to immune checkpoint blockade. Science (New York, NY). 2016;351(6280):1463-9.
87. Andre T, Shiu K-K, Kim TW, Jensen BV, Jensen LH, Punt CJA, et al. Pembrolizumab versus chemotherapy for microsatellite instability-high/mismatch repair deficient metastatic colorectal cancer: The phase 3 KEYNOTE-177 Study. J Clin Oncol. 2020;38(18_suppl):LBA4-LBA.
88. Cohen R, Bennouna J, Meurisse A, Tournigand C, De La Fouchardiere C, Tougeron D, et al. RECIST and iRECIST criteria for the evaluation of nivolumab plus ipilimumab in patients with microsatellite instability-high/mismatch repair-deficient metastatic colorectal cancer: the GERCOR NIPICOL phase II study. J Immunother Cancer. 2020;8(2).
89. Siegel RL, Miller KD, Fedewa SA, Ahnen DJ, Meester RGS, Barzi A, et al. Colorectal cancer statistics, 2017. CA Cancer J Clin. 2017;67(3):177-93.
90. Undevia SD, Gomez-Abuin G, Ratain MJ. Pharmacokinetic variability of anticancer agents. Nat Rev Cancer. 2005;5(6):447-58.
91. Gottesman MM, Fojo T, Bates SE. Multidrug resistance in cancer: role of ATP-dependent transporters. Nat Rev Cancer. 2002;2(1):48-58.
92. Dive C, Hickman JA. Drug-target interactions: only the first step in the commitment to a programmed cell death? British journal of cancer. 1991;64(1):192-6.
93. Watson RG, Muhale F, Thorne LB, Yu J, O'Neil BH, Hoskins JM, et al. Amplification of thymidylate synthetase in metastatic colorectal cancer patients pretreated with 5-fluorouracil-based chemotherapy. Eur J Cancer. 2010;46(18):3358-64.
94. Bohanes P, Labonte MJ, Lenz HJ. A review of excision repair cross-complementation group 1 in colorectal cancer. Clin Colorectal Cancer. 2011;10(3):157-64.
95. Bettegowda C, Sausen M, Leary RJ, Kinde I, Wang Y, Agrawal N, et al. Detection of circulating tumor DNA in early- and late-stage human malignancies. Sci Transl Med. 2014;6(224):224ra24.
96. Misale S, Arena S, Lamba S, Siravegna G, Lallo A, Hobor S, et al. Blockade of EGFR and MEK intercepts heterogeneous mechanisms of acquired resistance to anti-EGFR therapies in colorectal cancer. Sci Transl Med. 2014;6(224):224ra26.
97. Suggested technique for fecal occult blood testing and interpretation in colorectal cancer screening. American College of Physicians. Ann Intern Med. 1997;126(10):808-10.
98. Bhardwaj M, Gies A, Werner S, Schrotz-King P, Brenner H. Blood-Based Protein Signatures for Early Detection of Colorectal Cancer: A Systematic Review. Clin Transl Gastroenterol. 2017;8(11):e128.
99. Voronova V, Glybochko P, Svistunov A, Fomin V, Kopylov P, Tzarkov P, et al. Diagnostic Value of Combinatorial Markers in Colorectal Carcinoma. Front Oncol. 2020;10:832.
100. Sargent DJ, Marsoni S, Monges G, Thibodeau SN, Labianca R, Hamilton SR, et al. Defective mismatch repair as a predictive marker for lack of efficacy of fluorouracil-based adjuvant therapy in colon cancer. J Clin Oncol. 2010;28(20):3219-26.
101. Petrelli F, Ghidini M, Cabiddu M, Pezzica E, Corti D, Turati L, et al. Microsatellite Instability and Survival in Stage II Colorectal Cancer: A Systematic Review and Meta-analysis. Anticancer Res. 2019;39(12):6431-41.

102. Sinicrope FA, Mahoney MR, Smyrk TC, Thibodeau SN, Warren RS, Bertagnolli MM, et al. Prognostic impact of deficient DNA mismatch repair in patients with stage III colon cancer from a randomized trial of FOLFOX-based adjuvant chemotherapy. J Clin Oncol. 2013;31(29):3664-72.
103. Morse MA, Hochster H, Benson A. Perspectives on Treatment of Metastatic Colorectal Cancer with Immune Checkpoint Inhibitor Therapy. Oncologist. 2020;25(1):33-45.
104. Sahin IH, Akce M, Alese O, Shaib W, Lesinski GB, El-Rayes B, et al. Immune checkpoint inhibitors for the treatment of MSI-H/MMR-D colorectal cancer and a perspective on resistance mechanisms. British journal of cancer. 2019;121(10):809-18.
105. Yoon HH, Tougeron D, Shi Q, Alberts SR, Mahoney MR, Nelson GD, et al. KRAS codon 12 and 13 mutations in relation to disease-free survival in BRAF-wild-type stage III colon cancers from an adjuvant chemotherapy trial (N0147 alliance). Clin Cancer Res. 2014;20(11):3033-43.
106. Modest DP, Ricard I, Heinemann V, Hegewisch-Becker S, Schmiegel W, Porschen R, et al. Outcome according to KRAS-, NRAS- and BRAF-mutation as well as KRAS mutation variants: pooled analysis of five randomized trials in metastatic colorectal cancer by the AIO colorectal cancer study group. Ann Oncol. 2016;27(9):1746-53.
107. De Roock W, Claes B, Bernasconi D, De Schutter J, Biesmans B, Fountzilas G, et al. Effects of KRAS, BRAF, NRAS, and PIK3CA mutations on the efficacy of cetuximab plus chemotherapy in chemotherapy-refractory metastatic colorectal cancer: a retrospective consortium analysis. The Lancet Oncology. 2010;11(8):753-62.
108. Pietrantonio F, Petrelli F, Coinu A, Di Bartolomeo M, Borgonovo K, Maggi C, et al. Predictive role of BRAF mutations in patients with advanced colorectal cancer receiving cetuximab and panitumumab: a meta-analysis. Eur J Cancer. 2015;51(5):587-94.
109. Rowland A, Dias MM, Wiese MD, Kichenadasse G, McKinnon RA, Karapetis CS, et al. Meta-analysis of BRAF mutation as a predictive biomarker of benefit from anti-EGFR monoclonal antibody therapy for RAS wild-type metastatic colorectal cancer. British journal of cancer. 2015;112(12):1888-94.
110. Reece M, Saluja H, Hollington P, Karapetis CS, Vatandoust S, Young GP, et al. The Use of Circulating Tumor DNA to Monitor and Predict Response to Treatment in Colorectal Cancer. Front Genet. 2019;10:1118.
111. Loupakis F, Yang D, Yau L, Feng S, Cremolini C, Zhang W, et al. Primary t umor location as a prognostic factor in metastatic colorectal cancer. J Natl Cancer Inst. 2015;107(3).
112. Tejpar S, Stintzing S, Ciardiello F, Tabernero J, Van Cutsem E, Beier F, et al. Prognostic and Predictive Relevance of Primary Tumor Location in Patients With RAS Wild-Type Metastatic Colorectal Cancer: Retrospective Analyses of the CRYSTAL and FIRE-3 Trials. JAMA Oncol. 2017;3(2):194-201.
113. Lee MKC, Loree JM. Current and emerging biomarkers in metastatic colorectal cancer. Curr Oncol. 2019;26(Suppl 1):S7-S15.
114. Malumbres M. Cyclin-dependent kinases. Genome Biol. 2014;15(6):122.
115. Dhariwala FA, Rajadhyaksha MS. An unusual member of the Cdk family: Cdk5. Cellular and molecular neurobiology. 2008;28(3):351-69.
116. Shah K, Lahiri DK. Cdk5 activity in the brain - multiple paths of regulation. Journal of cell science. 2014;127(Pt 11):2391-400.

117. Kumazawa A, Mita N, Hirasawa M, Adachi T, Suzuki H, Shafeghat N, et al. Cyclin-dependent kinase 5 is required for normal cerebellar development. Mol Cell Neurosci. 2013;52:97-105.
118. Chen F, Wang Q, Wang X, Studzinski GP. Up-regulation of Egr1 by 1,25-dihydroxyvitamin D3 contributes to increased expression of p35 activator of cyclin-dependent kinase 5 and consequent onset of the terminal phase of HL60 cell differentiation. Cancer Res. 2004;64(15):5425-33.
119. Sahlgren CM, Mikhailov A, Vaittinen S, Pallari HM, Kalimo H, Pant HC, et al. Cdk5 regulates the organization of Nestin and its association with p35. Mol Cell Biol. 2003;23(14):5090-106.
120. Liebl J, Weitensteiner SB, Vereb G, Takacs L, Furst R, Vollmar AM, et al. Cyclin-dependent kinase 5 regulates endothelial cell migration and angiogenesis. The Journal of biological chemistry. 2010;285(46):35932-43.
121. Tang D, Chun AC, Zhang M, Wang JH. Cyclin-dependent kinase 5 (Cdk5) activation domain of neuronal Cdk5 activator. Evidence of the existence of cyclin fold in neuronal Cdk5a activator. The Journal of biological chemistry. 1997;272(19):12318-27.
122. Saito T, Yano M, Kawai Y, Asada A, Wada M, Doi H, et al. Structural basis for the different stability and activity between the Cdk5 complexes with p35 and p39 activators. The Journal of biological chemistry. 2013;288(45):32433-9.
123. Asada A, Yamamoto N, Gohda M, Saito T, Hayashi N, Hisanaga S. Myristoylation of p39 and p35 is a determinant of cytoplasmic or nuclear localization of active cyclin-dependent kinase 5 complexes. J Neurochem. 2008;106(3):1325-36.
124. Patrick GN, Zhou P, Kwon YT, Howley PM, Tsai LH. p35, the neuronal-specific activator of cyclin-dependent kinase 5 (Cdk5) is degraded by the ubiquitin-proteasome pathway. The Journal of biological chemistry. 1998;273(37):24057-64.
125. Kimura T, Ishiguro K, Hisanaga S. Physiological and pathological phosphorylation of tau by Cdk5. Front Mol Neurosci. 2014;7:65.
126. Patrick GN, Zukerberg L, Nikolic M, de la Monte S, Dikkes P, Tsai LH. Conversion of p35 to p25 deregulates Cdk5 activity and promotes neurodegeneration. Nature. 1999;402(6762):615-22.
127. Song H, Kim W, Choi JH, Kim SH, Lee D, Park CH, et al. Stress-induced nuclear translocation of CDK5 suppresses neuronal death by downregulating ERK activation via VRK3 phosphorylation. Sci Rep. 2016;6:28634.
128. Zhang J, Cicero SA, Wang L, Romito-Digiacomo RR, Yang Y, Herrup K. Nuclear localization of Cdk5 is a key determinant in the postmitotic state of neurons. Proc Natl Acad Sci U S A. 2008;105(25):8772-7.
129. Zeb A, Son M, Yoon S, Kim JH, Park SJ, Lee KW. Computational Simulations Identified Two Candidate Inhibitors of Cdk5/p25 to Abrogate Tau-associated Neurological Disorders. Comput Struct Biotechnol J. 2019;17:579-90.
130. Zukerberg LR, Patrick GN, Nikolic M, Humbert S, Wu CL, Lanier LM, et al. Cables links Cdk5 and c-Abl and facilitates Cdk5 tyrosine phosphorylation, kinase upregulation, and neurite outgrowth. Neuron. 2000;26(3):633-46.
131. Wei FY, Nagashima K, Ohshima T, Saheki Y, Lu YF, Matsushita M, et al. Cdk5-dependent regulation of glucose-stimulated insulin secretion. Nat Med. 2005;11(10):1104-8.
132. Liebl J. Cdk5 and Foxc2--a new relationship in the lymphatic vasculature. Oncotarget. 2015;6(26):21799-801.

133. Dorand RD, Nthale J, Myers JT, Barkauskas DS, Avril S, Chirieleison SM, et al. Cdk5 disruption attenuates tumor PD-L1 expression and promotes antitumor immunity. Science (New York, NY). 2016;353(6297):399-403.
134. Shupp A, Casimiro MC, Pestell RG. Biological functions of CDK5 and potential CDK5 targeted clinical treatments. Oncotarget. 2017;8(10):17373-82.
135. Mushtaq G, Greig NH, Anwar F, Al-Abbasi FA, Zamzami MA, Al-Talhi HA, et al. Neuroprotective Mechanisms Mediated by CDK5 Inhibition. Curr Pharm Des. 2016;22(5):527-34.
136. Ahmed D, Sharma M. Cyclin-Dependent Kinase 5/p35/p39: A Novel and Imminent Therapeutic Target for Diabetes Mellitus. Int J Endocrinol. 2011;2011:530274.
137. Cicenas J, Kalyan K, Sorokinas A, Stankunas E, Levy J, Meskinyte I, et al. Roscovitine in cancer and other diseases. Ann Transl Med. 2015;3(10):135.
138. Xi CL, Wang L, Yu J, Ye H, Cao LL, Gong ZL. Inhibition of cyclin-dependent kinases by AT7519 is effective to overcome chemoresistance in colon and cervical cancer. Biochem Bioph Res Co. 2019;513(3):589-93.
139. Robb CM, Kour S, Contreras JI, Agarwal E, Barger CJ, Rana S, et al. Characterization of CDK(5) inhibitor, 20-223 (aka CP668863) for colorectal cancer therapy. Oncotarget. 2018;9(4):5216-32.
140. Lenjisa JL, Tadesse S, Khair NZ, Kumarasiri M, Yu M, Albrecht H, et al. CDK5 in oncology: recent advances and future prospects. Future Med Chem. 2017;9(16):1939-62.
141. Zheng YL, Li C, Hu YF, Cao L, Wang H, Li B, et al. Cdk5 inhibitory peptide (CIP) inhibits Cdk5/p25 activity induced by high glucose in pancreatic beta cells and recovers insulin secretion from p25 damage. Plos One. 2013;8(9):e63332.
142. Sundaram JR, Poore CP, Sulaimee NH, Pareek T, Asad AB, Rajkumar R, et al. Specific inhibition of p25/Cdk5 activity by the Cdk5 inhibitory peptide reduces neurodegeneration in vivo. J Neurosci. 2013;33(1):334-43.
143. Bao HX, Bi Q, Han Y, Zhao C, Zou H. Potential mechanisms underlying CDK5 related Osteosarcoma progression. Expert Opin Ther Targets. 2017;21(5):455-60.
144. Liang Q, Li L, Zhang J, Lei Y, Wang L, Liu DX, et al. CDK5 is essential for TGF-beta1-induced epithelial-mesenchymal transition and breast cancer progression. Sci Rep. 2013;3:2932.
145. Zeng J, Xie S, Liu Y, Shen C, Song X, Zhou GL, et al. CDK5 Functions as a Tumor Promoter in Human Lung Cancer. J Cancer. 2018;9(21):3950-61.
146. Zhuang K, Zhang J, Xiong M, Wang X, Luo X, Han L, et al. CDK5 functions as a tumor promoter in human colorectal cancer via modulating the ERK5-AP-1 axis. Cell death & disease. 2016;7(10):e2415.
147. Zhang R, Lin P, Yang H, He Y, Dang YW, Feng ZB, et al. Clinical role and biological function of CDK5 in hepatocellular carcinoma: A study based on immunohistochemistry, RNA-seq and in vitro investigation. Oncotarget. 2017;8(65):108333-54.
148. Sharma S, Zhang T, Michowski W, Rebecca VW, Xiao M, Ferretti R, et al. Targeting the cyclin-dependent kinase 5 in metastatic melanoma. Proc Natl Acad Sci U S A. 2020;117(14):8001-12.
149. Lin JX, Xie XS, Weng XF, Zheng CH, Xie JW, Wang JB, et al. The prognostic value of Cyclin-Dependent Kinase 5 and Protein Phosphatase 2A in Gastric Cancer. J Cancer. 2018;9(23):4404-12.

150. Chiker S, Pennaneach V, Loew D, Dingli F, Biard D, Cordelieres FP, et al. Cdk5 promotes DNA replication stress checkpoint activation through RPA-32 phosphorylation, and impacts on metastasis free survival in breast cancer patients. Cell cycle (Georgetown, Tex). 2015;14(19):3066-78.
151. Huang PH, Chen MC, Peng YT, Kao WH, Chang CH, Wang YC, et al. Cdk5 Directly Targets Nuclear p21CIP1 and Promotes Cancer Cell Growth. Cancer Res. 2016;76(23):6888-900.
152. Goodyear S, Sharma MC. Roscovitine regulates invasive breast cancer cell (MDA-MB231) proliferation and survival through cell cycle regulatory protein cdk5. Exp Mol Pathol. 2007;82(1):25-32.
153. Mandl MM, Zhang S, Ulrich M, Schmoeckel E, Mayr D, Vollmar AM, et al. Inhibition of Cdk5 induces cell death of tumor-initiating cells. British journal of cancer. 2017;116(7):912-22.
154. Deng H, Tan S, Gao X, Zou C, Xu C, Tu K, et al. Cdk5 knocking out mediated by CRISPR-Cas9 genome editing for PD-L1 attenuation and enhanced antitumor immunity. Acta Pharm Sin B. 2020;10(2):358-73.
155. Su CY, Yan RL, Hsu WH, Chu CT, Chang HC, Lai CC, et al. Phosphorylation of adducin-1 by cyclin-dependent kinase 5 is important for epidermal growth factor-induced cell migration. Sci Rep. 2019;9(1):13703.
156. Li L, Kolodziej T, Jafari N, Chen J, Zhu H, Rajfur Z, et al. Cdk5-mediated phosphorylation regulates phosphatidylinositol 4-phosphate 5-kinase type I gamma 90 activity and cell invasion. FASEB J. 2019;33(1):631-42.
157. Feldmann G, Mishra A, Hong SM, Bisht S, Strock CJ, Ball DW, et al. Inhibiting the cyclin-dependent kinase CDK5 blocks pancreatic cancer formation and progression through the suppression of Ras-Ral signaling. Cancer Res. 2010;70(11):4460-9.
158. Eggers JP, Grandgenett PM, Collisson EC, Lewallen ME, Tremayne J, Singh PK, et al. Cyclin-dependent kinase 5 is amplified and overexpressed in pancreatic cancer and activated by mutant K-Ras. Clin Cancer Res. 2011;17(19):6140-50.
159. Pozo K, Hillmann A, Augustyn A, Plattner F, Hai T, Singh T, et al. Differential expression of cell cycle regulators in CDK5-dependent medullary thyroid carcinoma tumorigenesis. Oncotarget. 2015;6(14):12080-93.
160. Lin H, Chen MC, Chiu CY, Song YM, Lin SY. Cdk5 regulates STAT3 activation and cell proliferation in medullary thyroid carcinoma cells. The Journal of biological chemistry. 2007;282(5):2776-84.
161. Zhang S, Ulrich M, Gromnicka A, Havlicek L, Krystof V, Jorda R, et al. Anti-angiogenic effects of novel cyclin-dependent kinase inhibitors with a pyrazolo[4,3-d]pyrimidine scaffold. Br J Pharmacol. 2016;173(17):2645-56.
162. Ehrlich SM, Liebl J, Ardelt MA, Lehr T, De Toni EN, Mayr D, et al. Targeting cyclin dependent kinase 5 in hepatocellular carcinoma--A novel therapeutic approach. J Hepatol. 2015;63(1):102-13.
163. Courapied S, Sellier H, de Carne Trecesson S, Vigneron A, Bernard AC, Gamelin E, et al. The cdk5 kinase regulates the STAT3 transcription factor to prevent DNA damage upon topoisomerase I inhibition. The Journal of biological chemistry. 2010;285(35):26765-78.
164. Wang F, Zhao W, Gao Y, Zhou J, Li H, Zhang G, et al. CDK5-mediated phosphorylation and stabilization of TPX2 promotes hepatocellular tumorigenesis. J Exp Clin Cancer Res. 2019;38(1):286.

165. Merk H, Zhang S, Lehr T, Muller C, Ulrich M, Bibb JA, et al. Inhibition of endothelial Cdk5 reduces tumor growth by promoting non-productive angiogenesis. Oncotarget. 2016;7(5):6088-104.
166. Bisht S, Nolting J, Schutte U, Haarmann J, Jain P, Shah D, et al. Cyclin-Dependent Kinase 5 (CDK5) Controls Melanoma Cell Motility, Invasiveness, and Metastatic Spread-Identification of a Promising Novel therapeutic target. Transl Oncol. 2015;8(4):295-307.
167. Ambrosini G, Pratilas CA, Qin LX, Tadi M, Surriga O, Carvajal RD, et al. Identification of unique MEK-dependent genes in GNAQ mutant uveal melanoma involved in cell growth, tumor cell invasion, and MEK resistance. Clin Cancer Res. 2012;18(13):3552-61.
168. Abdullah C, Wang X, Becker D. Expression analysis and molecular targeting of cyclin-dependent kinases in advanced melanoma. Cell cycle (Georgetown, Tex). 2011;10(6):977-88.
169. Li X, Wang R, Zhang J, Yang S, Ji K, Du B, et al. Cyclin-dependent kinase 5 regulates proliferation, migration, tyrosinase activity, and melanin production in B16-F10 melanoma cells via the essential regulator p-CREB. In Vitro Cell Dev Biol Anim. 2019;55(6):416-25.
170. Liu JL, Gu RX, Zhou XS, Zhou FZ, Wu G. Cyclin-dependent kinase 5 regulates the proliferation, motility and invasiveness of lung cancer cells through its effects on cytoskeletal remodeling. Mol Med Rep. 2015;12(3):3979-85.
171. Zhou X, Gu R, Han X, Wu G, Liu J. Cyclin-dependent kinase 5 controls vasculogenic mimicry formation in non-small cell lung cancer via the FAK-AKT signaling pathway. Biochem Biophys Res Commun. 2017;492(3):447-52.
172. Zhang S, Lu Z, Mao W, Ahmed AA, Yang H, Zhou J, et al. CDK5 Regulates Paclitaxel Sensitivity in Ovarian Cancer Cells by Modulating AKT Activation, p21Cip1- and p27Kip1-Mediated G1 Cell Cycle Arrest and Apoptosis. Plos One. 2015;10(7):e0131833.
173. Quintavalle M, Elia L, Price JH, Heynen-Genel S, Courtneidge SA. A cell-based high-content screening assay reveals activators and inhibitors of cancer cell invasion. Sci Signal. 2011;4(183):ra49.
174. Lowman XH, McDonnell MA, Kosloske A, Odumade OA, Jenness C, Karim CB, et al. The proapoptotic function of Noxa in human leukemia cells is regulated by the kinase Cdk5 and by glucose. Mol Cell. 2010;40(5):823-33.
175. Kim E, Chen F, Wang CC, Harrison LE. CDK5 is a novel regulatory protein in PPARgamma ligand-induced antiproliferation. International journal of oncology. 2006;28(1):191-4.
176. Ruiz de Porras V, Bystrup S, Cabrero-de Las Heras S, Musulen E, Palomero L, Alonso MH, et al. Tumor Expression of Cyclin-Dependent Kinase 5 (Cdk5) Is a Prognostic Biomarker and Predicts Outcome of Oxaliplatin-Treated Metastatic Colorectal Cancer Patients. Cancers (Basel). 2019;11(10).
177. Lindqvist J, Imanishi SY, Torvaldson E, Malinen M, Remes M, Orn F, et al. Cyclin-dependent kinase 5 acts as a critical determinant of AKT-dependent proliferation and regulates differential gene expression by the androgen receptor in prostate cancer cells. Molecular biology of the cell. 2015;26(11):1971-84.
178. Hsu FN, Chen MC, Lin KC, Peng YT, Li PC, Lin E, et al. Cyclin-dependent kinase 5 modulates STAT3 and androgen receptor activation through phosphorylation of Ser(7)(2)(7) on STAT3 in prostate cancer cells. Am J Physiol Endocrinol Metab. 2013;305(8):E975-86.

179. Pozo K, Castro-Rivera E, Tan C, Plattner F, Schwach G, Siegl V, et al. The role of Cdk5 in neuroendocrine thyroid cancer. Cancer Cell. 2013;24(4):499-511.
180. Liu C, Zhai X, Zhao B, Wang Y, Xu Z. Cyclin I-like (CCNI2) is a cyclin-dependent kinase 5 (CDK5) activator and is involved in cell cycle regulation. Sci Rep. 2017;7:40979.
181. Lopes JP, Agostinho P. Cdk5: multitasking between physiological and pathological conditions. Prog Neurobiol. 2011;94(1):49-63.
182. Pozo K, Bibb JA. The Emerging Role of Cdk5 in Cancer. Trends Cancer. 2016;2(10):606-18.
183. Yu HP, Xie JM, Li B, Sun YH, Gao QG, Ding ZH, et al. TIGAR regulates DNA damage and repair through pentosephosphate pathway and Cdk5-ATM pathway. Sci Rep. 2015;5:9853.
184. Lee JH, Kim KT. Regulation of cyclin-dependent kinase 5 and p53 by ERK1/2 pathway in the DNA damage-induced neuronal death. J Cell Physiol. 2007;210(3):784-97.
185. Tian B, Yang Q, Mao Z. Phosphorylation of ATM by Cdk5 mediates DNA damage signalling and regulates neuronal death. Nature cell biology. 2009;11(2):211-8.
186. Martinez-Cardus A, Martinez-Balibrea E, Bandres E, Malumbres R, Gines A, Manzano JL, et al. Pharmacogenomic approach for the identification of novel determinants of acquired resistance to oxaliplatin in colorectal cancer. Molecular cancer therapeutics. 2009;8(1):194-202.
187. Zhang F, Zhang T, Gu ZP, Zhou YA, Han Y, Li XF, et al. Enhancement of radiosensitivity by roscovitine pretreatment in human non-small cell lung cancer A549 cells. J Radiat Res. 2008;49(5):541-8.
188. Cortes N, Guzman-Martinez L, Andrade V, Gonzalez A, Maccioni RB. CDK5: A Unique CDK and Its Multiple Roles in the Nervous System. J Alzheimers Dis. 2019;68(3):843-55.
189. Strock CJ, Park JI, Nakakura EK, Bova GS, Isaacs JT, Ball DW, et al. Cyclin-dependent kinase 5 activity controls cell motility and metastatic potential of prostate cancer cells. Cancer Res. 2006;66(15):7509-15.
190. Feldmann G, Mishra A, Bisht S, Karikari C, Garrido-Laguna I, Rasheed Z, et al. Cyclin-dependent kinase inhibitor Dinaciclib (SCH727965) inhibits pancreatic cancer growth and progression in murine xenograft models. Cancer Biol Ther. 2011;12(7):598-609.
191. Demelash A, Rudrabhatla P, Pant HC, Wang X, Amin ND, McWhite CD, et al. Achaete-scute homologue-1 (ASH1) stimulates migration of lung cancer cells through Cdk5/p35 pathway. Molecular biology of the cell. 2012;23(15):2856-66.
192. Xie W, Liu C, Wu D, Li Z, Li C, Zhang Y. Phosphorylation of kinase insert domain receptor by cyclin-dependent kinase 5 at serine 229 is associated with invasive behavior and poor prognosis in prolactin pituitary adenomas. Oncotarget. 2016;7(32):50883-94.
193. Jin JK, Tien PC, Cheng CJ, Song JH, Huang C, Lin SH, et al. Talin1 phosphorylation activates beta1 integrins: a novel mechanism to promote prostate cancer bone metastasis. Oncogene. 2015;34(14):1811-21.
194. Parvathy M, Sreeja S, Kumar R, Pillai MR. Potential role of p21 Activated Kinase 1 (PAK1) in the invasion and motility of oral cancer cells. BMC cancer. 2016;16 Suppl 1:293.
195. Danilov AV, Hu S, Orr B, Godek K, Mustachio LM, Sekula D, et al. Dinaciclib Induces Anaphase Catastrophe in Lung Cancer Cells via Inhibition of Cyclin-

Dependent Kinases 1 and 2. Molecular cancer therapeutics. 2016;15(11):2758-66.
196. Bhandari D, Lopez-Sanchez I, To A, Lo IC, Aznar N, Leyme A, et al. Cyclin-dependent kinase 5 activates guanine nucleotide exchange factor GIV/Girdin to orchestrate migration-proliferation dichotomy. Proc Natl Acad Sci U S A. 2015;112(35):E4874-83.
197. Weis SM, Cheresh DA. Tumor angiogenesis: molecular pathways and therapeutic targets. Nat Med. 2011;17(11):1359-70.
198. Sharma MR, Tuszynski GP, Sharma MC. Angiostatin-induced inhibition of endothelial cell proliferation/apoptosis is associated with the down-regulation of cell cycle regulatory protein cdk5. J Cell Biochem. 2004;91(2):398-409.
199. Li B, Chan HL, Chen P. Immune Checkpoint Inhibitors: Basics and Challenges. Curr Med Chem. 2019;26(17):3009-25.
200. Hossain DMS, Javaid S, Cai M, Zhang C, Sawant A, Hinton M, et al. Dinaciclib induces immunogenic cell death and enhances anti-PD1-mediated tumor suppression. J Clin Invest. 2018;128(2):644-54.
201. Bei Y, Cheng N, Chen T, Shu Y, Yang Y, Yang N, et al. CDK5 Inhibition Abrogates TNBC Stem-Cell Property and Enhances Anti-PD-1 Therapy. Advanced science (Weinheim, Baden-Wurttemberg, Germany). 2020;7(22):2001417.
202. Livak KJ, Schmittgen TD. Analysis of relative gene expression data using real-time quantitative PCR and the 2(-Delta Delta C(T)) Method. Methods (San Diego, Calif). 2001;25(4):402-8.
203. Dobin A, Davis CA, Schlesinger F, Drenkow J, Zaleski C, Jha S, et al. STAR: ultrafast universal RNA-seq aligner. Bioinformatics. 2013;29(1):15-21.
204. Li B, Dewey CN. RSEM: accurate transcript quantification from RNA-Seq data with or without a reference genome. Bmc Bioinformatics. 2011;12.
205. Love MI, Huber W, Anders S. Moderated estimation of fold change and dispersion for RNA-seq data with DESeq2. Genome Biol. 2014;15(12).
206. Reimand J, Kull M, Peterson H, Hansen J, Vilo J. g : Profiler - a web-based toolset for functional profiling of gene lists from large-scale experiments. Nucleic Acids Res. 2007;35:W193-W200.
207. Martinez-Balibrea E, Martínez-Cardús A, Musulén E, Ginés A, Manzano JL, Aranda E, et al. Increased levels of copper efflux transporter ATP7B are associated with poor outcome in colorectal cancer patients receiving oxaliplatin-based chemotherapy. Int J Cancer. 2009;124(12):2905-10.
208. Jenkins RW, Aref AR, Lizotte PH, Ivanova E, Stinson S, Zhou CW, et al. Ex Vivo Profiling of PD-1 Blockade Using Organotypic Tumor Spheroids. Cancer discovery. 2018;8(2):196-215.
209. Guinney J, Dienstmann R, Wang X, de Reynies A, Schlicker A, Soneson C, et al. The consensus molecular subtypes of colorectal cancer. Nat Med. 2015;21(11):1350-6.
210. Liu JF, Lichtenberg T, Hoadley KA, Poisson LM, Lazar AJ, Cherniack AD, et al. An integrated TCGA pan-cancer clinical data resource to drive high quality survival outcome analytics. Cancer Res. 2018;78(13).
211. Stange DE, Engel F, Longerich T, Koo BK, Koch M, Delhomme N, et al. Expression of an ASCL2 related stem cell signature and IGF2 in colorectal cancer liver metastases with 11p15.5 gain. Gut. 2010;59(9):1236-44.

212. Tuo QZ, Liuyang ZY, Lei P, Yan X, Shentu YP, Liang JW, et al. Zinc induces CDK5 activation and neuronal death through CDK5-Tyr15 phosphorylation in ischemic stroke. Cell death & disease. 2018;9(9):870.
213. Schonrath K, Klein-Szanto AJ, Braunewell KH. The putative Tumor Suppressor VILIP-1 Counteracts Epidermal Growth Factor-Induced Epidermal-Mesenchymal Transition in Squamous Carcinoma Cells. Plos One. 2012;7(3).
214. Guerrico AMG, Jaffer ZM, Page RE, Braunewell KH, Chernoff J, Klein-Szanto AJP. Visinin-like protein-1 is a potent inhibitor of cell adhesion and migration in squamous carcinoma cells. Oncogene. 2005;24(14):2307-16.
215. Akagi T, Hijiya N, Inomata M, Shiraishi N, Moriyama M, Kitano S. Visinin-like protein-1 overexpression is an indicator of lymph node metastasis and poor prognosis in colorectal cancer patients. Int J Cancer. 2012;131(6):1307-17.
216. Zehmer JK, Bartz R, Liu P, Anderson RG. Identification of a novel N-terminal hydrophobic sequence that targets proteins to lipid droplets. Journal of cell science. 2008;121(11):1852-60.
217. Zhou S, Shen Y, Zheng M, Wang L, Che R, Hu W, et al. DNA methylation of METTL7A gene body regulates its transcriptional level in thyroid cancer. Oncotarget. 2017;8(21):34652-60.
218. Jin X, Yang C, Fan P, Xiao J, Zhang W, Zhan S, et al. CDK5/FBW7-dependent ubiquitination and degradation of EZH2 inhibits pancreatic cancer cell migration and invasion. The Journal of biological chemistry. 2017;292(15):6269-80.
219. Hai CM, Gu Z. Caldesmon phosphorylation in actin cytoskeletal remodeling. European journal of cell biology. 2006;85(3-4):305-9.
220. Nalluri SM, O'Connor JW, Virgi GA, Stewart SE, Ye D, Gomez EW. TGFβ1-induced expression of caldesmon mediates epithelial-mesenchymal transition. Cytoskeleton (Hoboken, NJ). 2018;75(5):201-12.
221. Efremova M, Rieder D, Klepsch V, Charoentong P, Finotello F, Hackl H, et al. Targeting immune checkpoints potentiates immunoediting and changes the dynamics of tumor evolution. Nature communications. 2018;9(1):32.
222. Germano G, Lamba S, Rospo G, Barault L, Magri A, Maione F, et al. Inactivation of DNA repair triggers neoantigen generation and impairs tumour growth. Nature. 2017;552(7683):116-20.
223. Aref AR, Campisi M, Ivanova E, Portell A, Larios D, Piel BP, et al. 3D microfluidic ex vivo culture of organotypic tumor spheroids to model immune checkpoint blockade. Lab on a chip. 2018;18(20):3129-43.
224. Ried T, Meijer GA, Harrison DJ, Grech G, Franch-Expósito S, Briffa R, et al. The landscape of genomic copy number alterations in colorectal cancer and their consequences on gene expression levels and disease outcome. Molecular aspects of medicine. 2019;69:48-61.
225. Ooi A, Nakanishi I, Huang CD, Mai M. Numerical chromosome alterations in colorectal carcinomas detected by fluorescence in situ hybridization. Virchows Archiv. 1996;428(4):243-51.
226. Camins A, Verdaguer E, Folch J, Canudas AM, Pallàs M. The role of CDK5/P25 formation/inhibition in neurodegeneration. Drug news & perspectives. 2006;19(8):453-60.
227. Pallari HM, Lindqvist J, Torvaldson E, Ferraris SE, He T, Sahlgren C, et al. Nestin as a regulator of Cdk5 in differentiating myoblasts. Molecular biology of the cell. 2011;22(9):1539-49.

228. Liu Y, Mi Y, Mueller T, Kreibich S, Williams EG, Van Drogen A, et al. Multi-omic measurements of heterogeneity in HeLa cells across laboratories. Nature biotechnology. 2019;37(3):314-22.
229. Ben-David U, Siranosian B, Ha G, Tang H, Oren Y, Hinohara K, et al. Genetic and transcriptional evolution alters cancer cell line drug response. Nature. 2018;560(7718):325-30.
230. Asghar U, Witkiewicz AK, Turner NC, Knudsen ES. The history and future of targeting cyclin-dependent kinases in cancer therapy. Nature reviews Drug discovery. 2015;14(2):130-46.
231. Lochhead PA, Clark J, Wang LZ, Gilmour L, Squires M, Gilley R, et al. Tumor cells with KRAS or BRAF mutations or ERK5/MAPK7 amplification are not addicted to ERK5 activity for cell proliferation. Cell cycle (Georgetown, Tex). 2016;15(4):506-18.
232. de Jong PR, Taniguchi K, Harris AR, Bertin S, Takahashi N, Duong J, et al. ERK5 signalling rescues intestinal epithelial turnover and tumour cell proliferation upon ERK1/2 abrogation. Nature communications. 2016;7:11551.
233. McManus MJ, Boerner JL, Danielsen AJ, Wang Z, Matsumura F, Maihle NJ. An oncogenic epidermal growth factor receptor signals via a p21-activated kinase-caldesmon-myosin phosphotyrosine complex. The Journal of biological chemistry. 2000;275(45):35328-34.
234. Eppinga RD, Li Y, Lin JL, Mak AS, Lin JJ. Requirement of reversible caldesmon phosphorylation at P21-activated kinase-responsive sites for lamellipodia extensions during cell migration. Cell motility and the cytoskeleton. 2006;63(9):543-62.
235. Chi Y, Welcker M, Hizli AA, Posakony JJ, Aebersold R, Clurman BE. Identification of CDK2 substrates in human cell lysates. Genome Biol. 2008;9(10):R149.
236. Hedges JC, Oxhorn BC, Carty M, Adam LP, Yamboliev IA, Gerthoffer WT. Phosphorylation of caldesmon by ERK MAP kinases in smooth muscle. American journal of physiology Cell physiology. 2000;278(4):C718-26.
237. Nikolic M, Chou MM, Lu W, Mayer BJ, Tsai LH. The p35/Cdk5 kinase is a neuron-specific Rac effector that inhibits Pak1 activity. Nature. 1998;395(6698):194-8.
238. Kawauchi T, Chihama K, Nabeshima Y, Hoshino M. Cdk5 phosphorylates and stabilizes p27kip1 contributing to actin organization and cortical neuronal migration. Nature cell biology. 2006;8(1):17-26.
239. Dave JM, Bayless KJ. Vimentin as an integral regulator of cell adhesion and endothelial sprouting. Microcirculation (New York, NY : 1994). 2014;21(4):333-44.
240. Yao YB, Xiao CF, Lu JG, Wang C. Caldesmon: Biochemical and Clinical Implications in Cancer. Frontiers in cell and developmental biology. 2021;9:634759.
241. Zehmer JK, Bartz R, Bisel B, Liu P, Seemann J, Anderson RG. Targeting sequences of UBXD8 and AAM-B reveal that the ER has a direct role in the emergence and regression of lipid droplets. Journal of cell science. 2009;122(Pt 20):3694-702.
242. Qi L, Song Y, Chan THM, Yang H, Lin CH, Tay DJT, et al. An RNA editing/dsRNA binding-independent gene regulatory mechanism of ADARs and its clinical implication in cancer. Nucleic Acids Res. 2017;45(18):10436-51.

243. McKinnon CM, Mellor H. The tumor suppressor RhoBTB1 controls Golgi integrity and breast cancer cell invasion through METTL7B. BMC cancer. 2017;17(1):145.
244. Courapied S, Sellier H, de Carné Trécesson S, Vigneron A, Bernard AC, Gamelin E, et al. The cdk5 kinase regulates the STAT3 transcription factor to prevent DNA damage upon topoisomerase I inhibition. The Journal of biological chemistry. 2010;285(35):26765-78.
245. Martinez-Balibrea E, Martínez-Cardús A, Ginés A, Ruiz de Porras V, Moutinho C, Layos L, et al. Tumor-Related Molecular Mechanisms of Oxaliplatin Resistance. Molecular cancer therapeutics. 2015;14(8):1767-76.
246. Nabet B, Roberts JM, Buckley DL, Paulk J, Dastjerdi S, Yang A, et al. The dTAG system for immediate and target-specific protein degradation. Nature chemical biology. 2018;14(5):431-41.
247. Zhang Z, Zhou L, Xie N, Nice EC, Zhang T, Cui Y, et al. Overcoming cancer therapeutic bottleneck by drug repurposing. Signal transduction and targeted therapy. 2020;5(1):113.
248. Swanton C, Tomlinson I, Downward J. Chromosomal instability, colorectal cancer and taxane resistance. Cell cycle (Georgetown, Tex). 2006;5(8):818-23.
249. Olson B, Li Y, Lin Y, Liu ET, Patnaik A. Mouse Models for Cancer Immunotherapy Research. Cancer discovery. 2018;8(11):1358-65.

Annex

cancers

MDPI

Article

Tumor Expression of Cyclin-Dependent Kinase 5 (Cdk5) Is a Prognostic Biomarker and Predicts Outcome of Oxaliplatin-Treated Metastatic Colorectal Cancer Patients

Vicenç Ruiz de Porras [1,2,†], Sara Bystrup [1,2,†], Sara Cabrero-de las Heras [1,2], Eva Musulén [3,4], Luis Palomero [5,6], Maria Henar Alonso [6,7,8,9], Rocio Nieto [10], Diego Arango [10], Víctor Moreno [6,7,8,9], Cristina Queralt [1,2], José Luis Manzano [1,11,12], Laura Layos [1,11,12], Cristina Bugés [1,11,12] and Eva Martinez-Balibrea [1,2,*]

1 Program of predictive and personalized cancer medicine (PMPPC) Germans Trias i Pujol Research Institute (IGTP), Ctra. Can Ruti—Camí de les escoles s/n, 08916 Badalona, Spain; vruiz@igtp.cat (V.R.d.P.); sbystrup@igtp.cat (S.B.); scabrero@igtp.cat (S.C.-d.l.H.); cqueralt@iconcologia.net (C.Q.); jmanzano@iconcologia.net (J.L.M.); llayos@iconcologia.net (L.L.); cbuges@iconcologia.net (C.B.)
2 Program Against Cancer Therapeutic Resistance (ProCURE), Catalan Institute of Oncology, Ctra. Can Ruti-Camí de les escoles s/n, 08916 Badalona, Spain
3 Department of Pathology, Hospital Universitari Germans Trias i Pujol, Ctra. Can Ruti—Camí de les escoles s/n, 08916 Badalona, Spain; emusulen@hotmail.com
4 Department of Pathology, Hospital Universitari General de Catalunya, Grupo Quirónsalud, Pedro i Pons 1, 08195 Sant Cugat del Valles, Spain
5 Program Against Cancer Therapeutic Resistance (ProCURE), Catalan Institute of Oncology, 08908 L'Hospitalet del Llobregat, Barcelona, Spain; lpalomero@iconcologia.net
6 ONCOBELL Program, Bellvitge Institute for Biomedical Research, 08908 L'Hospitalet del Llobregat, Barcelona, Spain; mhalonso@iconcologia.net (M.H.A.); v.moreno@iconcologia.net (V.M.)
7 Oncology Data Analytics Program, Institut Català d'Oncologia (ICO), 08908 Barcelona, Spain
8 Consortium for Biomedical Research in Epidemiology and Public Health (CIBERESP), 28029 Madrid, Spain
9 Department of Clinical Sciences, Faculty of Medicine and Health Sciences, University of Barcelona, 08907 Barcelona, Spain
10 Group of Biomedical Research in Digestive Tract Tumors, CIBBIM-Nanomedicine, Vall d'Hebron University Hospital, Research Institute (VHIR), Universitat Autònoma de Barcelona, Passeig Vall d'Hebron, 119-129, 08035 Barcelona, Spain; rocio.nieto@vhir.org (R.N.); diego.arango@vhir.org (D.A.)
11 Medical Oncology Service, Catalan Institute of Oncology (ICO), 08908 Barcelona, Spain
12 B-ARGO group, Germans Trias I Pujol Research Institute (IGTP), Ctra. Can Ruti- Camí de les escoles s/n, 08916 Badalona, Spain
* Correspondence: embalibrea@iconcologia.net; Tel.: +34-93-497-8684; Fax: +34-93-497-8654
† Vicenç Ruiz de Porras and Sara Bystrup contributed equally.

Received: 5 September 2019; Accepted: 9 October 2019; Published: 11 October 2019

Abstract: In recent years, an increasing number of studies have shown that elevated expression of cyclin dependent kinase (Cdk5) contributes to the oncogenic initiation and progression of many types of cancers. In this study, we investigated the expression pattern of Cdk5 in colorectal cancer (CRC) cell lines and in a large number of tumor samples in order to evaluate its relevance in this pathogenesis and possible use as a prognostic marker. We found that Cdk5 is highly expressed and activated in CRC cell lines and that silencing of the kinase decreases their migration ability. In tumor tissues, Cdk5 is overexpressed compared to normal tissues due to a copy number gain. In patients with localized disease, we found that high Cdk5 levels correlate with poor prognosis, while in the metastatic setting, this was only the case for patients receiving an oxaliplatin-based treatment. When exploring the Cdk5 levels in the consensus molecular subtypes (CMS), we found the lowest levels in subtype 1, where high Cdk5 again was associated with a poorer prognosis. In conclusion, we confirm that Cdk5

is involved in CRC and disease progression and that it could serve as a prognostic and predictive biomarker in this disease.

Keywords: colorectal cancer; cyclin-dependent kinase 5 (Cdk5); prognostic and predictive biomarker; oxaliplatin

1. Introduction

Cyclin dependent kinase (Cdk5) belongs to the cyclin-dependent kinase family of serine/threonine kinases whose activity depends on a regulatory subunit named cyclin. However, Cdk5 is considered an atypical Cdk because it binds to non-cyclin proteins p35 (*CDK5R1*) and p39 (*CDK5R2*), phosphorylation in the T-loop is not required for its activation and most of its substrates are not involved in cell cycle control. The function of this kinase was thought to be restricted to the central nervous system, where it is indispensable for normal brain development during embryogenesis and controls neuronal migration or axonal guidance, among others. Deregulation of Cdk5 is widely described in neurodegenerative diseases such as Alzheimer's, Parkinson's, and Huntington's [1]. In recent years, several studies have demonstrated that Cdk5 also plays relevant physiological and pathological roles outside of the nervous system, including transcriptional regulation (through regulation of transcription factors such as p53 or signal transducer and activator of transcription 3 (STAT3)), cell migration, adhesion, angiogenesis, and apoptosis [2]. Given that some of these functions are deregulated in tumors and that a great similarity exists between the cellular and molecular mechanisms orchestrating neuronal migration during the development of the nervous system and cancer cell migration during metastasis, it is not surprising that Cdk5 plays a role in cancer.

Cdk5 phosphorylates the STAT3 transcription factor on its Ser-727 residue, leading to increased proliferation and promotion of tumor formation in medullar thyroid carcinoma and in prostate cancer cells through the activation of androgen receptor [3,4] or resistance to DNA-damaging agents through the increased transcription of the DNA-repair gene essential meiotic structure-specific endonuclease 1 (*EME1)* in colorectal cancer (CRC) cell lines [5]. Cdk5 is involved in the regulation of DNA-damage repair through the phosphorylation of ataxia telangiectasia mutated (ATM) [6]. Elevated expression has been described in human pancreatic [7], lung [8], prostate [9], and breast [10] tumors and has been associated with a worse prognosis. The role of Cdk5 in the proliferation of tumor cells is not clear, but many studies have demonstrated its implication in cancer migration, invasion, and anchorage-independent growth. For instance, in pancreatic cancer, two studies showed that Cdk5 inhibition affected tumor malignant progression in vitro and in vivo. The rat sarcoma (RAS) pathway was reported to have an important effect on the Cdk5-mediated tumor progression on the one hand because mutant Kirsten rat sarcoma (KRAS) increased its kinase activity [7] and on the other hand, by participating in its downstream signaling through phosphorylation of Ras-related (Ral) A and B proteins [11]. In prostate and melanoma cancer models, the inhibition of Cdk5 resulted in decreased cell motility and metastatic potential [9,12] and in breast cancer, Cdk5 controlled cancer cell migration and tumor formation by regulating the phosphorylation of focal adhesion kinase (FAK) at Ser-732, as a downstream step of transforming growth factor Beta (TGF-B1) signaling, and was shown to be essential for epithelial to mesenchymal transition (EMT) and cell motility [10]. In CRC, Cdk5 functions as a tumor promoter via modulating the extracellular receptor kinase 5 (ERK5)—activator protein 1 (AP-1) axis [13] and it has been associated with oxaliplatin resistance acquisition [14].

To date, little is known about the possible role of Cdk5 as a cancer biomarker. In the present study, we studied the role of Cdk5 in several CRC cell lines, reproducing results from Zhuang et al. [13] and most importantly, we investigated the expression patterns of Cdk5 at different molecular levels in a significant number of human tumor samples from patients at different disease stages with the aim of evaluating its role as a prognostic and predictive marker in this malignancy.

2. Results

2.1. Cdk5 and p35 Are Broadly Expressed in CRC Cell Lines

We studied protein levels of Cdk5 and p35 by western blotting in a panel of 10 human CRC cell lines and detected both at high levels in all cell lines tested (Figure 1A). In contrast, we did not detect the p35 calpain-cleaved product p25, which is recognized by the same antibody. It has been reported that Cdk5 activity is regulated through phosphorylation of Y15 [1], and this phosphorylation is commonly used as a measure of activity [5,15]. However, based on our experience, this is not a good approach because Y15 is a highly conserved residue in the Cdk family [16] and the epitope against which these antibodies are designed is highly homologous for Cdk1, Cdk2, and Cdk5, which could lead to misleading results. As Cdk5 kinase activity is strictly dependent on the binding with p35/p25, this interaction also serves as a measure of activity. To study this binding, Cdk5 was immunoprecipitated and p25 was found to co-immunoprecipitate with Cdk5 in HT29, LoVo, HCT116, and DiFi cell lines (Figure 1B). It was also found that p25 is more stable than p35 and leads to prolonged kinase activity of Cdk5 [17], suggesting a Cdk5 hyperactivation in these cell lines.

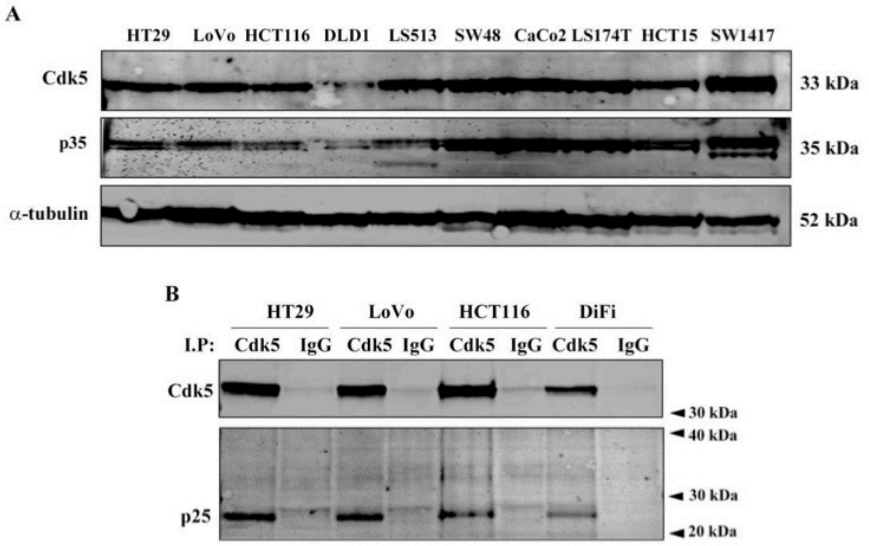

Figure 1. Cyclin dependent kinase 5 (Cdk5) and p35 (CDK5R1) expression in colorectal cancer (CRC) cell lines. (**A**) Western blot analysis of Cdk5 and p35 basal expression in a panel of 10 CRC cell lines. Alpha-tubulin was used as endogenous control. (**B**) Representative western blot images showing the co-immunoprecipitation of Cdk5 and p35/p25 in the indicated cell lines. Co-immunoprecipitation with an immunoglobin G (IgG) antibody was used as a negative control. The results were obtained from at least three independent experiments.

2.2. Cdk5 siRNA-Mediated Gene Silencing Impaired CRC Cells Migration and Invasion

We investigated how the transient silencing of Cdk5 affected three important characteristics of tumor cells: proliferation, migration and invasion. Forty-eight hours after siRNA gene silencing, Cdk5 knockdown (siCdk5) efficiency was between 90% and 95% at the protein level in HT29, LoVo, DiFi, and HCT116 cell lines (Figure S1A). Under these conditions, we did not observe any effect in cell proliferation (Figure 2A and Figure S2A).

However, we found significantly reduced migration and invasion in HT29 and LoVo siCdk5-transfected cell lines as compared to siRNA non-target control (siNTC) cells. In contrast, silencing of Cdk5 did not decrease the migration and invasion ability of DiFi cells (Figure 2B,C). As HT29 and LoVo cell lines harbor mutations in genes from the mitogen activated protein kinase (MAPK) signaling pathway [18] and the DiFi cell line is considered to be wild type [19], we wondered

whether an altered MAPK downstream signaling could be behind the observed differences. We took advantage of another KRAS wildtype (WT) cell line that was engineered to express a mutant form of *KRAS* (G12D). Cdk5 silencing caused a modest but statistically significant decrease in migration only in the SW48 *KRAS* G12D cell line and not in the *KRAS* WT. No differences in invasion ability after Cdk5 silencing were observed in either cell lines (Figure 2D,E).

Another important characteristic of cancer cells is their ability to undergo an unlimited number of divisions. To study the implications of Cdk5 in their long-term clonogenic capability of CRC cells, we performed colony formation assays in the HT29 and LoVo cell lines (Figure S2A,B). We observed a decrease in the number of colonies for siCdk5-transfected cells compared to siNTC cells in both lines, however, these were only statistically significant for the LoVo cells (p-values 0.198 and 0.046, respectively).

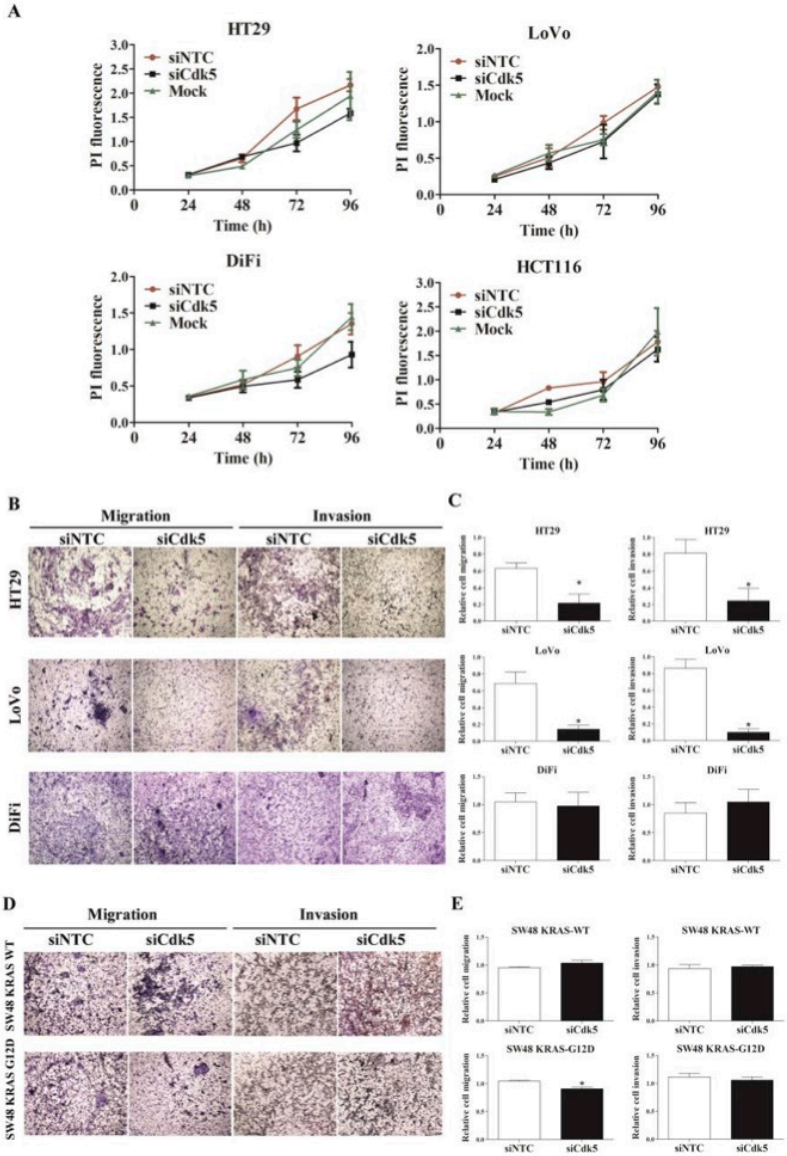

Figure 2. Effect of Cyclin dependent kinase 5 (Cdk5) siRNA-mediated gene silencing on colorectal cancer (CRC) cells proliferation, migration and invasion. (**A**) Graphic representation of HT29, LoVo, DiFi,

and HCT116 time-dependent cell proliferation after *Cdk5* gene silencing measured by propidium iodide (PI). (**B**,**D**) Representative Boyden chamber migration and invasion assays images (4× magnification) and (**C**,**E**) bar graphs showing (mean ± SD) relative cell migration and invasion after *Cdk5* silencing in the indicated cell lines. * p-value < 0.05 relative to control cells siRNA non-target control (siNTC). The results were obtained from at least three independent experiments.

2.3. Cdk5 and p35 Are Overexpressed in CRC Tumor Samples

We next evaluated Cdk5 and p35 expression in human samples. We included four different cohorts: A, B, D, and F (Table 1). In cohort A, Cdk5 and p35 proteins were clearly overexpressed as detected by western blot in tumor tissues as compared to the corresponding normal adjacent tissues (Figure 3A–C). Cdk5 was detected by immunohistochemistry (IHC) in primary colorectal tumors from cohort D and scored as either negative or positive (weak and strong staining) (Figure 3D). A total of 75% of the tumors were positive for Cdk5 staining. We also observed significantly higher *Cdk5* mRNA levels in tumor versus normal adjacent colon samples in two different publicly available data sets (Colonomics, cohort B, Figure 3E The cancer genome atlas (TCGA), cohort F, Figure 3F). Using TCGA data (cohort F), we analyzed the *Cdk5* gene copy number variation (CNV) (region chr7:151054008–151057848). We observed a statistically significant increase ($p = 7.58 \times 10^{-7}$) in the Cdk5 copy number in primary tumors as compared to the corresponding adjacent normal colon tissues (Figure 3G). The CNV of the *Cdk5* gene was strongly correlated (r = 0.55, $p = 7.16 \times 10^{-7}$) to Cdk5 expression levels in tumor tissue (Figure 3H) and also in a panel of 63 CRC cell lines (r = 0.54, $p = 4.6 \times 10^{-6}$) (Broad Institute Cancer Cell Line Encyclopedia) (Figure 3I).

Table 1. Overview of cohort used in the study.

Cohort	Type of Samples	Cdk5 Measurement	N	Sex	Age	Metastasis	Stage	Treatment	Origin of Samples	Available at	Molecular Data Available	Clinical Data Available
A	Frozen tissue Tumor/adjacent	WB	12	Male 7 (78%) Female 2 (22%)	72	Liver 8 (89%) Lung 1 (11%)	IV	N/A	Tumor Biobank	N/A	-	-
B	In silico data	Micro array	98	Male 72 (57%) Female 28 (43%)	72 (43-87)	-	II, MSS	Radical surgery 96 (98%)	Colonomics project	Colonomics.org	RAS, CMS, etc	DFS, OS
C	Frozen tissue	qPCR	37	Male 21 (57%) Female 16 (43%)	78 (37-91)	-	III	Radical surgery 36 (97%)	Duran and Reynals Hospital	N/A	-	DFS (mean 36.3 months) OS (mean 42 months)
D	FFPE – TMA	IHC	52	Male 29 (56%) Female 23 (44%)	62 (37-76)	Liver 37 (71%) Lung 5 (10%) Others 10 (19%)	IV	5-FU/OXA (77%) CAPE/OXA (23%)	Private collection	ISCIII	-	DFS (mean 9.6 months)
E	FFPE – TMA	IHC	139	Male 78 (69%) Female 35 (31%)	62 (29-75)	Liver 97 (70%) Lung 46 (33%) Others 20 (14%)	IV	5-FU/LV/IRI (47%) 5-FU/IRI (53%)	Private collection	ISCIII	-	DFS (mean 9.4 months) OS (mean 20.3 months)
F	In silico data	RNA seq	473	Male 259 (54%) Female 225 (46%)	66 (31-90)	-	I-IV	Various	TCGA project	https://cancergenome.nih.gov	CNV, RAS, CMS, etc	PFI, OS

Abbreviations: 5-FU/LV/IRI: 5-Fluorouracil/leucovorin/irinotecan; 5-FU/IRI: 5-Fluorouracil/irinotecan; 5-FU/OXA: 5-Fluorouracil/oxaliplatin; CAPE/OXA: Capecitabine/oxaliplatin; CMS: Consensus molecular subtype; CNV: Copy number variation; DFS: Disease-free survival; FFPE-TMA: Formalin-fixed paraffin-embedded tissue microarray; IHC: Immunohistochemistry; ISCIII: Instituto de Salud Carlos III; MSS: Microsatellite stable; N/A: Not available; OS: Overall survival; PFI: Progression-free interval; qPCR: Quantitative polymerase chain reaction; TCGA: The cancer genome atlas; RAS: Rat sarcoma oncogene; WB: Western blot.

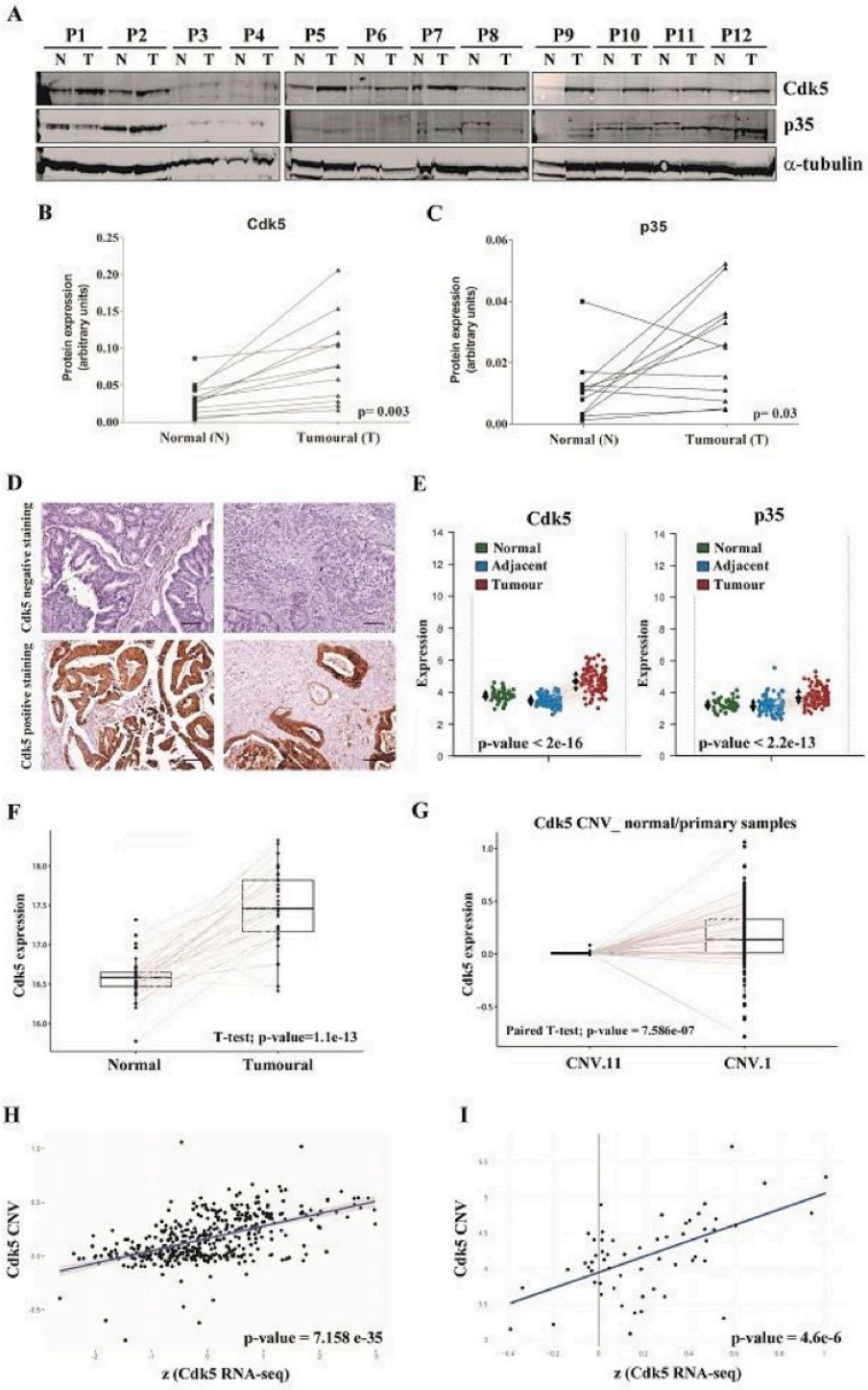

Figure 3. Cyclin dependent kinase (Cdk5) and p35 expression in colorectal cancer (CRC) tumor samples. Western blot (**A**) and graphic representation (**B**,**C**) of Cdk5 and p35 protein expression, respectively, in tumoral (T) and normal adjacent (N) tissues of 12 stage IV CRC patients (cohort A). Alpha-tubulin was used as endogenous control. The *p*-value was according to paired *t*-test. (**D**) Representative immunohistochemistry images of Cdk5 staining in CRC tumor tissues. The upper panel shows negative staining and lower panel positive staining. Scale bar: 100 μm. (**E**) Graphic representation of *Cdk5* and

p35 mRNA expression in 98-paired adjacent normal and tumoral tissues from stage II microsatellite stable (MSS) CRC patients (cohort B). (**F**) Graphic representation of *Cdk5* mRNA expression in normal and tumoral tissues of 38 I-IV CRC patients. Data were obtained from The Cancer Genome Atlas (TCGA) database (cohort F). (**G**) Graph representing the *Cdk5* copy number (CNV) change between normal and tumoral tissues in 67 stage I–IV CRC patients (cohort F). (**H**) Correlation between *Cdk5* CNV and *Cdk5* gene expression in 429 stage I–IV CRC patients. p-value according to Pearson correlation test (cohort F). (**I**) Correlation between *Cdk5* CNV and *Cdk5* gene expression in 63 CRC cell lines. The *p*-value was according to Pearson correlation test. Data from the Broad Institute Cancer Cell Line Encyclopedia.

2.4. High Cdk5 Levels Correlate with Poorer Prognosis in CRC Patients

Taking into account this data, we wondered whether Cdk5 expression could be a good prognostic and/or predictive biomarker in patients. To study this possibility, we used several cohorts in which the expression of Cdk5 was determined through different techniques (Table 1). We categorized data into high and low Cdk5 expression groups as follows: In cohorts using continuous data (cohorts B, C and F), patients were assigned to low or high groups according to Cdk5 values below or above the median, respectively; in those using categorical data (cohorts D and E), patients were grouped as low when IHC staining was negative or weak and as high when it was strong (Figure 3D). The prognostic value of Cdk5 expression was studied in two highly homogenous cohorts of localized microsatellite stable (MSS) CRC cancer patients (cohorts B and C, Table 1). Patients from cohorts B and C were diagnosed with stage II or stage III cancer, respectively, underwent surgery and did not receive any adjuvant treatment. In both the cohorts, high Cdk5 levels were associated with shorter disease free survival (DFS) ($p = 0.049$ 95%, confidence interval (CI) 0.98–5.88 for cohort B and $p = 0.048$, 95% CI 0.97–7.43 for cohort C) (Figure 4A,B), and also with overall survival (OS) in cohort B (p = 0.022, 95% CI 0.96–6.48), while no differences could be observed in OS in cohort C (Figure S3A,B). To study the predictive value of Cdk5 expression in the metastatic setting, we used two different, but again, quite homogenous cohorts of patients. Cohort D consisted of stage IV CRC patients treated with oxaliplatin and 5-fluorouracil as the first-line treatment, while patients from cohort E were treated with different schedules combining irinotecan and 5-fluorouracil (Table 1). As shown in Figure 4C,D, high Cdk5 levels were associated with shorter time to progression (TTP) only in the patients that received an oxaliplatin-based treatment (median 8.095 vs. 18.23 months, $p = 0.043$, 95% CI 1.01–4.71) (cohort D, Figure 4C), as no differences could be observed in the patients treated with irinotecan (median 8.95 vs. 8.42 months, $p = 0.45$, 95% CI 0.59–1.27) (cohort E, Figure 4D). These analyses were adjusted by age and sex; however, we performed an additional analysis including metastatic location as another co-variable, which resulted in an increased significance ($p = 0.018$, hazard ratio (HR) = 2.72, 95% CI 1.19–6.23). Similarly, when analyzing the response rates (Chi-square), we only found differences according to Cdk5 levels in the oxaliplatin-treated patients (cohort D) as 87% (13 out of 15 patients) of the low Cdk5 group had complete or partial response, while only 53% (18 out of 34) of the high Cdk5 group responded ($p = 0.029$). In view of these interesting results in the metastatic setting, we wanted to analyze whether Cdk5 was also predictive for adjuvant oxaliplatin-based therapy response. As we do not have our own cohort with this patient group, we used the TCGA data (cohort F). When splitting this subgroup ($n = 49$) based on high or low Cdk5, we could not observe any difference in the progression free interval (PFI) ($p = 0.64$, HR CI) nor OS ($p = 0.11$, HR CI). It is worth mentioning that when analyzing the entire TCGA cohort ($n = 473$, stages I to IV, treated and non-treated), no differences could be observed in PFI and OS (Figure S3C,D), highlighting the importance of choosing appropriate and well-defined cohorts of patients to conduct these studies.

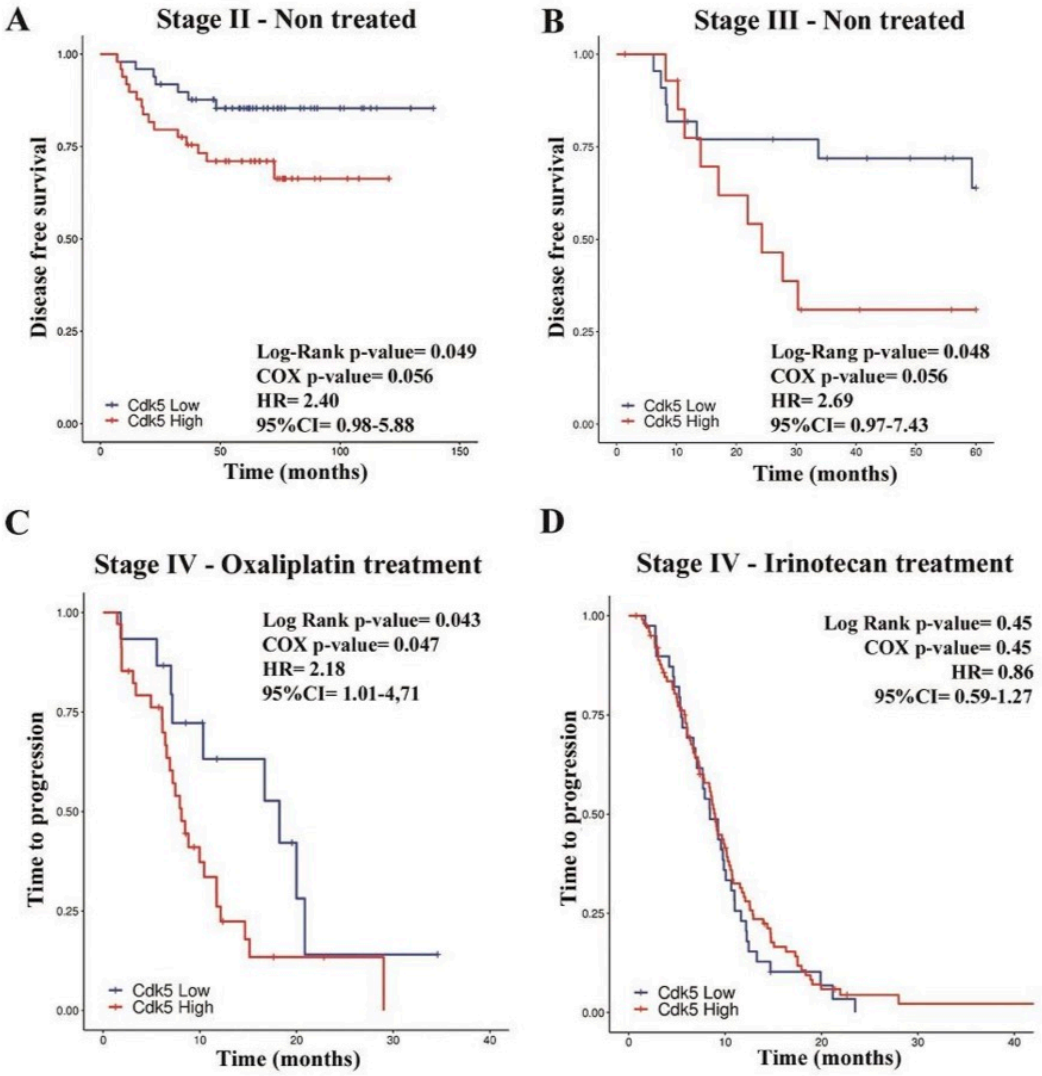

Figure 4. Kaplan–Meyer analysis of disease free survival (DFS) and time to progression (TTP) depending on Cyclin dependent kinase (Cdk5) levels. (**A**) DFS in 98 stage II colorectal cancer (CRC) patients split by the median of Cdk5 expression (cohort B). (**B**) DFS in 37 non-treated stage III CRC patients split by the median of Cdk5 expression (cohort C). (**C**) TTP in 52 stage IV oxaliplatin-treated patients, grouped depending on negative (n = 18) or positive Cdk5 (n = 34) immunohistochemistry (IHC) staining (cohort D). (**D**) TTP in 139 stage IV irinotecan-treated patients grouped depending on negative (n = 73) and positive (n = 66) Cdk5 IHC staining (cohort E).

As we observed a difference in migration and invasion when we silenced Cdk5 in our in vitro studies, we analyzed the link between Cdk5 expression and several gene sets related to EMT in the TCGA cohort. EMT is a well described process whereby cells undergo multiple biochemical changes that enable them to assume a mesenchymal phenotype, characterized by enhanced migratory capacity, invasiveness, and elevated resistance to apoptosis. We found that only for the TGF-β signaling within EMT did high Cdk5 levels correlate with higher pathway activation (p = 0.026, Figure S4).

We observed a difference in the effect of Cdk5 silencing in cell lines depending on their *KRAS* mutational status when studying the migration and invasion of the cells. Furthermore, it has been reported that Cdk5 is involved in the signaling cascade downstream of the epithelial growth factor receptor (EGFR) receptor [7]. Thus, we wanted to know whether there was a difference in the prognostic

value of Cdk5 according to *KRAS* mutations. Patients from cohort B were split according to *KRAS* mutational status (WT or mutated) and Cdk5 expression was again categorized as high or low. In the *KRAS* WT group, patients with high or low Cdk5 levels had similar DFS (Figure 5A); however, in the group with *KRAS*, mutated high Cdk5 levels predicted a statistically very significant poorer DFS compared to the Cdk5 low group (p = 0.004, 95% CI 1.56–36.46) (Figure 5B). We did not see any differences in OS in this cohort when grouping according to the *KRAS* mutational status (Figure S3E,F).

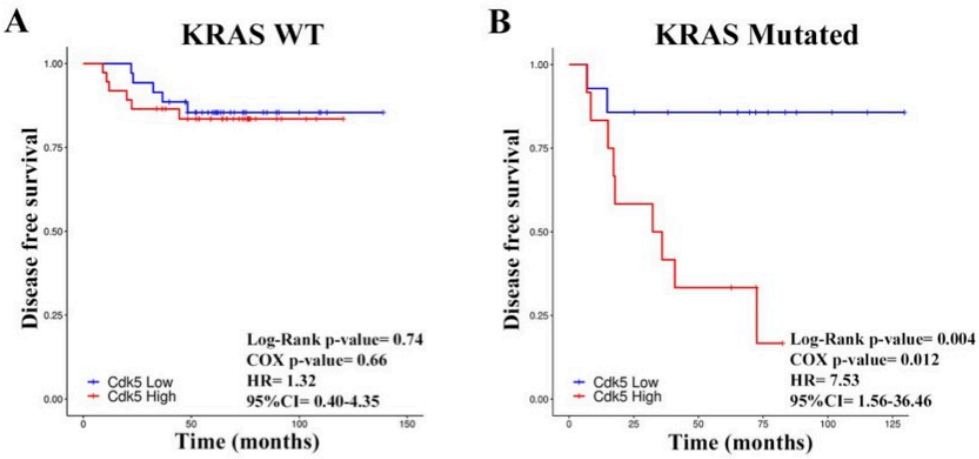

Figure 5. Kaplan–Meyer analysis of disease free survival (DFS) depending on Cyclin dependent kinase (Cdk5) expression and Kirsten rat sarcoma oncogene (*KRAS)* mutational status. (**A**) DFS for 72 stage II colorectal cancer (CRC) patients with wildtype (WT) *KRAS* and split by the median of Cdk5 expression. (**B**) DFS for 26 stage II CRC patients with mutated *KRAS* and split by the median of Cdk5 expression (cohort B).

2.5. Cdk5 Is Associated with Consensus Molecular Subtype 1

CRC has recently been classified into four consensus molecular subtypes (CMS) [20], namely, CMS1 (microsatellite instability immune), CMS2 (canonical), CMS3 (metabolic), and CMS4 (mesenchymal) subtypes. The subtype with the worst survival probability is the CMS4 [20]. Taking advantage of the fact that this information was available in cohort F, we wanted to explore whether there was an association between Cdk5 levels and a specific CMS. First, we checked if CMS-associated OS followed the same trend as reported previously and indeed, this was the case (Figure S5C). CMS1 displayed the lowest levels of Cdk5 (Figure 6A,B). For each molecular subtype, we then compared the OS between patients with high or low Cdk5 levels and did not observe any differences (Figure S5A). When we analyzed the progression-free interval (PFI), an endpoint similar to DFS and TTP used in our previous analysis which has been shown to be the most reliable endpoint when analyzing data from the TCGA-colorectal adenocarcinoma (COAD) database [21], we found that high Cdk5 in the CMS1 correlated with poorer outcomes (p = 0.036, 95% CI 1.07–8.10) (Figure 6C), while no differences were found in the three remaining molecular subtypes (Figure S5B). It is worth mentioning that the majority of the CMS1 group were non-metastatic patients (55 M0 and 4 M1).

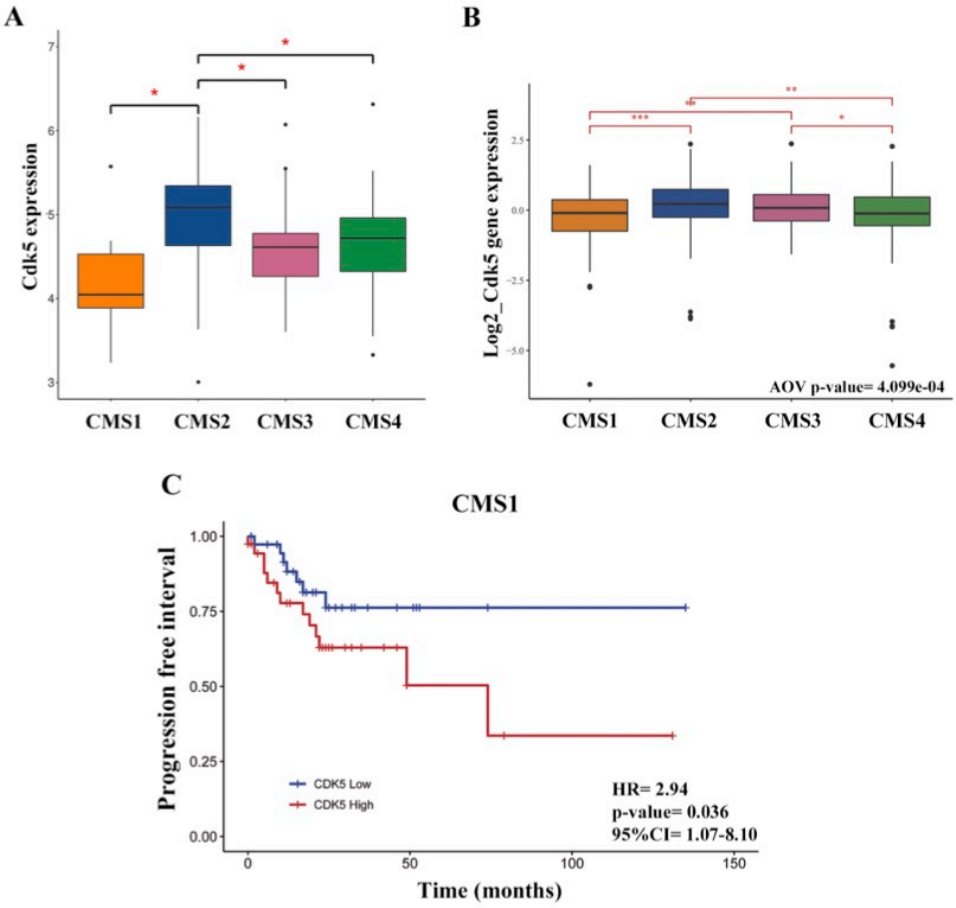

Figure 6. Cyclin dependent kinase 5 (Cdk5) expression in the four consensus molecular subtypes (CMS). (**A**) Dunn and Kruskal–Wallis multiple comparison of Cdk5 expression in CMS in 98 stage II tumors. Note that only six cases were classified as CMS1 as this cohort was restricted to microsatellite stabile (MSS) cases (**B**) ANOVA analysis of Cdk5 expression levels in the CMS in the cancer genome atlas - colorectal adenocarsinoma - rectal adenocarcinoma dataset (TCGA-COAD-READ) including 410 stage I–IV patients. * p-value < 0.05, ** p-value < 0.01, *** p-value < 0.001. (**C**) PFI in the TCGA-COAD CMS1 subgroup including 78 stage I–IV patients; patients were split according to the median of Cdk5 expression (cohort F).

3. Discussion

Cdk5 has emerged as a possible drug target in several tumors, including CRC. Here, we confirm previous results implicating its role in CRC pathogenesis [13], but importantly, we report its possible utility as a prognostic biomarker in this malignancy. It is worth mentioning that our study was performed in a large number of CRC patients' samples using different techniques to measure Cdk5 levels, and importantly, in selected groups according to tumor stage and clinical approaches. Given the relevance of the recent molecular classification of CRC into four consensus subtypes, we also explored the possible association of Cdk5 overexpression with specific CMS. To our knowledge, this is the most complete study of these characteristics so far.

Our results indicate that Cdk5 and its activator p35 are broadly expressed in human CRC cell lines; however, Cdk5 was found to be mainly bound to p25, the truncated form of p35. The binding of p25 to Cdk5 is indicative of constitutive activation of Cdk5 [17]. In human colorectal adenocarcinomas, Cdk5 and p35 were also highly expressed, especially when compared to normal adjacent tissue or to normal colonic mucosa from healthy donors. Our results are in agreement with those reported

by Zhuang et al. [13] and are possibly explained by the increased copy number of the *Cdk5* gene found in primary tumors as compared to normal adjacent tissues, a fact that was also pointed out by Robb et al. [22].

Reduced Cdk5 expression was associated with decreased migration and invasion in vitro but not with cell proliferation. This has been observed previously in cell lines from different tumor origins [7,9,11–13]. Our cell lines had mutations in *KRAS* (LoVo) or in rapidly accelerated fibrosarcoma B (*BRAF)* (HT29) genes. Indeed, signaling through the MAPKs is one of the main deregulated pathways in CRC and other authors had reported an interaction between Cdk5 and different effectors of this pathway. Unfortunately, in the only previous study conducted for Cdk5 in the context of CRC, all the cell lines tested had a deregulated MAPK pathway [13]. Therefore, we wanted to include cell lines with proficient MAPK pathways and compare the effects of silencing the *Cdk5* gene. We observed that in this case, Cdk5 downregulation had no effect on migration or invasion of cells, which is in agreement with previously published data [7]. It was previously shown that, in a context of *RAS*/*BRAF* mutant CRC, Cdk5 could phosphorylate ERK5 and that the effects of abrogation of Cdk5 expression were due to the inhibition of ERK signaling [13]. However, we think that this is unlikely as CRC cell lines with *KRAS* or *BRAF* mutations seem to preferentially activate the ERK1/2 pathway and when treated with ERK5 inhibitors, cell proliferation is unaffected [23,24].

We could successfully translate our results into a clinical setting as high levels of Cdk5 were associated with a higher risk of relapse in early-stage MSS CRC patients that did not receive any treatment after primary tumor resection, especially in patients with *KRAS*-mutant tumors. These results point to the prognostic value of Cdk5, which seems to be related with a more aggressive phenotype as we and others have reported in cell lines and in vivo models. Thus, those tumors expressing high levels of Cdk5 could have an enhanced capacity to invade and migrate from primary sites to metastatic sites. This is in agreement with what has been reported for other kinds of cancer, for example, breast cancer, where the Cdk5-FAK pathway downstream of TGF-β signaling is necessary for EMT [10]. Indeed, when we analyzed the connection between several gene sets related to EMT and Cdk5 expression in the TCGA cohort, we found that only for TGF-β signaling within EMT did high Cdk5 levels correlate with greater pathway activation.

We want to remark the homogeneity of these two cohorts of localized CRC patients and the fact that the patients did not receive any treatment, as this underscores the importance of Cdk5 as a biomarker in a priori good prognostic tumors. Whether treatment should be considered for these patients has to be explored in further studies.

We also investigated the predictive value of Cdk5 through analysis of the association between tumor protein expression and the outcome of metastatic CRC patients receiving two standard chemotherapy regimens: Oxaliplatin plus 5-fluorouracil and irinotecan plus 5-fluorouracil. Several studies have shown that Cdk5 plays a role in DNA damage repair and resistance, including the one induced by oxaliplatin and irinotecan [5,14]. However, we only observed a clear association of Cdk5 protein levels with response or TTP in patients treated with the former: the higher the Cdk5 levels, the worse the response or TTP. Whether patients with high Cdk5 tumor levels should be treated with irinotecan-based schedules rather than oxaliplatin-based schedules requires further investigation. Nevertheless, it should be noted that our results were based on the protein assessment in primary tumors and not in metastases.

For the moment, these results suggest that Cdk5 could be a good target to develop drugs against; on the one hand, they could be used in an adjuvant setting to prevent disease relapse and on the other hand, in a metastatic setting in combination with oxaliplatin. Another possibility would be a combination with poly (ADP-ribose) polymerase (PARP) inhibitors, as it was reported that *Cdk5* gene silencing conferred high sensitivity to this kind of drugs [25]. Unfortunately, although huge efforts have been made, the development of specific inhibitors is still an outstanding issue.

Finally, we wanted to explore the possible association between Cdk5 and the recently described CMSs [20] using the TCGA data. We found that in this cohort, CMS1 tumors had the lowest levels of Cdk5 and a high Cdk5 expression was only associated with worse progression-free interval in this

subtype. CMS1 is the so-called immune subtype and it is enriched in microsatellite instable (MSI), hypermutated, and highly lymphocyte-infiltrated tumors, which usually are responsive to immune checkpoint blockers. Dorand et al. reported a CD4+ T-cell-dependent rejection of Cdk5-deficient medulloblastoma cells in mice and an inverse correlation between Cdk5 and CD3+ T-cell infiltration in human medulloblastoma samples [26]. Experimentally, they showed that IFN-γ-induced programmed death ligand 1 (PD-L1) upregulation on medulloblastoma cells requires Cdk5. Therefore, we can speculate that in CMS1 tumors, which display high lymphocyte infiltration, high levels of Cdk5 would favor the expression of PD-L1 avoiding antitumor immunity. Nevertheless, it is important to stress that this cohort is very heterogeneous, containing both localized or metastatic tumors and a variety of treatments. Therefore, this hypothesis should be confirmed in further investigations.

4. Material and Methods

4.1. Human CRC Cell Lines

Human tumor-derived colorectal adenocarcinoma cell lines HT29, LoVo, DLD1, LS513, HCT116, DLD1, Caco2, LS174T, SW1417, SW480, HCT15, and DiFi from the American Type Culture Collection, along with SW48 parental and *KRAS* G12D/+ mutated cell lines (Horizon Discovery Ltd, Cambridge United Kingdom), were used in the present study. Cell lines were grown as a monolayer in RPMI 1640 (DLD1, LS513, HCT116, SW48, SW480, Caco2, and HCT15), DMEM (HT29, LS174T and SW1417) and Ham's F-12 (LoVo) media (Thermo Fisher Scientific, Waltham, MA, USA). DMEM and RPMI media were supplemented with 10% of heat-inactivated fetal calf serum (FCS) (Reactiva, 08004 Barcelona, Spain), 1% penicillin/streptomycin (Thermo Fisher Scientific, Waltham, MA, USA), 2 mmol/L L-glutamine (Sigma-Aldrich, St. Louis, MO, USA), and 10 mmol/L HEPES (Sigma-Aldrich, St. Louis, MO, USA). The Ham's medium was supplemented with 20% of heat-inactivated FCS and 1% penicillin/streptomycin (Thermo Fisher Scientific, Waltham, MA, USA). All cell lines were cultured at 37 °C in a humidified atmosphere of 5% CO_2. Cells were periodically tested for *Mycoplasma* contamination and authenticated by short tandem repeat profiling with in-house methods.

The molecular status of cell lines used for experiments: HT29: MSS, *KRAS* WT, and *BRAF* mut. V600E; LoVo: MSI, *KRAS* mut. G13D, and *BRAF* WT; HCT116: MSI, *KRAS* mut. G13D, and *BRAF* WT; DiFi: MSS, *KRAS* WT, and *BRAF* WT; SW48: MSI, *KRAS* WT, and *BRAF* WT.

4.2. Gene Silencing

Cdk5 was transiently silenced using a mix of three different siRNAs (s2825, s2826, and s2827; (Thermo Fisher Scientific, Waltham, MA, USA) and lipofectamine RNAiMAX in OptiMem medium according to the manufacturer's instructions (Thermo Fisher Scientific, Waltham, MA, USA). A negative transcription control (siNTC) (Cat No. AM4611; Thermo Fisher Scientific, Waltham, MA, USA) was used in all the experiments. Silencing was validated by western blotting and experiments with a minimum of 70% silencing levels were considered.

4.3. Cell Proliferation

Cell proliferation was analyzed 24, 48, 72, and 96 hours after siRNA Cdk5 silencing. Cells were permeabilized with 0.3% Triton X-100 and 30 µM propidium iodide (Sigma-Aldrich, St. Louis, MO, USA) was added and the fluorescence signal corresponding to the cell quantity was measured at 645 nm on the Varioskan reader (Thermo Fisher Scientific, Waltham, MA, USA).

4.4. Colony Formation Assay

HT29 and LoVo siNTC and siCdk5 cells were plated in six-well plates at a density of 300 cells/well. After 12 days in culture, the cells were washed with phosphate-buffered saline (PBS), fixed with a methanol/acetic acid (3:1) solution for 10 min and stained with a solution of crystal violet (0.5%) for 10 min. Colonies were counted manually.

4.5. Migration and Invasion

Migration and invasion assays were performed using transwell plates (HTS Transwell®Sigma-Aldrich, St. Louis, MO, USA). For the invasion assay, the upper chambers were coated with 21 µL of Geltrex™ (Thermo Fisher Scientific, Waltham, MA, USA). For both the assays, the lower chambers were filled with a medium containing 10% FCS and cells were seeded in 2% FCS medium in the upper chamber. Migrated/invasive cells that had reached the lower side of the membrane were fixed with 4% paraformaldehyde (PFA) and stained with 0.5% crystal violet. The ImageJ software was used for quantification.

4.6. Immunoprecipitation

Cells were homogenized in lysis buffer and the supernatant was incubated with a Cdk5 primary antibody (Santa Cruz Biotechnology, Santa Cruz, CA, USA; (J3): sc-6247) overnight at 4 °C. The mix was incubated 2 hours with protein G-coupled beads (Millipore, St. Louis, MO, USA) and the beads were washed and boiled for 5 minutes in a loading buffer to detach the protein complex. The protein levels were examined by western blotting.

4.7. Western Blotting

Cells were homogenized in a radioimmunoprecipitation assay (RIPA) plus buffer. Frozen tissue samples were disintegrated manually and were homogenized with RIPA plus buffer using the gentleMACS Dissociator system (Milteny Biotech, Bergisch Gladbach, Germany). Protein concentration was determined using the DC™ Protein Assay (Bio-Rad Laboratories, Inc., Richmond, CA, USA) and 50 µg of the protein was loaded and subjected to electrophoresis in 10% Sodium dodecyl sulfate-polyacrylamide gel electrophoresis (SDS-PAGE) gels (Thermo Fisher Scientific, Waltham, MA, USA) and transferred onto Polyvinylidene fluoride or polyvinylidene difluoride (PVDF) membranes (Bio-Rad Laboratories, Inc., Richmond, CA, USA). After blocking (LICOR Biosciences, Lincoln, NE, USA), membranes were incubated overnight with specific primary antibodies against Cdk5 (Cell Signaling, Danvers, MA, USA, #2506, 1:1000), p35 (Cell Signaling, Danvers, MA, USA, #2680, 1:300), and α-Tubulin (Sigma-Aldrich, St. Louis, MO, USA, #T6074, 1:20,000). Membranes were incubated with IRDye rabbit and mouse secondary antibodies (1:10,000) (LICOR Biosciences, Lincoln, NE, USA) and scanned and analyzed on the Odyssey imaging system (LICOR Biosciences). Non-cropped western blots from Figure 1B, Figure 3A, and Figure S1 can be seen in Figure S6.

4.8. Patients' Samples

Six different cohorts (named A to F), with a total of 811 samples from different patients, were used in this study. Table 1 shows the characteristics of each cohort. Samples from cohort C were collected at the Duran i Reynals Hospital. Samples from cohorts D and E belong to a private collection (ISCIII registered number C.0001505). All the samples were collected according to standard local protocols and after obtaining informed consent. The Clinical Research Ethical Committee from Hospital Germans Trias i Pujol provided approval for the study (BB14002; date: 7th March 2014).

4.9. Tissue Microarray and Immunohistochemistry (IHC) Staining

A tissue microarray (TMA) was built for cohorts D and E as previously described [27]. Subsequent immunohistochemistry procedures were applied as reported [27,28], and specific Cdk5 antibodies were used (Abcam, Cambridge, MA, USA, ab40773, 1:200 and Cell Signaling, Danvers, MA, USA, 2506, 1:200 for validation). Cells with siNTC or siCdk5 gene silencing were used to evaluate antibody specificity.

4.10. qPCR

CDK5 gene expression was studied by qPCR in cohort C as previously described [14,28]. Briefly, retrotranscription was performed with moloney murine leukemia virus (MMLV) reverse transcriptase (Thermo Fisher Scientific, Waltham, MA, USA) and the Cdk5 assay no. Hs00762869_s1 was used (Thermo Fisher Scientific, Waltham, MA, USA). Relative gene expression quantification was calculated according to the comparative Ct method as described elsewhere using β-Actin (Thermo Fisher Scientific, Waltham, MA, USA) as the endogenous control.

4.11. In Silico Data

Two publicly available cohorts were used: Colonomics (NCBI BioProject PRJNA188510) and TCGA. The colonomics cohort (cohort B) consisted of 98 paired adjacent-normal and tumor tissues from stage II microsatellite stable patients and 50 colon mucosae samples from healthy donors (246 samples in total). Gene expression data, assessed by Affymetrix Human Genome U219 expression array, had previously been analyzed [29].

For studies using the TCGA cohort (cohort F), we included all samples annotated as TCGA-colon adenocarcinoma (COAD) ($n = 448$) and 25 samples annotated as stage IV TCGA-rectum adenocarcinoma (READ), 473 samples in total. The classification of TCGA samples into four CMS was in agreement with Guinney et al. [20]. Different survival event data were retrieved according to Liu et al. [21].

4.12. Statistical Analysis

The data coming from in vitro experiments are presented as mean ± standard error of the mean (SEM) of at least three independent experiments and statistical analysis was performed with Graphpad Prism V.4 software (San Diego, CA, USA). Comparisons among different experimental conditions were carried out through the T-student or two-way ANOVA test followed by Bonferroni post-test. Values of $p \leq 0.05$ were considered significant.

A survival analysis was performed with the survival and survminer R packages. Kaplan–Meier curves depicting disease-free survival (DFS), time to progression (TTP), progression-free interval (PFI), and overall survival (OS) were accompanied with the log-rank test to verify significance in survival curve differences. The Cox regression hazards models were performed to quantify the effect of gene expression and survival (adjusted for age and stage). Differences in response to treatment were evaluated in cohorts D and E by contingency tables and chi-square or Fisher's exact tests as appropriate.

Regarding TCGA data, comparison between primary and normal tumor samples (gene expression and copy number alteration segment mean) were performed using paired samples T-tests. Both variables were compared using the Pearson correlation test. *Cdk5* gene expression comparison between different CMS subtypes was performed using one-way ANOVA.

The GSVA R-package (gene set variation analysis, PMC3618321) was used to compare the gene expression levels of EMT and TGF-β signaling in EMT pathways in Cdk5 low vs. Cdk5 high tumors. A Wilcox's test was performed to evaluate the statistical significance.

5. Conclusions

We combined in vitro studies with the analysis of a high number of tumor samples from different CRC stages and confirmed that Cdk5 is involved in CRC progression and that it could serve as a prognostic and predictive biomarker in this disease. Our findings also suggest that Cdk5 could help decide which patients should receive adjuvant therapy and whether oxaliplatin or irinotecan should be used in the treatment of metastatic disease.

Supplementary Materials: The following are available online at http://www.mdpi.com/2072-6694/11/10/1540/s1, Figure S1: Cdk5 siRNA-mediated gene silencing in CRC cells, Figure S2: Effect of Cdk5 siRNA-mediated gene silencing on HCT116 cell proliferation and HT29 and LoVo colony formation, Figure S3: Kaplan–Meier analysis of OS and PFI depending on Cdk5 expression and *KRAS* mutational status, Figure S4: EMT-related enriched hallmark correlations with Cdk5 expression, Figure S5: Kaplan–Meier analysis of OS and PFI depending on Cdk5

expression and CMS group, Figure S6: Images displaying non-cropped western blots from Figure 1B, Figure 3A, and Figure S1.

Author Contributions: Conceptualization, V.R.d.P., S.B., and E.M.B; Data curation, L.P.; formal analysis, V.R.d.P., S.B., L.P., and M.H.A.; funding acquisition, E.M.-B.; investigation, V.R.d.P., S.B., S.C.-d.l.H., E.M., L.P., M.H.A., R.N., D.A., and C.Q.; methodology, V.R.d.P., S.B., E.M., D.A., and E.M.-B.; project administration, E.M.-B.; supervision, E.M.-B.; validation, E.M. and R.N.; visualization, V.R.d.P., S.B., L.P., and M.H.A.; writing—original draft, V.R.d.P., S.B., and E.M.-B.; writing—review and editing, V.R.d.P., S.B., E.M., D.A., V.M., J.L.M., L.L., C.B., and E.M.-B.

Funding: This work has been funded by the ISCIII grants from the Spanish Government, project numbers PI09/01334 and PI12/02228, and the Departament d'Innovació, Universitats i Empresa, Generalitat de Catalunya, project numbers 2014-SGR-1494, 2017-SGR-1705 and 2017-SGR-723. The group from Eva Martinez Balibrea is furthermore funded by the PIE16/00011 and the group from Diego Arango by the PI16/00540 and AC15/00066 grants.

Acknowledgments: The tumor biobank at the IGTP-HUGTP. ICOBIOBANC, sponsored by the Catalan Institute of Oncology. We thank the CERCA Program, Generalitat de Catalunya for institutional support.

Conflicts of Interest: All authors have read the journal's policy on disclosure of potential conflicts of interest. All authors disclose not to have neither financial nor personal relationship with organizations that could potentially be perceived as influencing the described research.

References

1. Shah, K.; Lahiri, D.K. Cdk5 activity in the brain—Multiple paths of regulation. *J. Cell Sci.* **2014**, *127 Pt 11*, 2391–2400. [CrossRef] [PubMed]
2. Contreras-Vallejos, E.; Utreras, E.; Gonzalez-Billault, C. Going out of the brain: Non-nervous system physiological and pathological functions of Cdk5. *Cell Signal.* **2012**, *24*, 44–52. [CrossRef] [PubMed]
3. Fu, A.K.; Fu, W.Y.; Ng, A.K.; Chien, W.W.; Ng, Y.P.; Wang, J.H.; Ip, N.Y. Cyclin-dependent kinase 5 phosphorylates signal transducer and activator of transcription 3 and regulates its transcriptional activity. *Proc. Natl. Acad. Sci. USA* **2004**, *101*, 6728–6733. [CrossRef] [PubMed]
4. Hsu, F.N.; Chen, M.C.; Lin, K.C.; Peng, Y.T.; Li, P.C.; Lin, E.; Chiang, M.C.; Hsieh, J.T.; Lin, H. Cyclin-dependent kinase 5 modulates STAT3 and androgen receptor activation through phosphorylation of Ser(7)(2)(7) on STAT3 in prostate cancer cells. *Am. J. Physiol. Endocrinol. Metab.* **2013**, *305*, E975–E986. [CrossRef]
5. Courapied, S.; Sellier, H.; de Carne Trecesson, S.; Vigneron, A.; Bernard, A.C.; Gamelin, E.; Barre, B.; Coqueret, O. The cdk5 kinase regulates the STAT3 transcription factor to prevent DNA damage upon topoisomerase I inhibition. *J. Biol. Chem.* **2010**, *285*, 26765–26778. [CrossRef]
6. Yu, H.P.; Xie, J.M.; Li, B.; Sun, Y.H.; Gao, Q.G.; Ding, Z.H.; Wu, H.R.; Qin, Z.H. TIGAR regulates DNA damage and repair through pentosephosphate pathway and Cdk5-ATM pathway. *Sci. Rep.* **2015**, *5*, 9853. [CrossRef]
7. Eggers, J.P.; Grandgenett, P.M.; Collisson, E.C.; Lewallen, M.E.; Tremayne, J.; Singh, P.K.; Swanson, B.J.; Andersen, J.M.; Caffrey, T.C.; High, R.R.; et al. Cyclin-dependent kinase 5 is amplified and overexpressed in pancreatic cancer and activated by mutant K-Ras. *Clin. Cancer Res.* **2011**, *17*, 6140–6150. [CrossRef]
8. Liu, J.L.; Wang, X.Y.; Huang, B.X.; Zhu, F.; Zhang, R.G.; Wu, G. Expression of CDK5/p35 in resected patients with non-small cell lung cancer: Relation to prognosis. *Med. Oncol.* **2011**, *28*, 673–678. [CrossRef]
9. Strock, C.J.; Park, J.I.; Nakakura, E.K.; Bova, G.S.; Isaacs, J.T.; Ball, D.W.; Nelkin, B.D. Cyclin-dependent kinase 5 activity controls cell motility and metastatic potential of prostate cancer cells. *Cancer Res.* **2006**, *66*, 7509–7515. [CrossRef]
10. Liang, Q.; Li, L.; Zhang, J.; Lei, Y.; Wang, L.; Liu, D.X.; Feng, J.; Hou, P.; Yao, R.; Zhang, Y.; et al. CDK5 is essential for TGF-beta1-induced epithelial-mesenchymal transition and breast cancer progression. *Sci Rep.* **2013**, *3*, 2932. [CrossRef]
11. Feldmann, G.; Mishra, A.; Hong, S.M.; Bisht, S.; Strock, C.J.; Ball, D.W.; Goggins, M.; Maitra, A.; Nelkin, B.D. Inhibiting the cyclin-dependent kinase CDK5 blocks pancreatic cancer formation and progression through the suppression of Ras-Ral signaling. *Cancer Res.* **2010**, *70*, 4460–4469. [CrossRef] [PubMed]
12. Bisht, S.; Nolting, J.; Schutte, U.; Haarmann, J.; Jain, P.; Shah, D.; Brossart, P.; Flaherty, P.; Feldmann, G. Cyclin-Dependent Kinase 5 (CDK5) Controls Melanoma Cell Motility, Invasiveness, and Metastatic Spread-Identification of a Promising Novel therapeutic target. *Transl. Oncol.* **2015**, *8*, 295–307. [CrossRef] [PubMed]

13. Zhuang, K.; Zhang, J.; Xiong, M.; Wang, X.; Luo, X.; Han, L.; Meng, Y.; Zhang, Y.; Liao, W.; Liu, S. CDK5 functions as a tumor promoter in human colorectal cancer via modulating the ERK5-AP-1 axis. *Cell Death Dis.* **2016**, *7*, e2415. [CrossRef] [PubMed]
14. Martinez-Cardus, A.; Martinez-Balibrea, E.; Bandres, E.; Malumbres, R.; Gines, A.; Manzano, J.L.; Taron, M.; Garcia-Foncillas, J.; Abad, A. Pharmacogenomic approach for the identification of novel determinants of acquired resistance to oxaliplatin in colorectal cancer. *Mol. Cancer Ther.* **2009**, *8*, 194–202. [CrossRef] [PubMed]
15. Lin, H.; Chen, M.C.; Chiu, C.Y.; Song, Y.M.; Lin, S.Y. Cdk5 regulates STAT3 activation and cell proliferation in medullary thyroid carcinoma cells. *J. Biol. Chem.* **2007**, *282*, 2776–2784. [CrossRef]
16. Morgan, D.O. Principles of CDK regulation. *Nature* **1995**, *374*, 131–134. [CrossRef]
17. Patrick, G.N.; Zukerberg, L.; Nikolic, M.; de la Monte, S.; Dikkes, P.; Tsai, L.H. Conversion of p35 to p25 deregulates Cdk5 activity and promotes neurodegeneration. *Nature* **1999**, *402*, 615–622. [CrossRef]
18. Mouradov, D.; Sloggett, C.; Jorissen, R.N.; Love, C.G.; Li, S.; Burgess, A.W.; Arango, D.; Strausberg, R.L.; Buchanan, D.; Wormald, S.; et al. Colorectal cancer cell lines are representative models of the main molecular subtypes of primary cancer. *Cancer Res.* **2014**, *74*, 3238–3247. [CrossRef]
19. Montagut, C.; Dalmases, A.; Bellosillo, B.; Crespo, M.; Pairet, S.; Iglesias, M.; Salido, M.; Gallen, M.; Marsters, S.; Tsai, S.P.; et al. Identification of a mutation in the extracellular domain of the Epidermal Growth Factor Receptor conferring cetuximab resistance in colorectal cancer. *Nat. Med.* **2012**, *18*, 221–223. [CrossRef]
20. Guinney, J.; Dienstmann, R.; Wang, X.; de Reynies, A.; Schlicker, A.; Soneson, C.; Marisa, L.; Roepman, P.; Nyamundanda, G.; Angelino, P.; et al. The consensus molecular subtypes of colorectal cancer. *Nat. Med.* **2015**, *21*, 1350–1356. [CrossRef]
21. Liu, J.; Lichtenberg, T.; Hoadley, K.A.; Poisson, L.M.; Lazar, A.J.; Cherniack, A.D.; Kovatich, A.J.; Benz, C.C.; Levine, D.A.; Lee, A.V.; et al. An Integrated TCGA Pan-Cancer Clinical Data Resource to Drive High-Quality Survival Outcome Analytics. *Cell* **2018**, *173*, 400–416.e11. [CrossRef] [PubMed]
22. Robb, C.M.; Kour, S.; Contreras, J.I.; Agarwal, E.; Barger, C.J.; Rana, S.; Sonawane, Y.; Neilsen, B.K.; Taylor, M.; Kizhake, S.; et al. Characterization of CDK(5) inhibitor, 20-223 (aka CP668863) for colorectal cancer therapy. *Oncotarget* **2018**, *9*, 5216–5232. [CrossRef] [PubMed]
23. Lochhead, P.A.; Clark, J.; Wang, L.Z.; Gilmour, L.; Squires, M.; Gilley, R.; Foxton, C.; Newell, D.R.; Wedge, S.R.; Cook, S.J. Tumor cells with KRAS or BRAF mutations or ERK5/MAPK7 amplification are not addicted to ERK5 activity for cell proliferation. *Cell Cycle* **2016**, *15*, 506–518. [CrossRef] [PubMed]
24. de Jong, P.R.; Taniguchi, K.; Harris, A.R.; Bertin, S.; Takahashi, N.; Duong, J.; Campos, A.D.; Powis, G.; Corr, M.; Karin, M.; et al. ERK5 signalling rescues intestinal epithelial turnover and tumour cell proliferation upon ERK1/2 abrogation. *Nat. Commun.* **2016**, *7*, 11551. [CrossRef]
25. Turner, N.C.; Lord, C.J.; Iorns, E.; Brough, R.; Swift, S.; Elliott, R.; Rayter, S.; Tutt, A.N.; Ashworth, A. A synthetic lethal siRNA screen identifying genes mediating sensitivity to a PARP inhibitor. *EMBO J.* **2008**, *27*, 1368–1377. [CrossRef]
26. Dorand, R.D.; Nthale, J.; Myers, J.T.; Barkauskas, D.S.; Avril, S.; Chirieleison, S.M.; Pareek, T.K.; Abbott, D.W.; Stearns, D.S.; Letterio, J.J.; et al. Cdk5 disruption attenuates tumor PD-L1 expression and promotes antitumor immunity. *Science* **2016**, *353*, 399–403. [CrossRef]
27. Martinez-Balibrea, E.; Martinez-Cardus, A.; Musulen, E.; Gines, A.; Manzano, J.L.; Aranda, E.; Plasencia, C.; Neamati, N.; Abad, A. Increased levels of copper efflux transporter ATP7B are associated with poor outcome in colorectal cancer patients receiving oxaliplatin-based chemotherapy. *Int. J. Cancer* **2009**, *124*, 2905–2910. [CrossRef]
28. Gines, A.; Bystrup, S.; Ruiz de Porras, V.; Guardia, C.; Musulen, E.; Martinez-Cardus, A.; Manzano, J.L.; Layos, L.; Abad, A.; Martinez-Balibrea, E. PKM2 Subcellular Localization Is Involved in Oxaliplatin Resistance Acquisition in HT29 Human Colorectal Cancer Cell Lines. *PLoS ONE* **2015**, *10*, e0123830. [CrossRef]
29. Sanz-Pamplona, R.; Berenguer, A.; Cordero, D.; Molleví, D.G.; Crous-Bou, M.; Sole, X.; Paré-Brunet, L.; Guino, E.; Salazar, R.; Santos, C.; et al. Aberrant gene expression in mucosa adjacent to tumor reveals a molecular crosstalk in colon cancer. *Mol. Cancer* **2014**, *13*, 46. [CrossRef]